UNIVERSIDAD COMPLUTENSE DE MADRID

FACULTAD DE CIENCIAS BIOLÓGICAS

DEPARTAMENTO DE GENÉTICA

TESIS DOCTORAL

Alteraciones inducidas por cambios gravitatorios en células proliferantes en cultivo de *Arabidopsis thaliana*

MEMORIA PARA OPTAR AL GRADO DE DOCTOR

PRESENTADA POR

Khaled Youssef Kamal Moustafa

Directores

Francisco Javier Medina Díaz
Raúl Herranz Barranco

Madrid, 2014

UNIVERSIDAD COMPLUTENSE DE MADRID

FACULTAD DE BIOLOGÍA

DEPARTAMENTO DE GENÉTICA

Alteraciones inducidas por cambios gravitatorios en células proliferantes en cultivo de *Arabidopsis thaliana*

Khaled Youssef Kamal Moustafa

Licenciado en Ingeniería Agronómica

Madrid, 2014

Departamento de Biología Medioambiental

Centro de Investigaciones Biológicas

Consejo Superior de Investigaciones Científicas

UNIVERSIDAD COMPLUTENSE DE MADRID

FACULTAD DE BIOLOGÍA

DEPARTAMENTO DE GENÉTICA

Alterations induced by gravity changes in proliferating culture cells of *Arabidopsis thaliana*

Khaled Youssef Kamal Moustafa

Licenciado en Ingeniería Agronómica

Madrid, 2014

Departamento de Biología Medioambiental

Centro de Investigaciones Biológicas

Consejo Superior de Investigaciones Científicas

UNIVERSIDAD COMPLUTENSE DE MADRID

FACULTAD DE BIOLOGÍA

DEPARTAMENTO DE GENÉTICA

Alteraciones inducidas por cambios gravitatorios en células proliferantes en cultivo de *Arabidopsis thaliana*

*(*ALTERATIONS INDUCED BY GRAVITY CHANGES IN PROLIFERATING CULTURE CELLS OF *ARABIDOPSIS THALIANA)*

Khaled Youssef Kamal Moustafa

Licenciado en Ingeniería Agronómica

Madrid, 2014

Bajo la dirección de los doctores:
Francisco Javier Medina Díaz
Raúl Herranz Barranco

Tutor de la Facultad de Ciencias Biológicas (UCM):
Francisco Javier Gallego Rodríguez

Vº Bº Directores de tesis doctoral:

Dr. Francisco Javier Medina Díaz

Dr. Raúl Herranz Barranco

Vº Bº Tutor de doctorado:

Dr. Francisco Javier Gallego Rodríguez

My Dear Mother

Mom, who behind and the secret of my happiness

I Love You…..

ACKNOWLEDGEMENTS

It gives me great pleasure in expressing my gratitude to all those people who have supported me and their contributions in making this thesis possible. First and foremost, I must acknowledge and thank The Almighty Allah for blessing, protecting and guiding me throughout this period. I could never have accomplished this without the faith I have in Allah.

I express my profound sense of reverence to my supervisor and head of our laboratory Dr. Medina for his constant guidance, support, motivation and untiring help during my predoctoral stay at CIB. His in-depth knowledge on a broad spectrum of different microscope techniques and cellular biology topics has been extremely beneficial for me. He has given me enough freedom to explore on my own and at the same time the guidance to recover when my steps faltered. I will always remember his calm and relaxed nature, and the way he asks "YES! How can I help you? *"In English instead of Spanish*", whenever I enter his office. I am thankful to the Allah for giving me a mentor like him.

Furthermore, my deepest gratitude is to my co-supervisor, Dr. Raúl Herranz. Raúl taught me how to question thoughts and express ideas that helped me sort out the technical details specially, genomic and proteomic analysis. His patience and support helped me overcome many crisis situations and finish this dissertation. I am also thankful to him for encouraging the use of correct grammar and consistent notation in my writings and for carefully reading and commenting on countless revisions of this manuscript.

I also would like to acknowledge my current and previous colleagues in the CIB lab; Miguel (the person who help me most in my first steps in Spain, thank you so much Miguel), Aranzazu, the newest student at our lab, and Dr. Manzano. Moreover, I will always be grateful to Mercedes for all her technical help and lovely social lab interactions.

I would like to thanks all the member of the CIB services and departments who participated in the works conducting to this thesis. Special thanks to Dr. Pedro Lastres for his help, discussion, and work inspiration about flow cytometry analyses. Thanks a lot Pedro, without you almost the whole thesis project will not been finished.

Finally, I would like to express my gratitude to the researchers and technical staff from different scientific groups in Europe part of the GBF projects coordinated by Dr. Raúl Herranz. Using LDC and RPM in the European Space Research and Technology Centre (ESTEC), the Pipette clinostat in DLR German Aerospace Center (DLR), and also the magnetic levitation in High Field Magnet Laboratory at the Radboud University in the Netherlands was not only a demand of the project but a great opportunity to understand the European societies more extensively.

It's very important to have a nice social environment outside the lab; Tantway, Alaa, Ahmed, Rahma, Ahmed kamal, Dalia and our beautiful angel Sandrilla (*Thanks a lot all of you, I have spent the best 4 years ever in all my life*). The city, Madrid, itself has taught me several good lessons and also has given me several good friends.

I will finish with Egypt, My Lovely Home, where the most basic source of my life energy resides: my family. I have an amazing family, unique in many ways, and the stereotype of a *perfect* family in many others. Their support has been unconditional all these years and among all my life; they have given up many things for me to be at this situation now; they have cherished with me every great moment and supported me whenever I needed it. And I need to thank them in Arabic now...

كلمات الوفاء فى هذا الزمان قد ندرت. أستدعى بالذاكره سنوات حياتى الى أن وصلت الى ما أنا فيه الأن, ولا أتذكر إلا عائلتى: والداى وأخوتى. لا أستطيع أن أتخيل حياتى ذو قيمه بدون عائلتى الصغيره. والدتى الحبيبه: (امى أنتى مصدر السعاده والراحه والأمان والاطمئنان الأوحد فى حياتى. لا يوجد اى كلمات تستطيع ان تعبر عن عمق حبى وشكرى لك يا امى. اديت لك بكل شئ يا أمى فبدون وجودك فى حياتى لا اساوى شيئا. ربنا يحميك ويخليكى لى. أحبك يا اغلى الناس). والدى الحبيب (انت ركيزه حياتى. اتذكر دائما انك الاصل والاساس فى محبتى للعلم والبحث ولطالما كنت السند لنا فى حياتنا). اخوتى الاحباء (وفاء وسلمى), ملائكه حياتى الجميلات. يامصدر البهجه والسعادة فى حياتى ربنا يخليكم لى.

This work has been financially supported by a JAE-preDoc 2010 fellowship funded by CSIC to cover my four years contract. Scientific research funding was received from the Ministerio de Economía y Competitividad (AYA2009-07952 & AYA2012-33982), the European Space Agency (GBF projects #4000105761 & 4200022650) and European Union (EUROMAGNET II Project 2010.17 (NSO06-209)).

RESUMEN

La gravedad es el único factor ambiental, esencial para el desarrollo de la vida en la tierra, que ha permanecido constante durante la evolución. La gravedad es un desafío constante para el crecimiento de las plantas terrestres y la alteración o la ausencia de la gravedad es un cambio ambiental nuevo y filogenéticamente desconocido para estos seres vivos. Los efectos del cambio de la gravedad ambiental sobre las células meristemáticas de *Arabidopsis* se han abordado en nuestro laboratorio en un número relativamente pequeño de experimentos en microgravedad en el Espacio y en instalaciones de simulación en Tierra, en los que hemos descubierto una importante alteración de la coordinación entre la proliferación y el crecimiento celular que es característica de estas células indiferenciadas, altamente proliferantes. En la base de estas alteraciones se encuentran mecanismos específicos de respuesta de la planta a la señal gravitatoria, como la graviresistencia o el gravitropismo, en los que está implicada la regulación del transporte polar de auxinas, aunque el mecanismo específico que opera en las células meristemáticas es desconocido.

El **objetivo principal** de esta Tesis Doctoral es definir si estas respuestas gravitatorias son puramente celulares o dependen de la organización tisular, y para ello hemos utilizado un sistema modelo de cultivo celular *in vitro* de plantas de *Arabidopsis thaliana*, en el que no se conoce la presencia de estructuras especializadas para la gravisensibilidad, como los estatolitos, ni la de cascadas de señalización tisular, como el transporte de auxinas. Mediante nuevos abordajes experimentales, disponibles en este modelo en cultivo *in vitro*, se pretende investigar la respuesta de las células individuales al estrés gravitatorio, concretada en los procesos de proliferación y crecimiento celular y en los mecanismos implicados.

Para desvelar el impacto de la gravedad en los procesos biológicos de las plantas se precisan instalaciones de microgravedad simulada en tierra (*Ground Based Facilities* - GBF) adecuadas. Las GBF son valiosas para la preparación de experimentos espaciales, y también como instalaciones independientes en investigación gravitacional. En primer lugar hemos realizado un estudio comparativo y sistemático de la idoneidad de varias GBFs para proporcionar una simulación de microgravedad fiable para los cultivos de células vegetales en suspensión. Los estudios realizados en el clinostato de pipetas 2D y en las instalaciones de levitación magnética mostraron que estos dispositivos no daban una respuesta totalmente satisfactoria a los requerimientos exigidos. El método finalmente seleccionado consistió en la inclusión de las células en agarosa previa a su incubación en la Máquina de Posicionamiento Aleatorizado (*Random Positioning Machine* - RPM) para experimentos en microgravedad simulada, o en la Centrifuga de Gran Diámetro (*Large Diameter Centrifuge* - LDC), para experimentos en hipergravedad. El abordaje experimental de inmovilización del cultivo en suspensión, adaptado y desarrollado en este trabajo, ha sido un éxito, tanto por su reproducibilidad de los ambientes de gravedad alterada como por la preservación de la viabilidad del cultivo celular de plantas. Además, se han investigado nuevos modos de operación de la RPM (RPM^{HW} y RPM^{SW}) para obtener gravedad parcial (entre 0g y 1g). Esta nueva capacidad del dispositivo, enfocada a la simulación de las condiciones de la Luna y Marte, ha dado resultados de gran interés y promete nuevos avances de la investigación en esta línea.

Los cultivos celulares *in vitro* de *Arabidopsis* se expusieron a diferentes niveles de gravedad alterada para estudiar el crecimiento y la proliferación celular así como los efectos a nivel de genoma completo, incluidos los cambios transcriptómicos y el remodelado de la cromatina. Los cultivos celulares asincrónicos se expusieron a las condiciones simuladas de microgravedad (RPM), la gravedad de la Luna (RPM^{HW}), la de Marte (RPM^{SW}), así como a la hipergravedad 2g (LDC) durante 3h, 14h y 24h. El crecimiento y la proliferación celular se desacoplaron de forma similar a lo observado en células meristemáticas de plántulas. Estas alteraciones fueron mayores en condiciones de gravedad reducida, pero más leves en hipergravedad. La distribución de células en las fases del ciclo celular se fue alterando gradualmente con el tiempo de exposición; además, se observaron cambios en la expresión de genes reguladores del ciclo celular, como Ciclina B1 o el antígeno “Prolifera”. La biogénesis de ribosomas disminuyó, según mostró la

disminución en los niveles de nucleolina y fibrilarina, y el aumento en el número de nucleolos inactivos. Además, se detectó un efecto sobre la regulación epigenética de la expresión génica, comprendiendo un aumento en la metilación del DNA y una disminución en la acetilación de histonas.

El uso de sincronización por afidicolina permitió un estudio en profundidad de cada una de las fases del ciclo celular y de la tasa de proliferación celular, a lo largo de un período de 72 h. En condiciones de gravedad 1*g* control se definió un patrón ultraestructural concreto del nucleolo y de sus subcomponentes para cada fase del ciclo celular. Los nucleolos del tipo morfológico compacto aparecieron en las fases G1 y S, en esta última con un tamaño incrementado al doble. La fase G2 se caracterizó por nucleolos de gran tamaño, algunos de ellos del tipo vacuolado, y por los más altos niveles de las proteínas nucleolares nucleolina y fibrilarina, como reflejo de una elevada tasa de síntesis de ribosomas. En condiciones de microgravedad simulada la actividad nucleolar descendió respecto al control 1*g*, sobre todo en la subpoblación G2/M. Además, la trascripción extra-nucleolar por la RNA polimerasa II se redujo y se encontró un incremento en la proporción de cromatina condensada. Se demostró la aceleración del ciclo celular, debida esencialmente a un acortamiento de la fase G2/M. Este periodo muestra una duración variable, dependiendo de los niveles de gravedad, cuya ordenación, de menor a mayor es: la Luna (simulada), microgravedad (simulada), Marte (simulada), La Tierra hasta el periodo más largo en el caso de la hipergravedad. Por tanto, el punto de control G2/M aparece como una diana clave para los efectos de la gravedad alterada sobre el ciclo celular y su perturbación parece ser la causa principal de los cambios en la duración del ciclo inducidos por los cambios gravitatorios.

Por último se realizaron estudios sobre los cambios en el transcriptoma que aparecían tras la exposición a la gravedad alterada de los cultivos celulares *in vitro*. Comparamos la respuesta global del genoma a la microgravedad simulada, tanto en las subpoblaciones G1 y G2/M de cultivos sincrónicos, como en cultivos asincrónicos expuestos durante 14 h, apareciendo la transcripción global generalmente reprimida en todos ellos. Los principales grupos GO que aparecieron afectados incluyeron genes de estrés abiótico, regulación del ciclo celular y genes mitocondriales de función desconocida. De hecho, los genes que regulan el punto de control G2/M se mostraron claramente reprimidos, provocando un ciclo celular acelerado, mientras que la regulación del punto de control G1 estaba levemente potenciada, permitiendo una

recuperación parcial de la aceleración del ciclo originada en la transición G2/M. En consecuencia, la respuesta de las plantas a la microgravedad opera a través de un mecanismo único y complejo; la activación diferencial de varias rutas del estrés ambiental sugiere un efecto sinérgico en diferentes subpoblaciones del ciclo celular. Una nueva ruta de señalización, que incluye genes mitocondriales, se ha relacionado con la respuesta a la gravedad alterada, posiblemente en conexión con la actividad mitocondrial y producción adicional de radicales libres (ROS) como respuesta rápida a la microgravedad.

Una contribución adicional de este trabajo a los procedimientos metodológicos de nuestro laboratorio es la producción de protocolos y materiales adaptados para próximos experimentos espaciales. La definición de modelos nucleolares morfofuncionales, junto al desarrollo de cultivos transgénicos fluorescentes de *Arabidopsis* permitirá el uso de muestras *in vivo* para observación microscópica. Su implementación en experimentos de vuelo a la ISS potenciará los retornos científicos futuros de los programas de biología espacial.

Las conclusiones obtenidas de este trabajo de Tesis Doctoral son las siguientes:

1. Hemos comprobado que el mejor método para exponer un cultivo celular de plantas a un ambiente de gravedad alterada, en instalaciones de simulación en tierra, es la inmovilización por inclusión en agarosa. Este método mantiene la viabilidad celular, permite la sincronización celular y evita estímulos mecánicos no deseados.
2. Mediante el sistema biológico de cultivo celular vegetal *in vitro*, las instalaciones que mejor reproducen varios ambientes de gravedad alterada fueron la Máquina de Posicionamiento Aleatorizado (RPM), para microgravedad simulada, la Centrífuga de Gran Diámetro (LDC) para hipergravedad, y una versión de la RPM que usa modos de funcionamiento nuevos basados en Hardware o Software, para simular gravedad parcial, es decir, niveles de gravedad entre 0 y 1g, que incluyen las condiciones gravitatorias de La Luna y de Marte. En este último caso, se requiere investigación adicional para confirmar la equivalencia de los equipamientos. Otros instrumentos utilizados no han proporcionado resultados satisfactorios. El clásico clinostato 2D de pipetas para sistemas celulares no es adecuado, especialmente para experimentos a largo plazo, debido a problemas técnicos de los controles 1g (incluida una viabilidad celular comprometida). El abordaje de levitación magnética, aunque muy

versátil para simulación de gravedad parcial, despierta importantes preocupaciones tanto por la presencia de campos magnéticos muy intensos como por los problemas técnicos de varias simulaciones alternativas para $0g$*.

3. Otros avances técnicos conseguidos durante la realización de esta tesis con cultivos celulares de plantas en condiciones de gravedad alterada son:
   a. La adaptación de potentes técnicas de biología celular a nuestro sistema modelo *in vitro* de *Arabidopsis* por primera vez: los modelos morfofuncionales del nucléolo, el ensayo de tinción con EdU, la sincronización celular y técnicas cuantitativas de colocalización.
   b. La obtención de nuevos cultivos transgénicos, que han sido derivados con éxito desde líneas mutantes o con genes marcadores prestablecidas en nuestro grupo.
4. Tal y como se observó en las células meristemáticas de la raíz de plántulas expuestas a microgravedad, tanto real (Experimento "Root" en la ISS) o simulada, la coordinación de los procesos celulares fundamentales en el desarrollo de las plantas se pierde en condiciones de gravedad reducida (microgravedad simulada y gravedad parcial; la Luna y Marte) en cultivos celulares de planta, mientras que la hipergravedad (2g) produce un desequilibrio menor y en sentido opuesto entre el crecimiento y la proliferación celular.
5. El ciclo celular se acelera en las condiciones de microgravedad simulada y la Luna, debido a una relajación en los puntos de control del ciclo celular, concretamente en la transición G2/M, causando una mayor tasa de proliferación celular. Este aumento en la proliferación se acompaña de una reducción en el tamaño celular, corroborado por una actividad nucleolar disminuida, considerada como una estimación del crecimiento celular.
6. El ciclo celular se retrasa en las condiciones de hipergravedad, causando un ciclo celular significativamente más largo. Aunque el tamaño celular y algunos parámetros del crecimiento celular no están afectados significativamente, se puede inferir un aumento en la actividad nucleolar cuando se analiza la distribución de los modelos nucleolares a $2\ g$.
7. Las condiciones gravitatorias de Marte producen un efecto intermedio; aunque la proliferación celular aumenta inicialmente, debido a un periodo G2/M acortado, y el crecimiento celular disminuye (como en otras condiciones de gravedad reducida), la fase G1 es particularmente extendida hasta el punto de promover un ciclo celular más largo, por lo tanto recordando el efecto de la hipergravedad.

8. Los efectos de la gravedad alterada en cultivos celulares vegetales *in vitro* se debería explicar en el contexto de un sistema en el que las células gravisensibles profesionales, como los estatolitos de las plántulas, están ausentes o se desconocen. Una explicación probable sería considerar que el mecanismo inespecífico de la graviresistencia implica la gravisensibilidad en las células no diferenciadas. Por otro lado, un mecanismo universal, aun no descrito para la percepción de la gravedad, que sería responsable de la plétora de procesos fisiológicos que afectan a la polaridad celular y la organización espacial de las células, también podría estar jugando un papel fundamental. El solapamiento de diferentes sistemas de gravipercepción podría provocar la "confusión" del sistema con señales contradictorias, lo que explicaría los resultados de la gravedad parcial simulada.
9. La microgravedad simulada provoca un efecto extensivo y diferencial durante las fases del ciclo celular a nivel de genoma completo. Las respuestas transcriptómicas han sido confirmadas por análisis proteómicos y concuerdan con las modificaciones epigenéticas.
10. Las modificaciones epigenéticas, tanto la hipermetilación del DNA como la deacetilación de histonas, son componente clave de la regulación de la expresión génica que permite a las células vegetales lidiar con ambientes de gravedad alterada. Las modificaciones y la remodelación de la cromatina probablemente están relacionados con la alteración de las tasas de proliferación del ciclo celular de *Arabidopsis*, dado que el estado de condensación/decondensación de la cromatina varía con la progresión del ciclo celular.
11. La respuesta de las plantas a la gravedad alterada, más que basarse en un pequeño grupo de genes o cascadas de transducción especificas descansa en un mecanismo complejo, caracterizado por una respuesta única ante un estrés ambiental novedoso, que sugiere un efecto sinérgico que combina elementos de muchas vías de respuesta a estrés abiótico. La implicación de estos resultados a la agricultura sostenible en la Tierra y los sistemas de soporte vital en el Espacio es evidente.

ABSTRACT

Gravity is a key environmental cue for life on Earth, the only one that has remained constant throughout evolution. Environmental gravity is a particular challenge for the growth of terrestrial plants and alteration of absence of gravity is a novel and phylogenetically unknown environmental change for them. The effects of a change in the environmental gravity on *Arabidopsis* root meristematic cells have been approached up to now in our laboratory in a relatively small number of microgravity experiments performed in space and in ground based facilities (GBFs). A disruption of the coordination of cell growth and proliferation was shown to occur in response to altered gravity in these undifferentiated, highly proliferating cells. This response may be specifically triggered in the meristem by general mechanisms of graviresponse, such as graviresistance and gravitropism, including altered regulation of auxin polar transport, although the specific mechanisms of gravity sensing and response which operating on meristematic cells are unknown.

In this work we aim to define whether these gravity responses are purely cellular, or depend on the tissue level. To achieve this objective we have used a biological model system consisting of *Arabidopsis thaliana* cell cultures *in vitro*, in which neither specialized structures for gravity sensing, such as statoliths, nor extracellular signal transduction pathways, like auxin polar transport, are known to be present. Novel cellular and molecular methods, available for the *in vitro* cell culture model, have been used to get a deeper understanding on the mechanisms operating at individual cells to alter cell growth and proliferation under gravitational stress.

To disclose the impact of gravity on the plant biological processes, we require suitable ground based facilities (GBFs) for microgravity simulation. GBFs are valuable tools for preparing spaceflight experiments, and they also serve as stand-alone platforms for gravitational research. First of all, we performed a systematic and comparative study of the suitability of several available GBFs to provide a reliable microgravity simulation for plant cell cultures. The 2D pipette clinostat and magnetic levitation facilities were found to do not comply with our requirements. The method of choice consisted of a first embedding of cells in agarose followed by incubation, either in the Random Positioning Machine (RPM; microgravity), or in the Large Diameter Centrifuge (LDC; hypergravity). This immobilization approach, adapted and

developed by us, has proved successful to reproduce several altered gravity environments while preserving plant cell culture viability. Plus, novel modes of operation of the RPM (RPM^{HW} and RPM^{SW}) were assayed for partial *g* simulation. This approach, directed towards the simulation of the Moon and Mars gravity conditions, yielded interesting data and revealed as highly promising.

We exposed *in vitro* cell cultures to different levels of altered gravity to study cell growth, cell proliferation and whole genome effects, including transcriptomic changes and chromatin remodeling. Asynchronous cell cultures were exposed to the simulated microgravity (RPM), the Moon (RPM^{HW}), Mars (RPM^{SW}), and 2*g* hypergravity (LDC), for 3h, 14h and 24h. Cell growth and cell proliferation were similarly uncoupled by altered gravity as in meristematic cells from seedlings. These alterations were stronger under hypogravity conditions, while the hypergravity effect was weaker. Distribution of cell cycle phases was gradually disrupted through the exposure time, in addition to cell cycle regulators; Cyclin B1 expression was altered, while the antigen "Prolifera" was increased. Ribosome biogenesis was decreased as inferred by decreased nucleolin and fibrillarin levels, and the increased number of inactive nucleoli. In addition, an effect on the epigenetic regulation of gene expression was noted, including increased DNA methylation and depleted histone acetylation.

The use of aphidicolin synchronization allowed a deep study of each cell cycle phase and of the cell proliferation rate through a period of 72h. Under 1*g* control we linked the morphofunctional features of the nucleolus to cell cycle phases. Compact nucleoli appeared at G1 phase and S phase (double sized). The G2 phase was characterized by large nucleoli, some of them vacuolated, and by the highest nucleolar protein levels, reflecting a high rate of ribosome synthesis. Under simulated microgravity nucleolar activity was reduced versus 1*g*, especially during G2/M. Furthermore, in these conditions, the extra-nucleolar transcription by RNA polymerase II was depleted, while condensed chromatin increased. Cell cycle acceleration was demonstrated, being particularly observed at the G2/M phase. The length of this phase showed a considerable variation in the different gravity conditions studies, whose arrangement, from shortest to longest was: the Moon (simulated), microgravity (simulated), Mars (simulated), Earth, and hypergravity. Consequently, G2/M checkpoint disruption was considered a key cell cycle target for altered gravity effects.

Finally, transcriptomic analyses were performed. Global transcriptome response to simulated microgravity was obtained in both G1 and G2/M subpopulations of synchronous cultures and in asynchronous cultures after 14h of incubation, being generally repressed. Differential GO groups affected were abiotic stress, cell cycle regulation and mitochondrial (unknown function) genes. In fact, G2/M checkpoint genes were clearly downregulated, causing an accelerated cell cycle, while the G1 checkpoint genes were slightly upregulated, allowing the cell to partially compensate the acceleration. Plant response to microgravity alteration works through a unique and complex mechanism; differential activation of several environmental stress pathways suggests synergistic effects at different cell cycle subpopulations. A new pathway, including mitochondrial genes, has been involved in altered gravity responses, maybe connected to additional mitochondrial activity and ROS production as a rapid response to microgravity.

An additional methodological contribution of this work was the production of adapted protocols and materials for future spaceflight research. The definition of morphofunctional nucleolar models, together with the development of transgenic fluorescent *Arabidopsis* cultures will allow the use of "*in vivo*" observation of the samples by microscopic techniques. They can be implemented in ISS experiments to enhance the scientific outcomes of the space biology programs.

The conclusions we have reached from this Doctoral Thesis Work are as follows:

1. We have found that the best method to expose a plant cell culture system to altered gravity environments, using ground based facilities, is the immobilization by agarose embedding. This method preserves cell viability, allows cell synchronization and avoids unwanted mechanical stimuli.
2. Using the biological system of in vitro plant cell culture, the best instruments to reproduce several altered gravity environments were the Random Positioning Machine (RPM), for simulated microgravity, the Large Diameter Centrifuge (LDC) for hypergravity, and the modified RPM, based on Hardware or Software modes of operation, for simulated partial g, i.e. levels of gravity between 0 and 1, comprising the Moon and Mars gravity conditions. In this latter case, further research is required to

confirm their interchangeability. Other instruments tested have not given satisfactory results. The 2D Pipette Clinostat, often used for animal cellular systems, is not suitable, especially for long term experiments, due to technical problems in the $1g$ control samples (including cell viability issues). The magnetic levitation approach, while quite versatile in terms of partial g simulation, raises important concerns due to the high energy magnetic fields, and also to technical problems in the $0g*$ alternative experiences.

3. Other important technical achievements have also resulted from the work with plant cell cultures under altered gravity conditions. These achievements include:
    a. The adaptation of powerful cell biology techniques to be used in our *Arabidopsis in vitro* model system for the first time: morphofunctional nucleolar models, EdU labelling assay, cell synchronization and quantitative colocalization techniques.
    b. The establishment of new transgenic cell cultures, which have been successfully derived from previously established mutant/marker lines.
4. Similarly to the effects observed in root meristematic cells of seedlings exposed to microgravity, either real ("Root" experiment performed in the ISS) or simulated, the coordination of fundamental plant cell developmental processes is disrupted under reduced gravity conditions (simulated microgravity and partial gravity - the Moon and Mars) in plant cell cultures, while hypergravity ($2g$) produces an opposite and weaker misbalance on the plant cell growth and proliferation equilibrium.
5. Cell cycle is accelerated under simulated microgravity and the Moon conditions, due to relaxation of the cell cycle checkpoints, particularly at the G2/M transition, resulting in a higher cell proliferation rate. This proliferation increase is accompanied by a reduced cell size, corroborated by a depleted nucleolar activity, taken as an estimation of cell growth.
6. Cell cycle is decelerated under hypergravity conditions, producing a significantly longer cell cycle. While cell size and some cell growth parameters are not significantly affected, an increase in the nucleolar activity is inferred from the analysis of nucleolar models.
7. Mars gravity conditions produce an intermediate effect: while cell proliferation is initially increased, due to a shorter G2/M phase, and cell growth is decreased (as in other reduced gravity conditions), G1 phase is particularly extended to produce a longer cell cycle, thus resembling the effect of hypergravity.

8. The effects of altered gravity on the plant cell culture *in vitro* should be explained in the context of a system without known professional gravisensitive cells, such as seedling statoliths. A likely interpretation should take into account the unspecific graviresistance mechanism, which involves gravity sensing by non-differentiated cells, but a universal, still unknown mechanism of gravity perception would also play a prominent role. The existence of this mechanism is supported by the plethora of known physiological processes which involve cell polarity or spatial organization of cells. The overlapping of different systems of graviperception could lead to "confusing" the system with contradictory signals, which could explain the results of the partial gravity simulation, somehow striking.
9. An extensive effect of simulated microgravity at the overall genome level has been differentially detected through the cell cycle phases. Transcriptomic responses have been confirmed by proteomic analyses and this is consistent with epigenetic modifications.
10. Epigenetic modifications, both hypermethylation of DNA and histone deacetylation, are a key component in the regulation of gene expression that allows the plant cells to cope with altered gravity environments. Chromatin modifications and remodeling effects are probably influencing the altered progression rates of *Arabidopsis* cell cycle, since variable condensed/decondensed chromatin states have been observed through the cell cycle.
11. Plant response to altered gravity, rather than being based in a small group of genes or transduction pathways, relies in a complex mechanism, characterized by a unique response against a novel environmental stress, suggesting a synergistic effect which combines elements of multiple abiotic stress pathways. The implication of these results for sustainable agriculture on Earth and in Life Support Systems in space is certain.

INDEX

ACRONYMS AND ABBREVIATIONS

µ	Micro
3D/2D	**D**imension
ABA	**Ab**scisic **A**cid
ANOVA	**A**nalysis **O**f **V**ariance
BSA	**B**ovine **S**erum **A**lbumin
CDK	**C**yclin-**D**ependent **K**inase
CIB	**C**entro de **I**nvestigaciones **B**iológicas
CMT	**C**hromo**me**t**h**ylase 1
CYC	**C**yclin
DABCO	Glycerol based mounting medium
DAPI	4',6-**d**iamidino-2-phenyl**i**ndole
DESC	**D**utch **E**xperiment **S**upport **C**entre
DFC	**D**ense **F**ibrillar **C**omponents
DLR	German Aerospace Center
DNA	**D**eoxyribo**n**ucleic **a**cid
EdU	5-**e**thynyl-2'-**d**eoxy**u**ridine
ESA	**E**uropean **S**pace **A**gency
ESTEC	**E**uropean **S**pace Research and **T**echnology **C**enter
F	**F**orce
FC	**F**ibrillar **C**enters
g	**G**ravity
g	**G**ram
G1	**G**ap **1** (cell cycle)
G2	**G**ap **2** (cell cycle)
G2/M	**G**ap **2** / **M**itosis
GBF	**G**round **B**ased **F**acilities
GC	**G**ranular **C**omponents
GFP	**G**reen **F**luorescence **P**rotein
GIA	From **G**BF to **I**SS with ***A****rabidopsis thaliana*
GLU	**Glu**taraldehyde
GO	**G**ene **O**ntology
GUS	β-**gl**ucu**c**uronidase
h	**H**our
HAT	**H**istone **A**cetyl**t**ransferase
HDAC	**H**istone **De**a**c**etylase
HFML	**H**igh **F**ield **M**agnet **L**aboratory
IF	**I**mmuno**f**luorescence
IgG	**I**mmuno**g**lobulin **G**
ISS	**I**nternational **S**pace **S**tation

KOH	Potassium Hydroxide
l	**L**iter
LDC	**L**arge **D**iameter **C**entrifuge
LIS	**L**ife and Physical Sciences **I**nstrumentation and Life **S**upport Lab
M	**M**olar
M/AI	**M**etaphase/**A**naphase **I**ndex
MET	**Met**hyl**t**ransferase
mg	**M**illi**g**ram
min	**M**inutes
ml	**M**illiliter
MM2D	A type of Rapidly dividing *Arabidopsis* cell suspensions cultures maintained in Dark
mRNA	Messenger RNA
MSS	MS medium, **M**urashige and **S**koog + Succarose
NAA	α-**n**aphthalene **a**cetic **a**cid
NAOH	Sodium hydroxide
NASA	**N**ational **A**eronautics and **S**pace **A**dministration
ºC	**C**elsius degree
PBS	**P**hosphate **B**uffered **S**aline
PCR	**P**olymerase **C**hain **R**eaction
PFA	**P**ara**f**orm**a**ldehyde
PH	Negative *log* of hydrogen ion concentration
p-value	Statistical test **p**rovability **v**alue
qPCR	**Q**uantitative real-time **PCR**
RNA	**R**ibo**n**ucleic **a**cid
RNA POL II	**R**NA **p**olymerase **II**
ROS	**R**eactive **O**xygen **S**pecies
RPM	**R**andom **P**ositing **M**achine
rpm	**R**evolutions **p**er **m**inute
RPM^{HW}	RPM (Hardware)
RPM^{SW}	RPM (Software)
rRNA	**R**ibosomal **RNA**
RT	**R**oom **T**emperature
RT-PCR	**R**everse **T**ranscription **P**olymerase **C**hain **R**eaction
s	**S**econds
T	**T**ime sampling
TEM	**T**ransmission **E**lectron **M**icroscopy
w/v	**W**eight/**V**olume

Space Biology is a fundamental component of Space Life Sciences. By studying plants in the microgravity environment both in space or simulated conditions, we can understand the basic concepts of the interaction of gravity with these organisms, such as perception, signal transduction, and response to stimuli.

INTRODUCTION

Biology in Space!
Arabidopsis cell cultures
Cell proliferation
Cell growth
Epigenetics

INTRODUCTION

1. BIOLOGY IN SPACE!

Space Biology is a fundamental component of *Space Life Sciences.* Space life sciences include the sciences of physiology, medicine, and biology, which are linked with the sciences of physics, chemistry, geology, engineering, and astronomy. Space life sciences research not only helps to increase a new knowledge of the human function and the capacity of the human being to live and work in space, but also explores fundamental questions about the role of gravity in the origin, evolution, maintenance, and aging processes of life on Earth. As with *Space Physiology* and *Space Medicine*, Space Biology experiments have the goal of using the space environment as a tool to help in the understanding of the influence of gravity on functional processes of living organisms, such as microorganisms, cells, animals and plants. Furthermore, this discipline allows us to look at the role of gravity in the evolution and development of terrestrial organisms and ecological systems, as well as to investigate how the organisms react and adjust themselves to the effects of different gravity levels (Clément 2005, Clément & Slenzka 2006). As in any research discipline, a distinction needs to be made between the factors that are of *applied* nature, and those that concern basic aspects of biology as studied in the space environment. Therefore, the basic research objectives of space biology are:

- To understand the gravity alterations on microorganisms, cells, animals and plants.
- To determine the combined effects of microgravity and other environmental stresses (e.g., radiation, absence of day/night cycles) on the biological systems.
- To improve the quality of life on Earth through the use of the space environment to advance the knowledge in the biological sciences (Becker & Souza 2013).

1.1. PLANTS IN SPACE, WHY?

There are a number of reasons to study plant biological systems in the space environment. Plants respond to the gravity and to other environmental factors in fundamental ways. By studying plants in the microgravity environment of the space, we can understand the basic concepts of the interaction of gravity with these organisms, such as perception, signal transduction, and response to stimuli. In turn, on Earth, it depends upon plants to feed and sustain all living beings.

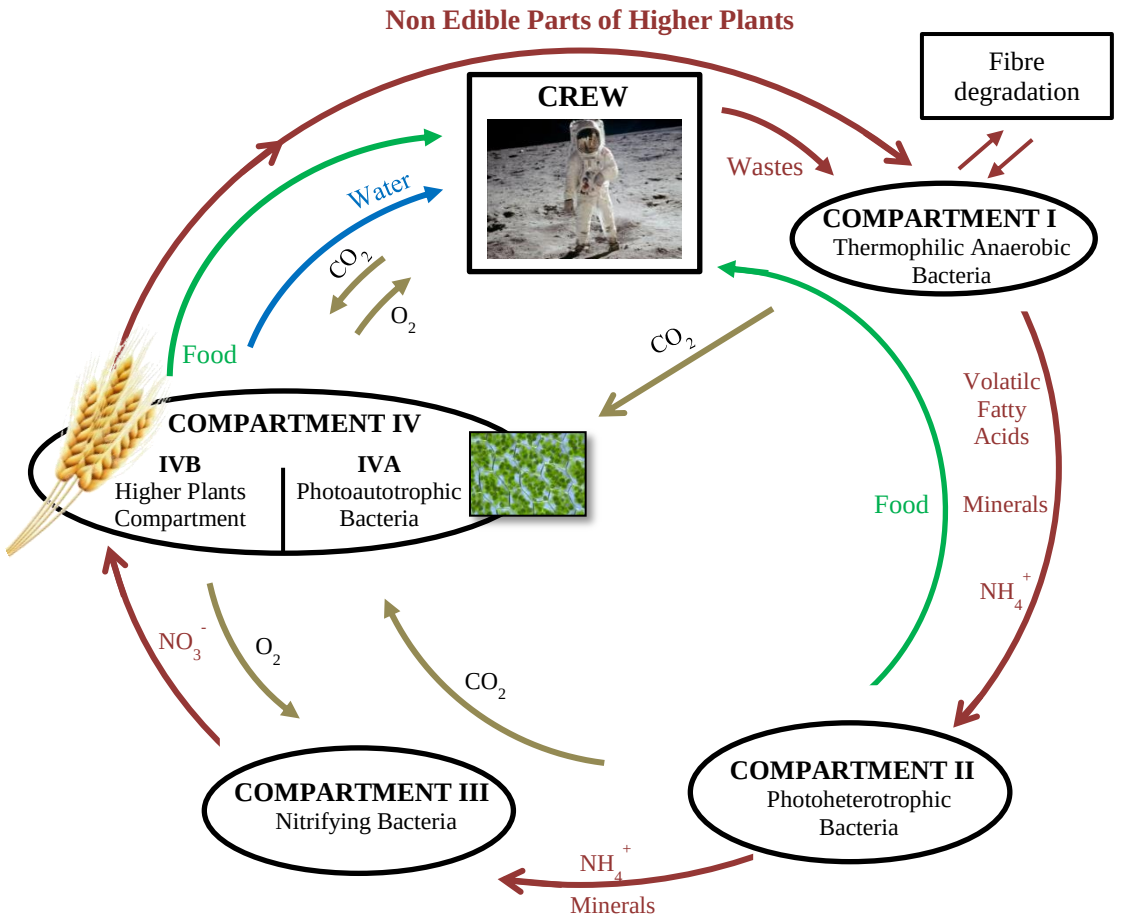

Figure 1: Plant-based Advanced Life support project (MELiSAA loop), European Space Agency. MELIiSSA (Micro-Ecological Life Support System Alternative) has been conceived as a micro-organisms and higher plants based ecosystem intended as a tool to gain understanding of the behavior of artificial ecosystems, and for the development of the technology for a future regenerative life support system for long term manned space missions, e.g. a lunar base or a mission to Mars. The driving element of MELIiSSA is the recovering of food, water and oxygen from waste (faeces, urea), carbon dioxide and minerals (Hendrickx et al 2006, Mastroleo et al 2010, Mergeay et al 1988). Based on the principle of an "aquatic" ecosystem, MELISSA is comprised of 5 compartments colonized respectively by Thermophilic Anaerobic Bacteria **(I)**, Photoheterotrophic Bacteria (*Rhodospirillum rubrum*) **(II)**, Nitrifying Bacteria (*Nitrosomonas/Nitrobacter*) **(III)**, Photoautotrophic Bacteria (*Arthrospira platensis*) **(IVA)**, Higher Plants **(IVB)**, and the crew. Unwanted waste products and air pollutants are processed using the natural function of plants which in turn provide food as well as contributing to water purification and oxygen for air revitalization. Many other important benefits are being examined for related industrial projects. ***Maintained by ESA/ESTEC/TEC-MCT (http://ecls.esa.int/ecls/?p=melissa).***

Plants play a critical role in the complex food network. Powered by light from the sun, CO_2 from the air, and nutrients from the soil, plants pass on this energy to the life forms that consume them. The same qualities that make plants essential to life on Earth-food production, absorption of CO_2, and release of O_2 and water vapor make them highly desirable on long term human space missions, as essential components of the so-called "Regenerative Life Support Systems".

Virtually all scenarios for the long term habitation of spacecraft and other extraterrestrial structures involve plants as important part of the contained environment that would support humans **(Figure 1).** So, plant growth in space remains a priority to be fully understood before plant-based life support systems can become a reality in the coming future (Ferl et al 2002, Freed & Vunjak-Novakovic 2002).

1.1.1. The Role of Gravity in Plant Evolution and Physiology

Plants on Earth are subjected to a constant gravitational field, which has played a major role in their evolution (Hoson et al 1996a, Ishii et al 1996). The action of gravity on plants has been studied for more than a century (Larsen 1962, Sack 1991, Sievers 1991). Gravity is the only parameter which has remained constant on Earth since life appeared on the surface of our planet, regarding both the direction and magnitude of the gravity vector (Herranz & Medina 2014, Morita 2010). Thus, the strategy followed by plants with respect to this environmental factor has consisted of using it to modulate important physiological activities, such as nutrients production and growth. However, despite plants have evolved collections of mechanisms to adapt to extreme environmental conditions, the existing plants are not known to be endowed with specific mechanisms for adaptation to altered gravity environments.

1.1.2. How Do Plants Sense The Gravity Direction?

Two hypotheses have been proposed to explain the gravity directions perceived by the plant. First of them is the classic starch-statolith hypothesis connecting gravity sensing and gravitropism; statoliths are starch-accumulating amyloplasts that sediment in the direction of gravity within specialized cells called statocytes (Blancaflor et al 1998, Kiss 2000, Morita & Tasaka 2004, Tsugeki et al 1998). The second one is the protoplast-pressure model, where the mass of the cytoplasm causes tension on the top and bottom of the plasma membrane (relative to the gravity vector) and a reinforcement of the cell wall is produced in response to gravity vector reorientation (Hoson et al 1996b, Staves 1997).

1.1.3. Gravity Alteration Influences Plant Response to Biotic and/or Abiotic Stresses

By studying plants in microgravity on board a spacecraft, biologists seek to understand how plants respond to the absence of the gravity vector. Otherwise, plants respond to environmental stimuli such as light, temperature, water, wind, magnetic or electric fields and also they interact with other living beings. These responses are at least partially masked on Earth by the overriding response of plants to gravity (Dutcher et al 1994, Halstead & Dutcher 1987, Krikorian et al 1992). Significant changes in these environmental factors produce stress in plants, altering the physiological processes. Plants counteract these alterations by changing the expression of specific genes, namely the stress genes among which the heat shock genes (Timperio et al 2008). In these stress conditions, produced by biotic and/or abiotic factors, the result of gravity alteration is a synergistic effect that promotes a complex environmental stress response (Beckingham 2010, Herranz et al 2010). Recent evidence from studying the influence of microgravity on other environmental factors revealed that altered gravity conditions produce specific changes in gene expression, involving heat shock-related and stress-related genes, thus modulating the pathways of plant responses to environmental changes (Paul et al 2012, Zupanska et al 2013). Also the phototropic response to red light wavelengths detected in *Arabidopsis* is altered under microgravity conditions (Millar et al 2010).

1.2. PLANT BIOLOGY RESEARCH IN MICROGRAVITY CONDITIONS; PROBLEMS, FACILITIES, AND FUTURE ASPECTS

Research in microgravity conditions is indispensable to disclose the gravity alterations on the biological processes and organisms. This research should be conducted in real microgravity conditions during spaceflight missions, as a unique opportunity to successful space exploration strategies (Des Marais et al 2008). Spaceflights to the International Space Station (ISS) provide unique conditions to investigate the plant biology in space. ISS is well equipped with biological specific laboratories. However, research in the near Earth orbit and access to ISS is severely constrained by the limited number of flight opportunities. To overcome this constraint, ground based facilities (GBFs) for simulated microgravity are valuable tools for preparing spaceflight experiments, and also for facilitating stand-alone studies and thus, providing additional cost-efficient platforms for gravitational research (Herranz et al 2013a). This strongly emphasizes the

need for using the GBFs to define baselines and enable testing of biological systems to address gravity-related issues prior to space experiments.

1.2.1 Different Altered Gravity Paradigms Used In Space Biology Research

Real Microgravity (μ*g*). The term "microgravity" is frequently used as a synonym of ¨weightlessness" and "zero-*g*¨, but actually, under microgravity there is a remaining *g*-force which is not zero, but just very small. Strictly speaking, the term "microgravity" should be applied to *g*-forces equal or lower than 10^{-6} *g*. Real microgravity can be achieved exclusively in spaceflights (ISS or satellites), or in sounding rockets (minutes), drop towers (seconds), or aircrafts during parabolic flight (seconds, in alternance with hypergravity periods). Mid- and long-term experiments in real microgravity can only be performed in space (Herranz et al 2013a).

Simulated Microgravity Conditions. It had been proposed to use the term "simulated microgravity" to describe the state of acceleration, such as it is perceived by a biological organism, which is assumed to be achieved using GBF (Herranz et al 2013a). In simulated microgravity experiments, the magnitude of Earth gravity vector cannot be changed, only its influence can be nullified by different methods (Briegleb 1992). In consequence, real microgravity cannot be achieved with a simulator. Rather, such a simulator may generate functional weightlessness from the perspective of the organisms or cells, being crucial the decision on the best GBF to be used for each biological question and model system (Herranz et al 2013a).

Hypergravity Conditions. Hypergravity is defined as the condition where the force of the gravity exceeds that existing on the surface of Earth (1*g*). Studying the effects of hypergravity is also quite interesting, since recently located potentially habitable exoplanets can be more massive than Earth (Vogt et al 2012) **(Figure 2B)**, and also since a flight Earth-Mars, with an expected duration of 6 months, will first require acclimation to microgravity conditions and then a change to a higher gravity level (from 0 to 3/8*g*). A broad gravity spectrum has to be explored to complete the scientific picture of how gravity has an impact on a system: samples have to be exposed to a variety of acceleration values, below and above 1*g*.

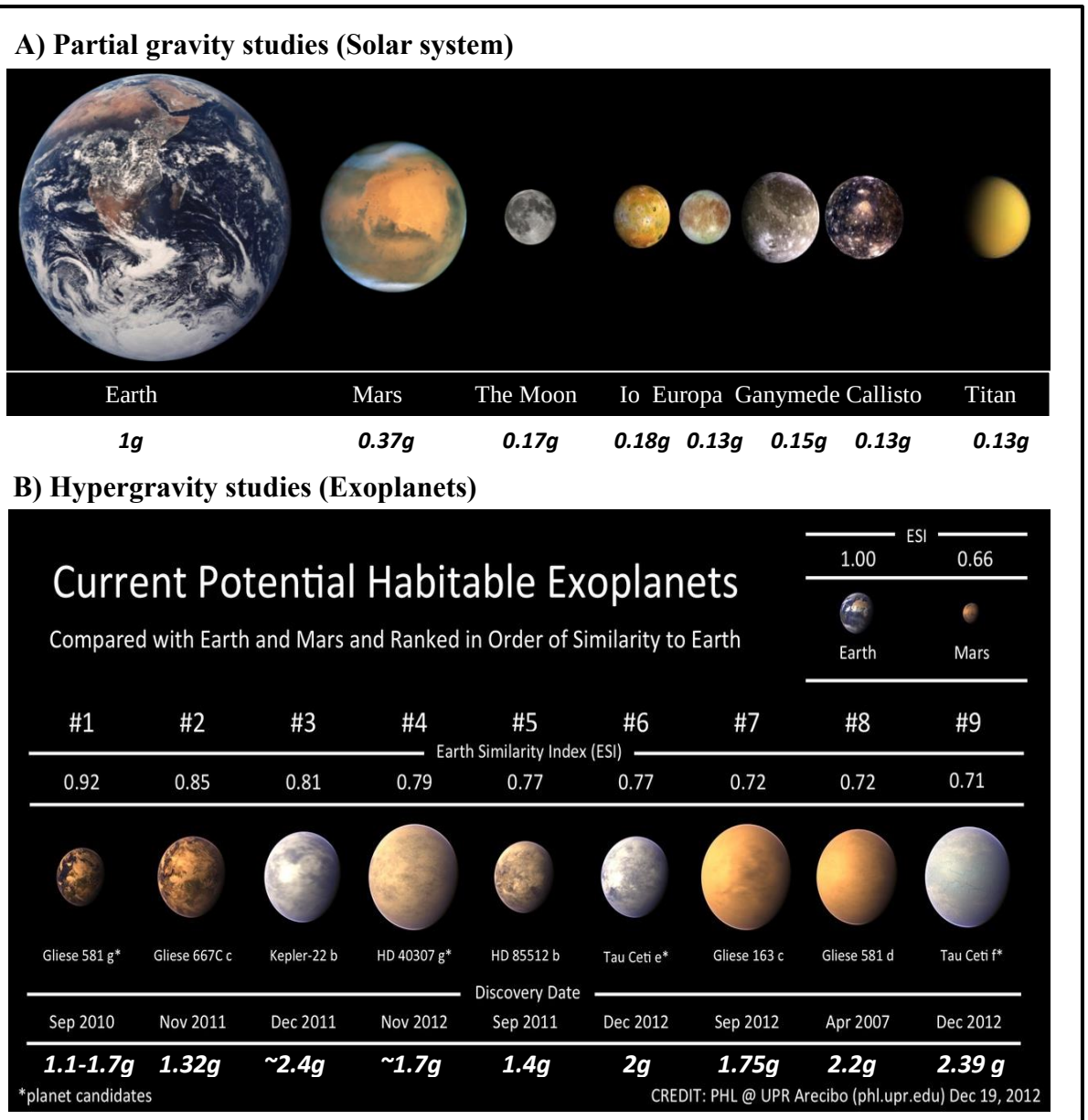

Figure 2: Gravity levels in potentially life-compatible solar system celestial bodies and current potential habitable exoplanets A) Gravity level of some solar system celestial bodies in a comparison with the Earth gravity reveals that the importance of the partial gravity studies. **B)** Recent potentially habitable exoplanets were discovered in a comparison with the earth gravity, arguing for the hypergravity interest to be investigated. Gravity has a positive relation with the mass and density of each planet.

Partial Gravity; the Moon and Mars Gravity Conditions. Plant behavior under partial gravity environments (less than the nominal 1*g* that occurs on Earth, such as the Moon (0.17*g*) and Mars (0.37*g*)) are understudied **(Figure 2A)** despite their potential interest (Garshnek 1994). The necessity to investigate plant biology under partial gravity environments comes from the fact that the European Space Agency (ESA), the National Aeronautics and Space Administration

(NASA) and other international space agencies have cited human exploration of the Moon and Mars as important goals in the upcoming years (Nair et al 2008). Therefore, it is important to take advantage of a new partial gravity GBFs in order to better prepare us for the eventual trip back to the Moon and to Mars. In addition, since plants are likely to be part of life-support systems on extended stays on the Moon/Mars, we need to understand plant biology at the Moon ($0.17g$) and Mars ($0.37g$) gravitational levels (Kiss 2014).

1.2.2. Ground Based Facilities (GBF) used for Altered Gravity Simulation

Various GBFs based on different physical concepts have been constructed to produce different gravity level environments on the ground and particularly to be used for simulating microgravity (Herranz et al 2013a) **(Figure 3)**. In our experiments, the following simulation techniques were used to study the influence of altered gravity on plant biological processes:

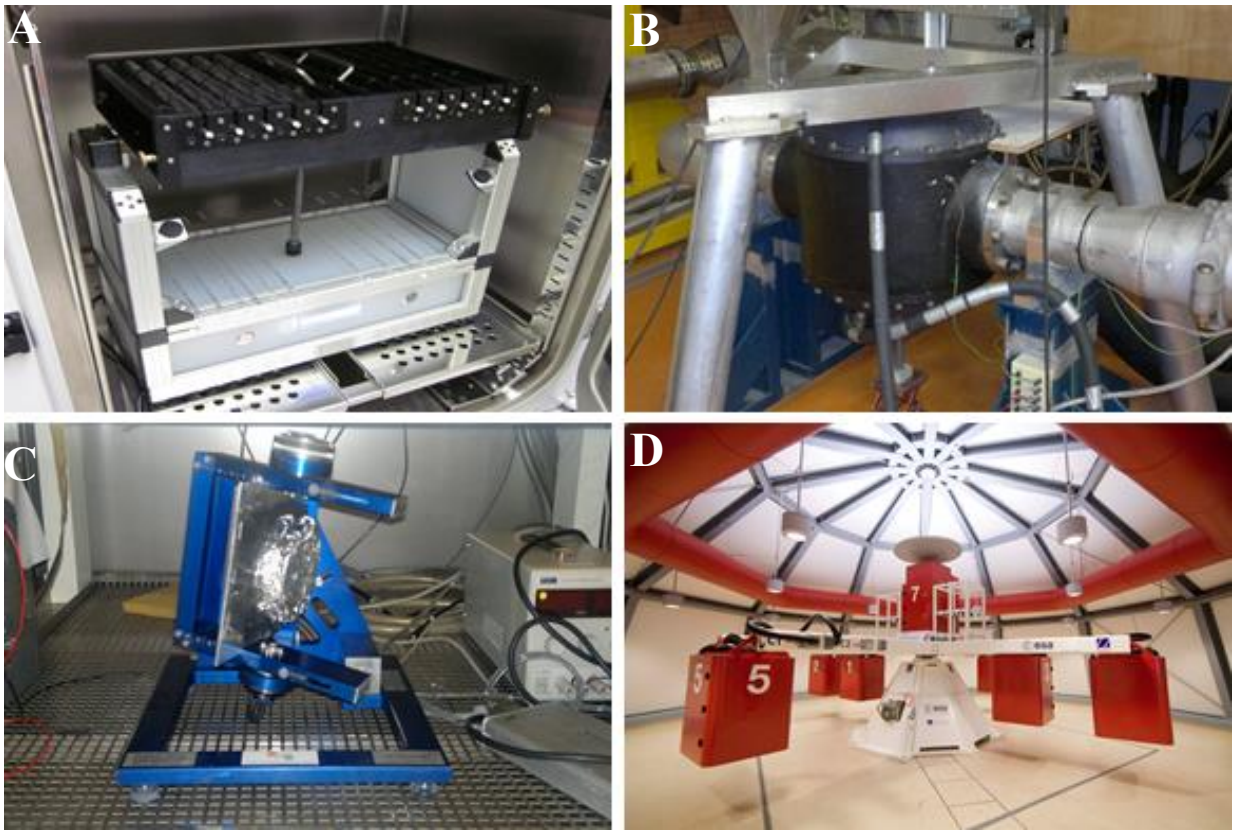

Figure 3: Several common ground based facilities (GBFs) used in plant biology research. A) 2D clinostat, located at German Aerospace Center (DLR), Cologne, Germany. **B)** Magnetic levitation facility, located at the HFML, Nijmegen, the Netherlands. **C)** Desktop RPM, **D)** LDC for hypergravity studies, both of them located at DESC/ESA-ESTEC, Noordwijk, The Netherlands.

Clinostats & RPMs. A clinostat is a device in which samples are rotated to prevent the biological system from perceiving the gravitational acceleration vector. Different configurations exist with respect to the number of rotation axes, the speed and the direction of rotation (Briegleb 1992, Hader et al 1995, Klaus 2001, Klaus et al 1997). Clinostat with one rotation axis, which runs perpendicular to the gravity direction, is called a 2D clinostat. Pipette 2D clinostat with a fast rotating clinostat (Clinostat mode **(Figure 4A)**) was used to achieve ¨functional weightlessness¨ for single cells (Briegleb 1992). By fast and constant rotation it is assumed that sedimentation is prevented physically by a continuous and constant change of the direction of the gravity vector by rotating the particles in small tube vertically. Particles are forced to move on circular paths according to the rotation speed and finally reach a non-sedimentation effect (Hemmersbach et al 2006, Klaus 2001).

Clinostats with two axes are called 3D clinostats, being the most commonly used the Random Positioning Machine (RPM) (3D Random Mode **(Figure 4B)**), in which the quality of simulation is increased by rotating around two axes following a randomized speed profile compared with a classic 2D clinostat, especially for large objects (Kraft et al 2000, van Loon 2007). These 3D systems have two independently rotating frames; both frames can be operated with different speeds and different directions (Borst & van Loon 2009). With random mode setting the individual frame speed and the rotation direction are randomly varied, resulting in an unpredictable and symmetrical path (Borst & van Loon 2009). Main limitation of this technology is sample size, since centripetal accelerations appear as long as we place the sample far from the rotation center, especially when using high rotation speed (van Loon 2007).

Centrifuges for Hypergravity Research: The Large Diameter Centrifuge (LDC). There are a large number of centrifuges available for the biological research community working on hypergravity environments. A Large Diameter Centrifuge (LDC) has been recently developed by ESA, allowing the acquisition of measurement points in the range from 1 to 20g. This instrument can indeed provide a stable hypergravity environment for fundamental research on cells, plants and small animals (van Loon et al 2005).

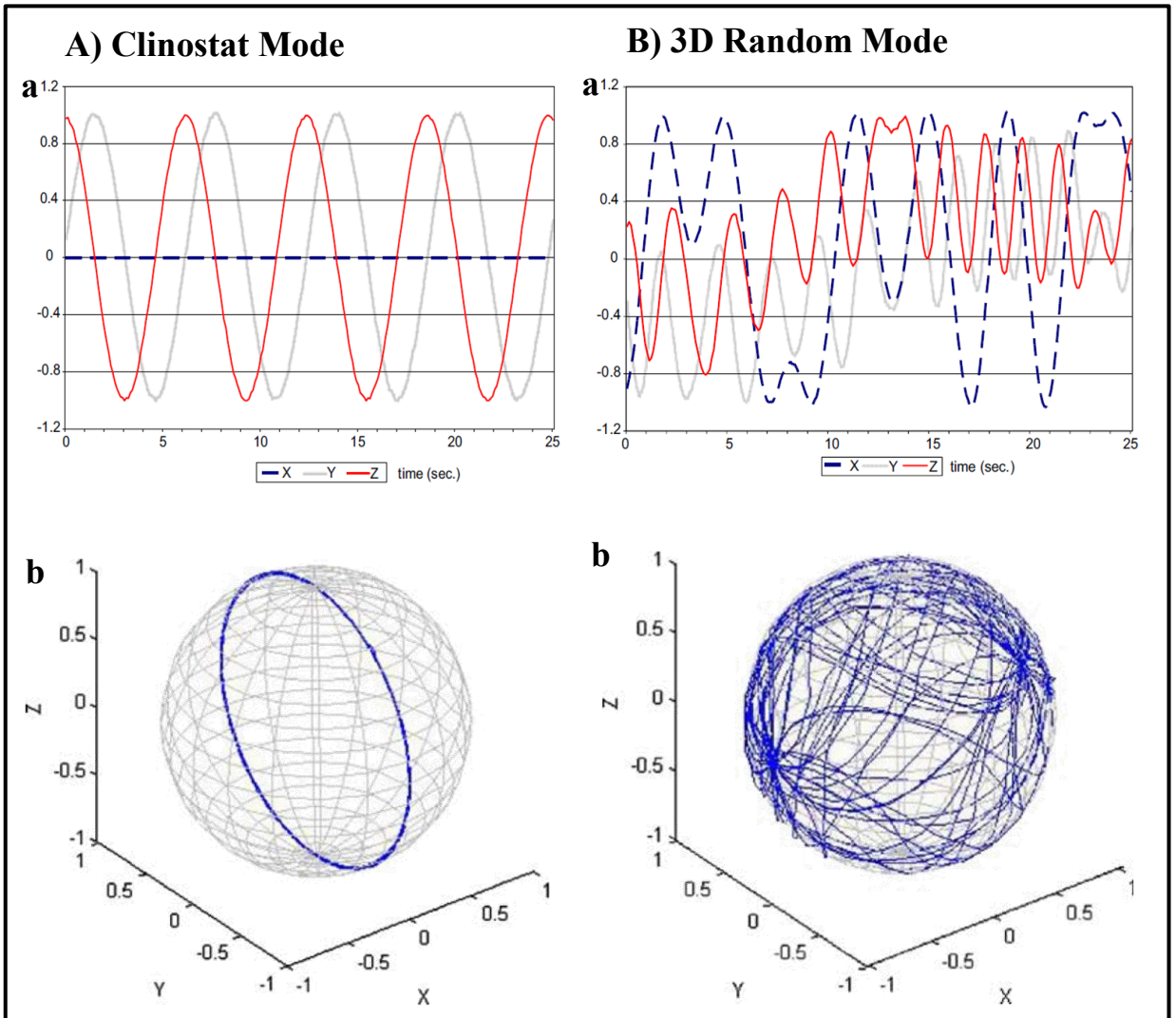

Figure 4: Basic RPM control Modes. A) Clinostat mode; a Gravity values in a standard clinostat mode. *Y* and *Z* are changing sinusoidal between +1 *g* and −1 *g*. **b** the clinostat mode results in a 2D motion trajectory, in this graph projected on an imaginary sphere. The abscissa in **a** as well as the three axes in **b** is accelerations expressed as '*g*'. Time displayed in seconds is displayed at the ordinate in **b. B) 3D Random mode; a** Gravity values measured on the RPM, rotated in random speed and random direction mode, the inner and outer frame rotate (in this example) are at a varying speed between 60–120"/s. It should be noted that most users apply a speed of ±60"/s for both frames. **b** Motion trajectory in random speed and random direction mode, displayed on an imaginary sphere. The abscissa in **a** as well as the three axes in **b** is accelerations expressed as '*g*'. Time displayed in seconds is displayed at the ordinate in **b.**

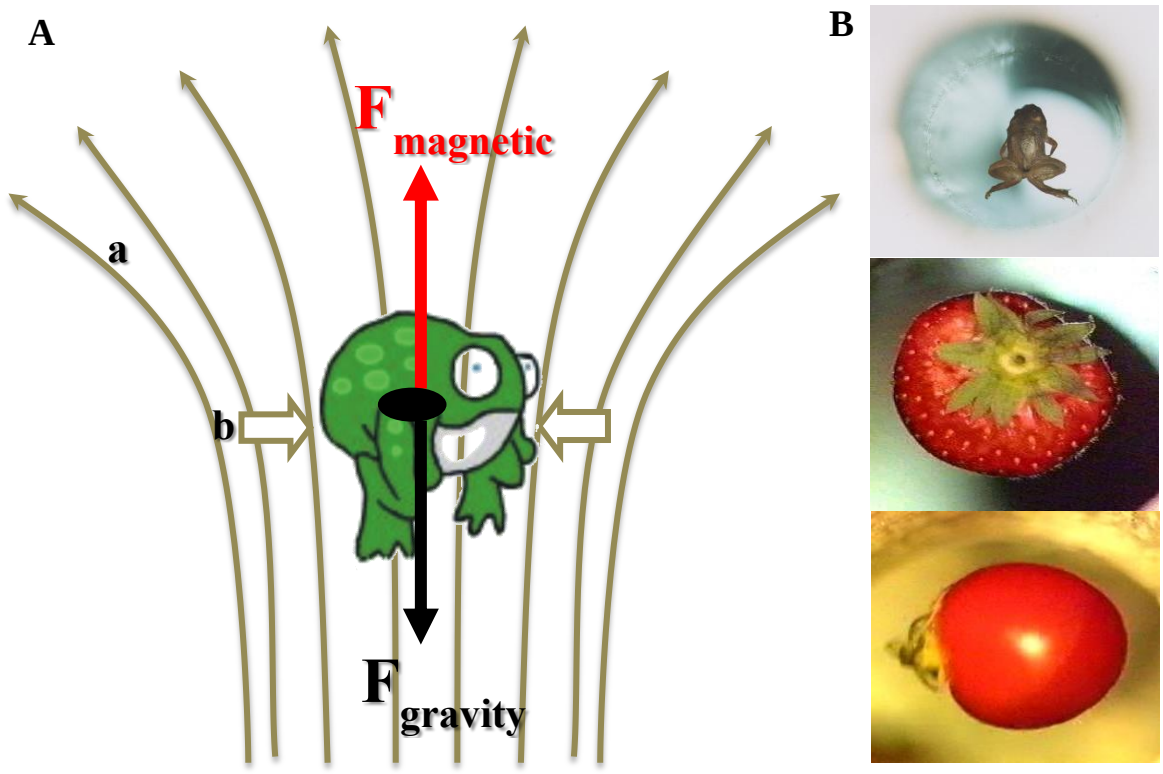

Figure 5: Magnetic levitation force to generate simulated microgravity: **A)** Magnetic levitation force affecting biological samples inside the magnet affecting with two forces, Magnetic force (**Red**) and in opposite direction Gravity force (**Black**). (**a**) refers to the magnet force lines, (**b**) Lateral stabilizing magnetic force. **B)** Some of the success levitated biological samples, Animals (frogs, flies) and plants (strawberry, grapes)

Magnetic Levitation. The phenomenon of levitation has attracted wide attention due to its peculiarity and potential applications. Among various types of levitation methods that have been invented, diamagnetic levitation is the most suitable for levitating large biological organisms (Berry & Geim 1997, Geim et al 1999). Placing a biological material in a strong magnetic field with a strong magnetic field gradient creates a diamagnetic force on the system (Brooks et al 2000, Ueno & Iwasaka 1997). Orienting this force against the gravitational force leads to the absence of any net force on the object, thus, levitation occurs **(Figure 5).** Adjusting the polarity of the gradient field can vary magnetic force.

The effective gravity acting on a diamagnetic body in the magnetic field is defined as the net force, that is, the sum of the gravitational (m·g) and magnetic force (F_m), per unit of mass.

$$F_m = xVB\frac{dB}{dZ}\mu_0^{-1}$$

where: X = Magnetic susceptibility, $\boldsymbol{B}$ = Magnetic field, $\boldsymbol{V}$ = Volume object, and $\boldsymbol{\mu_0}$= Constant.

For biological materials in the magnetic field, it is useful to calculate the effective gravity acting on water, assuming that water (a diamagnetic molecule) is the major component of the living matter and that magnetic susceptibilities of all tissues of interest are similar to that of water (Herranz et al 2013a). Thus, living beings can be levitated using an appropriate magnetic field. Indeed, magnetic levitation of frogs, flies, grasshoppers, *Arabidopsis* seedlings and other biological systems has been demonstrated (Guevorkian & Valles 2004, Hill et al 2012, Manzano et al 2013, Simon & Geim 2000, Valles et al 2005).

It is reported that such a strong magnetic field alone may have a significant effects on the behavior and development of living organisms (Glover et al 2007, Maret & Dransfeld 1985), inhibition of *Drosophila* oogenesis (Herranz et al 2012), altered the transcriptional *Arabidopsis* genome (Manzano et al 2012c). In addition, because diamagnetic levitation force depends on the magnetic susceptibility of the materials at the molecular level, together with reduced gravitational stress we can observe induced internal stresses within the cells. The extend of these secondary effects should be confirmed in each experiment (Berry & Geim 1997, Herranz et al 2013a)

2. CELL PROLIFERATION, CELL GROWTH & EPIGENETIC IN *ARABIDOPSIS THALIANA* MODEL SYSTEM

Arabidopsis thaliana has become the model system of choice in plant biology research, including space research. Some of the factors that have contributed towards its popularity include its short life cycle, completely sequenced genome, and the existence of a multitude of mutants and transgenic plants due to the available molecular biology tool box in this species. This is why *Arabidopsis* was chosen for recent space biology experiments examining fundamental questions on plant growth in microgravity (Clément & Slenzka 2006, Ferl et al 2002, Kiss 2000, Matía et al 2010, Medina et al 2010, Medina & Herranz 2010, Millar et al 2010, Paul et al 2012). *Arabidopsis* has also been used in our laboratory to understand cell growth and proliferation mechanisms under simulated microgravity (Herranz et al 2013b, Herranz & Medina 2014, Manzano et al 2012a, Manzano et al 2013, Matía et al 2010, Medina & Herranz 2010). Different types of *Arabidopsis* biological systems have been used in microgravity investigations including plant seedlings (Millar et al 2010, Paul et al 2013), root meristematic tissue (Manzano et al 2013, Matía et al 2010) and semisolid cell cultures (Herranz et al 2013c, Zupanska et al 2013).

2.1. IN VITRO PLANT CELL CULTURES, A POWERFUL TOOL IN SPACE BIOLOGY RESEARCH

Experiments on the effect of altered gravity on cell growth and proliferation have recently been extended on the use of *in vitro* plant cell cultures (Herranz & Medina 2014, Manzano et al 2012a, Manzano et al 2012c). As it occurs in root meristematic cells from seedlings, cultures are composed of a population of actively proliferating cells. The reason under the use of a specific biological system, such as seedling roots, in order to investigate the influence of microgravity on plant cell growth and proliferation is that they have a specific mechanism for sensing gravity, located in the statocytes of the collumela, at the root tip, containing amyloplasts which move according to the gravity vector and are capable of transducing this signal to other regions of the root by a mechanism affecting the transport of the phytohormone auxin. The known target of the transduced signal is the elongation (transition) zone, but the meristematic region has also been

shown to react to gravitational changes, being probably an additional target of the signal sensed at the root tip (Medina & Herranz 2010). On the contrary, non-differentiated cells from a cell suspension culture sense the gravity by an unknown mechanism, in a pure individual cellular response. Among various types of cell cultures, dispersed plant cell suspension cultures allow the study of cell division in the absence of developmental processes, by providing a homogeneous population of near-identical cells (Gould 1984). A cell suspension culture of *Arabidopsis thaliana* with a reported 4C DNA was used for the derivation of fast growing cell line MM2d (Menges & Murray 2002). MM2d consists of similarly small clumps of creamy-colored cells with fast growth and high density **(Figure 6).**

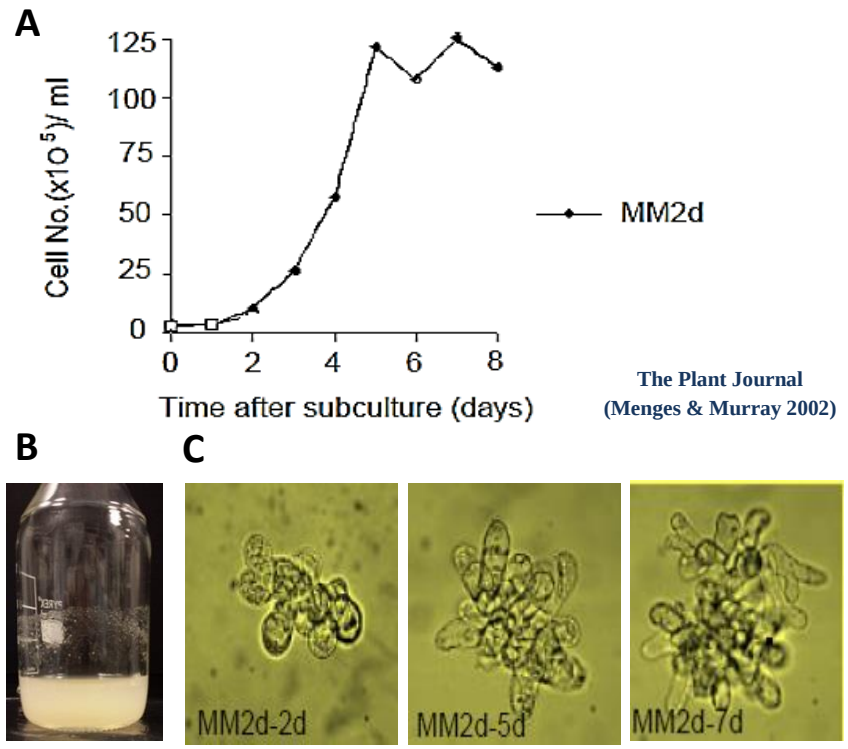

Figure 6: Growth characteristics of *Arabidopsis* cell line MM2d (Menges & Murray 2002). **A)** Early stationary phase for 7 days, cells were subculture, and cell growth monitored of cell line MM2d. **B)** MM2d cell suspension maintains after 7 days in dark conditions. **C)** Cell morphology of MM2d through the cultivation time 2, 5, and 7days.

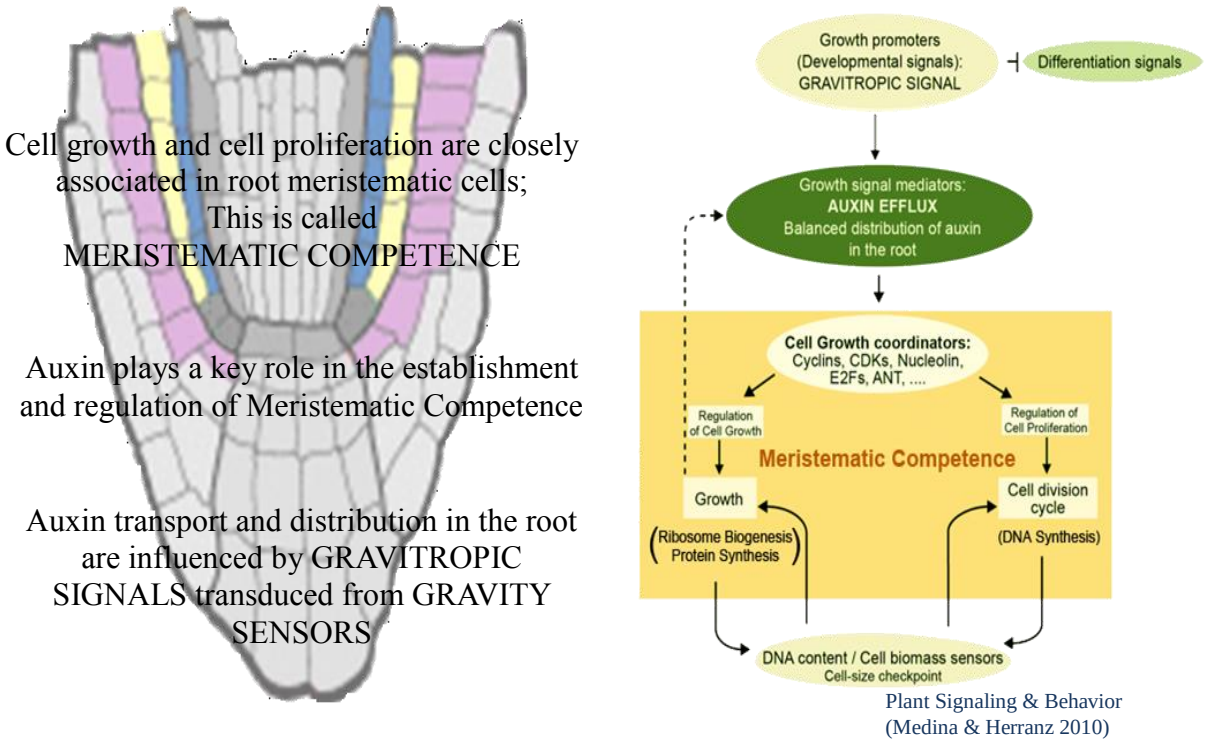

Figure 7: Model of actions and interactions leading to the maintenance of the meristematic competences (involving the coordination between cell growth and cell proliferation) specifically showing the players involved in the transduction of the gravitropic signal under normal ground conditions. Scheme is adapted and modified by (Medina & Herranz 2010) from (Mizukami 2001).

2.2. PLANT MECHANISMS POTENTIALLY DISRUPTED BY GRAVITY ALTERATION

Gravity plays a role in plant growth and development, and its alteration induces changes in these processes (Ferl et al 2002, Perbal 2001). These processes of growth and development affect the whole plant, but they rely on cellular mechanisms, including cell proliferation, growth and differentiation, which are basic and essential functions for the cell life, specifically in the root meristem, which constitute the supply of cells for the developmental processes. It is well known that signals transduced between different plant organs are capable of activating key modulators of cell growth and cell division in a coordinated manner, in meristems; the reception of these signals and the response to them is indeed called ¨*meristematic competence*¨ **(Figure 7)** (Mizukami 2001). The absence of gravity has been shown to result in the uncoupling of cell growth and cell proliferation, which are strictly coordinated under normal ground gravity conditions (Herranz & Medina 2014, Manzano et al 2012a, Manzano et al 2013, Matía et al 2010).

2.2.1. Cell Cycle Regulation in Plant Development

The cell cycle is one of the most comprehensively studied biological processes, particularly given its importance for growth and development; indeed, the role of the cell cycle machinery during development remains an important scientific challenge (Inze & De Veylder 2006). In contrast to animals, plant development is largely post-embryonic. New organs, such as roots, stem, leaves, and flowers, originate from life-long iterative cell divisions followed by cell growth and differentiation (Grafi & Avivi 2004, Steward et al 1964). Cell division therefore plays a role both in the development processes that create plant architecture and in the modulation of plant growth rate in response to the environment (Beemster et al 2002, Cockcroft et al 2000).

2.2.1.1. *Arabidopsis thaliana* Cell Cycle

The cell cycle encompasses four sequential ordered phases **(Figure 8)** that temporally distinguish the replication of genetic material from the segregation of duplicated chromosomes into two daughter cells. Lag or gap (G) phases therefore separate the replication of the DNA (S phase) and the segregation of the chromosomes (M phase, mitosis). The G1 phase (the first gap) intercedes between the previous mitosis and the entry into the next S phase, whereas the G2 phase separates the S phase from the subsequent M phase. Cells in G2 are therefore discriminated from G1 cells by possessing a double DNA content. The gap phases allow the operation of controls that ensure that the previous phase has been accurately and fully completed, and not surprisingly the major regulatory points in the cell cycle operates at the G1/S and G2/M transitions, which correspond to points of potential arrest as a consequence of evaluation of external conditions (Dewitte & Murray 2003, van´t Hof 1986). Differentiating plant cells often display an alternative cycle known as endoreduplication, characterized by an increase in the nuclear ploidy level that results from repeated S phases with no intervening mitosis (Joubes & Chevalier 2000). In all cases, endoreduplication appears to occur only after cells have ceased normal mitotic cycles (De Veylder et al 2001, Foucher & Kondorosi 2000).

2.2.1.2. Synchronous Cell Cycle Systems

The biochemical and molecular analysis of the cell division cycle is greatly facilitated in cell systems that allow populations of cells to be synchronized (Banfalvi 2008, Dolezel et al 1999, Harper 2005, Kumagai-Sano et al 2006, Lin et al 2012, Vassilev 2006, Zhang & Zou 2012).

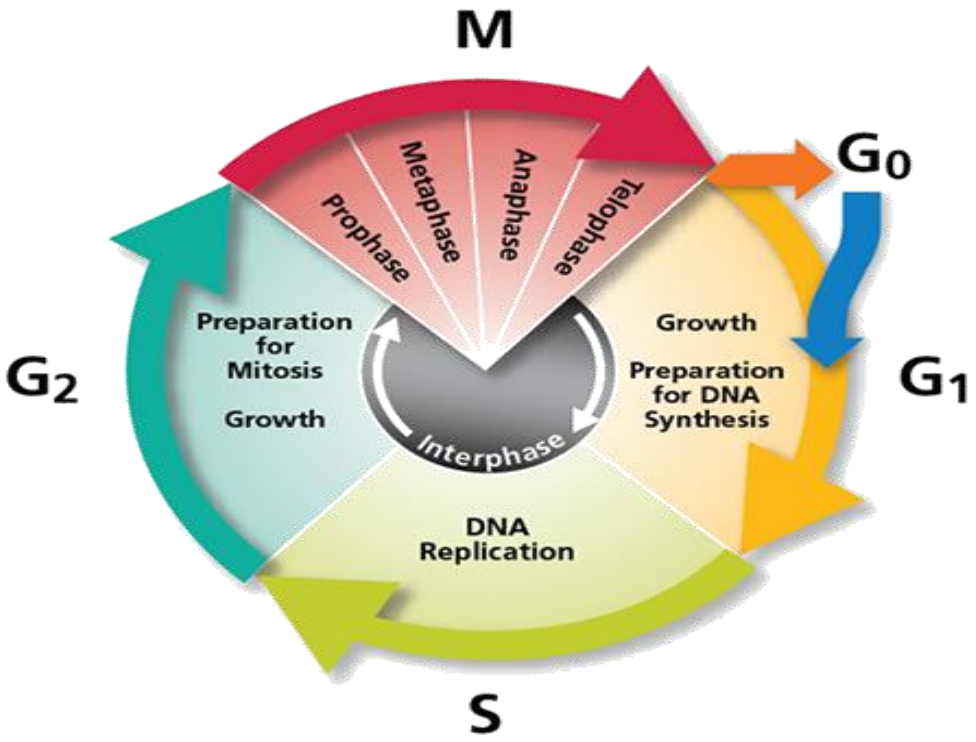

Figure 8: Schematic of the cell (division) cycle. Cell cycle consists of four essential phases, **G1** (Gap 1), **S** (Synthesis), **G2** (Gap 2), and **M** (Mitosis for cell division).

The most suitable systems for detailed analysis are *in vitro* suspension cultures of plant cells (Dewitte & Murray 2003). In such systems, cell division is removed from any developmental context. Ideally, all cells progress through the cell cycle at the same rate from the same initial starting point, and various procedures have been developed for different cultures that allow an approximation to this ideal. These procedures involve some method of accumulating cells at a specific point in the cycle, followed by the reactivation of cell cycle progression. The major approaches are the use of reversible inhibitors of specific cell cycle processes to block progression through the cycle, followed by release of the synchronized cells, and the removal and resupply of specific nutrients or other factors that may be combined with cycles of sub-culturing. The application of inhibitors to cell cycle studies has been reviewed (Planchais et al 2000); one of the agents of choice is the DNA-polymerase inhibitor Aphidicolin, which blocks cell cycle progression in early S phase (Matherly et al 1989, Menges & Murray 2006, Sourlingas & Sekeri-Pataryas 1996). However, rather few plant cell suspensions can be synchronized to a high degree except tobacco BY-2 cell line which is widely used in cell cycle studies (Nagata et al

1992, Samuels et al 1998). More recently, it has been reported that *Arabidopsis* cell cultures synchronized by means of Aphidicolin block/release are suitable for following both the re-entry of cells into the cell cycle and progression from S phase. Synchronization with Aphidicolin produced up to 80% S phase cells, with constitutes a clear separation of different cell cycle phases versus 60% of synchronization achieved by using sucrose starvation (Menges & Murray 2002, Menges & Murray 2006).

2.2.1.3. Cell Cycle Regulation

Any discussion on the role of cell division in plant development and growth requires a thorough understanding of the basic machinery that controls the cell cycle (Inze & De Veylder 2006). Eukaryotic cell cycle is regulated at multiple points, but all or most of these checkpoints involve the activation of a special class of serine-threonine protein kinases, which are functionally defined as requiring for their activity the binding to regulatory proteins known as cyclins, and are therefore named cyclin-dependent kinases (CDKs). Cyclins provide the primary mechanisms for control of CDK activity because the CDK subunit is inactive unless it is bound to an appropriate cyclin **(Figure 9)** (De Veylder et al 2007, Dewitte & Murray 2003, Inze & De Veylder 2006).

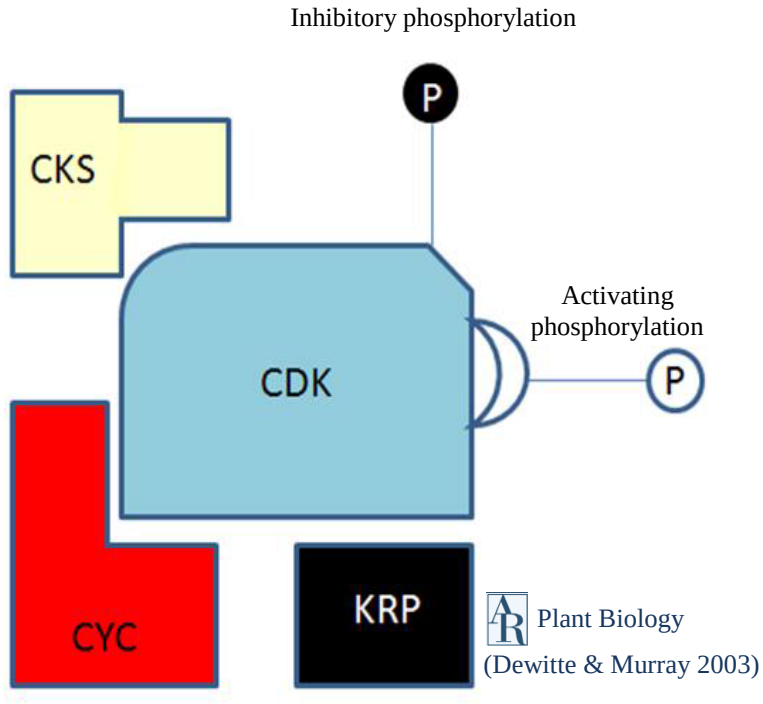

Figure 9: Cyclin-dependent kinase (CDK) activity is regulated at multiple levels. Monomeric CDK lacks activity until it complexes with cyclins (CYC) and activated by phosphorylation by CDK-activating kinase (CAK). Its activity can therefore be regulated by the abundance of the CDK or cyclin components through controlled transcription, translation, intracellular localization, or regulated destruction, or by the regulated activity of CAK. In addition, activity can be inhibited by phosphorylation by WEE1 kinases or the binding of inhibitor proteins such as Kip-related proteins (KRP). Inhibitors may block the assembly of CDK/cyclin complexes or inhibit the kinase activity of assembled dimers. CDK subunit (CKS) proteins scaffold interactions with target substrates (Dewitte & Murray 2003).

Cyclins. *Arabidopsis thaliana* genome encodes at least 32 cyclins with a putative role in cell cycle progression, *Arabidopsis* gene annotation identified 10 A-type, 11 B- type, 10 D-type and 1 H-type cyclins, in addition to 17 other cyclin-related genes which are classified in types C, P, L, and T (Torres Acosta et al 2004, Vandepoele et al 2002, Wang et al 2004). A-type cyclins generally appear at the beginning of S phase, are involved in S phase progression, and are destroyed around the G2/M transition (Dewitte & Murray 2003). B-type cyclins appear during G2, control G2/M transition and mitosis, and are destroyed as cells enter anaphase. All identified B-type cyclins were initially subdivided into two subclasses, CYCB1 and CYCB2 (Renaudin et al 1996), but the presence of a B-type cyclin gene in the *Arabidopsis* genome, which encodes for a B-type-cyclin-like protein without the typical B-type destruction box, was predicted and assigned to a third class, CYCB3 (Vandepoele et al 2002). D-type cyclins control progression through G1 and into S phase and differ from A and B types by generally not displaying a cyclical expression or abundance (Dewitte & Murray 2003, Renaudin et al 1996, Van Leene et al 2010). The levels of cyclins are generally determined by their highly regulated transcription as well as by specific protein-turnover mechanisms. A-and B-type cyclins possesses ¨*destruction boxes*¨ targeting their timely removal by the anaphase-promoting complex during early to mid-mitosis. D-type cyclins are conjugated to ubiquitin by an SCF complex and then subjected to proteasome degradation (Genschik et al 1998, King et al 1996).

Prolifera (MCM7). The *Prolifera* (*PRL*) gene in *Arabidopsis* encodes a homologue of the MCM proteins which plays a critical role in DNA replication initiation and cell proliferation (Springer et al 1995). Prolifera protein accumulates during the G1 phase of the cell cycle, and it is transiently localized to the nucleus. During mitosis, the fusion protein rapidly disappears, returning to daughter nuclei during G1 (Springer et al 2000). There are six MCM proteins (MCM2-7) that form one or more protein complexes which enter into the nucleus, bind to chromatin and regulate replication (Springer et al 2000). After forming the pre-replication complex (pre-RC) with other components, the MCM2-7 complex is activated by CDK/cyclin-dependent kinase to initiate DNA replication; this is accomplished by accurate cell cycle-dependent licensing control (Wei et al 2013). During late mitosis and early G1 phase, origin recognition complex, Cdt1, and Cdc6 are loaded at replication origins independently and then recruit the mini-chromosome maintenance MCM2–7 complex onto chromatin sequentially under

regulation of mitotic kinases (Lei & Tye 2001, Tye 1999). Then, the MCM2–7 complex is triggered into an active helicase at replication forks by concerted activity of Cdc7/dbf4 and cyclin E/Cdk2 at the G1-S transition. When cells enter into S-phase, the pre-RC is disassociated by high cyclin-dependent kinase (CDK) activity, which will cause destruction of selected pre-RC components, avoiding pre-RC re-binding onto chromatin to prevent DNA re-replication. Therefore, the substrates of each kinase complex are the key subjects to be investigated in detail for a comprehensive study of tight cell cycle regulation (Porter 2008, Tanaka et al 2007, Wei et al 2013). However, each MCM component functions differently in cell cycle regulation, it has been reported that, MCM7 is a substrate of Cyclin E/Cdk2 that phosphorylates MCM7 at Ser-121 and regulates its distribution in cells, a phosphorylation of MCM7 by Cyclin/CDKs plays an important role in S phase checkpoint activation as well as in the regulation of proper M phase progression (Blow & Dutta 2005, Wei et al 2013).

2.2.1.4. Cell Cycle Transitions and Progression

Different CDK-cyclin complexes phosphorylate a plethora of substrates at the key G1 to S and G2 to M transition points, triggering the onset of DNA replication and mitosis, respectively.

G1/S Transition. Control model **(Figure 10A)** has been proposed in which D-type cyclins are primary mediators of the G1/S transition and hence have a major responsibility for stimulating the mitotic cell cycle in the presence of growth factors such as sucrose, auxin, cytokinin, and brassinosteroids. Transcription of D-type cyclins is activated by extracellular signals and leads to the formation of active CDKA-CYCD complexes (Dewitte & Murray 2003, Francis 2007, Inze & De Veylder 2006). These phosphorylate and hence inactivate the Rb protein, so that it loses its E2F association and can no longer block the activation of E2F-regulated genes. E2F is then able to activate transcription of genes involved in S phase and other growth and cell-cycle processes (Chaboute et al 2002, De Veylder et al 2002).

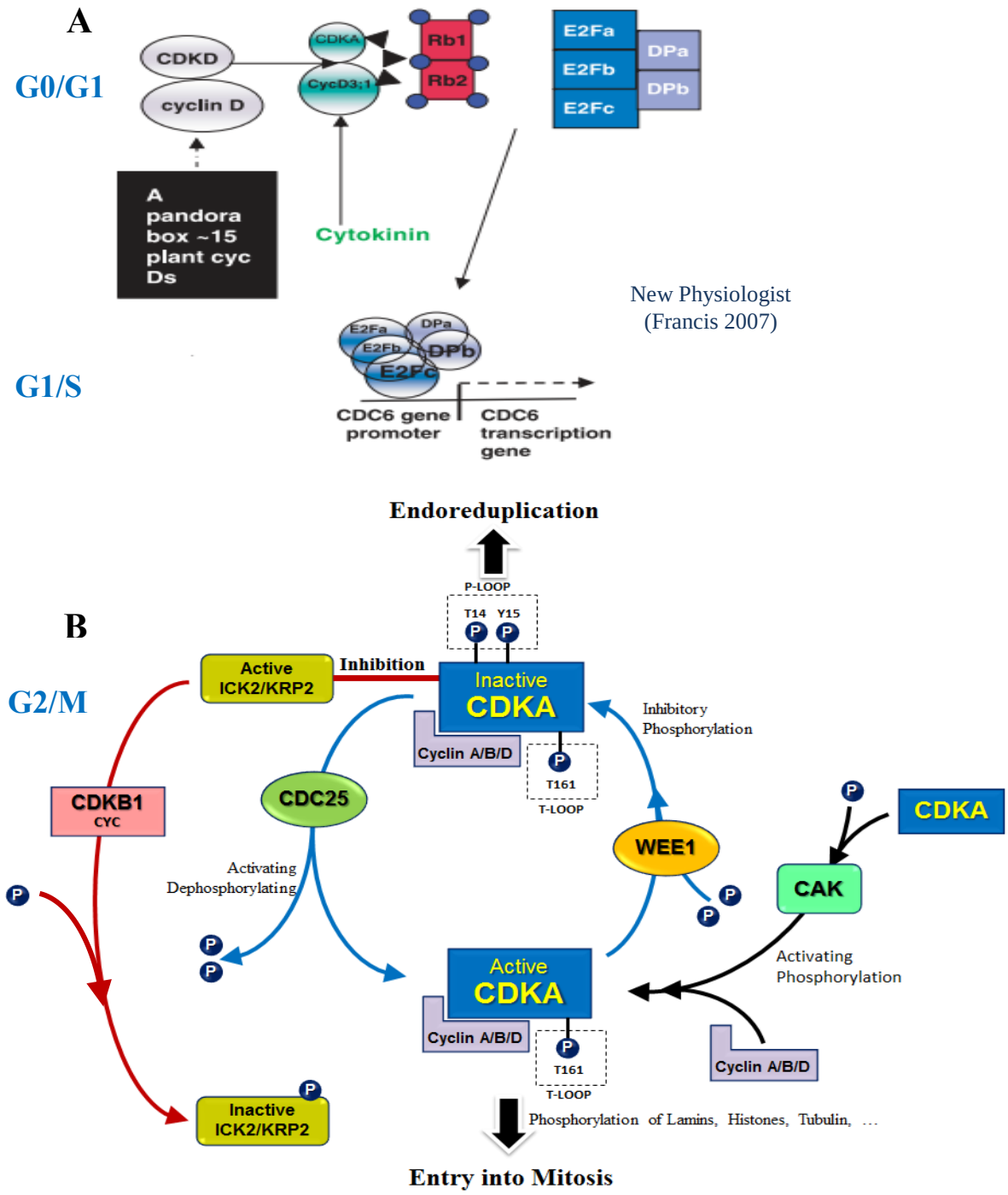

Figure 10: Different cyclin-dependent kinase (CDKs) and Cyclins regulate G1/S and G2/M transition points through cell cycle progression. A) At G1/S, CDKD/cyclin D phosphorylates CDKA enabling CycD3;1 to bind. A cytokine-induced transcellular induction culminates in CyCD3;1, which activates CDKA that, in turn, phosphorylates Rb1 and 2. This releases the E2F complex, which then induces the expression of S phase-specific genes (e.g. CDK6) (Francis 2007). **B)** G2/M transition is regulated by the activation/inactivation of complex CDKA/cyclins (A,B,D) where several theories of control, is identical to that of animals based on complex regulating CDK-CDC25-WEE1 or by CDKB activity. The activity of the CDKA–CYCD complexes can be inhibited by their association with CDK inhibitory proteins (ICK/KRP) that respond to stress stimuli or developmental signals (De Veylder et al 2007).

G2/M Transition. is controlled by the level of CDKA-CYC kinase activity **(Figure 10B)**, and inhibition of CDKs arrests cells in G2 and stabilizes the pre-prophase band (Binarova et al 1998). During the G2 phase of the cell cycle, cyclins of the A, B and probably D types (CYCA, CYCB, and CYCD) associate with both CDKs of the A and B type (CDKA and CDKB). Some B-type CDKs are under transcriptional control of the E2F pathway, properly providing a mechanism by which G1/S and G2/M transitions are regulated. Further regulation of CDK activity by both KRP proteins and inhibitory phosphorylation by WEE1 kinases is likely. Once the CDK/CYC complexes are active, they trigger the G2/M transition through the phosphorylation of a plethora of different substrates. The activity of the CDKA–CYC complexes can be inhibited by their association with CDK inhibitory proteins (ICK/KRP and SIM) that respond to stress stimuli or developmental signals (Churchman et al 2006, Verkest et al 2005b). Furthermore, the protein kinase CK2 shows discrete activity peaks at G1/S and M in tobacco BY-2 cells, and blocking its activity during G1 abolishes the G2/M checkpoint, resulting in premature entry into prophase; this is an evidence of links between G1 processes and G2 controls (Espunya et al 1999). Finally, exit from mitosis requires the proteolytic destruction of the cyclin subunits. This destruction is initiated by the activation of the anaphase-promoting complex (APC) through its association with the CCS52 protein (Dewitte & Murray 2003, Inze & De Veylder 2006).

2.2.2. *Arabidopsis* Cell Growth

2.2.2.1. Concept of *Arabidopsis* Cell Growth *VS* Cell Enlargement

The concept of cell growth in meristematic cells is meant for the production of cell biomass, essentially proteins. Therefore, specifically in these cells, cell growth is determined largely by the activity of the ribosome biogenesis and the protein synthesis (Baserga 2007, Bernstein & Baserga 2004, Bernstein et al 2007). Ribosome biogenesis occurs in a well-defined nuclear territory ¨*the nucleolus*¨ as a nucleolar activity structural marker. It should be stressed here that the strict connection of cell growth and nucleolar activity is not valid for cell types other than meristematic, actively proliferating. An increase of cell size may occur, for example, in cells experiencing differentiation processes, where it is common to observe large vacuoles increasing the cell size, but not connected with a high rate of protein synthesis, and therefore, a high nucleolar activity. When cell size increase is not connected to proliferation demands, we should refer to it, strictly speaking, as a process of cell enlargement, but not as cell growth (Doerner 2008, Li et al 2005).

2.2.2.2. The Nucleolus and Nucleolar Structure

Nucleoli are nuclear domains present in almost all eukaryotic cells. They were recognized as the ribosome-producing factories of the cell (Melese & Xue 1995). They not only specialize in the production of ribosomal subunits but also play roles in many other fundamental cellular activities. The nucleolus is a prominent nuclear organelle which morphologically expresses all functional steps necessary for the synthesis of ribosomes from transcription of rRNA genes to the assembly and maturation of pre-ribosomal particles and their transport to the cytoplasm. This process involves the transcription of the genes encoding rRNA as a single pre-rRNA molecule, and the processing of this molecule up to the assembly of mature rRNA species with specific ribosomal proteins (Sáez-Vásquez & Medina 2008).

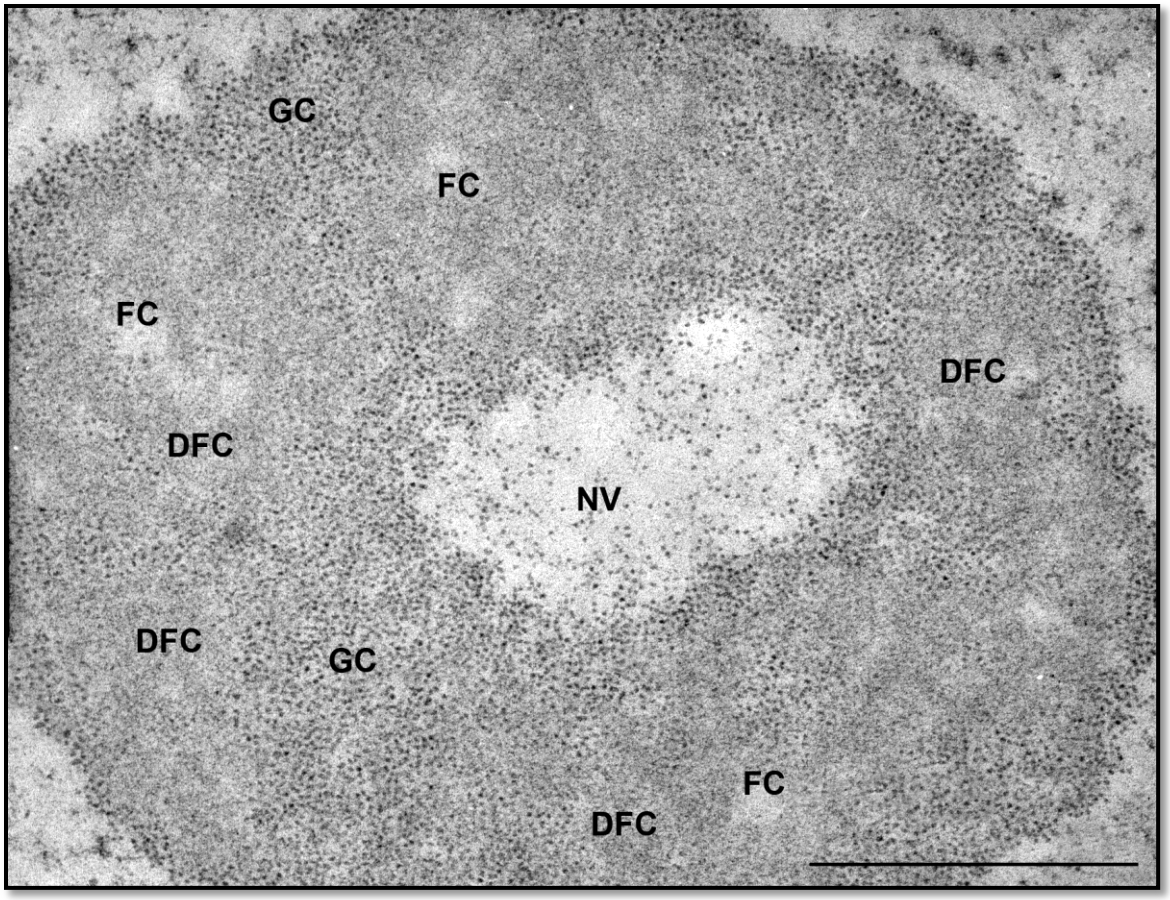

Figure 11. ***Arabidopsis thaliana*** **meristematic cells nucleolus structure.** Ultrastructure subcomponents is defined as: fibrillar centers (FC), dense fibrillar components (DFC), granular component (GC), and Nucleolar vacuole (NV). Scale bar represents 1µm. This ultrastructure image is obtained from (Pontvianne et al 2007).

Nucleolar Organization. Structurally, the nucleolus has some common basic components for all cell types, namely fibrillar centers (FCs), the dense fibrillar component (DFC), and the granular component (GC) (Goessens 1984, Shaw & Jordan 1995) **(Figure 11)**. The relative distribution of these structural components is highly variable, depending on the cell type, cellular activity and the cell cycle stage (Medina et al 2000, Sáez-Vásquez & Medina 2008, Stepinski 2014). For instance, the major component of an active nucleolus form plant meristematic cell is the DFC, and GC may be absent in very low active nucleoli (Medina et al 2000).

The Nucleolus during the Cell Cycle. It was verified that under normal physiological conditions, an increase in the rate of cell proliferation is accompanied by an increase in the biosynthesis of ribosomes (Baserga 1984, Hannan & Rothblum 1995). Therefore, the positive correlation between cell proliferation and the activity of pre-rRNA transcription and processing is the cause of alterations in the size of the nucleolus and in the distribution of the nucleolar components. Furthermore, cell cycle progression involves differences in the ribosome synthesizing activity, which can be detected as changes in the nucleolus morphology (Medina et al 2000). Different nucleolar structural models for proliferating plant root meristematic cells were proposed **(Figure 12)** (Gonzalez-Camacho & Medina 2006, Manzano 2011, Stepinski 2014); according to them, the nucleolar size is constant during G1, and S phases and it is doubled in G2. GC enlargement occurs in G2 phase as a consequence of an enhanced nucleolar activity (Hadjiolov 1985, Smetana & Busch 1974). On their part, FCs show a clear association with the cell cycle progression; the number of FCs increased by the progression of cell cycle, whereas, structurally, heterogeneous FCs (containing small condensed chromatin inclusions) are present in G1 and completely homogeneous (exclusively decondensed chromatin) in G2 nucleoli (Gonzalez-Camacho & Medina 2006, Medina et al 1983, Risueño et al 1982).

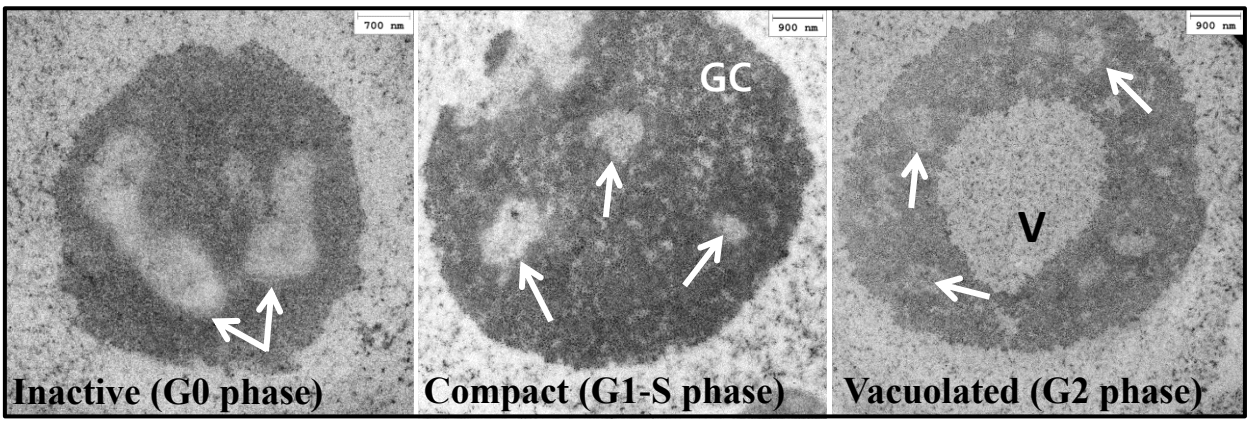

Figure 12. Nucleolar morphofunctional models in *Arabidopsis* semi-solid culture (callus). Three types of morphofunctional nucleoli (Inactive, Compact and Vacuolated) have been characterized by electron. Each morphological model shows a distinct amount and distribution of the nucleolar subcomponents, and can be associated with a differentiated level of nucleolar activity as well as, preferentially, with a period of the cell cycle (Manzano 2011).

2.2.2.3. Nucleolar Proteins: Their Role in Ribosome Biogenesis and Plant Development

The evolution of the nucleolus during cell cycle is associated with changes detected in nucleolar proteins. These proteins, are acting as targets of factors controlling cell proliferation and cell cycle progression, and at the same time, as regulators of the pre-RNA transcription and processing, thus confirming that the major function of the nucleolus is the ribosome biogenesis (Medina & González-Camacho 2003, Volkov et al 2004). Recently, 217 nucleolar proteins in *Arabidopsis* were found (Brown et al 2005), however, there are other stable and/or transitory unknown nucleolar proteins in plants.

Nucleolin. It is the major nucleolar protein of proliferating cells in eukaryotes. Nucleolin is one of the most abundant non-RPs in the nucleolus (Ginisty et al 1999). It plays a key role in the different steps involved in ribosome biogenesis, including RNA pol I transcription and processing of pre-rRNA (Roger et al 2003)., In plants, it is referred to as "nucleolin-like protein(s)", since the first description in onion cells, being localized in the nucleolus (Martin et al 1992). Nucleolin-like proteins have been cloned and characterized in *A. thaliana*, where two nucleolin-like genes *AtNUC-L1* and *AtNUC-L2* were reported (Kojima et al 2007, Petricka & Nelson 2007, Pontvianne et al 2007), in contrast to animals and yeast, where a single nucleolin gene is present. However, only the *AtNUC-L1* gene is ubiquitously expressed in normal growth conditions (Pontvianne et al 2007). Regarding the function of nucleolin, it was demonstrated that *Arabidopsis* nucleolin-like proteins play a major role in growth and plant development. *Arabidopsis* mutants displayed reduced growth rate, a prolonged life cycle, pointed leaves, and a defective vascular pattern (Kojima et al 2007, Petricka & Nelson 2007, Pontvianne et al 2007). In addition, it was suggested that nucleolin in *Arabidopsis* might be involved in auxin-dependent organ growth and patterning (Petricka & Nelson 2007), potentially indicating a way by which nucleolin may be controlling plant development. Expression of *AtNUC-L1* was reported to control growth and plant development by coordinating the expression of diverse factors involved in ribosome synthesis, including ROS and rRNA (Pontvianne et al 2007, Sáez-Vásquez & Medina 2008). Although nucleolin has been involved essentially in ribosome biogenesis, it has also been implicated in a number of additional processes that take place in the nucleus and in the cytoplasm, including RNA pol II transcription regulation, DNA replication, mRNA stability/translation and assembly of RNP complexes (Medina et al 2010, Sáez-Vásquez & Medina 2008). Furthermore, there exists a correlation of increased nucleolin-like protein

expression with the cell cycle and cell proliferation, in which, there is a relationship between the increase of the nucleolar activity, cell cycle progression, and the activity of the nucleolin-like proteins. In onion cells, variations of the nucleolin levels throughout the cell cycle have been investigated, and the highest levels have been found in G2 phase, the period characterized by the highest rate of pre-rRNA synthesis and processing (Gonzalez-Camacho & Medina 2006).

Fibrillarin. It is a key nucleolar protein in eukaryotes for pre-rRNA processing conserved from archaebacteria to vertebrates, located in the nucleolus (Barneche et al 2000, Schimmang et al 1989). Fibrillarin has been shown by various approaches to be involved in rRNA maturation (Cerdido & Medina 1995). It is associated with box C/D small nucleolar RNAs directing RNA methylation (Barneche et al 2000). It was found two genes encoding fibrillarins proteins were found in *A. thaliana*, namely *AtFib1* and *AtFib2* (Barneche et al 2000). Fibrillarin immunolocalization has consistently resulted in its detection in the nucleolar dense fibrillar component (DFC), and it is functionally homogeneous (Ochs et al 1985), and participates in different stages of the processing of pre–RNA (Cerdido & Medina 1995, Mougey et al 1993, Stanek et al 2000). However, the morphologically homogeneous localization of Fibrillarin in DFC may not be uniform in function (Cerdido & Medina 1995). Furthermore, with regards to the sub-nucleolar location of Fibrillarin and its levels during the cell cycle, available results show that the amount of Fibrillarin increases when nucleolar activity increases in G2 phase, and probably decreases when nucleolar activity decreases during differentiation (Cerdido & Medina 1995, Medina et al 2000, Sáez-Vásquez et al 2004).

2.2.2.4. Nucleolar Dynamics under Stress Conditions

The nucleolus is a very dynamic structure that may vary both in size and appearance, from one cell type to another, and also depending on transcriptional activity. There are several lines of evidence suggesting that the nucleolus has a role in sensing and responding to stresses (Boulon et al 2010). The varied effects on ribosome subunit production and cell growth induced by different types of cellular stress are often accompanied by dramatic changes in the organization and composition of the nucleolus (Mayer & Grummt 2005, Shaw & Brown 2012). Several stresses induced the nucleolar segregation in which the DFC and GC are subsequent separated with the formation of the nucleolar caps around the nucleolar remnant (Shav-Tal et al 2005). This

disruption on the nucleolar component is the consequence of alterations in the nucleolar activity and ribosome biogenesis. Microgravity conditions, taken as a stress, alter plant nucleolus structure and disrupt the nucleolar components; it was found that the nucleolar ultrastructure on microgravity-exposed cells, corresponded to that of a proliferating cell actively engaged in the production of ribosomes, but showing a smaller nucleolus with abnormal distributions of the nucleolar components (Matía et al 2010).

2.2.3. Epigenetic Regulation of Gene Expression: A Chromatin Perspective of Plant Cell Cycle Progression

Epigenetics is defined as the study of heritable changes in gene activity and expression that occur without any alterations of DNA sequence. It is known that these non-genetic alterations are tightly regulated by two major epigenetic modifications: chemical modification of the cytosine residues of DNA (DNA methylation) and of the histone proteins associated with DNA (histone acetylation). Functionally the patterns of epigenetic modifications can serve as epigenetic markers to represent gene activity and expression, as well as chromatin state (Bird 2007, Goldberg et al 2007). Chromatin unfolding involves the action of ATP-dependent remodeling complexes, covalent modifications of histone proteins, deposition of histone variants, or DNA methylation changes. These changes in chromatin status could have either positive or negative impact on gene expression (Jerzmanowski 2007, Kouzarides 2007, Zilberman 2008).

2.2.3.1. Chromatin Structure

Genomic DNA in eukaryotic cells is packaged with special proteins termed histones enabling protein/DNA complexes that constitute the chromatin. The basic unit of chromatin is the nucleosome, which is composed of ~ 146 base pairs of DNA wrapped around an octamer of the four core histones (H2A, H2B, H3, H4). The nucleosome structure is then compacted in turn into higher-order structures that comprise chromosomes. This organization of chromatin (with the additional participation of internucleosome histone H1) allows DNA to be tightly packaged, accurately replicated, and sorted as chromosomes into daughter cells during cell division (Luger et al 1997, Routh et al 2008). The degree of chromatin condensation is crucial in the regulation of accessibility and activity of the genome. Chromatin composition during different stages of the cell cycle is dynamic and regulated through multiple epigenetic mechanisms **(Figure 13)** (Groth et al 2007, Ruthenburg et al 2007).

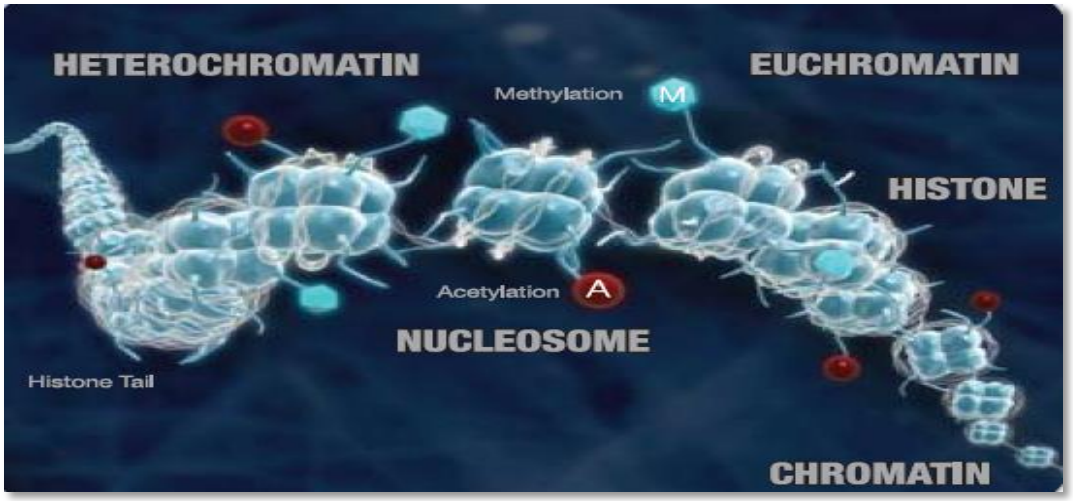

Figure 13: Basic epigenetic mechanism of chromatin organization. DNA associates with histone proteins packaged into chromatin to form high-order structures that comprise chromosomes. This composition of chromatin is crucial for regulation the accessibility and functions of the genome, and is controlled by epigenetic modification, such as DNA methylation and histone modifications. Figure from (ASBiosciences 2008).

In plants, a complex epigenetic network monitors the developmental state of the plant (Araki 2001, Blazquez & Weigel 2000), and this coordination is decisive for reproductive success. Several reports have demonstrated the correlation between epigenetic mechanisms such as DNA methylation and histone modification (Dennis & Peacock 2007, Henderson & Dean 2004). To understand the biological significance of epigenetic markers in the regulation of cell cycle progression, it is necessary to identify the distribution of DNA methylation and histone modifications (histone acetylation) among the different cell cycle phases.

DNA Methylation. DNA methylation, the first recognized and best characterized epigenetic modification, is linked to transcriptional silencing and is important for gene regulation and development; it refers to the addition of a methyl group to the cytosine base of DNA to form 5-methylcytosine (Esteller 2008, Jones & Baylin 2007). Three classes of enzymes are necessary for *de novo* and maintenance methylation. MET1 (DNA methyltransferase 1) and CMT1 (chromomethylase 1) contribute to the *de novo* cytosine methylation, and DRM2 (Domains Rearranged Methylase 2) plays a role in maintaining symmetric DNA methylation in *Arabidopsis* (Aufsatz et al 2004, Cao & Jacobsen 2002). The different phases of the cell cycle represent different physiological states of the cells and the gene expression programs adapt to them. It was reported that DNA methylation pattern varies during a single cell cycle, where the

global level of DNA methylation decreases in G1 and increases during S phase in HeLa cells (Brown et al 2007).

Histone Acetylation. Among the epigenetic mechanisms that alter chromatin to regulate gene expression, modifications of the nucleosome core histones (H2A, H2B, H3, and H4) is well studied. The amino terminals of the core histones are subjected to several types of multivalent modifications, including acetylation, methylation, phosphorylation, etc. All histone modifications are removable, which may therefore provide a flexible way for regulation of gene expression (Luo et al 2012a). The acetylation of histones was the first epigenetic modification connected with biological activity (Feinberg & Tycko 2004, Ruthenburg et al 2007). The lysine residues at the N-terminal tails of histones are subjected to reversible acetylation and deacetylation catalyzed by histone acetyltransferase (HATs) and histone deacetylases (HDACs), respectively. Acetylation removes positive charges and reduces the affinity between histones and DNA, thereby opening the condensed chromatin structure to allow easier access of transcriptional machineries to promoter regions; thus, histone acetylation is considered a reliable epigenetic regulator of transcriptional activation (Feinberg & Tycko 2004, Jenuwein & Allis 2001, Ruthenburg et al 2007).

RNA Polymerase II (pre-mRNA transcription) through Chromatin Remodeling. In eukaryotic cells, mRNA transcripts are synthesized from protein-coding genes by RNA polymerase II (Kadonaga 1998). Because of this, RNA pol II has been the focus of most studies of transcription in eukaryotes (Roeder 1996). Active RNA pol II is recruited to gene promoters during transcription initiation, in a process involving the modulation of the chromatin structure at promoter sites. The machinery that transcribes protein-coding genes in eukaryotic cells must contend with repressive chromatin structures in order to find its target DNA sequences. Chromatin decondensation facilitates access to DNA has been most widely studied for RNA polymerase II-mediated transcription of protein-coding genes, a process that requires rapid access to genes for the response to environmental signals and programmed cellular events, but the underlying principles are equally applicable to any process requiring interaction with DNA (Orphanides & Reinberg 2000, Sproul et al 2005, Wang et al 2014). Thus, remodeling of the local chromatin such as decondensed chromatin is associated with transcriptionally RNA pol II.

2.2.3.2. Chromatin Dynamics (Controlled by Epigenetics) during the Cell Cycle

Chromatin reveals as a highly dynamic and major player in cell cycle regulation, not only owing to the changes that occur as a consequence of cell cycle progression but also because some specific chromatin modifications are crucial to move across the cell cycle **(Figure 14)**. These are particularly relevant for controlling transcriptional activation and repression as well as initiation of DNA replication and chromosome compaction (condensation and decondensation) (Costas et al 2011, Sanchez et al 2008). Chromatin decondensation is typically associated with transcriptional activation. In the interphase polytene chromosomes it has been clearly shown that activation of particular genes gives rise to chromatin decondensation at the site of the gene, due to DNAse hypersensitivity assays within and beyond the transcriptionally active region (Callan 1986, Daneholt 1975, Muller et al 2001). A plethora of proteins affecting various aspects of chromatin dynamics has been shown to be essential for the regulation of cell proliferation and cell cycle progression, as a mechanism complementary to the oscillating activity of various complexes of cyclins and cyclin-dependent kinases (CDK). Furthermore, it was reported recently that core cell cycle regulators control gene expression by modifying histone patterns (Raynaud et al 2014). Due to the cell cycle demands, chromatin becomes locally decondensed during replication in S phase, increasingly condensed during G2 phase, maximized by the chromosomal structures which appear in mitosis, and decondensed again at the beginning of interphase in daughter cells. The decondensed state extends through G1 before G1/S transition, when histone acetylation is required for the specification and activation of replication origins. Chromatin condensation during mitosis is temporally associated with an increase in several histone modifications including histone phosphorylation (Costas et al 2011, Green et al 2011, Xu et al 2009). Another epigenetic mechanism by which chromatin organization is controlled is through DNA methylation. Heavily methylated regions of DNA are related to the chromatin activity. In an interestingly coordinated process, proteins that bind to methylated DNA also form complexes with proteins involved in deacetylation of histones. Therefore, when the DNA is in a methylated state, nearby histones are deacetylated (Phillips & Shaw 2008). Summarizing, compact, condensed chromatin has a disproportionately low content of acetylated histones, due to the lysine modifications and it contains a disproportionately large fraction of the nuclear content of methyl cytosine bases (DNA methylated).

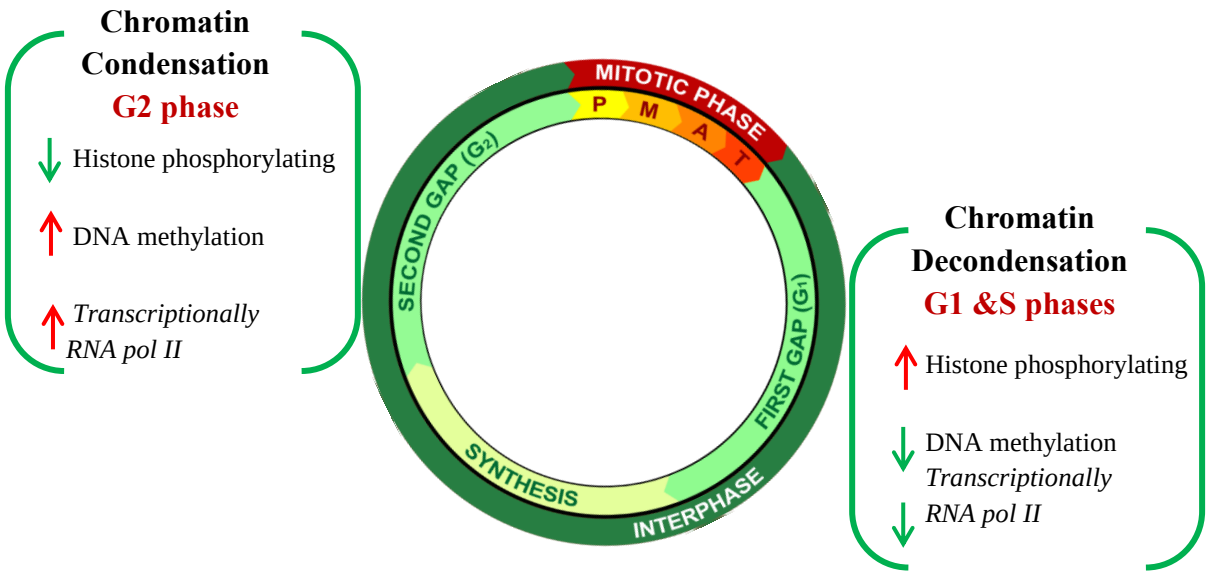

Figure 14: Chromatin modifications through cell cycle controlled by epigenetic modifications; DNA methylation and Histone Acetylation. Chromatin condensation and decondensation characterized by a determinant of transcriptional activity, involves enzymes for histone acetylation, DNA methylation, and RNA polymerase activity. Arrows refer to the activity (high (red), and low (green)).

2.2.3.3. Chromatin Modifications and Remodeling in Plant Abiotic Stresses Responses

The ability of epigenetic mechanisms to alter rapidly and reversibly the gene expression could be a key component of plant responses to environment cues (Jaskiewicz et al 2011, Luo et al 2012a). It was suggested that exposure to environmental stress could leave epigenetic marks in chromatin and keep the chromatin region in a permissive state that may facilitate quicker and more potent response to the environmental changes (Bruce et al 2007). Epigenetic mechanisms, such as histone modifications, may have decisive functions in the plant response to abiotic stresses. *Arabidopsis* cells show dynamic changes in histone modifications in response to high salinity and cold stresses, manifested by transient upregulation of H3 phosphoacetylation (Sokol et al 2007), suggesting that functionally related gene groups are regulated coordinately through histone modifications in response to abiotic stress in plant cells (Chen et al 2010). Recent reports have shown that environmental stresses altered methylation status of DNA and nucleosome histones modifications; salt and cold stresses induced hypomethylation of the coding sequences of stress responsive genes in tobacco, suggesting that the transcription of stress responsive genes might be controlled by DNA methylation (Wada et al 2004). The hypermethylation pattern is correlated with the stress dosage (Labra et al 2002, Labra et al 2004).

3. PREVIOUS RESULTS: GRAVITATIONAL FIELD VARIATION ALTERED *ARABIDOPSIS THALIANA* CELL PROLIFERATION AND GROWTH

Through 10 years, microgravity alteration on *Arabidopsis* had been investigated in our lab under the leadership of Dr. Francisco Javier Medina. Experiments performed on the real microgravity conditions in the International Space Station (ISS) using the spaceflight opportunity supporting form European Space Agency (ESA) and the National Aeronautics and Space Administration (NASA) projects. Complementary, experiments on ground based facilities (GBF project) were done, even to support the real microgravity results or to study additional scientific points not addressed yet in Space experiments. A description of those experiments it is provided in the following pages and summarized in **Table 1**.

3.1. *ARABIDOPSIS* SEEDLINGS: PLANT CELL PROLIFERATION AND GROWTH WERE ALTERED BY REAL MICROGRAVITY IN SPACEFLIGHT

Experiments performed on orbit ("Root" experiment, Cervantes Soyuz mission in 2003 to ISS) evidenced that, in root meristematic cells, the absence of gravity results in the uncoupling of cell growth and cell proliferation (Matía et al 2010, Matía et al 2007). Proliferation rate measured by counting the number of cells per mm was found to be higher in microgravity conditions. Cell growth, estimated by means of ribosome biogenesis rate, using the level of the nucleolar protein nucleolin, was depleted under microgravity conditions compared with the 1g control. However, the nucleolar size was significantly smaller in samples grown in space under microgravity conditions compared with the 1g ground control. Considering the amount and distribution of nucleolar components, microgravity disrupted the nucleolar components distribution; granular component (GC) and dense fiber component (DFC) compared with the 1g ground control. Finally, cell growth and proliferation, which are strictly associated functions under normal 1g ground conditions, appeared divergent under gravity absence: cell proliferation was enhanced, whereas cell growth was depleted (Matía et al 2010, Matía et al 2005).

3.2. *ARABIDOPSIS* SEEDLINGS: PLANT CELL PROLIFERATION AND GROWTH WERE ALTERED BY SIMULATED MICROGRAVITY & HYPERGRAVITY ON GBF

Experiments were performed using different ground based facilities, such as the Random Position Machine (RPM), Large Diameter Centrifuge (LDC) and Magnetic levitation instruments. It was found that growing seedlings on the RPM and the Diamagnetic levitator for simulated microgravity conditions showed similar trends as the spaceflight experiments. Seedlings were longer compared with the 1*g* control (increased the number of cells per mm as an indicator for the cell proliferation rate, compared with the 1*g* control). In addition to the regulation of cell cycle progression, determined by the expression of levels of cyclin B1 using the GUS reporter gene was disrupted, it showed a significant decrease altered by simulated microgravity. The same results indicated to depletion on the nucleolar activity and ribosome biogenesis (Manzano et al 2009, Manzano et al 2013, Matía et al 2010). Whereas, exposing *Arabidopsis* seedling to hypergravity (2*g*), both in the case of magnetic levitation and the Large Diameter Centrifuge (LDC) had less impact on plants than microgravity, as shown by the effects on cell growth and proliferation, which were quantitatively lower and with an opposite trend than those obtained in microgravity (Manzano et al 2012b, Manzano et al 2013).

3.3. *ARABIDOPSIS* SEMI-SOLID CELL CULTURES (CALLUS CULTURES): PLANT CELL PROLIFERATION AND GROWTH WERE ALTERED BY SIMULATED MICROGRAVITY

As a first attempt to use a cell culture model system to obtain large amount of proliferating materials, semi-solid non-synchronized cell cultures were tested. *Arabidopsis thaliana in vitro* callus cultures were used to validate the previous observations of the gravity effects on the cell growth and cell proliferation carried out on seedlings exposed to altered gravity environments. *In vitro* callus culture was exposed to different gravity levels (0*g*, 0.1*g*, 1.9*g* and 2*g*) using different ground based facilities (Magnetic levitation, RPM, LDC) (Manzano et al 2012c). Under microgravity, it was detected that, an increment of the cell proliferation rate was decoupled from a decreased cell growth and the opposite trend was observed under hypergravity conditions. Moreover, a morphofunctional nucleolar model was defined, as an easy and reliable indicator of

functional changes; increased frequency of the inactive nucleoli model under microgravity conditions (RPM) compared with 1g control in which the compacted nucleoli is the most common. In opposite to microgravity conditions, hypergravity was richer with compacted nucleoli. These results were coherent with an increase in nucleolar activity under hypergravity, associated with the nucleolar enlargement opposite to the microgravity response. Determined the cell cycle progression by the means of flow cytometry, it was found that, a significant changes in cultures grown under simulated microgravity, specifically an increase in the percentage of cells in S phase and subsequent increase of the G2/M population due to a highly significant decrease of G1 population. On the other hand, the hypergravity induced a slight increase in the S population and a decrease in the G2/M population. Genetic analyses were applied to validate the previous results using qPCR analysis; it revealed that, nucleolar activity related genes; Nucleolin and Fibrillarin were increased in both, simulated microgravity and hypergravity. Whereas the cell cycle regulated genes (CdkB1 and cyclin B1) were depleted influenced by microgravity conditions and increased under hypergravity (Manzano 2011). The overall gene expression was analyzed by the means of microarray analysis. Microarray analysis indicted that, changes in the overall gene expression of cultured cells exposed to altered gravity (Magnetic levitation, RPM, LDC) was observed; a significant effect, mainly on structural, abiotic stress genes and secondary metabolisms genes (Manzano et al 2012c). This effect was more extensive when both environmental stressors (partial gravity and magnetic field intensity) were magnified (0.1g* and 1.9g* samples).

Table 1: Summary of the results obtained in exposing *Arabidopsis thaliana* (seedling and cell cultures) to gravity alteration. (µ*g*) refers to real microgravity by the space flight. (Sim µ*g*) refers to simulated microgravity by the RPM. (2*g*) refers to the hypergravity by LDC. (*g) refers to the high energy magnetic field exposed samples.**

These results suggest that altered gravity is a serious stress on the plant cell, capable of uncoupling cell proliferation and cellular growth (loss of meristematic competence) in b in both, root meristematic cells and callus cultures.

Parameter (Plant seedling 4days)		**µ*g***	**Sim µ*g***	**2*g***	**Magnetic Levitation**		
					0*g**	**1*g****	**2*g****
Cell proliferation	Seedling and root length	**++**	**++**	**=**	**++**	**+**	**+**
	Cell proliferation rate (No. cells/mm)	**++**	**++**	**--**	**++**	**=**	**=**
	Cyclin B1 expression		**--**	**++**	**--**	**-**	**--**
Cell growth	Ribosome Biogenesis (Nucleolar Size and GC proportion)	**--**	**--**	**-**	**--**	**=**	**-**
	Ribosome Biogenesis (Nucleolin Levels)	**--**	**--**	**--**	**=**	**-**	**-**
Parameter (callus cultures)		**µ*g***	**Sim µ*g***	**2*g***	**Magnetic Levitation**		
					0*g**	**1*g****	**2*g****
Cell proliferation	Cell cycle alteration		**Yes**	**No**	**Yes**	**Yes**	**Yes**
	Cyclin B1 expression		**--**	**++**	**=**	**=**	**--**
Cell growth	Ribosome Biogenesis (Nucleolar Size)		**--**	**++**	**=**	**=**	**=**
	Ribosome Biogenesis (Nucleolin qPCR)		**++**	**=**	**=**	**++**	**=**

OBJECTIVES

Gravity is a key factor for life on Earth; gravity removal or alteration produces substantial changes in essential functions, such as cell growth and proliferation, which appear uncoupled under altered gravity, whereas they are strictly coordinated under normal ground gravity conditions. This gravity effect was detected in root meristematic cells from seedlings, where the mechanisms of gravity sensing and response involve different tissues and are mediated by the active transport of the phytohormone auxin. However, the identity and characteristics of the response to gravity of individual cells, whether or not they are differentiated, are not known.

Are individual undifferentiated cells sensitive to gravity alterations? And, if yes, Is the response depending on similar mechanisms to those operating in seedlings, or each individual cell has its own response mechanism?

The main purpose of the thesis is, therefore, to validate plant cell cultures *in vitro* as a model system in which neither specialized structures for gravity sensing nor signal transduction pathways are known to be present, in order to get a deeper understanding on the mechanisms operating at the level of individual cells in their response to gravitational stress affecting cell growth and cell proliferation, the basic essential functions of this cellular system.

This general objective could be achieved by fulfilling several specific sub-objectives:

1. To validate the readiness of the currently available ground based facilities (GBFs) to recreate an altered gravity environments compatible with the specific requirements of cell cultures (*Arabidopsis in vitro* cell cultures). We will particularly test the 2D Pipette clinostat and the Random Positioning Machine (RPM) as reliable simulators of microgravity, the Large Diameter Centrifuge (LDC) as generator of hypergravity, the magnetic levitation instrument as a device producing all gravity levels between 0*g** and 2*g**, and two systems using the RPM for generating conditions of partial gravity (intermediate g-levels between 0 and 1, especially those corresponding to the Moon and Mars gravity), namely the combined use of an RPM and a centrifuge (Hardware version RPM^{HW}) and the operation of RPM by specific dedicated software for this purpose (Software version RPM^{SW}).

2. To perform an exhaustive study of the alterations induced in the functions of cell growth and cell proliferation using selected GBFs considered optimal for the growth of cell cultures in an altered gravity environment, including:

    a. Precise determination of the cell proliferation status of the cell, i.e. the identification of changes in the duration of the cell cycle and of each one of its different phases under altered gravity conditions.
    b. Precise determination of the cell growth status as reflected by the protein biosynthetic activity, faithfully evaluated by estimating the status of the ribosome-producing machinery in the cell nucleolus. This will include the definition of the correlation of nucleolar activity with cell cycle phases by the analysis of changes in the nucleolar morphofunctional patterns throughout the cell cycle.

3. To perform a genome-scale analysis to unravel the specific alterations of biological mechanisms which are responsible of the global changes in cell proliferation /cell growth induced by altered gravity conditions. The analysis will be carried out at three levels:
    a. Proteomic level: Specific antibody-based techniques will be used to monitor the activity of key proteins previously known to be involved in altered gravity effects.
    b. Transcriptional level: Microarrays and qPCR will be used to monitor the expression of key genes previously known to be involved in altered gravity effects, and also to identify novel genes whose expression is found to be changed in the experimental conditions.
    c. Epigenetic level: Assays on the activity of chromatin-remodeling factors will be carried out to gain insights into the interaction and regulation of epigenetic modifications (histone modifications and DNA methylation) through the cell cycle, which appear under gravitational alteration.

4. To optimize the use of transgenic *in vitro* cultures in Earth-based or future space experiments under altered gravity conditions. The induction of transgenic callus containing fluorescence promoters will lead us to detect the gravitational alteration on the cells *in vivo* in future experiments, and, especially, to extend the use of the fluorescence microscope in the gravitational investigations on cellular systems, both in space and on Earth.

Material & Methods

Cell Culture
GBF
Microscopy

Flow cytometry
Microarray

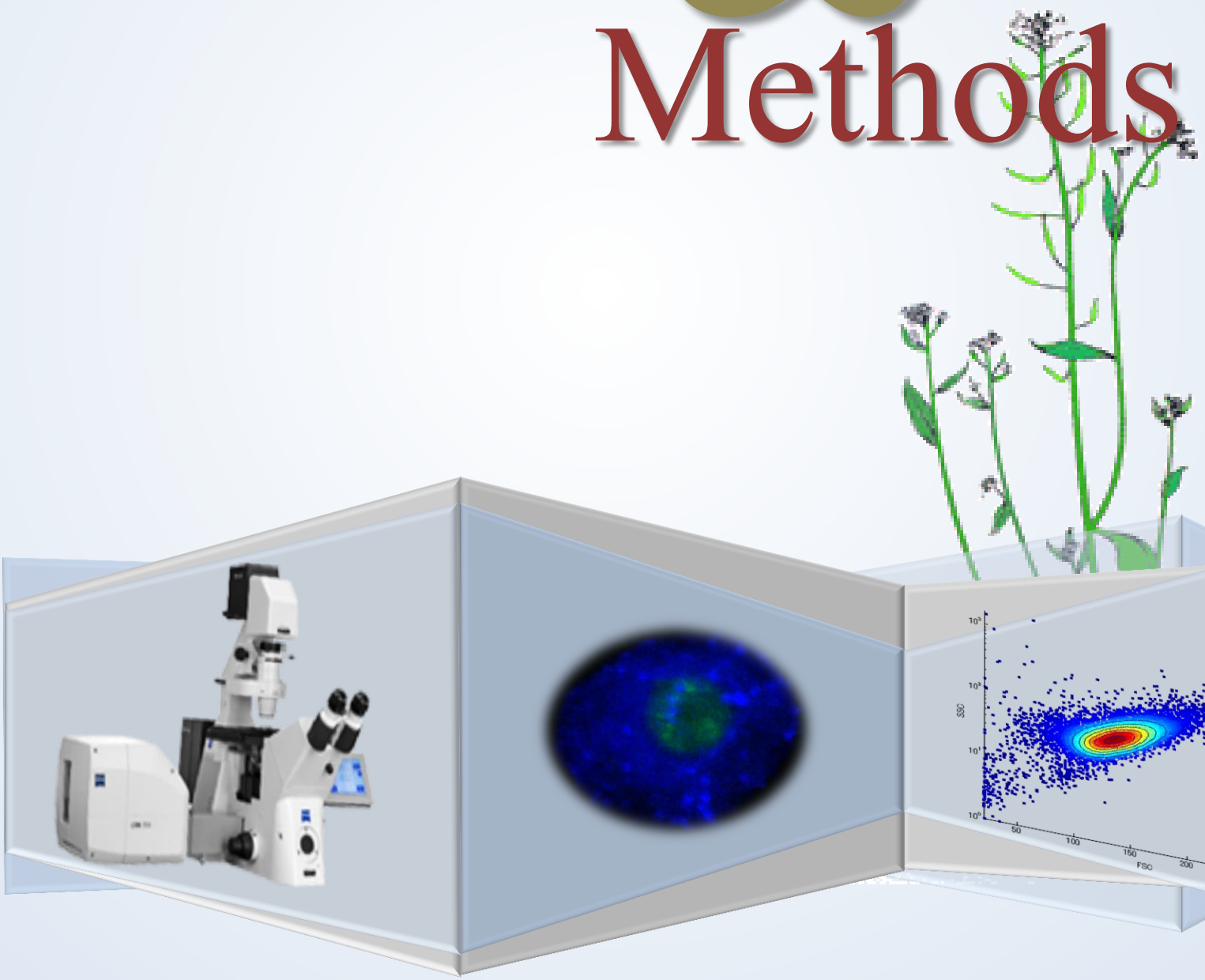

MATERIAL AND METHODS

1. *ARABIDOPSIS* CELL CULTURE TECHNIQUES

1.1. CULTIVATION OF FAST GROWING *ARABIDOPSIS* CELL SUSPENSION CULTURES (MM2D)

Arabidopsis thaliana cell suspension culture (ecotype *Landsberg erecta*), originally described by (May & Leaver 1993) and kindly supplied by us from Dr. Crisanto Gutierrez at CBM (UAM-CSIC) was the source material in most of the experiments described in hereafter. MM2d were grown in MSS medium (MS medium, Murashige and Skoog, Duchefa, The Netherlands), supplemented with 3% (*w/v*) sucrose and pH 5.8 (adjusted with 1M NaOH). This medium was autoclaved at 110ºC and stored at 4ºC for no more than two weeks before use, moment in which it is supplemented with 50 mg/l MS vitamins (Murashige and Skoog vitamin mixture, Duchefa), 0.5 mg/l NAA (α-naphthalene acetic acid, Duchefa) and 0.05 mg/l kinetin (Kinetin, Duchefa) sterilized by filtration using Minisart® filter unit.

Faster growing derivatives of MM2d cells were selected uniquely by subculture in MSS medium (1:20 dilution every 7 days in 250 ml Pyrex flask), under shaking and darkness conditions (120 rpm in an Excella^{TM} E24 shaker incubator, New Brunswick product by Eppendorf, USA) at 27°C (Menges & Murray 2006).

1.2. IMMOBILIZATION OF CELL SUSPENSION CULTURES BY EMBEDDING IN LOW MELTING AGAROSE

A procedure published by (Sieberer 2009) to immobilize cells in agarose to be used in spaceflight was adapted by us. MM2d cultures were sub-cultured (in a dilution 1:20) at the 7th day of the growth in a fresh MSS medium and kept in a sterile 50 ml Falcon tube in darkness. Low melting agarose (2% (*w/v*); gelling at 26-30ºC; SeaPlaque™ Agarose, BDH, Pool, UK) was dissolved in MSS medium in a sterile glass flask by boiling for 10 seconds in a microwave and

was allowed to cool down to 28-27ºC. The agarose solution was then mixed with an equal volume of the prepared cell suspension, resulting in a final concentration of 1% (*w/v*) agarose and a 1:40 dilution of cells in MSS medium.

After gentle mixing, 10 ml of agarose-cell mixture were poured into Petri dishes. After the agarose had solidified, Petri dishes were sealed with Micropore^{TM} tap. All steps were carried out at room temperature and under sterile conditions. Then it was kept in 27ºC in dark conditions according to each experiment design. Embedded cells in agarose were recoved at the end of each experiment as follow:

Fixed samples. Embedded cells in agarose were fixed by adding 1 ml of 4% (*w/v*) paraformaldehyde (PFA, Electron Microscopy Science, England) or 3% (*w/v*) glutaraldehyde (Glu, TAAB, England) in PBS buffer on to the surface of the plate for 1 hour. Fixative arrive to the cells by free-diffusion through the agarose. Fixed samples were washed with 1 ml PBS buffer for 15 min after the chemical fixation to prevent over fixation and the cytoplasmic extraction. The agarose including the fixed cells was transferred to 15 ml Falcon tubes and disolved by inmersion in a water bath at 63ºC untill disolved. Centrifugation of the disolved solution at 2500 rpm for 5 min is enough to recover the pellet of the fixed cells (without agarose) in order to use them in others protocols.

Frozen samples. Cells were fixed with 1 ml 1% (*w/v*) PFA for 15 min to stop the biological activity. Agarose were disolved at 63ºC using a water bath and cells were extracted by centrifugation and directly be frozen by inmersion in liquid nitrogen. The time to collect frozen samples was always less than 1 hour after the end of each experiment.

1.3. SYNCHRONIZATION OF IMMOBILIZED CELL SUSPENSION CULTURES

We used aphidicolin synchronization method described by (Menges & Murray 2006) to arrest cell cycle progression at the G1/S transition to obtain synchronic subpopulation of cells (Aphidicolin block/release):

1. 5 ml of MM2d cell suspensions (7 days old) was sub-cultured into 100 ml fresh MSS medium. It was incubated at 27ºC, 120 rpm in the darkness for 7 days to have an early stationary phase cell suspension. 20 ml of the cell suspension was transferred into 100 ml of fresh MSS medium (dilution 1:5).

2. Incubation with 4.16 µg/ml of aphidicolin (100 µl of a 5 mg/ml aphidicolin stock solution from *Nigrospora sphaerica*, Sigma added to 120 ml of diluted cell suspension) at 27ºC, 120 rpm in the dark for 24 hours. Aphidicolin was removed by filtering the cell suspension through a homemade sterile filtration unit (using nylon mesh 50µm). Cell suspensions were rinsed in 100 ml fresh MSS medium. Carefully swirl the beaker to wash the cells. Change the medium several times (use a total of 1L of MSS medium for 10 times) by simply lifting the filtration unit out of the glass beaker and discarding the washing solution. After 10 min rinse the cell suspension in 100 ml of MSS medium and vigorously swirl before pouring the cells from the filtration unit into a second sterile glass beaker. Cell suspensions were transferred into 50 ml Falcon tubes and were centrifuged at 1800 rpm for 1 min without braking applied. The washing procedure should not take more than 15 min in total.

3. Cell pellets were rinsed in 120 ml of fresh MSS medium (in a 300 ml Erlenmeyer flask) and were incubated following each experiment cultivation requirements. Take a T0 sample control directly after washing and hourly sampling according to the experimental conditions. A typical flow cytometry analysis (*see 2.1 later*) was used to check synchrony at different times once the aphidicolin block is released.

1.4. PRODUCTION OF TRANSGENIC SEMI-SOLID CELL CULTURES (CALLUS) FROM TRANSGENIC SEEDS

During the thesis we used *Arabidopsis thaliana* ecotype "Columbia" (Col 0) as our model plant species reference strain. Different transgenic plant lines containing different reporters were used:

- Line Col 0 wild genotype (wild type).
- Transgenic line CYCB1 Line:*uidA*, carrying a reporter gene "GUS" under the control of the promoter of cyclin B1(Ferreira et al 1994), provided by Dr. Eugenie Carnero-Díaz (University Pierre et Marie Curie, Paris VI, France).
- Transgenic line NUCL1:mGFP, carrying a reporter gene "GFP" under the control of the promoter of NUCL1 **(Figure 15)**, generated in our lab (Manzano 2011).
- Transgenic line CYCB1;1:mGFP, carrying a reporter gene "GFP" under the control of the promoter of CYCB1 **(Figure 15)**, generated in our lab (Manzano 2011).

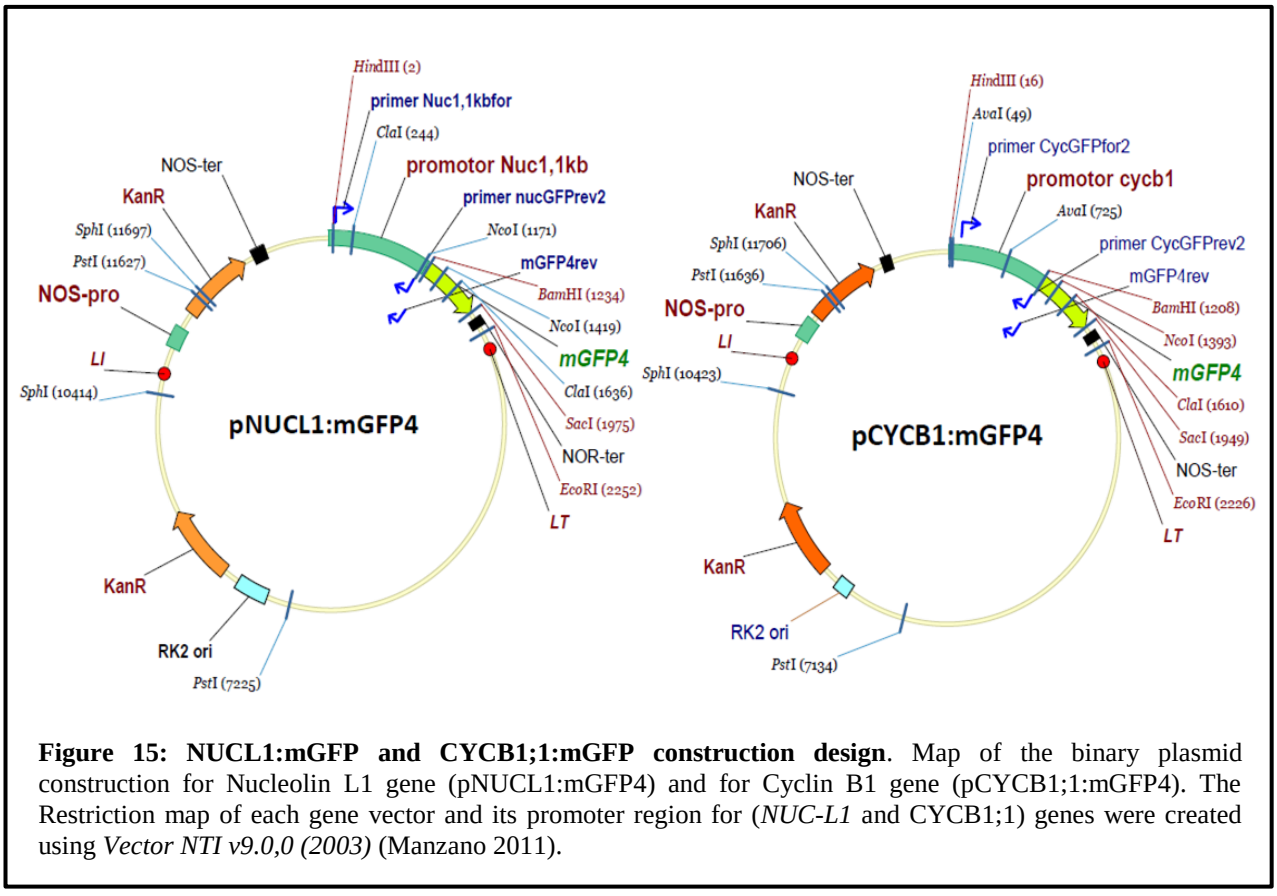

Figure 15: NUCL1:mGFP and CYCB1;1:mGFP construction design. Map of the binary plasmid construction for Nucleolin L1 gene (pNUCL1:mGFP4) and for Cyclin B1 gene (pCYCB1;1:mGFP4). The Restriction map of each gene vector and its promoter region for (*NUC-L1* and CYCB1;1) genes were created using *Vector NTI v9.0,0 (2003)* (Manzano 2011).

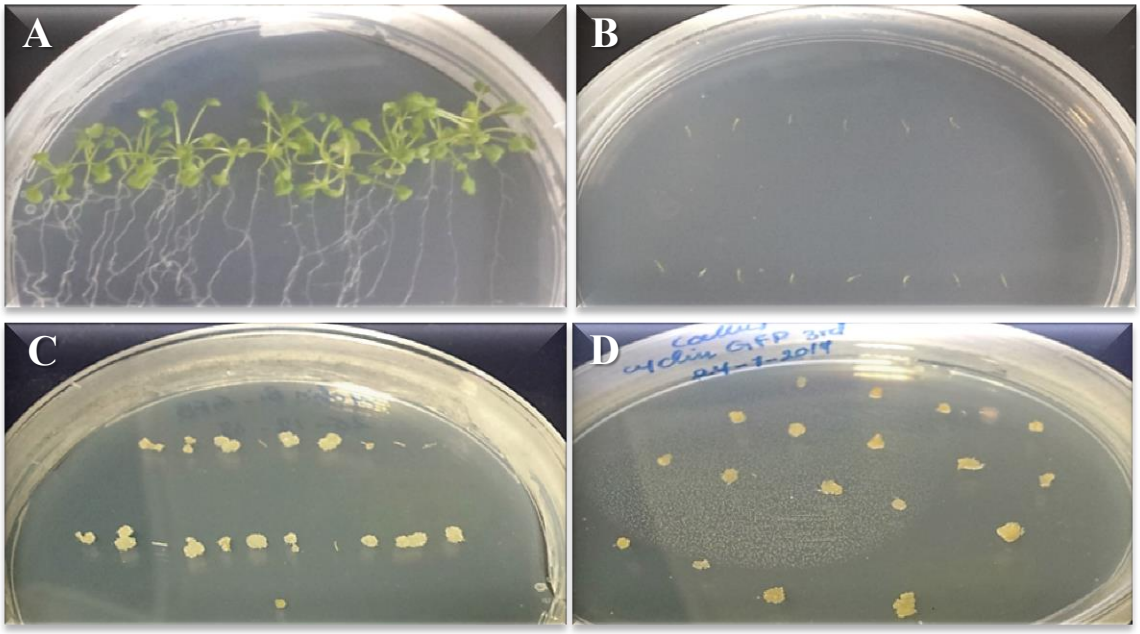

Figure 16. Callus induction from *Arabidopsis* seedling: **A)** *Arabidopsis* transgenic lines (AtNUC-L1;GFP, CYCB1;1;GFP or CYCB1:Gus) cultivation for 2-3 weeks. **B)** Transfer the hypocotyl cuts onto callus medium (about 2mm thick) and grow at (23°C 16h light/ 8h dark) for 2-5 weeks. **C)** After 2-3 weeks, callus should start to develop from the tips of hypocotyls. **D)** Transfer the callus onto new

***ARABIDOPSIS* SEEDLING CULTIVATION.** Seeds were sterilized with 1ml ethanol 70% and 1µl 100% Triton for 5 min. Then, seeds were washed with ethanol 90% for 3 times. Seeds were dried onto sterile paper and stored in sterile Eppendorf. Seeds germination was carried out in a sterile medium composed of Murashige and Skoog (MS Salt) with sucrose (10g/l), MES (0.5g/l) and 0.8% agar (*w/v*), pH was adjusted to 5.6 (1M KOH). Seedlings were grown at 22ºC, relative humidity of 80% and a photoperiod of 16/8 hours light/dark for 2-3 weeks up till the hypocotyl thick reach approximately 2mm.

CALLUS INDUCTION. Transfer the hypocotyl pieces onto a callus medium (MSS medium (MS salt (4.4g/l), 1ml MS vitamins, 300 µl NAA 1mg/ml, and 10g/l agar) supplemented with sucrose (0.9g/l)). After MSS medium was prepared and autoclaved at 110ºC, it was supplemented with 2 mg/ml Kinetin (stored always at 4ºC) at RT before the gelling occurs. The plate will remain in a growth cabinet (23ºC, 16/8h light/dark) for 2-5 weeks **(Figure 16).** During that time, we should transfer hypocotyl pieces onto a fresh medium every 5 days. In 2-3 weeks, callus should start to develop from the tips of hypocotyls. When it becomes more than 1 mm in size, callus was cut off from the hypocotyls and were transferred onto a fresh callus medium and stored at RT. Callus sub-cultures was carried out every one week to initiate new callus cultures.

2. MICROSCOPY TECHNIQUES

2.1. PREPARATION OF SAMPLES FOR ULTRASTRUCTURAL ANALISIS (TRANSMISSION ELECTRON MICROSCOPY (TEM))

The preparation of samples for electron microscope requires five steps: Fixation, dehydration, resin embedding, validation of embedding in semithin sections (optical microscope) and preparation/Staining of slides for TEM.

Sample Fixation. Fixation is the first and most important step in any EM study. For the nucleolar ultrastructure studies, cells were fixed using 3% (*v/v*) glutaraldehyde in PBS for 2 hours at RT. And for immunecytochemical studies for EM, cells were fixed using 4% (*v/v*) paraformaldehyde in PBS for 2 hours at RT. Cells should pipetted and rinsed in the fixative during the fixation period. Fixed cells were washed twice with PBS for 5 min at RT.

Dehydration. Cells were dehydrated through a series of methanol (GLU fixation) /ethanol (PFA fixation) **(Table 2)** at RT as follow:

Table 2: Dehydration process protocols used in fixative sample preparation for microscopic analysis

***Note:* *Methylation-acetylation method* is described by (Testillano et al 1995, Testillano et al 1991). Fixation and dehydration was continued until 70% by the method described below. Later, continued dehydration with 100% methanol (3 washes of 30 min each) and the samples were left overnight in a solution of methanol-acetic anhydride 5:1 (*v/v*) at 25ºC. The following day they were washed three times with 100% methanol for 30 min each.**

Paraformaldehyde fixation		Glutaraldehyde fixation	
30% ethanol	30 minutes	**30% Methanol**	30 minutes
50% ethanol	30 minutes	**50% Methanol**	30 minutes
70% ethanol	30 minutes / overnight	**70% Methanol**	30 minutes
90% ethanol	1 hour	**90% Methanol**	30 minutes
100% ethanol	3x 1 hour changes	**100% Methanol**	3x30min changes

Resin Embedding. Cells were treated a resin infiltration using a mixture dilution of the LR White resin (London resin, EMA, England) and ethanol (1:2) for 2 hours at 4ºC, and then with a dilution (2:1) for 2 hours at 4ºC. Fresh pure resin will be added to embed the cells, and will be refurbished twice a day for 2-3 days at 4ºC. Samples will be filled into gelatin capsules with fresh pre-polymerized resin. Samples inside the capsules will polymerize for 22 hours at 62ºC.

Validation of Resin-Embedding under Optical microscopy. In order to perform an optical microscopy structural study and to locate the proper zone for ultrastructure study, we performed semi thin 2 microns thick on the blocks included in LR White visualized by phase contrast microscope coupled with a Leica DM2500 CCD digital camera Leica DFC320. The images obtained were processed for quantitative studies programs QWin Standard image analysis (Leica Microsystems) and Image *J2.0* (*imagejdev.org*). When it came to continue the study to electron microscopy, selected area on a pyramid are carved with "Pyramitome LKB 11800" to then ultrathin sections on a ultramicrotome "Reichert Ultracut E", which were mounted on nickel grids coated Formvar film (TAAB).

Staining for Electron microscope. All samples displayed a stained electron microscopy previously for 30 min in uranyl acetate 5% (*w/v*) and lead citrate 0.3% (*w/v*) for one minute and a half. Between the two treatments and ultimately washed in distilled water. Samples were observed on a transmission electron microscope JEOL 1230 at 100kV acceleration voltage. Images taken were digitized and were processed for quantitative studies with image analysis programs: Qwin Standard (Leica Microsystems) and Image *J 2.0* (*imagejdev.org*).

2.2. IMMUNOFLUORESCENCE CONFOCAL MICROSCOPY TECHNIQUE

A number of techniques are based in the use of specific antibodies in combination with secondary antibodies chemically conjugated to fluorescent dyes such as fluorescein isothiocyanate (FItC). Immunofluorescence (IF) based on pioneering work by (Coons & Kaplan 1950) had been widely used both in research and clinical diagnostics, applications include the quantification and subcellular localization of specific proteins in cell suspensions, cultured cells or tissues. The labeled antibodies bind indirectly using secondary antibodies to amplify the detection of the antigen of interest through fluorescence techniques. The fluorescence can then be visualized “in situ” by confocal microscopy and even quantified in single cells by using a flow cytometer (*see Methods 3*). Immunofluorescence techniques using specific antibodies for staining particular areas in the cell are an important tool for demonstrating both the presence and the subcellular localization of an antigen, especially by an image analyzer. Immunofluorescence protocol can be divided into four steps: cell fixation, specific hybridization with first and secondary antibody, confocal laser scanning and images evaluation.

Cell Fixation. Fresh cells were rapidly fixed using 4% PFA in PBS for 1 hour at room temperature. Fixed cells were washed twice with PBS with a centrifugation at RT (5 min, 2000 rpm). Cell wall was digested with 898 µl enzyme digestive cocktail (2% cellulose + 1% Pectinase + 0.05% Macerozime + 0.4% D-Manitol), 100µl 10% glycerol and 2µl 0.2% Triton X-100 for 30 min at 37ºC. Cells were washed twice with 898 µl PBS, 100µl 10% glycerol and 2µl 0.2% Triton X-100 with a centrifugation at RT (5 min, 2000 rpm). Cells were dehydrated with 100% methanol and then squashed onto 0.1% poly-L-lysine coated multi-well slides (Teflon printed slides, ES-239W, Electron Microscopy Sciences, England). Slides were stored at -20ºC until required.

Use of Antibodies. Cell staining against particular proteins involves incubation of cell preparations with primary antibody. Unbound primary antibody is removed by washing, and the bound antibody is detected using a fluorochrome-labeled secondary antibody. During our experimental analysis for the immunofluorescence techniques, several specific antibodies were used in order to study different proteins expression under the experimental conditions. The primary antibodies were used, generally, in a dilution 1:1000, while the proper secondary antibody linked to the fluorochrome Alexa 488 in a green fluorescence (FITC) was used in a dilution 1:100 as shown in **Table 3.** Dried samples recovered from the -20ºC freezer will be hydrated with PBS twice for 5 min. Cells were incubated with block solution (PBS + 0.05 % Tween + 2% BSA) for 30 min at RT. Incubate cells with the primary antibody over night at 37ºC. Cells were washed with PBS (3x5min) to remove the primary antibody (*the number of washes depend on the type of the antibodies* **(Table 3**). Negative controls were prepared by omitting the primary antibody.

Cells were incubated with the secondary antibody for 3 hour at 37ºC, and then washed with PBS (3x5min) to remove the unspecific binding signal. DNA was labelled with 1µl DAPI staining for 5 min at RT. Samples were washed twice with PBS (2x5min) and H2Odd (2x5min). Coverslips were placed under PVA-DABCO™ (a glycerol based mounting medium containing an anti-fading reagent for use with immunofluorescence preparations) and invert onto glass slides.

Table 3: List of the specific antibodies used in the Immunofluorescences bases-analysis with the references and its dilutions in the blocking solutions.

Note: Dilution percentage is equal in all the antibodies (1:1000) in primary and (1:100) in secondary antibodies except 5mdc (1:25) for DNA methylation and AcH4 (1:50) for histone acetylation. Thus the number of washing should be increased to 5 times more in these two antibodies compared with 3 times in the rest of the antibodies.

Protein of interest	Specific antibodies	
	Primary (1:1000)	**Secondary (1:100)**
Nucleolin L1	Rabbit polyclonal Ani-AtNUC-L1 (1:1000) Provided by Dr. Julio Sáez Vásquez	Anti-Rabbit (Alexa 488-Green)
Fibrillarin	Mouse monoclonal Anti-Fibrillarin (1:1000) Abcam, ab4566, Cambridge, UK	Anti-Mouse (Alexa 488-Green) (Alexa 568-Red)
Cyclin B1	Goat polyclonal anti B-like cyclin (1:1000) Santa cruz, sc-12859, Texas, USA	Anti-Goat (Alexa 488-Green)
Prolifera	Goat polyclonal anti Prolifera (1:1000) Santa cruz, sc-12853, Texas, USA	Anti-Goat (Alexa 488-Green)
RNA polymerase II	Rabbit monoclonal anti RNA polymerase II (1:1000) Abcam, ab5408, Cambridge, UK	Anti-Mouse (Alexa 488-Green)
DNA methylation	Mouse Monoclonal Anti 5-Methylcytidine (1:25) Eurogentec , BI-MECY-0500, Belgium	Anti-Mouse (Alexa 488-Green)
Histone Acetylation	Rabbit Polyclonal Anti acetyl-Histone H4 (1:50) Milipore, Cat.# 06-866, Temecula, USA	Anti-Mouse (Alexa 488-Green)

Confocal Laser Scanning and Image Analysis. Confocal laser microscopy scanning was performed using Leica TCS SP5 with AOBS (Acousto Optical Beam Splitter, Mannheim, Germany) with 63X oil immersion optics. Laser lines at 488nm (Green) and 561nm (Red) for excitation of GFP and TxR (x-Ray system) were provided by an Ar laser and a DPSS laser. Detection ranges were set to eliminate crosstalk between fluorophores. Images were analyzed using Leica LAS AF, image analysis software *v2.4*.

2.3. QUANTITATIVE COLOCALIZATION ANALYSIS OF MULTICOLOR CONFOCAL IMMUNOFLUORESCENCE MICROSCOPY IMAGES

Colocalization is detected by correspondent antibodies with different excitation spectra when staining of antigens visualized in different colors overlaps. Although observation of colocalization does not provide a direct proof, it provides a solid support for there to have a common structure and/or similar functional characteristics (Swaney et al 2006, Tsutsumi et al 2006). Colocalization can be explained as an existence of the signal at the same pixel location when examination multi-channel fluorescence microscopy images (Zinchuk et al 2007).

How Colocalization Analysis is Performed. **(a)** Make sure that your chosen fluorophores have well separated excitation and emission spectra. **(b)** Using the same protocol of immunofluorescence (*see 3.2*), in additional to put the both primary antibodies (AtNuCL1 + Fibrillarin) with the proper concentration with blocking solution (1: 1000) in the same moment. It was incubated at 37ºC overnight. Secondary antibodies were added (Alexa 488 (green) for AtNuCL1 and Alexa 647 (Red) for Fibrillarin) at the same moment with the proper concentration with blocking solution (1: 100).

Colocalization Quantifications and Estimations. Colocalization is estimated using specially developed algorithms which calculate a number of respective coefficients, which colocalization can be evaluated quantitatively using Leica LAS AF, image analysis software *v2.4*. These coefficients use different approaches to evaluate colocalization and have different sensitivity and applicability (Zinchuk et al 2007):

a) **Pearson´s correlation coefficient** is one of the standard measures in pattern recognition:

$$R_r = \frac{\sum_i (S1_i - S1_{aver}).(S2_i - S2_{aver})}{\sqrt{\sum_i (S1_i - S1_{aver})^2}.\sum_i (S2_i - S2_{aver})^2}$$

where *S1* represents signal intensity of pixels in the channel 1 (AtNuCL1 (green)) and *S2* represents signal intensity of pixels in the channel 2 (Fibrillarin (Red)); $S1_{aver}$ and $S2_{aver}$ reflect the average intensities of these respective channels. It is used for describing the correlation of the intensity distributions between channels.

It takes into consideration only similarity between shapes, while ignoring the intensities of signals. Its values range between −1.0 and 1.0, where 0 indicates no significant correlation and −1.0 indicates complete negative correlation.

b) Colocalization coefficients m1 and m2 describe contribution of each one from two selected channels to the pixels of interest:

$$m_1 = \frac{\sum_i S1_{i,coloc}}{\sum_i S1_i} \qquad m_2 = \frac{\sum_i S2_{i,coloc}}{\sum_i S2_i}$$

where $S1_{i,coloc}$ represent the intensity colocalization for channel 1 and $S2_{i,coloc}$ represent the intensity colocalization for channel 2. For example, if the Green-Red pair of channels is selected and *m1* and *m2* are 1.0 and 0.2, respectively, this means that all green pixels (100%) colocalize with red pixels, but only 20% of green pixels colocalize with red ones. The value of 1.0 for both channels indicates perfect colocalization.

2.4. COMPLEMENTARY OPTICAL MICROSCOPY TECHNIQUES

Trypan Blue Viability TEST. Trypan Blue staining was used to discriminate between live (blue stained) and dead cells (unstained). A cell sample was diluted in Trypan Blue dye of an acid azo exclusion medium (Trypan Blue, LONZA) by preparing a 1:1 dilution of the cell suspension using a 0.4% Trypan Blue solution. Cells were counted under the optical microscope to determine the cell viability rate (stained-living cells/total cells).

Sample Processing for GUS Staining Analysis. For GUS analysis, samples were fixed in 90% acetone at −20°C for 24 hours. Samples were washed with 100 mM phosphate buffer. The GUS signal was revealed by enzymatic reaction (5 mM potassium ferrocyanide and ferricyanide, 100 mM phosphate buffer and 40 mM XGlc) in the dark. Callus samples were washed and mounted on 8 mm 8-well slides and observed with optical Leica microscope. Images were recorded digitally using a Leica CCD camera and were processed using the Image J 2.0 (imagejdev.org) software packages. The integrated optical density (IOD) was calculated from the stained area multiplied by the Optical Density (OD) in blue light.

3. FLOW CYTOMETRY AND OTHER CELL CYCLE ANALYSES

3.1. DETERMINATION OF INDIVIDUAL CELL DNA CONTENT *(% OF CELLS IN G PHASES*)

Frozen samples (500 mg cells pellet) were treated with the High Resolution Kit for plant ploidy level analysis (Kit Cystain UV precise P; type P containing ***solution A*** (Nuclei extraction buffer) and ***solution B*** (Nuclei staining buffer containing DAPI), Partec GmbH, Munster, Germany) to determine the DNA content for each individual cell using flow cytometry approach. To release cell nuclei, cells were carefully chopped with a sharp razor blade in 300 µl of ***solution A***, and then incubate for 2 min at 4ºC.

Extracted nuclei solution were filtered prior to addition of 600 µl ***solution B*** (in our case using *Arabidopsis thaliana*, it required to add also 10µl DAPI staining solution (1µg/µl) to increase the efficiency of the staining buffer due to the small *Arabidopsis* genome) (Menges & Murray 2006) using a nylon mesh (50µm) at 4ºC in dark conditions (samples could be stored in this conditions overnight before the sample count).

On average, 10000 particles were counted by flow cytometry approach (Cell sorter FACS Vantage, Becton-Dickinson, San Diego, California) equipped with an argon ion laser tuned at 360 nm and detection of emission using a blue fluorescence emission filter (band pass filter of 424/44 nm Ban Pass).

FACS analysis results will be analyzed using BD CellQuest™ software for windows XP to determine the ratios of cell cycle phases according to the DNA content of individual cells (2n for phase G1, 2<n<4 for S, 4n for G2/M phases) **(Figure 17A)**.

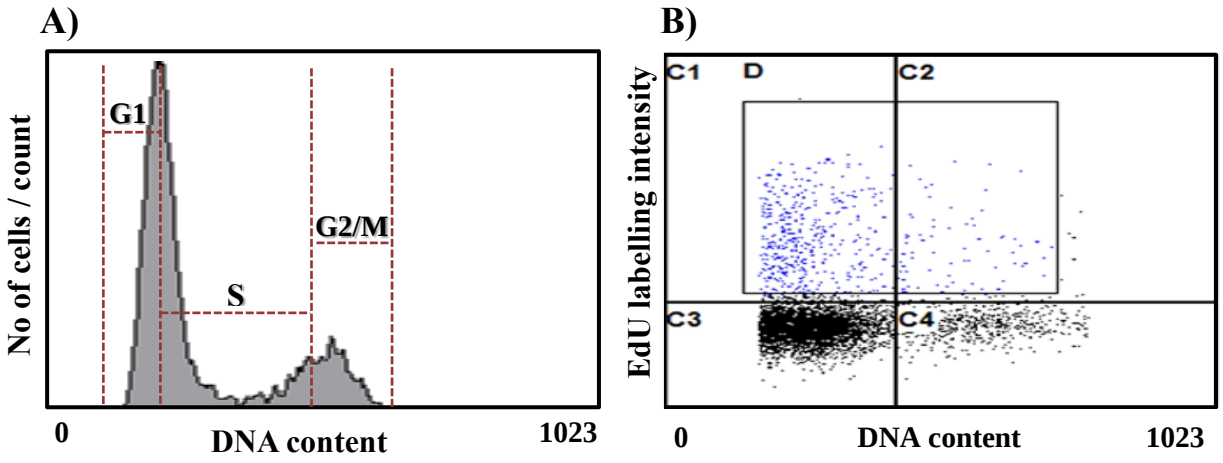

Figure 17: Cell cycle analysis protocols using Flow cytometry approach using BD CellQuest™ software. A) Cell cycle phases determination according to the DNA content (DAPI staining). Each panel represents the relative number of cells according to the DNA content in each cell. First peak (2n) reveals that G1 phase and the second peaks (4n) reveal that G2/M phase the rest of the DNA content (100%) refer to cells in S phase (which is manually estimated). **B) Cell cycle analysis with EdU assay staining using flow cytometry.** Biparametric dot-plot analysis of EdU labelling intensity (Alexa Fluor 488) (logarithmic scale) versus DNA content (DAPI staining intensity). Vertical line to differentiate cells in different cell cycle phases (C1/C3 = G1 and C2/C4= G2/M) and the horizontal one is to determine the background level and the labelled cells which represent the S phase. Background signal (Unspecific signal) was sited (C3, and C4). Labeled cells sited in **Blue**, and the Non-labeled cells in **Black**. Scatter D represents all cells labeled with Edu.

3.2. EDU LABELLING: EDU-BASED PROLIFERATION ASSAY (% OF CELLS IN S PHASE)

EdU (5-ethynyl-2'-deoxyuridine) is a method for detecting and quantifying newly synthesized DNA. EdU is a nucleoside analog of thymidine and is incorporated into DNA during active DNA synthesis (Buck et al 2008). Detection of the incorporated EdU with Alexa Fluor® azide, is based on a click reaction between EdU and azide modified dye. EdU assay is fully compatible with DNA staining, including dyes for cell cycle analysis. Here we describe the complete successful protocol for using EdU assay for the plant cells especially for *Arabidopsis* cell proliferation studies as a modified/enhanced version of the one used with other plant species by (Kotogany et al 2010).

1. *Arabidopsis* cultures 7 days old were incubated with 10 µm EdU (ethynyl deoxyuridine) for 2 hours. EdU treatment time determined according the experiment design; ***to estimate the percentage of cells in S phase***. 10µM of EdU were added on the surface of the experimental Petri dishes (cells embedded in agarose) before the end of each experiment with 2 hours. Cells were directly frozen at the end of the experiment (*see 1.2*) and then processed for nuclei isolation protocol (*see 3.1*).

2. Isolated nuclei were fixed for 15 min in 1% (*w/v*) paraformaldehyde solution in PBS with 0.1% Triton X-100. Adding the detergent Triton X-100 in the fixer prevents cell shrinkage and it also partially permeabilizes the plasma membranes for small detection reagents required in the EdU assay. Following 3×5 min PBS washes. 20-30 µl packed cell volume of cells were directly incubated 30 min at RT in EdU detection cocktail (Invitrogen, Click-iT EdU Alexa Fluor 488 HCS assay, cat no: A10027). For 1 sample reaction, following amounts of the kit components are mixed in 144 µl distilled water: 1.6 µl buffer additive (component F, kept frozen in small aliquots), 14 µl reaction buffer (Component D), 6.7 µl Copper (II) sulfate solution (Component E, 100 mM CuSO4) and 0.07 µl Alexa Fluor 488 azide (Component B, in 70 µl DMSO). The detection cocktail should be prepared freshly. Although the click reaction is not light sensitive, fluorochrome containing solutions should not be exposed to strong light.

3. Nuclei were stained with 100 ng/ml DAPI and analyzed on a FACS cell sorter. Two fluorescence detectors, for DAPI detection (DNA content) 424/44 emission range, and the boundary of EdU-Alexa Fluor 488-labeled nuclei (Alexa 488 green channel). To locate the EdU labelled nuclei in bi-parametric plots (EdU threshold value) counts versus (Alexa 488-EdU channel, log scale) histograms were used. The horizontal axis is representing to EdU labelling intensity corresponding to the vertical axis which representing the DNA content. The vertical line divided the histogram reveal to the major peak of the unlabeled nuclei represented in C3 and C4 quarters determined by the background intensity regarding to the negative control. Quarter C1 and C2 are represented to the labelled nuclei **(Figure 17B)**.

3.3. DETERMINATION OF THE MITOTIC INDEX (% OF CELLS IN M PHASE)

The metaphase/ anaphase index (M/AI) determination in the same sample was carried out by the microscopic examination through counting the proportion of DAPI-stained cells in mitosis (metaphase and anaphase figures **(Figure 18)**) compared to the total number of cells. Score at least 1000 cells in total in 5 replicate.

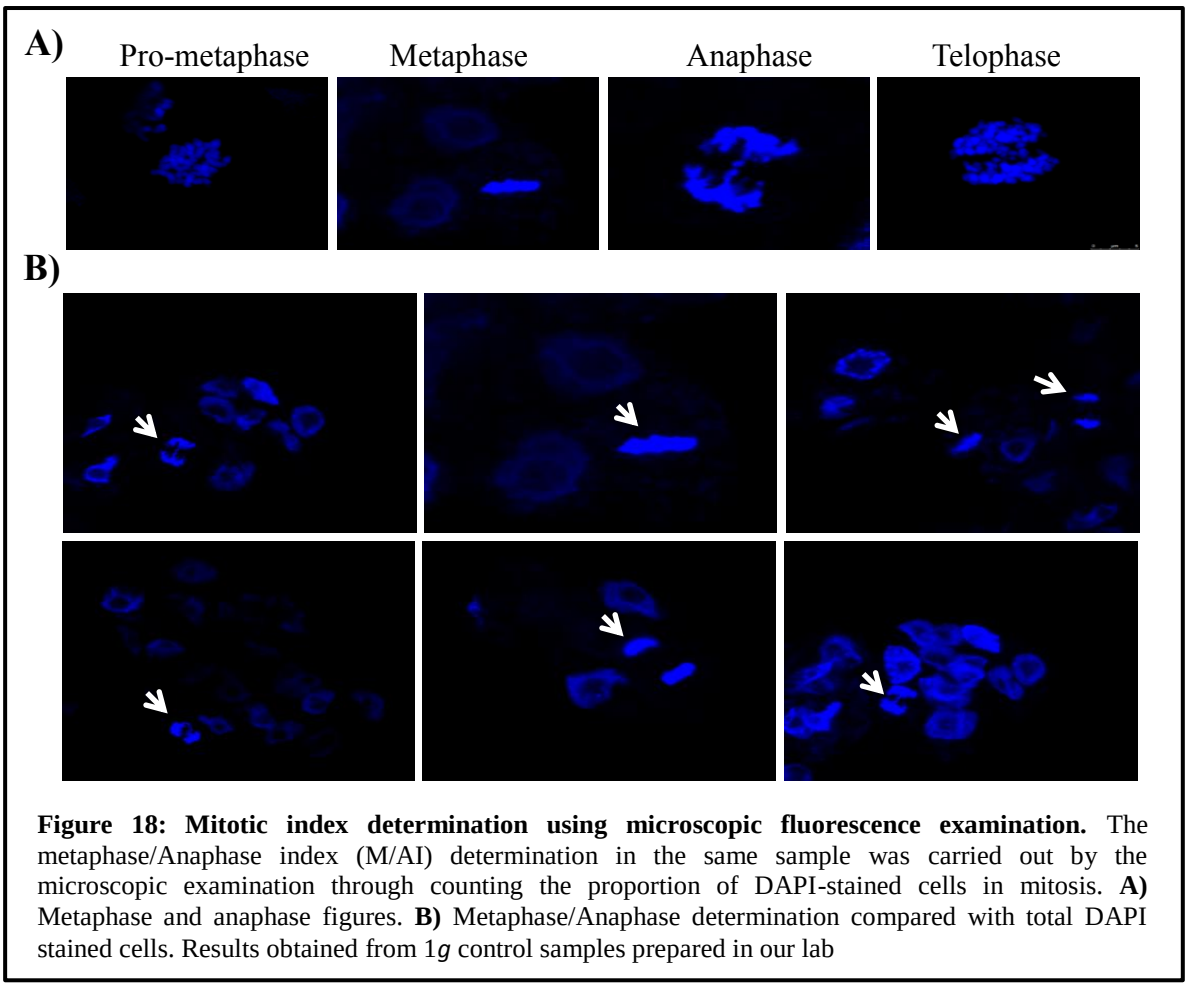

Figure 18: Mitotic index determination using microscopic fluorescence examination. The metaphase/Anaphase index (M/AI) determination in the same sample was carried out by the microscopic examination through counting the proportion of DAPI-stained cells in mitosis. **A)** Metaphase and anaphase figures. **B)** Metaphase/Anaphase determination compared with total DAPI stained cells. Results obtained from 1*g* control samples prepared in our lab

3.4. SPECIFIC PROTEIN QUANTIFICATION IN SINGLE CELLS USING FLOW CYTOMETRY

Immunofluorescence signal associated to a particular protein can be quantified at the single cell level by flow cytometry. Here we adapted and developed the techniques and protocols from (Gonzalez-Camacho & Medina 2006) required detecting plant (especially *Arabidopsis thaliana*) cells proteins fluorescent by flow cytometry approach as follows:

1. Frozen samples were processed to release nuclei as described before on the flow cytometry preparation samples (*see 3.1*). Isolated nuclei were incubated in isolation buffer after filtration on ice for 2 min.

2. Nuclei pellet after centrifugation at 4ºC (5 min, 1500 rpm), fixed on ice for 15 min by 1% PFA. Fixed nuclei were washed twice with 0.01% Triton X-100 containing PBS by centrifugation at 4ºC (5 min, 1500 rpm).

3. Washed nuclei were blocked in 500 µl of PBS blocking solution for 30 min at 4ºC. Then centrifuge at 4ºC (5 min, 1500 rpm). Incubate with the first antibody **(Table 3)** in blocking solution dilution for 45 min at 4ºC. Wash with PBS (2x5 min) using centrifugations 1500 rpm. Alexa Fluor® 488-labelled secondary antibody was used diluted 1:100 for 30 min at 4ºC. Wash with PBS (3x5 min) using centrifugations 1500 rpm.

4. Staining the nuclei with the staining *solution B,* containing DAPI labelling.

5. Two fluorescence detectors are used with the standard 360 nm laser. Alexa Fluor® 488-protein florescence intensity was detected between 530/30 nm (FL1 channel). For detection of DAPI intensity (DNA content) 424/44 nm blue fluorescence emission range was used at FL2 channel.

6. Data was analyzed using BD CellQuest™ software for protein fluorescence intensity detected by flow cytometry. Side scatter versus forward scatter diagrams were used to locate and gate nuclear populations by particle size.

4. TRANSCRIPTOMIC STUDIES

During gene expression studies, several specific primers were used in order to detect the different genes of interest expression under the experimental conditions. Also, to validate the results obtained by the microarray studies using the Rt-qPCR techniques. These primers were generated by using scientific programs such as UGENE *v* 1.13 and/or Primer 3 *Plus* and ordered to Integrated DNA Technology. **Table 4** shows a list of the all the primers used in our study.

4.1. RNA EXTRACTION

The REAL TOTAL RNA SPIN PLANTS AND FUNGI kit (REAL, Durviz S.L. Lot/21015) was used for the RNA extraction in our experiments. It is necessary to ground the cells with liquid nitrogen due to the omnipresence of RNases and in order to obtain an optimal lysis of the tissues. Directly the ground cells were mixed with the lysis solution (350 ml of Lysis solution I + 50ml PVP solution and 3.5ml of β-mercaptoethanol) with vortex. Samples were filtered using a filtration column with a centrifugation (13000 rpm for 1 min). Add 350ml of ethanol 70% to the filtrate and mix by vortex, and then all of the precipitate was load on the column with a centrifugation at 10000 rpm for 3 seconds. Add 350 ml of Membrane Desalting Buffer and centrifuge at maximum speed 13000 rpm for 1 minute to dry the membrane. DNase I Reaction mixture was prepared for each extraction, add 10 ml of reconstituted DNase I to 90 ml of DNase I Reaction Buffer, and then add directly onto the samples and incubate for 15 min at RT. Add 200 ml of STOP/DNAse I Solution to the RNA binding column. Centrifuge at 10000 rpm for 30 seconds. Wash the RNA pellet with 600 ml Wash Solution with a centrifuge at 10000 rpm for 30 seconds. Remove the liquid and place the column back in the collection tube. Wash again with 250ml washing solution with a centrifugation 13000 rpm for 2 min to completely dry the membrane. RNA was eluted in 30 ml of Nuclease-free water and centrifuge at 13000 rpm for 1 min. Add again 30 ml of Nuclease-free water to the same column, with the same collection tube. Centrifuge at 13000 rpm for 1 min. Finally it will be obtained 60 µl of RNA.

RNA concentration & quality was estimated by measuring the absorbance (absorbance ratio 260nm / 280nm should be between 1.6 and 2.0) using a spectrophotometer (Nano Drop ND-1000, Thermo, USA).

Table 4: Sequence of the different primers (5´-3´) used to follow the expression of key functions genes

Functions	Interested Genes	Primer (Forward)	Primer (Reverse)
Ribosome biogenesis	***AtNUC-L1*** (At1g48920)	ATGGGAAAGTCTAAATCCGC	TCCACGACC ACGATCACT T
	AtFIB1 (At5g52470)	CGTCTTTCGTTCTTCACTTTTAGACAAG	GCCCACTACGGCCTCTGTCA
Cell cycle core	***CYCB1;1*** (At4g37490)	CAGCAATGGAAGCAACAAGA	ATGVAGTGTTTGGGATTGAA
	Prolifera PRL (At4g02060)	TGGGTGGAAGAGGAAAATTG	CTGGCTCCTTCATCCTTCAG
Epigenetics	**MET1** (At5g49160)	GCTTAATCCAGCCCAGCATA	CACCTTTACCAGCAGCCTTC
	CMT3 (At1g69770)	AACGCCAATGGAACAAAATC	CAGGAAGCTTTCCCAGTGAT
	AUR2 (At2g25880)	TGAAAGGCACATGGCACTAA	TGAAGAGCCAGGGAAAGAGA
Abiotic stress	**Unknown** (At2g20560)	GGCCACTTAATGCAAACACA	GCATGCCAATGTCCATGTAA
	CYP71A12 (At2g30750)	TGGGTGGAAGGAAATCTGAG	CCTACTGGAGGTGGAGGACA
Unknown function /mitochondria	**ORF113** (Atmg01220)	ATCCACAGACTCGCAACCTT	CTGTCATGTCCGAATTGTGC
	Unknown (At2g07728)	GGATAGGACATGCAGGGAGA	TTCTTTCCGCTTATCCAACG
	Unknown (At2g07674)	CAATGCACCATTTGCAGAAC	CACAAGGTAGCCAAGGGAAA
	Unknown (At2g07702)	AATGCACGGATTCTCACCTC	TCTGACGCTCCTCAAGGACT

4.2. REVERSE TRANSCRIPTION POLYMERASE CHAIN REACTION (RT-PCR)

Reverse Transcription. Reverse Transcription is carried out using 2µg RNA with 1µl oligo-dT and complete the volume up to 15µl with Nuclease-free water. Mixture was incubated for 5 min at 70ºC, and then directly passes into ice for 5 min. Add the reaction mixture (5µl Buffer 5x of AMV RT + 2.5µl dNTPs + 1µl RNAsina and 1.5µl of AMV RT) to the RNA primer mixture. Mix briefly and incubate for 1 hour at 42ºC. Store the cDNA at -20°C until use for RT-PCR.

RT-PCR. PCR amplification mixture was prepared up to 25µl (1 µl cDNA + 0.5 µl dNTPs (deoxynucleotide triphosphates) (10mM) + 1 µl of each 10 mM specific primers (forward and reverse) + 0.5 µl Taq HF enzyme (Phusion® Hot Start II high-Fidelity DNA Polymerase F- 549) + 2.5 µl Enzyme buffer 10x + 18.5 µl Nuclease-free water. The polymerase chain reaction amplification carried out using BOECO Thermal cycler (Boeckel-Co (GmbH + Co) KG,

Hamburg, Germany) using the PCR thermo protocol. PCR product samples were examined by PCR gel electrophoresis at 100 V for 30 min in a 1% (*w/v*) agarose gel (Agarose D-1 Medium EEO, CONDA, Spain) in TAE buffer. The marker used a 1 kb DNA ladder. The electrophoresis gel was soaked in Ethidium bromide for 30 min then scanned in UV light.

4.3. QUANTITATIVE REAL-TIME PCR VALIDATION (RT-qPCR)

This technique has the advantage of combining the one-step reaction reverse transcriptase, with the real time monitoring of the chain reaction polymerase amplification. With this method we can make a relative quantification of each amplicon, allowing us to compare differences expression of a particular sequence among our samples. Relative quantification is based on the use of a fluorescent DNA intercalating agent, SYBR green that allows further amplification in real time during the reaction. The used primers are having a high efficiency at a given concentration of RNA. To do this, we must check that efficiency by standard curves; consist of using a first, at a given concentration, with serial dilutions RNA (assuming the maximum concentration of 70 ng / µl). Its efficiency is observed for each range of concentrations to choose optimal RNA concentration.

Sample Purification - Release Genomic DNA using DNase. It is necessary to purify the RNA samples from the genomic DNA completely before starting the quantitative real time RT-PCR using the DNase treatment. 4 µg of RNA samples will incubate with 1µl DNase enzyme (Turbo DNA-free; Ambion AM1907) and 5µl of 10X enzyme buffer at 37ºC for 1 hour. Inactive the DNase enzyme with 5µl stopped DNase for 2 min at room temperature. Sample was centrifuged at 13000 rpm for 2 min, and then collected the supernant containing the purified RNA sample. Measure the RNA concentration using Nanodrop. The final RNA sample concentration should be 7ng / µl to be ready for the Rt-qPCR analysis.

Sample Preparation for Rt-qPC*R*. Rt-qPCR will performed with 3 µl RNA using DNA amplification and quantification kit (SYBR Green QRT-PCR, Agilent, USA) using 7.5 µl of 2sy6 + 0.75 µl of RT + 0.15 µl of DTT + 0.9 µl of each specific primers forward and reverse 10 µM. Complete the experimental volume up to 12 µl by adding 1.8 µl Nuclease-free water. Vortex the sample and be ready for the quantitative real time PCR reaction.

Rt-qPCR Thermo Protocol. Rt-qPCR running was performed by the genomic service at (CIB-CSIC, Madrid) using the iQ™5 Multicolor Real-Time PCR Detection System, BIO-RAD. Rt-qPCR profile (**Table 5**). Optimizing qPCR performance was validated with several standard curves for each probe. Three different biological replicates in two technical replicates (only *2 of* these *3 replicates will be used in the microarray studies (see 4.4)*) were used beside to different internal controls; no-reverse transcriptase control (negative control using water), reverse transcriptase control (positive control 1 using general RNA samples) and actin as a positive control 2 for the expression. Data analyses were performed using iQ™5 optical system software *v2.1*. Gene expression was estimated as a relative fold expression (using the positive control 1 for each gene as a reference control).

Table 5: Rt-qPCR thermal cycler.

			PCR Cycle3 (40X)			Melting Cycle (36X)
Reverse Transcription	**Polymerase activation**	**Denature**	**Hybridization**	**amplification**	**Anneal, read fluorescence**	**Dissociation / Melting curve**
10 min/ 50ºC	3min/ 95ºC	10sec/ 95ºC	20sec/ 60ºC	30sec/ 72ºC	1min / (95-60 ºC)	10sec/60ºC

4.4. MICROARRAY ANALYSIS

Array Design. Microarray analysis was carried out at the Unité de Recherche en Génomique Végétale (Evry, France), using the CATMA*v6.2* array based on Roche-NimbleGen technology. A single high density CATMA*v6.2* microarray slide contains twelve chambers, each containing 219684 primers representing all the *Arabidopsis thaliana* genes: 30834 probes corresponding to CDS TAIR*v8* annotation (including 476 probes of mitochondrial and chloroplast genes) + 1289 probes corresponding to EUGENE software predictions. Moreover, it included 5352 probes corresponding to repeat elements, 658 probes for miRNA/MIR, 342 probes for other RNAs (rRNA, tRNA, snRNA, and soRNA) and finally 36 controls. Each long primer is triplicate in each chamber for robust analysis and in both strand. 2 of 3 replicates were hybridized. For each biological repetition and each point, RNA samples were obtained by pooling RNAs from 0.5g of cell pellet (*Arabidopsis* cell cultures). Three different experimental conditions were collected to be analyzed by the means of microarray approach; G1, G2 and 14 hours experiment in both 1*g* control and simulated microgravity by RPM. Total RNA was extracted (*see 5.1*) from each

sample. For each comparison, two technical replicate with fluorochrome reversal was performed for each two biological replicates (i.e. four hybridizations per comparison). The labeling of cRNAs with Cy3-dUTP or Cy5-dUTP (Perkin-Elmer-NEN Life Science Products) was performed as described in (Lurin et al 2004). The hybridization and washing were performed according to NimbleGen Arrays User's Guide *v5.1* instructions. Two micron scanning was performed with InnoScan900 scanner (Innopsys^{R}, Carbonne, FRANCE) and raw data were extracted using Mapix^{R} software (Innopsys^{R}, Carbonne, FRANCE).

Statistical Analysis of Raw Microarray Data. Experiments were designed with the statistics group of the Unité de Recherche en Génomique Végétale. For each array, the raw data comprised the logarithm of median feature pixel intensity at wavelengths 635 nm (red) and 532 nm (green). For each array, a global intensity-dependent normalization using the loess procedure (Yang et al 2002) was performed to correct the dye bias. The differential analysis is based on the log-ratios averaging over the duplicate probes and over the technical replicates. Hence the numbers of available data for each gene equals the number of the biological replicates and are used to calculate the moderated t-test (Smyth 2004). Under, the null hypothesis, no evidence that the specific variances vary between probes is highlighted by Limma and consequently the moderated t-statistic is assumed to follow a standard normal distribution. To control the false discovery rate, adjusted p-values found using the optimized FDR approach of (Storey & Tibshirani 2003) are calculated. It was considered as being differentially expressed the probes with an adjusted p-value ≤ 0.05. Analysis was done with the R software. The function SqueezeVar of the library Limma has been used to smooth the specific variances by computing empirical Bayes posterior means. The library kerfdr has been used to calculate the adjusted p-values.

Data Deposition. Microarray data from our experimental results were deposited at Gene Expression Omnibus (http://www.ncbi.nlm.nih.gov/geo/), accession no. GSE is pending and at CATdb (http://urgv.evry.inra.fr/CATdb/; Project: ***Au13-11_Gravity***) according to the "Minimum Information About a Microarray Experiment" standards.

Results Analysis and Data Processing (Bioinformatics). R-software curated microarray data was further processed and analyzed using different bioinformatics tools for different processing purpose:

- **GEDI clusters were performed using *Gene Expression Dynamic Inspector (GEDI program v2.1)***

Global expression pattern were calculated using the GEDI *v2.1* program analysis (Eichler et al 2003). GEDI profile allows the visualization of the gene expression across the transcriptome generating a mosaic image or dot matrix, consisting of 20 x 23 pixels (average of <46 probe sets/tile) using the self-organizing maps algorithm and standard setting of the software using the signal log_2 ratio of the selected probe sets through using the 20961 probes with any significant expression level from the total of 73229 probes included on the CATMA arrays. Each pixel on the figure represents a group or cluster of genes that behave similarly in all the experimental conditions.

- **Gene ontology analysis**

Gene ontology (GO) was performed using The *Arabidopsis* Information Resource Tool (TAIR, *https://www.arabidopsis.org/*) providing the GO biological process depends on the number of genes associated to each biological functions regardless to the significant impact of the gene in the function. Thus, in order to provide significance to each altered function, we performed the GO using GeneMANIA tools (GeneMANIA (*http://www.genemania.org/*) (Montojo et al 2010)).

- **Protein-protein network**

In order to study specific network in our study, Protein-protein network was performed using STRING *v9.1* (*http://string-db.org/*) (Franceschini et al 2013). Interested genes were selected and placed to generate the protein-protein network based on the protein structure and function data already available in the online databased.

- **Heat map**

Heat map was generated by coloring manually the excel datasheet cells depending on the *log2ratio* values. Red colors level reflect up regulated genes (*log2ratio*>1) while down regulated genes are displayed in green (*log2ratio*<1). Black was used as background (1>*log2ratio*>1).

5. STATISTICAL ANALYSES

Data were collected from different analysis after each experiment in an Excel datasheet (Microsoft office 2010). The average, data range and standard deviation in each experiment were estimated. In quantitative studies involving data comparison between different experimental means, data were analyzed according to (Steel 1980). Using SigmaPlot *v.12.5* and SPSS *v.22* program to be statistically analyzed the variance of differences using ANOVA test including Fisher test analysis and student t test. Degree of freedom was followed as $p \leq 0.05$ (95%) considers statistically meaning significant (*).

6. GROUND BASED FACILITIES MODE OF OPERATION, HARDWARE AND EXPERIMENTAL DESIGN

Access to different altered gravity recreating instruments, so called Ground based facilities (GBF), in different European laboratories was possible due to short stays (up to more than 3 months in total) in the frame of the ESA GBF Access GIA project "From GBF to ISS with *Arabidopsis thaliana*". Here we describe different GFB instruments, its mode of operation, hardware constrains and experimental design conditions.

1.1. EXPERIMENTS ON THE 2D PIPETTE CLINOSTAT LOCATED AT DLR

The fast rotating 2D clinostat with 50-100 rpm is mainly used in cellular systems experiments (Hemmersbach et al 2006). The first facility we used in this thesis was the so-called Pipette 2D clinostat (located at the German Aerospace Centre (DLR)) **(Figure 19),** enable the rotation of a sample around one axis perpendicular to the gravitational field producing a residual force of 4.2 x 10^{-3} g at 60 rpm (Hemmersbach et al 2006). It allows to simultaneously expose to simulated microgravity (2D-clinostat) ten pipettes placed into the rotating clinostat **(Figure 19A, upper part)** while an internal 1*g* control is provided by similar 10 pipettes without rotation **(Figure 19B, lower part)** to get the same environmental/vibration influences on the samples. Additionally, an alternative external 1*g* control was possible, just using the suspension culture in regular incubation shaker conditions.

Experiment 1: **Using the 2D clinostat as a microgravity simulator is valid for cellular systems investigations**

7 days *Arabidopsis* cell suspension cultures MM2d was used to investigate the impact of simulated microgravity using the clinorotation by 2D pipetted clinostat **(Figure 19)**. MM2d culture was grown at 27ºC in shaker incubator, 120 rpm in dark conditions for 7 days in (CIB laboratory- Madrid, Spain). Samples translocate to DLR (Cologne, Germany) in order to perform the experiment.

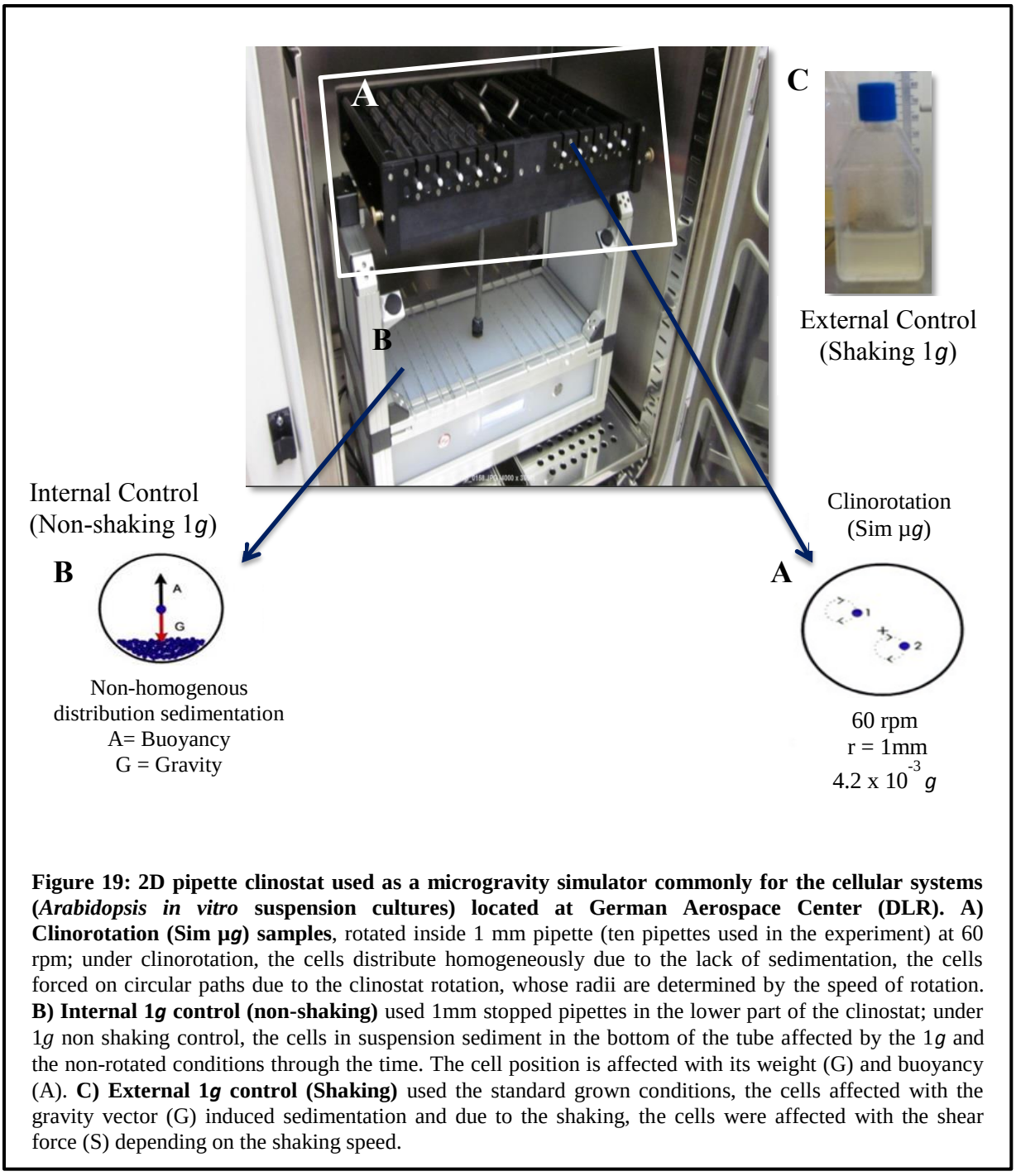

Figure 19: 2D pipette clinostat used as a microgravity simulator commonly for the cellular systems (*Arabidopsis in vitro* suspension cultures) located at German Aerospace Center (DLR). A) Clinorotation (Sim µ*g*) samples, rotated inside 1 mm pipette (ten pipettes used in the experiment) at 60 rpm; under clinorotation, the cells distribute homogeneously due to the lack of sedimentation, the cells forced on circular paths due to the clinostat rotation, whose radii are determined by the speed of rotation. **B) Internal 1*g* control (non-shaking)** used 1mm stopped pipettes in the lower part of the clinostat; under 1*g* non shaking control, the cells in suspension sediment in the bottom of the tube affected by the 1*g* and the non-rotated conditions through the time. The cell position is affected with its weight (G) and buoyancy (A). **C) External 1*g* control (Shaking)** used the standard grown conditions, the cells affected with the gravity vector (G) induced sedimentation and due to the shaking, the cells were affected with the shear force (S) depending on the shaking speed.

2D clinostat experiments using cell suspension was performed for different exposing duration, for short term experiments (3.5 hours) and for mid-term experiments (14 hours) in three replicates. Ten 1ml pipettes are used as clinorotation samples (Sim µ*g*) at 60 rpm in the upper rotated part at 27ºC in dark conditions. Two 1*g* control conditions were used in this experiment.

Internal 1g control (non-shaking) used the same condition of the clinorotation samples, 1ml pipette, vibration effect, and environmental conditions but in a stopped condition without movements. Whereas, External 1g control (shaking) used the standard culture growing conditions, 27ºC, 120 rpm in shaking incubator at dark conditions. Samples were recovered directly after each experiment (3 replicates for each different duration) for different analysis.

- **Fixed samples**. Cells in suspension were directly passed into a fixative solution (4% PFA) for immunofluorescence analysis (*see 2.2*, Protocol procedure finished at pass fixed cells into the poly-L-lysine coated multi-wells slides).
- **Frozen samples**. Cells in suspension were directly filtered using nylon mesh 50µm and directly frozen using liquid nitrogen. This sample is suitable for Flow cytometry analysis.

6.2. EXPERIMENTS ON DIAMAGNETIC LEVIATION AT HFML

The magnetic levitator is a unique facility which allowed us to observe simultaneously several altered gravity levels into the same high energy magnetic field environment of up to 16.26 T. We indicate the presence of high intensity magnetic fields in the samples by an (*). The facilities at the High Field Magnet Laboratory (HFML) at the Radbound University in Nijmegen (The Netherlands) require a high power consumption of about 5.8 MW which results in a significant restriction on hours required for use. In addition, the system needs to be cooled with a flow of 142 L/s of cold water at 12ºC (Christianen 2010) **(Figure 20)**, so we can't normally operate for more than 4-5 hours consequently. This levitator also has a central cylinder; where the tubes (cut to be 26.5 mm height) are inserted at different distances from the center of the apparatus (maximum field), and consequently exposed to differential magnetic field and effective gravity conditions. This system allowed us to obtain 4 different altered gravity and magnetic field samples **(Figure 20D)**:

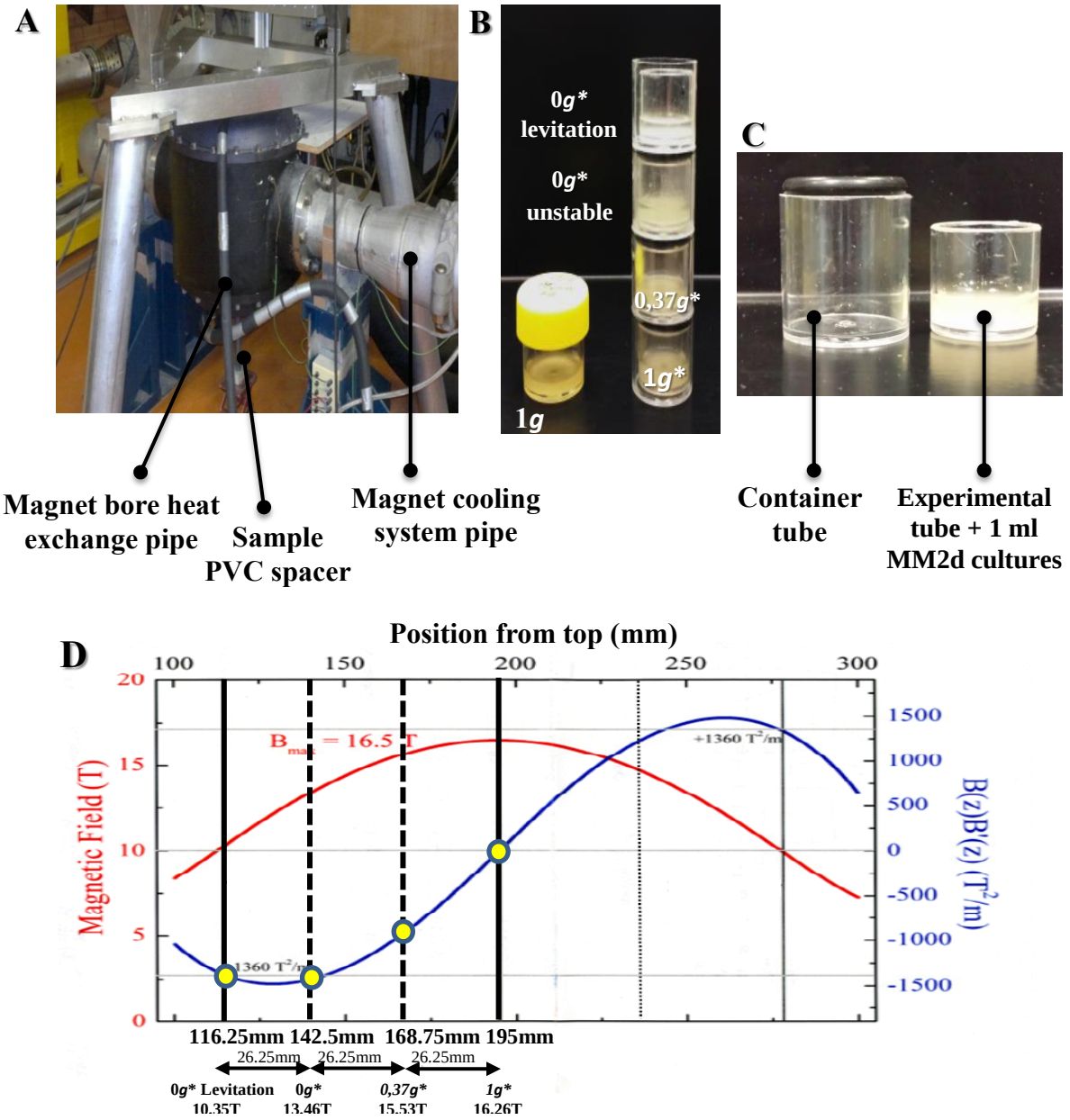

Figure 20: Magnetic levitation set up. A) Photo of the water-cooled duplex-Bitter magnet located at HFML with the samples positioned inside the magnet bore. The temperature is controlled by a double-walled metal tube connected to a 22ºC water bath. A PVC spacer is used to place the stack of samples in the correct position. **B)** The samples are contained in 26.25 mm high tubes placed on top of each other at four effective *g** levels. The space between the samples was 26.25 mm and all samples were in the dark before and during the experiment (no light reached the magnet bore). **C)** Closer view of a sample tube, 1ml of MM2d suspension cultures into the tube (layer 1-2mm) to ensure a similar force throughout the whole biological samples. **D)** Profile of the magnetic field strength (*B*) magnetic levitation force along the magnet bore. The samples were placed symmetrically in relation to the centre of the bore (195 mm above the top) indicated in the graph by vertical lines (straight lines for 0*g** levitation, 0*g** unstable, 0.37*g** and 1*g**). The red curve shows the magnetic field strength as a function of the vertical position (*z*) in the magnet. The blue curve indicates the product of the field strength *B(z)* and the field gradient ($B'(z) = dB/dz$), which is the derivative of the field strength with respect to the vertical position. The corresponding value of the effective gravity is equal to $g\ (1 + B(z)\ B'(z)/1360)$, so a magnetic force of -1360 T²/m is able to levitate water.

- **Two Simulated Microgravity Samples (0*g** unstable, 0*g** levitated).** In these positions, magnetic field intensity is 13.46T (52.5mm form the center), and 10.35T respectively (78.75mm from the center), but the magnetic field gradient is maximized so producing a magnetic levitation force high enough to compensate our planet 1*g* force (calculated for pure water), required to generate two alternative simulated microgravity conditions. The first one is an unstable 0*g** point and the second one is stabilized by the own magnetic field corresponding to the 0*g** levitation point.
- **Partial gravity (0.37*g** Mars condition).** At the same time, it is possible to generate an effective force similar to the Mars gravity (0.37*g**), if we place the sample 26.25mm from the center (15.53T is the magnetic force intensity at that distance from the center of the magnetic bore).
- **Internal control (1*g**).** At the center of the apparatus, the more intense magnetic field, 16.26T, cause no diamagnetic force since magnetic field gradient is null in this point (so the net 1*g** gravity force is present).

Experiment 2: **Diamagnetic levitation used as multi-gravity levels simulator**

7 days *Arabidopsis* cell suspension cultures MM2d was grown at 27ºC in shaker incubator, 120 rpm in dark conditions in (CIB laboratory- Madrid, Spain). Samples translocate to HFML (Nijmegen, The Netherland) in order to perform the experiment.

3 hours experiments in 3 replicates were performed using 7 days *Arabidopsis thaliana* suspension cultures in the magnetic levitation. 1ml of the suspension culture was placed into 5 container tubes (4 localized in different distances from the center to generate different gravity levels **(Figure 20)** plus one located outside of the magnet as 1*g* control) at RT. After the end of each replicate, cells were recovered and distributed as fixed and frozen sample depending on the different analysis to be performed *(see Experiment 1)*.

6.3. EXPERIMENTS ON THE RANDOM POSITIONING MACHINE (RPM) AND THE LARGE DIAMETER CENTRIFUGUE (LDC) AT ESA-ESTEC

The Random Positioning Machine (RPM) hosted and operated at the Life and Physical Sciences Instrumentation and Life Support (LIS) Laboratory of ESTEC (ESA's technical centre located in the Netherlands), in collaboration with the Dutch Experiment Support Centre (DESC), is probably the most versatile version of a 3D-clinostat able to simulate microgravity conditions on the ground. The RPM is an instrument which was designed to provide an experiment with continuous random orientation and angular speed changes in 3 dimensional spaces relatively to Earth's gravity vector, also referred to as "3D Random mode",. The RPM is able to recreate on the ground effects close to those of a real microgravity environment in plants, although some biological systems (quick responders) are severely stresses into the RPM (Herranz et al 2013a).

In life-science experiments, it is interesting to emphasis the impact of mechanical stresses generated through the altered gravity on the mass of the organism. Although of Random Positioning Machines (RPM) is widely used to simulated microgravity environment (Borst & van Loon 2009, Pardo et al 2005, Yuge et al 2003), cells grown on the RPM are subjected to changes in gravity and mechanical stress due to the vibration of the machine (Coinu et al 2006) and can even be considered as an omnilateral stimulation more than the absence of gravitational stimuli.

The design of the RPM consists of two cardanic frames and the platform accommodating the experiment. The movements of the frames are generated via belts and two electro-motors. Both motors are controlled on the basis of feedback signals generated by encoders, mounted on the motor-axes, and by 'null position' sensors on the frames. The RPM is controlled by a computer hosting dedicated software in 3D Random mode. Gravity values measured on the RPM, rotated in 3D clinostat mode, the inner and outer frame rotate, both at a constant speed of 60º/s (van Loon 2007). For the experimental optimal conditions that are performed on the RPM, temperature and humidity control is well controlled. In the case of using liquids on the RPM, it is mandatory to fill the experimental chamber completely, without any gas bubbles and avoids loss of liquid during rotation. Gas bubbles movement results in unwanted fluid motion and associated shear stress to the sample completely ruining the simulation experience (Borst & van Loon 2009). In fact, shear stresses appearing in various platforms for the culture cells in suspension

such as 2D Pipette clinostat (Thiel et al 2012), rotating wall vessel (Wolf & Schwarz 1991, Wolf & Schwarz 1992) and also in the RPM can diminish simulated microgravity quality. Cells collisions with the container walls or undesirable fluid motion can cause stresses that there are not present in real microgravity conditions. Moreover, it is found that using cell culture in rotating wall vessels and 2D clinostat activates shear stress dependent genes, due to the equal and opposite hydronamic forces required to compensate gravity (Crabbe et al 2008, Kaysen et al 1999, Morin et al 2003). It is reported that rotating wall vessel produce shear forces affect plant cell suspension cultures (Sun & Linden 1999). However, comparative studies performed with the RPM using cultures cells were unable to produce the spaceflight results (Hoson et al 1997), suggesting that these differences associated by other stresses are not present in spaceflight caused by internal fluid motion and wall shear stresses (Leguy et al 2011).

By means of a different mode of operation, the RPM can be used to generate partial gravity levels by controlling the angle and the rotational speed. It would be possible to generate altered gravity to mimic for instance $0.37g$ (Mars) or $0.17g$ (Moon) gravity levels depending on the amount of time the sample is the upper or the lower part of the sphere during rotation. Rotation rate (ω) and geometrical distance from the center of rotation (R) enable the definition of "g-contours" through the following formula: $g = \omega^2 \cdot R \cdot g_{0\text{-}1}$ (where $g_0 = 9.81\ m \cdot s^{-2}$) **(Figure 21)**.

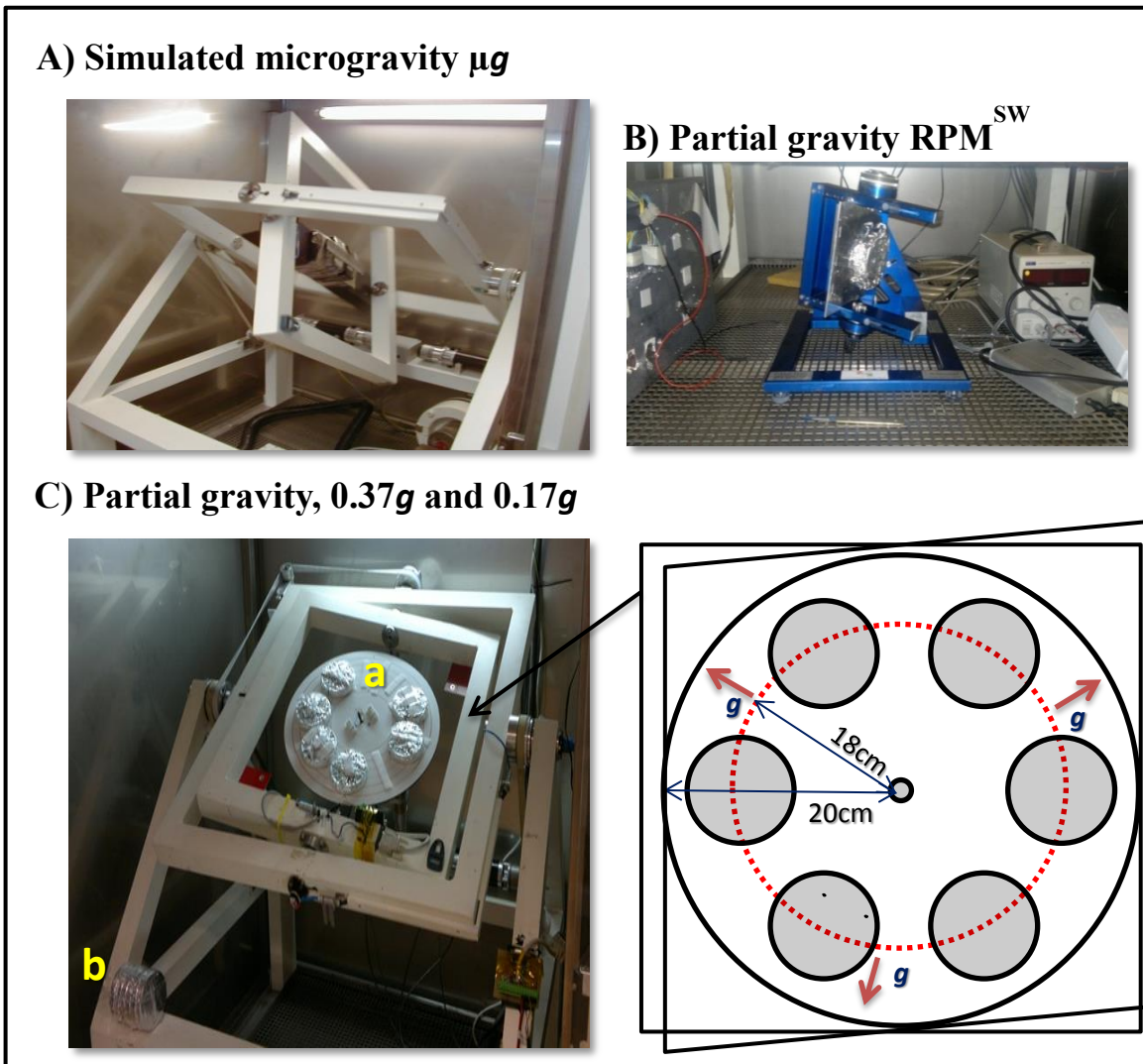

Figure 21: The Random Position Machine (RPM) can be used to simulate both, simulated microgravity (µ*g*) and partial gravity (the Moon (0.17*g*) and Mars (0.37*g*)). A) The Random Position Machine (RPM) with two independently driven perpendicular frames located inside an incubator based at the LIS Laboratory of ESTEC-ESA. **B)** Desktop RPM applicable to be used in a standard incubator. This desktop is used to simulate microgravity and also partial gravity using specific software (RPM^{SW}) controlling the speed, axis angles. Experimental samples placed in the center between the two axes to increase the quality of the simulated microgravity. **C)** RPM used in simulating partial gravity using hardware (RPM^{HW}); the combination between the random speed of the RPM and the rotated speed of the centrifuge **(a)** inside the RPM will simulated different partial gravity levels. Experimental samples located on the centrifuge **(a)** and the 1*g* control samples **(b)** are placed in the same incubator outside the RPM. **D)** Scheme of the (RPM^{HW}) for partial gravity simulation. It consists of the two frames as a part of the rotated RPM. Inside the RPM, a centrifuge is located with a diameter 20 cm. Samples will be placed in a proper place to produce the interested partial gravity level. For simulate the Moon gravity (0.17*g*). Plates will be positioned 18 cm diameter from the center with a centrifuge speed 28.6 rpm. And in the same position with a centrifuge speed 43.5 rpm to simulate Mars gravity (0.37*g*).

A Large Diameter Centrifuge (LDC) has been developed recently by ESA as a complement to the micro-/partial gravity RPM facilities. A large diameter centrifuge can provide the hyper gravity environment to cells, allowing the acquisition of the measurement points in the range from 1 to 20 *g*. The LDC is also part of the Life and Physical Sciences Instrumentation and Life Support Laboratory (LIS) at ESTEC (the Netherlands), dedicated to serving the science and technology user communities throughout Europe.

The diameter of the LDC is eight meters. It has four arms **(Figure 22)**, each of which can support two gondolas with a maximum payload of 80 kg per gondola. In practice, six gondolas are available, plus one gondola in the center for control or reference experiments. The rotation of the LDC then creates the Hypergravity field at the experiment site inside each gondola and minimize the lateral forces (Shear forces) generated during rotation (van Loon et al 2004). The LDC is flexible in terms of experiment scenarios, duration and possible equipment to use. This means that the system is able to execute and manage experiments that last from one minute up to six months, without stopping.

Figure 22: **Long LDC system description** located used for Hypergravity experiments at the Life Support Laboratory (LIS) at ESTEC-ESA (the Netherlands).

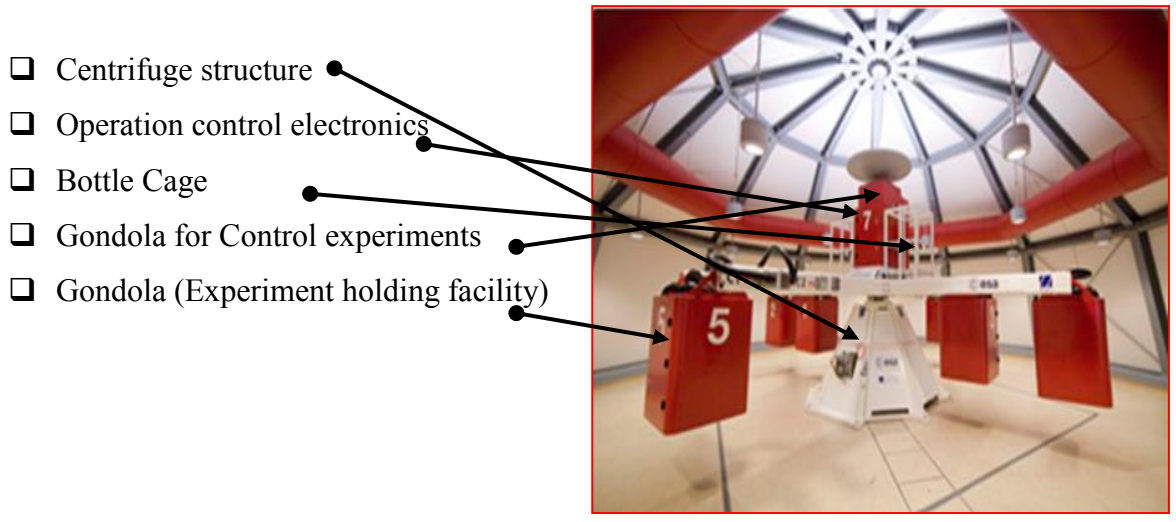

Experiment 3: **Impact of altered gravity levels on *Arabidopsis* cell cultures**

Arabidopsis thaliana cell suspension cultures 7 days old were embedded in agarose and used to detect the impact of altered gravity levels using various simulators (µ*g*/ simulated microgravity using RPM, 0.17*g*/ Moon condition using RPM^{SW} (RPM operated by software), 0.37*g*/Mars condition using RPM^{HW} (RPM operated by hardware) and 2*g*/ Hypergravity using LDC) to be compared with 1*g* control. Experiments were performed for different exposing times; short (3hr), mid (14hr), and long term (24 hours) in 3 replicates at 27ºC in dark conditions. At the end of each experiment cells were recovered from the embedded agarose (*see 1.2*) for

- **Fixed samples:** As described earlier, cells were fixed with Paraformaldehyde after extracting from the agarose. Cells were passed to the immunofluorescence protocol up to the preservation on the poly-L-lysine slide. Samples were used for the different immunofluorescence studies.
- **Fixed samples:** Other fixed samples with Glutaraldehyde fixation (*see 2.1)*.
- **Frozen samples:** Cells were frozen after extraction from the agarose. Frozen samples were used for Nuclei isolation for cell cycle analysis with flow cytometry, RNA extraction for gene expression studies, and protein extraction for proteomic studies.

Experiment 4: Impact of altered gravity levels on Arabidopsis cell cycle acceleration by detecting the proportion of cells in S-phase using EdU labelling assay

Arabidopsis thaliana cell suspension cultures 7 days old were embedded in agarose and used to detect the impact of different altered gravity level in the same conditions than *Experiment 3*.

In **Experiment 4**, the only difference was 2 hours incubation with EdU *before the end* of each experiment by passing 1 ml of 10µM of EdU assay on the surface of the embedded agarose. Simulators were stopped for the EdU incubation for 5 min before restarting the machine again. By the end of each experiment, samples were recovered as frozen samples to complete the EdU assay protocol.

Experiment 5: **Impact of altered gravity levels on Arabidopsis cell cycle progression using synchronic cell cultures**

Arabidopsis thaliana cell suspension cultures 7 days old were incubated with Aphidicolin for 24 hours at 27ºC, 120 rpm in shaking incubator in dark conditions. Then, cells were washed as described in the synchronization protocol earlier (*See 1.3*). T0 samples were collected just after washing and before starting the experiments. Then cells were embedded in agarose and exposed to various simulators (µ*g*/ simulated microgravity using RPM, 0.17*g*/ Moon condition using RPM^{SW} (RPM operated by software), 0.37*g*/Mars condition using RPM^{HW} (RPM operated by hardware) and 2*g*/ Hypergravity using LDC) to be compared with 1*g* control. Time-course experiments were performed for 72 hours to sample at different times on two different experiments through four days for three replicates. Cells were recovered as frozen samples (*see 1.2*) in order to isolate nuclei for cell cycle analysis using flow cytometry approach.

- **1st experiment (72h) sampling times**
  - First day: T0 – T12 (T0, T1, T2, T4, T6, T8, T10, T12)
  - Second day: T24 – T36 (T24, T26, T28, T30, T32, T34, T36)
  - Third day: T48 – T60 (T48, T52, T56, T60)
  - Fourth day: T72

- **2nd experiment (72h) sampling times**
  - First day: T0
  - Second day: T12 – T24 (T12, T14, T16, T18, T20, T22, T24)
  - Third day: T36 – T48 (T36, T40, T44, T48)
  - Fourth day: T60 – T72 (T60, T64, T68, T72)

Experiment 6: ***Arabidopsis*** **cell cycle phases characterization under simulated microgravity (Sim µ*g* RPM) compared with 1*g* control**

Depending on the results of Experiment 5, a reference time was determined for each phase subpopulation peak during the first cell cycle (S, G2/M, and G1 phase, see *Results 4.1*). The experiments were performed using synchronized cells embedded in agarose exposed to simulated microgravity (RPM) compared with 1*g* control for 3 different replicates. Cells were recovered for different studies.

- **Fixed samples**. Cells were fixed after extracting from the agarose (*see 1.2*). Cells were passed to the immunofluorescence protocol up to the preservation on the poly-L-lysine slide. Samples were used for the different immunofluorescence studies.
- **Fixed samples**. Other fixed samples with Glutaraldehyde fixation (*see 2.1*).
- **Frozen samples:** Cells were frozen after extraction from the agarose. Frozen samples were used for Nuclei isolation for cell cycle analysis with flow cytometry, RNA extraction for gene expression studies including CATMA microarray (*including additional sample for Asynchronous cultures exposed to RPM for 14h*), and protein extraction for proteomic studies.

Experiment 7: **Expose transgenic callus (induced from transgenic seedling lines) to simulated microgravity and hypergravity conditions**

Transgenic callus induced from different transgenic lines; CYCB1;1:Gus, CYCB1;1:GFP, and AtNUCL1:GFP. 7days old *Arabidopsis* transgenic callus were transferred to new MSS agar medium in petri dishes in dark conditions. Samples were placed directly into the simulators (RPM and LDC), and other sample at 1*g* control in the same environmental conditions; 24ºC in dark conditions. Experiments were performed for 4 days using 3 internal replicates (different medium, different age callus, replicates performed in the same time). Samples were recovered directly after the end of the each experiment as fixed samples for microscopy analysis.

- **CYCB1;1:GUS.** Samples were recovered for GUS staining protocol (*see 2.4*).
- **CYCB1;1:GFP & AtNUCL1:GFP.** Samples were fixed directly using 4% PFA.

Seeking the optimal simulation facility is important to validate plant cell cultures *in vitro* as a model system without specialized structures for gravity sensing. Furthermore, GBF allow to get a deeper understanding on the mechanisms operating at the level of individual cells; cell growth and cell proliferation, and epigenetics using the advantages of synchronous cell cultures.

RESULTS

Optimal GBF
Asynchronous cell cultures
Cell cycle in Synchronous cultures
Partial gravity
Transcriptome analysis

RESULTS

CHAPTER 1: *SEEKING THE OPTIMAL MICROGRAVITY SIMULATOR APPROPRIATE FOR THE PLANT CELLULAR SYSTEMS INVESTIGATIONS*

1.1. Using the 2D Clinostat as A Microgravity Simulator for Cellular Systems (*Cells In Suspension*) investigations

1.2. Using Diamagnetic Levitation as A Multigravity Level Simulator for Ground Studies (*Cells In Suspension*)

1.3. Using RPM and LDC to Simulate Microgravity, Partial Gravity, and Hypergravity for Cellular Systems *(Immobilized Cells in Agarose)*

CHAPTER 1: SEEKING THE OPTIMAL MICROGRAVITY SIMULATORS APPROPRIATE FOR THE PLANT CELLULAR SYSTEMS INVESTIGATIONS

Using plant cell cultures to investigate the impact of gravity alteration is justified precisely when studying plant development at the cellular level. At the beginning of our work, the recommend simulators for using cell cultures, especially cells in suspensions, was the 2D clinostat and magnetic levitation. Furthermore, adapting a new cellular system suitable for the use of other simulators such as the RPM, and LDC has recently become necessary. In this chapter we are going to test the possibility of using the 2D clinostat ***(Experiment 1)***, magnetic levitation ***(Experiment 2)***, RPM, and LDC ***(Experiment 3)*** in the *Arabidopsis* cell suspension investigations, in order to redefine the best GBF to study the impact of altered gravity levels on the fundamental plant cell processes as cell growth and cell proliferation.

1.1. USING THE 2D CLINOSTAT AS A MICROGRAVITY SIMULATOR FOR CELLULAR SYSTEMS *(CELLS IN SUSPENSION)* INVESTIGATIONS

A method commonly used to simulate microgravity (clinorotation) conditions on cellular systems is the 2D clinostat. A 7 days old *Arabidopsis* cell suspension was used in the clinorotation experiment for different exposure duration, 3.5 hours (short term) and 14 hours (mid-term). Clinorotation experiment was provided with two different controls, internal 1g control (non-shaking) to provide the same experimental conditions and external 1g control (shaking), the laboratory standard conditions for cell cultures maintains. Samples were recovered for different analysis

- To investigate the impact of simulated microgravity on *Arabidopsis* cell proliferation
- To investigate the impact of simulated microgravity on *Arabidopsis* cell growth

1.1.1. Simulated Microgravity and Static Controls Alter *Arabidopsis* Cell Proliferation

In order to demonstrate the impact of altered microgravity on the cell proliferation rate, the proportion of cells in G1, S and G2/M phases was determined by the means of flow cytometry; i.e. by determination of the DNA content for each individual cell.

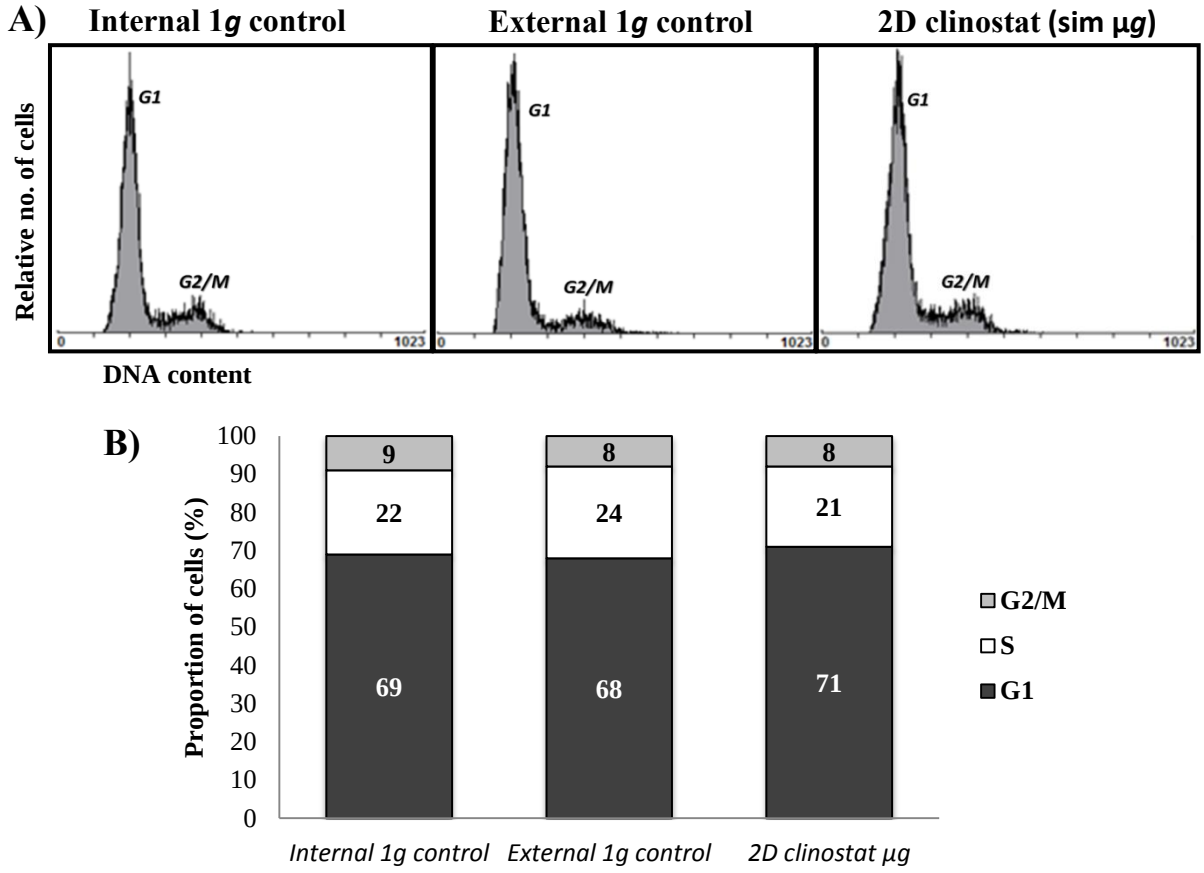

Figure 23: *Arabidopsis* cell cycle phases affected by simulated microgravity (2D clinostat) and the controls for the short term experiment. A) Flow cytometry analysis, each panel represents the relative number of cells according to the DNA content in each cell. First peak (2n) reflects G1 phase and the second peaks (4n) reflects G2/M phase. **B)** DNA content histogram. G1 peak is integrated to quantity the percentage of cells in G1 and similarly, the G2/M peak. The rest of the cells are considered at the S phase percentage by indirect estimation.

Data reveal that, there are no significant differences on the distribution of the cell cycle phases influenced the simulated microgravity for the short term exposure compared with the control conditions, either the internal or the external 1*g* controls **(Figure 23)**. Moreover, if we increase the exposure time **(Figure 24)**, cell cycle is disrupted significantly. Data reveals that significant increments on the percentage of cells in G1 with a decrease on the G2/M, affecting by the simulated microgravity for mid-term exposure compared with the external 1*g* control.

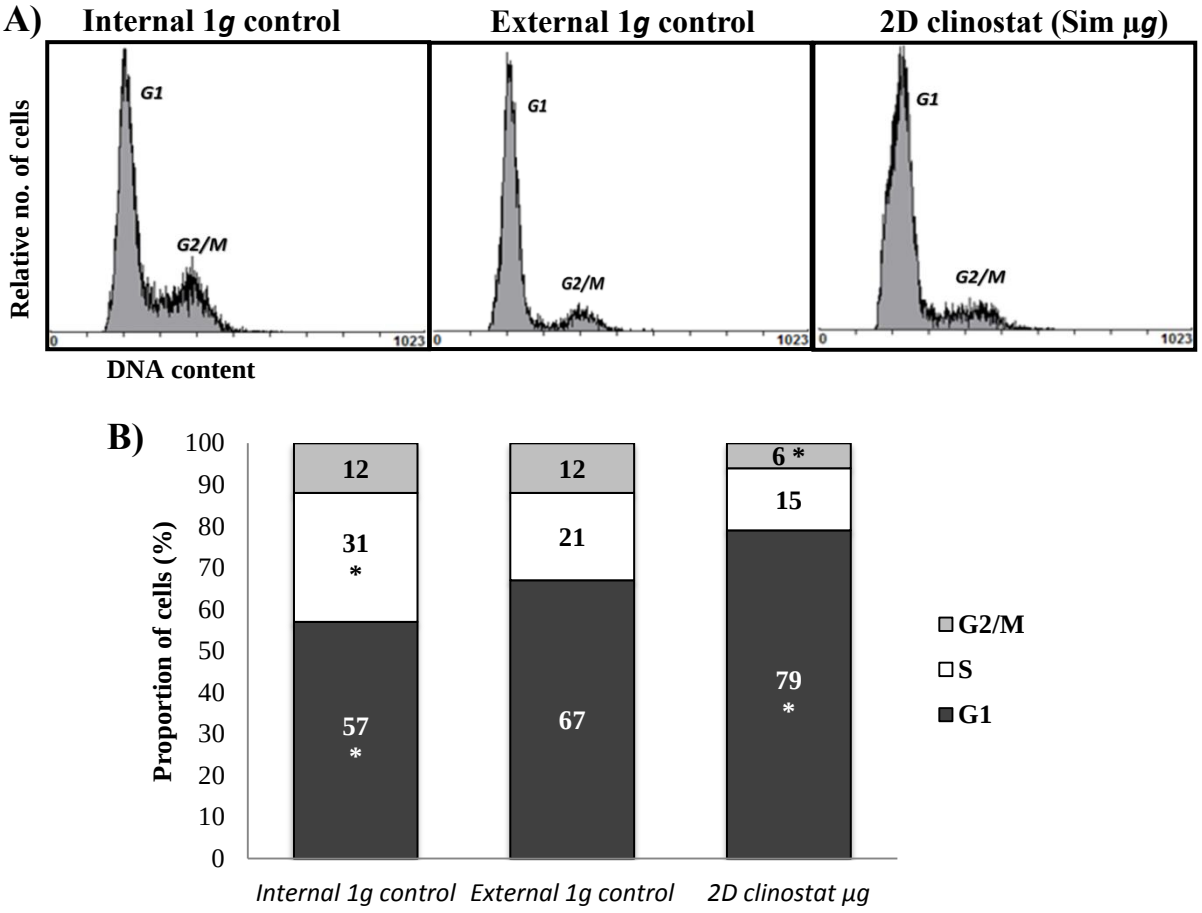

Figure 24: ***Arabidopsis*** **cell cycle phases affected by simulated microgravity (2D clinostat) and the controls for the mid-term experiment**. **A)** Flow cytometry analysis, each panel represents the relative number of cells according to the DNA content in each cell. First peak 2n reflects G1 phase and the second peak 4n reflects G2/M phase. **B)** DNA content histogram. Significant differences versus the external 1*g* control (in the same cell cycle phase) are shown, P-Value <0.05 (*).

On the other hand, cells are running up accumulating on S phase with a depletion of G1 cells proportion significantly under the internal 1*g* control compared with the external 1*g* control.

As a complementary approach for the cell proliferation studies, cell division rate was determined by estimating the mitotic index to evaluate the impact of simulated microgravity on *Arabidopsis* cell proliferation. The mitotic index was estimated by the proportion of cells stained with DAPI relative to metaphase/anaphase mitotic figures. **Figure 25** shows that, to increase the experimental exposure to simulated microgravity significantly reduced the mitotic index in both 2D-clinostat and the external 1*g* control.

1.1.2. Simulated Microgravity Influences *Arabidopsis* Cell Growth

Since the nucleolus is a reliable indicator of the cell growth in the proliferating cells (Medina et al 2000), we used a nucleolar protein, AtNucL1, to quantify the nucleolar area. Statistical analyses reveal that, the simulated microgravity alteration has not significance impact after a short term exposure compared with controls. When the exposure was longer, nucleolus area is significantly decreased under simulated microgravity, reaching statistically meaningful independently of the internal 1*g* control or the external 1*g* control **(Figure 26)**.

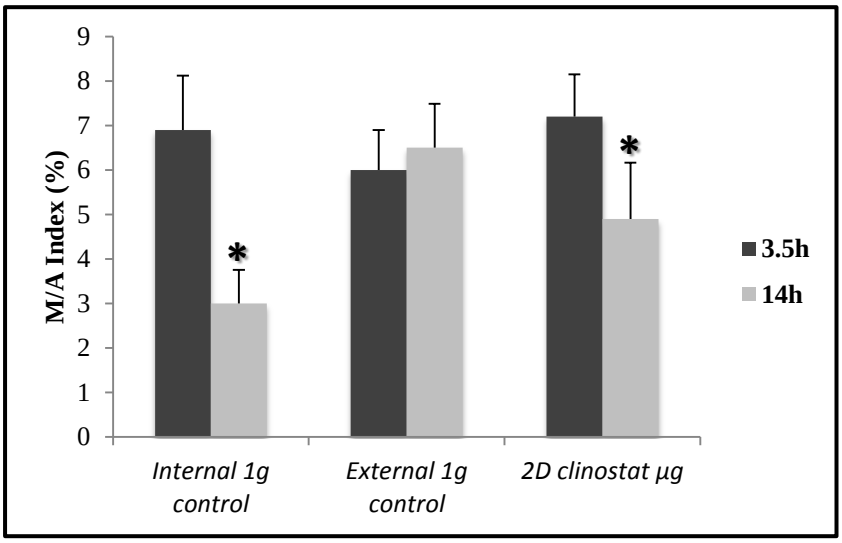

Figure 25: Cell division influenced by altered microgravity (2D clinostat) and other controls conditions for 3.5 and 14 hour experiments. Metaphase /Anaphase cells (M/A) index was determined as the proportion of mitotic cell per the rest of population. Significant difference versus the external 1*g* control (in the same exposure experiment) are shown, P-Value <0.05 (*).

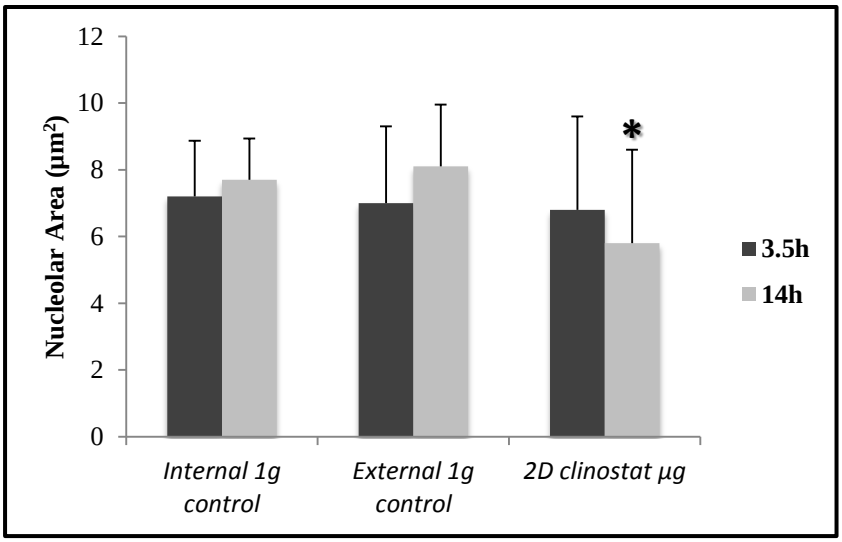

Figure 26: Nucleolar area is altered with altered microgravity (2D clinostat) and other control conditions for 3.5 and 14 hour experiment. More than 50 nucleolus area (α-nucleolin staining) of *Arabidopsis* cells were measured for each experiment conditions. Significant difference versus the external 1*g* control (in the same exposure experiment) are shown, P-Value <0.05 (*).

1.1.3. Cells Viability is Altered by Clinorotation and Its 1*g* Controls

To determine the number of viable cells present in our cell suspension altered through the clinorotation experiment, we used the Trypan blue dye exclusion. Cell viability test **(Figure 27)** reveals that, cell viability is not influenced by simulated microgravity (clinorotation) compared with the external 1*g* control (the standard control conditions explained by (Menges & Murray 2006) in both, short and mid-term experiments. On the other hand, internal 1*g* control condition has a deleterious influence on the viability of the cells, becoming statistically meaning in the mid-term experiment.

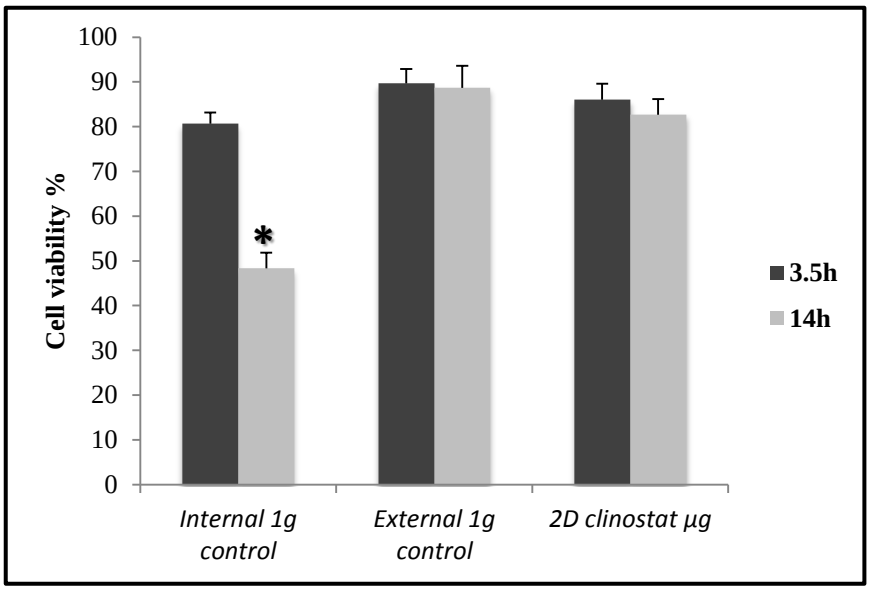

Figure 27: Cell viability under simulated microgravity (2D clinostat) and other control conditions for 3.5 and 14 hours experiment. Trypan Blue dye is used to determine the viable cells (stained cells reveal to dead cells). More than 100 cells were counted each experiment conditions for 3 different replicates. Significant difference versus the external 1*g* control (in the same exposure experiment) are shown, P-Value <0.05 (*).

1.2. USING DIAMAGNETIC LEVITATION AS A MULTIGRAVITY LEVEL SIMULATOR FOR GROUND STUDIES *(CELLS IN SUSPENSION)*

An alternative technology to investigate the impact of altered gravity, diamagnetic levitation, was used to simulate different gravity levels using *Arabidopsis* cell culture systems. 7 days-old cell suspensions were expose inside the magnet bore to different altered gravity levels (internal control (1g*), Mars gravity (0.37g*), simulated microgravity (unstable 0g*), and levitated microgravity (stable 0g*) for 3 hours (short term). Samples were recovered for different analysis:

- To investigate the impact of altered gravity by diamagnetic levitation on *Arabidopsis* cell proliferation.
- To investigate the impact of altered gravity by diamagnetic levitation on *Arabidopsis* cell growth.
- To confirm that plant cell suspension is actually levitating into a droplet.

1.2.1. Magnetically Altered Gravity Cause Little Effects on *Arabidopsis* Cell Proliferation on the Short Term

Distribution of the *Arabidopsis* cell cycle was determined by the means of flow cytometry. Results reveal insignificant differences among the altered gravity positions and the external 1g control **(Figure 28)**. Otherwise, **Figure 29** indicates a significant decrease in the mitotic index under simulated microgravity (0g* unstable and levitation) conditions compared with the external 1g control, while it does not reach the significance under the internal 1g* control or Mars (0.37g*) conditions.

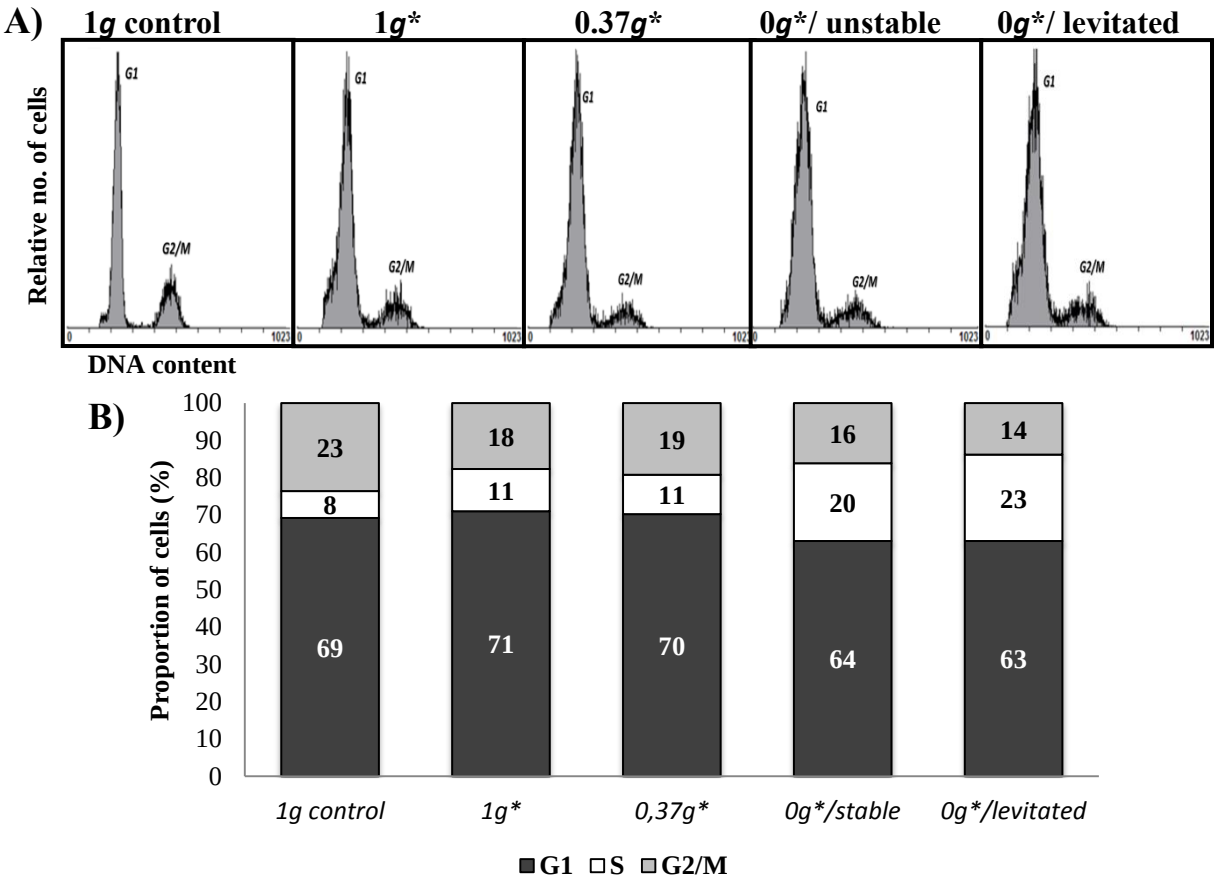

Figure 28: *Arabidopsis* cell cycle phase distribution after magnetic levitation experiment for 3 hours. **A)** Flow cytometry analysis, each panel represents the relative number of cells according to the DNA content in each cell. First peak (2n) reflects G1 phase and the second peak (4n) reflects G2/M phase. **B)** DNA content histogram.

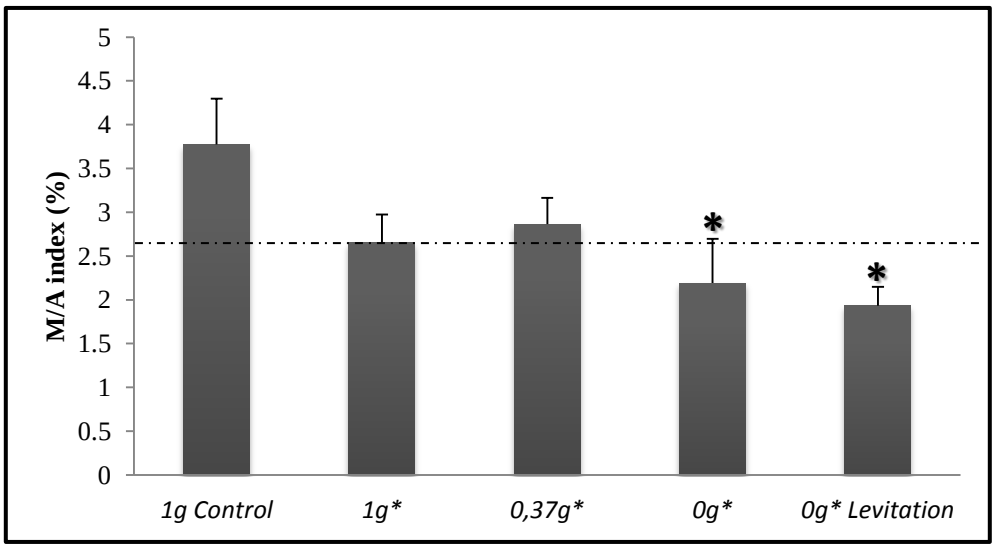

Figure 29: Cell division figures induced by magnetic levitation for 3 hours experiment. Metaphase /Anaphase cells (M/A) index was determined as the proportion mitotic cell per the rest of population. Significant differences versus the external 1*g* control are shown, P-Value <0.05 (*). (*) in *g* levels refers to the magnetic field induced this simulated gravity. A baseline effect of the magnetic field at the 1*g** position is indicated with a horizontal line.

1.2.2. *Arabidopsis* Cell Growth is Barely Influenced by Short term exposure to Diamagnetic Levitation

Nucleolus area, staining with AtNucL1 was used, in order to detect the effect of altered gravity levels generated by diamagnetic levitation on the *Arabidopsis* cell growth and nucleolar activity. Data **(Figure 30)** reveals a general reduction in all magnetic field samples versus the external 1*g* control, but the nucleolus area reduction is significant only under the unstable altered microgravity (0*g**/unstable) compared with the external 1*g* control.

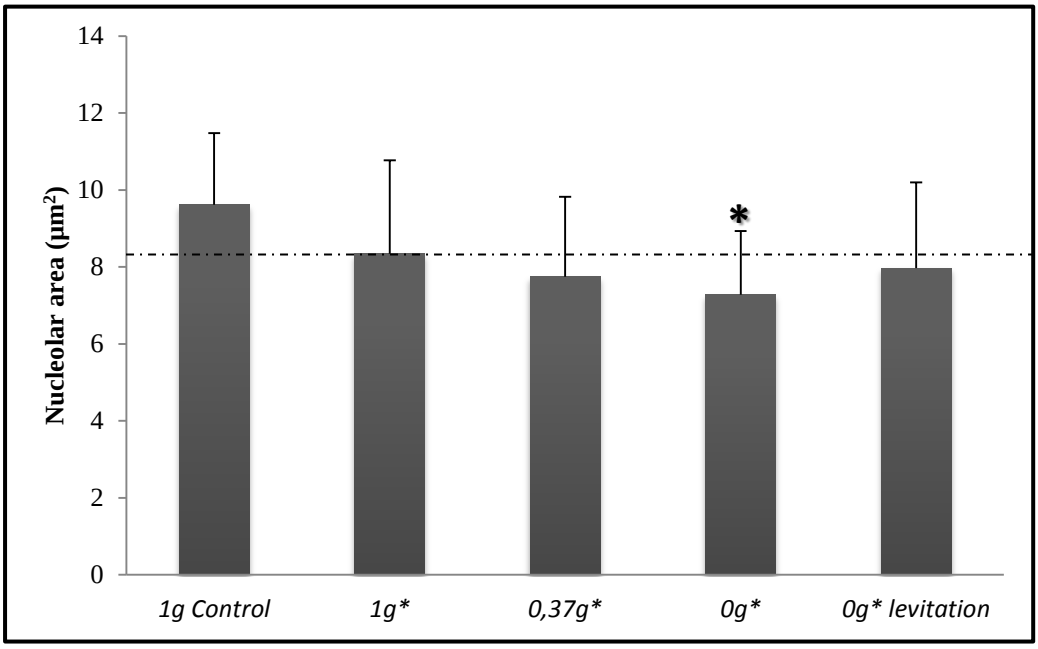

Figure 30: Nucleolar area under magnetic levitation 3 hours experiment. More than 50 nucleolus areas (α-nucleolin staining) of *Arabidopsis* cells were measured for each experimental condition. Significant differences versus the external 1*g* control are shown, P-Value <0.05 (*). (*) in *g* levels refers to the magnetic field induced this simulated gravity. A baseline effect of the magnetic field at the 1*g** position is indicated with a horizontal line.

1.2.3. 0*g** Levitation Simulated Microgravity: Do Cells Levitate Inside the Levitated Suspension Droplet?

It was reported a successful levitation of water droplets using magnetic levitation as a microgravity simulator (Liu et al 2010b). Levitation of complex non-uniform material, such as biological organisms is due to the interaction of the magnetic field with an average diamagnetic susceptibility of the subject. Biological entities, including living things, mostly consist of diamagnetic molecules such as water, and thus can be levitated using an appropriate magnetic field. Indeed, magnetic levitation of live frog, grasshoppers, *Arabidopsis* seedling and other biological systems have been demonstrated (Guevorkian & Valles 2004, Manzano et al 2013, Simon & Geim 2000, Valles et al 2005). In particular, it is interesting to distinguish if magnetic levitation can be applied to individual cells in suspension within a cell culture droplet using the magnetic levitation point of water or the cells are experiencing a differential magnetic force than the surrounding media leading to sedimentation of the cells.

Arabidopsis cells suspension droplet was installed inside the magnet bore to stabilize the levitation (0*g** stable levitation position). Then video record **(http://youtu.be/7vBiSZ7QNyQ)** and image management was performed front the top of the magnetic bore in order to discern the levitation of the cell suspension into the drop. In a first view the cells seems to be uniformly distributed into the drop, but we decided to take advantage of a side mirror **(Figure 31A)** to observe at the same time a top and a lateral view of the levitating droplet. *Arabidopsis* cell suspension droplet was introduced into the levitation region, showing floating in air and then stable levitation **(Figure 31B1, B2).** Increase of the magnetic force up to 16T, exclude the cell suspension droplet out of the magnet bore or stuck the bore wall after escaping out of the levitation zone **(Figure 31B3)**. When the suspension droplet levitates at the level of the lateral mirror **(Figure 31B4)** it is shown that cells are not equally distributed into the drop neither in the center of the drop but they are sediment in the bottom of the levitated drop. The magnet remained fully charged at the level as for the water drop levitation, i.e., 10.1 and 13T. The cells movements inside the levitated drop are clearly displayed that the cells are not experiencing a magnetic levitation force strong enough to remain in suspension. From time to time, it is observed some individuals cells seemed of being levitated **(Figure 31B5)**, but most of the cells are sediment.

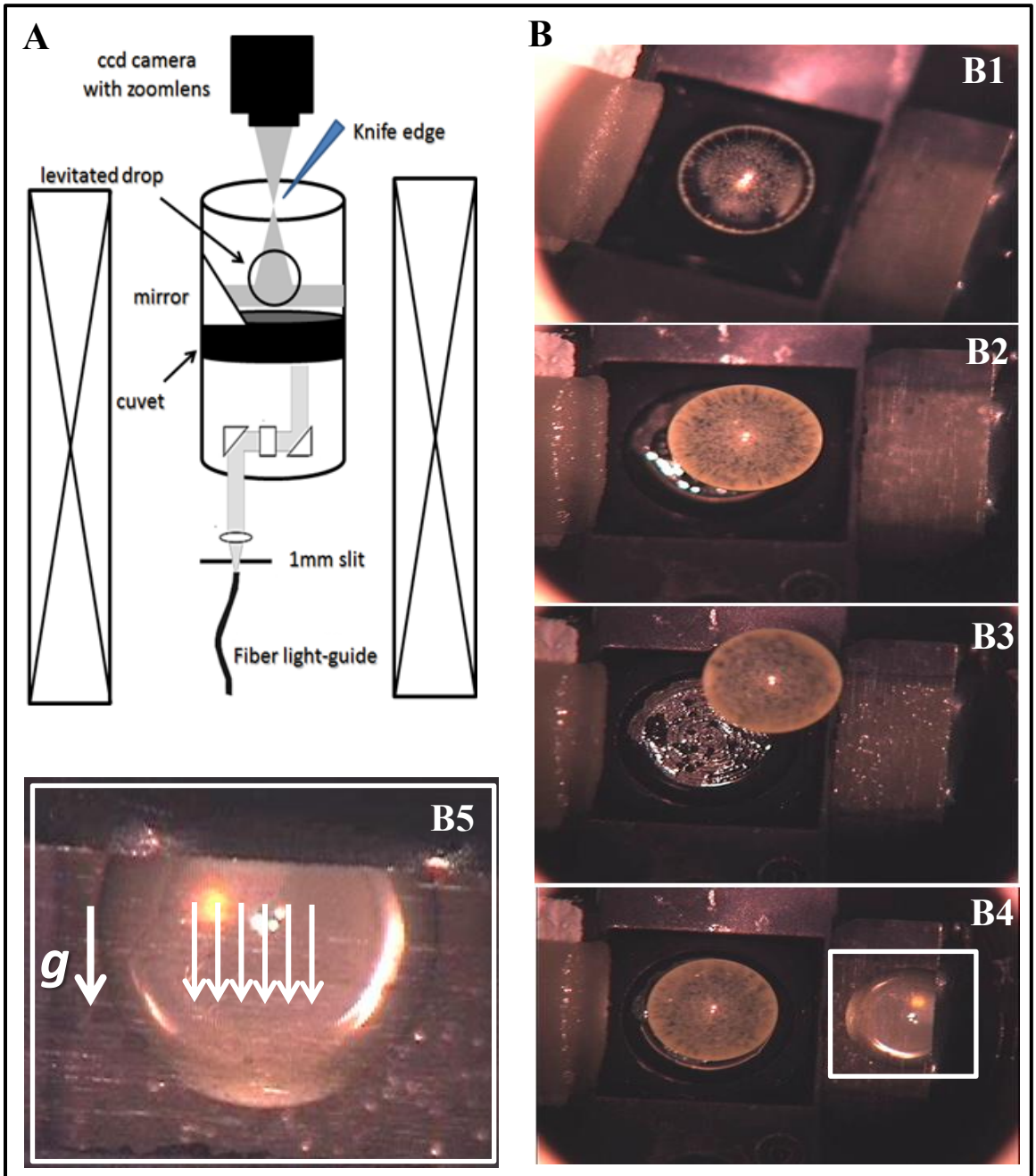

Figure 31: *Arabidopsis* cell suspension droplet levitation. Cell droplet is levitated using diamagnetic levitation instrument. **A)** Experimental design for the droplet levitation video record using a side mirror for the 2D video record. **B)** Cell droplet images extracted from the video (http://youtu.be/7vBiSZ7QNyQ) show different statement of the droplet levitation and the cells behavior during the levitation.

1.3. USING RPM AND LDC TO SIMULATE MICROGRAVITY, PARTIAL GRAVITY, AND HYPERGRAVITY FOR CELLULAR SYSTEMS (IMMOBILIZED CELLS IN AGAROSE)

Since previous attempts to obtain simulated microgravity suitable for the plant cellular system was not completely satisfactory, we prepared an alternative method to simulate different gravity levels such as simulated microgravity (Sim μ*g* using RPM) and hypergravity (2*g* using LDC). Recently, these facilities have been improved to produce partial gravity such as the Moon (0.17*g*) and Mars (0.37*g*) levels using two alternative paradigms (RPM^{HW}, and RPM^{SW}). Using such simulators provides us a new challenge of using cells in suspension because of immobilization requirements and the flooding problem. Thus, we aim in this part:

- To validate a new biological cellular systems used in these simulators without the flooding problem.
- To distinguish the differences of using the partial *g* RPM paradigms: Hardware (RPM^{HW}) or Software (RPM^{SW}) driven.

1.3.1. Embedding Cells In Agarose as A Suitable Biological System Used for The RPM and LDC Simulators

In order to use different GBF such as RPM and LDC in the plant cellular system experiments, it was important to immobilize the cells and to avoid the flooding problems which occur in the suspension cultures. *Arabidopsis* cell suspension were embedded in low melting agarose **(Figure 32A)** to immobilize the cells according to (Sieberer 2009) to be used in the coming experiments using the RPM and LDC.

Different tests were performed to check the viability of using immobilized cells in order to define whether or not it has an impact on the viability of the cells due to mechanical stress or containment on the cells. Embedding cells in agarose does not affect the cell morphological shape compared with the reference control **(Figure 32B).**

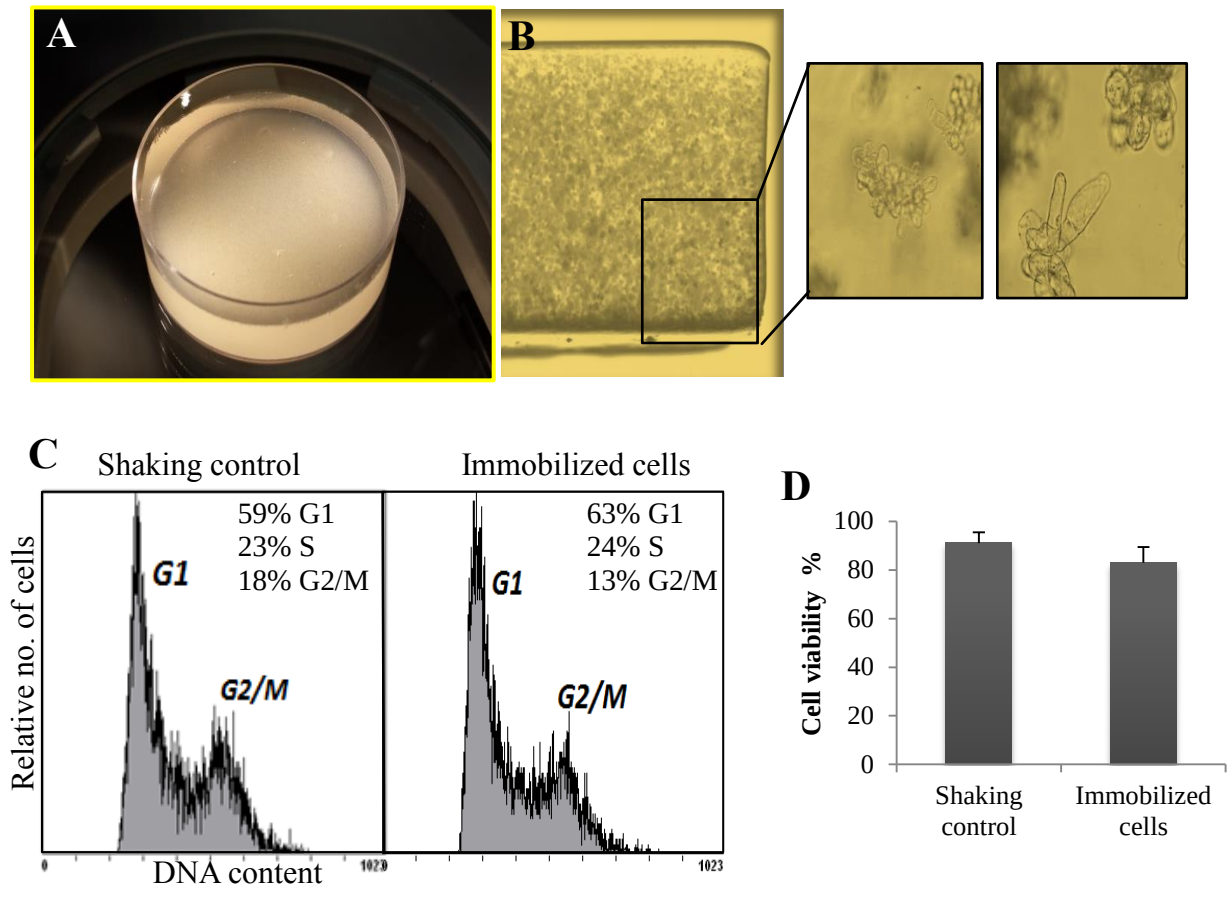

Figure 32: Immobilized cells in Agarose. *Arabidopsis* cells suspension were embedded in low melting agarose. **A)** Cell embedded in agarose in the experimental plate for 24 hours. B) Morphological status of the cells embedded in agarose after 24 hours. **C)** Cell cycle analysis by flow cytometry in a comparison with the standard shaking control. **D)** Cell viability test using Trypan blue dye.

Furthermore, the distribution of the cell cycle phases after 24 hours of immobilization in agarose is not significantly altered compared with the standard shaking control conditions. Cell viability rate was also determined to validate our system; reflecting that immobilization did not produced significant differences compared with the standard control after 24 hours.

1.3.2. Using Different RPM Paradigms for Lunar and Martian Partial Gravity

Two ways to induce a net partial gravity level, similar to the Moon ($0.17g$) or Mars ($0.37g$), are available at the Random Position Machine (RPM); based on neutralize gravity first (RPM) and apply the partial gravity with a built-on centrifuge (RPM^{HW}) or by partial neutralization of $1g$ by software (RPM^{SW}). Here we are going to distinguish the differences between using RPM^{HW} and RPM^{SW} for 3 (short term), 14 (mid-term), and 24 hours (long term) experiments. *Arabidopsis* cell cycle phases distribution is similarly influenced by RPM^{SW} and RPM^{HW} in both, the Moon and Mars conditions **(Figure 33)**. Exceptionally, using RPM^{HW} for Mars gravity level alters the distribution of cell cycle significantly compared with the use of RPM^{SW} for mid-term experiment, in which cells are accumulated in G2/M phase compared with the alternative one in RPM^{SW}. Furthermore, partial gravity, the Moon and Mars using (RPM^{SW} and RPM^{HW}) shows insignificant differences on the alteration on the nucleolus area **(Figure 34)**. Similarly, only one significant difference was detected on the nucleolus area when use of RPM^{SW} to induce Mars gravity level for the long term experiments compared with the use of RPM^{HW}.

Finally, it seems that using RPM^{SW} and RPM^{HW} for the Moon gravity made no differences, while there are variations (2/3 of the results are validated) for the Mars gravity simulation. Thus, due to the limitations in the number of experiments we can perform simultaneously, and the small differences observed between RPM^{SW} and RPM^{HW} paradigms; the more reliable simulator will be used for the Mars gravity, RPM^{SW}, while the remaining RPM^{HW} is going to be used to induce the Moon gravity level.

1.3.3. Impact of Different Gravity Levels on *Arabidopsis* Cell Proliferation

Expose *Arabidopsis* cells to different gravity levels, disrupts the cell cycle. Distribution of the proportion of cells through the cell cycle phases is disrupted also by the exposure duration in the different gravity levels. Results **(Figure 33)** indicate that, among different gravity levels, there are no significant alterations on the distribution of the cell cycle for the short term exposure.

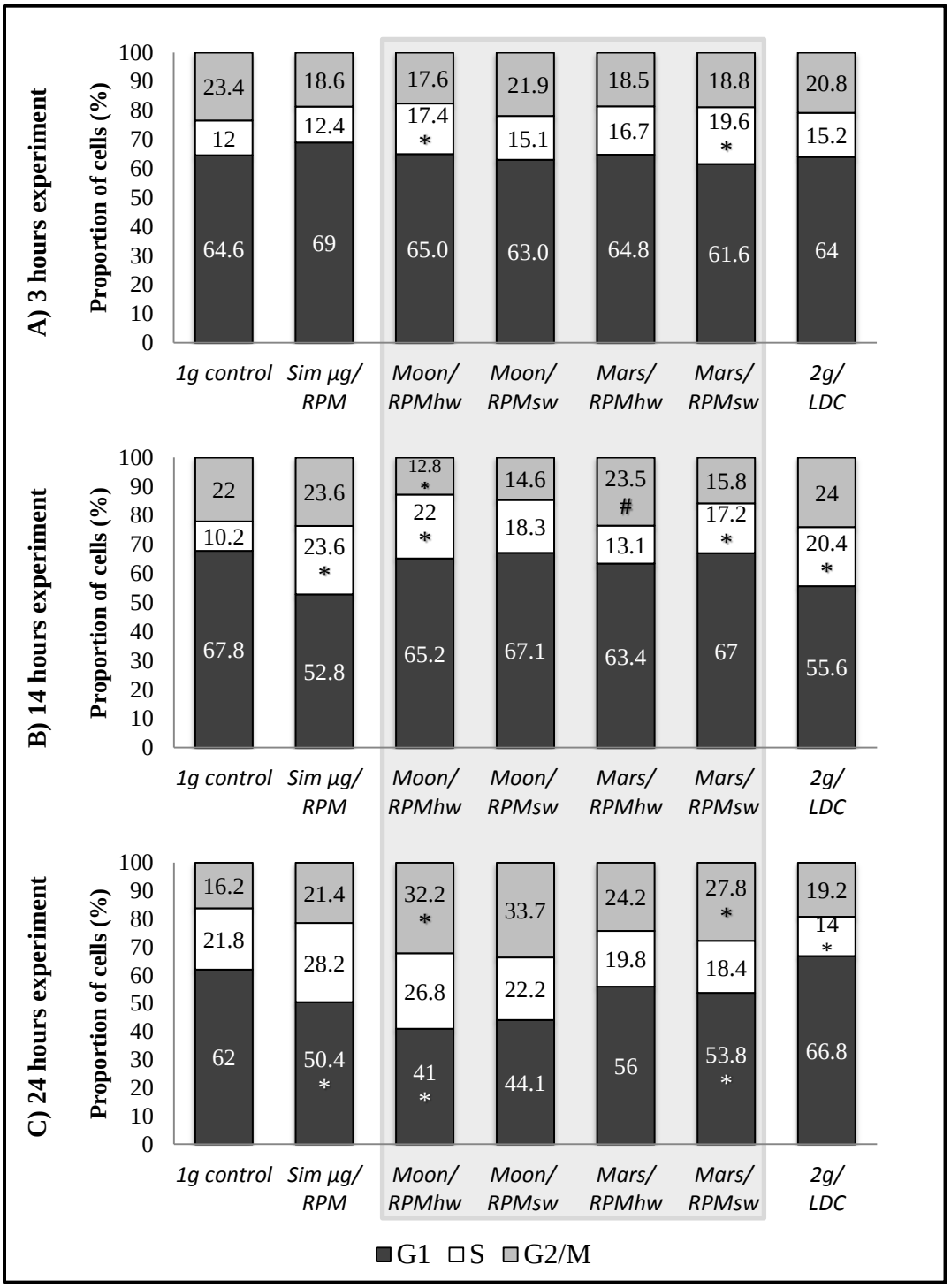

Figure 33. ***Arabidopsis*** **cell cycle phases distribution under** simulated microgravity (Sim µ*g*/RPM), partial gravity (0.17*g*/ the Moon and 0.37*g*/Mars) using (RPM, Hardware (RPM^{HW}) and software (RPM^{SW})), and hypergravity (2*g*/LDC) compared with 1*g* control for different experimental durations **A)** Short term (3 hours). **B**) Mid-term (14 hours). **C)** Long term (24 hours). DNA content histogram is obtained by flow cytometry analysis. Total DNA content is around 100%. G1 peaks present the percentage of cells in G1 and as the same the G2/M peaks. The rest of the 100% is considered the S phase percentage in indirect estimation. Significant differences are shown versus 1*g* control, P-Value <0.05 (*). Gray shadow part displays the comparison between RPM^{HW} and RPM^{SW} in the partial *g* simulation; significant differences within the same gravity level are shown, P-Value <0.05 (#).

Slightly indication for a significance increment on the proliferated cells on S phase is observed on the Moon and Mars condition compared with the 1*g* control. By extend the exposure time up to 14 hours (*Arabidopsis* cell cycle is approximately 24 hours), significant alterations are detected. Simulated microgravity (µ*g* /RPM) alters cell cycle phases distribution compared with the 1*g* control. Significant increments are detected on the S phase population (23.6%), with a depletion on the proportion of cells in G1 (52.8%) compared with 1*g* control (10.2% and 67.8%, respectively). Continuously, the Moon and Mars conditions alter the cell cycle by increasing the proliferating cells in S phase (17.2%, and 22%, respectively). Hypergravity condition shows the same effect of the simulated microgravity and the partial gravity, enhances the proportion of proliferating cells in S phase (20.4%) by significant depression of cells on G1 (55.6%), versus the 1*g* control. Long term experiments show an extreme influence of changing the gravity levels on the cell cycle phases distribution. Simulated microgravity and partial gravity conditions show the same influence, significantly increment on the G2/M cell population (21.4%, 32.2%, and 27.8, respectively) compared with the 1*g* control (16.2%). In addition, proportion of cells in G1 is running down among the simulated microgravity and partial gravity conditions through the exposure duration. Number of cells in G1 is depleted after long term exposure (Sim µ*g* (50.4%), the Moon (41%), Mars (53.8%)) compared with mid-term (52.8%, 65.2%, 67%, respectively) and short term (69%, 65%, and 61.6%). Moreover, it is significantly noticed compared with the 1*g* control for long term experiment (62%). Proportion of S phase *Arabidopsis* cells is significantly lessening (14%) and starting to accumulate in G2/M (19.2%) insignificantly after long term exposure under hypergravity condition compared with the 1*g* control (21.8%, and 16.2%, respectively). Hypergravity condition shows insignificant increase on the population of cells on G2/M compared with the 1*g* control.

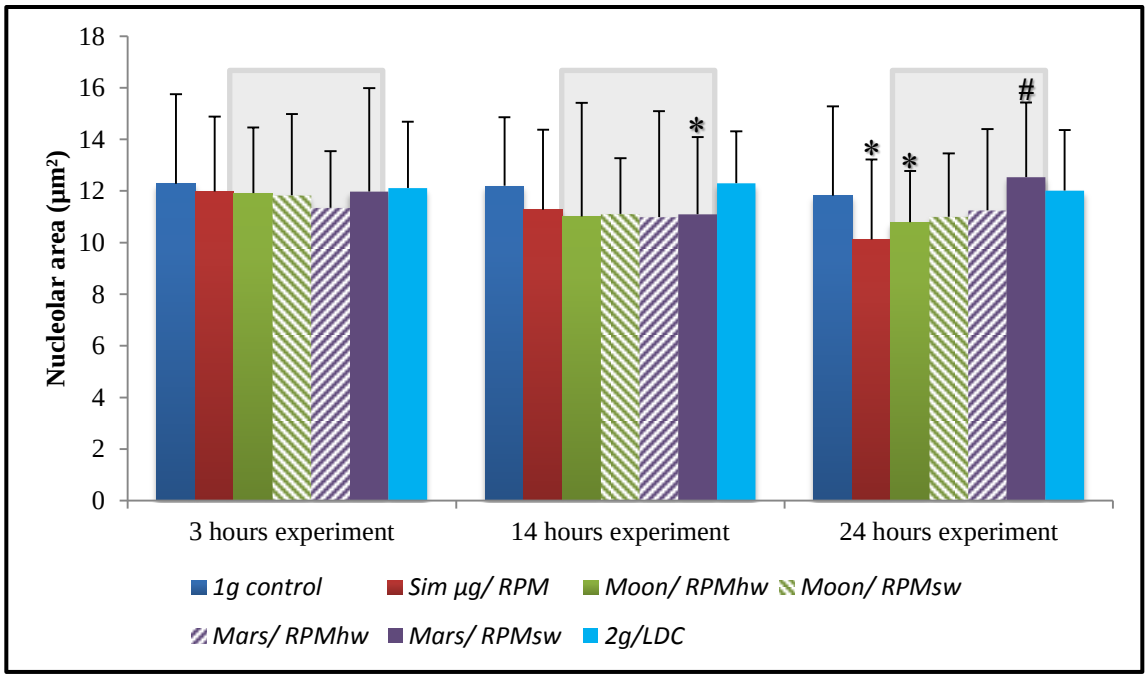

Figure 34: Nucleolar area under simulated microgravity (Sim µ*g*/RPM), partial gravity (0.16*g*/ the Moon and 0.37*g*/Mars) using (RPM, Hardware (RPM^{HW}) and software (RPM^{SW})), and hypergravity (2*g*/LDC) compared with 1*g* control for different experimental durations; 3 hours, 14 hours, 24 hours. More than 50 nucleolus area (α-nucleolin staining) of *Arabidopsis* cells were measured for each experiment conditions. Significant differences are shown versus the 1*g* control in the same exposure experiment, P-Value <0.05 (*). Gray shadow part displays the comparison between RPM^{HW} and RPM^{SW} in the partial *g* simulation RPMs; significant differences within the same gravity level are shown, P-Value <0.05 (#).

1.3.4. Impact of Different Simulated Gravity Levels on *Arabidopsis* Cell Growth

Exposing *Arabidopsis* cultures to different gravity levels produces an impact on the nucleolus area. Results obtained from **Figure 34** supports that; short exposure experiment for 3 hours has not enough influence to modify the nucleolus area. Increase the exposure duration up to 14 hours experiment has an impact on the nucleolus area. Data **(Figure 34)** indicates, there are decreases on the nucleolar area affected by the simulated microgravity, the Moon and Mars conditions. Nevertheless, it is only significant decrease on Mars condition compared with the 1*g* control. Hypergravity condition shows no differences compared with the 1*g* control. Expose to long term exposure shows deeper alterations on the nucleolus area. There are significant depletions on the nucleolus area under simulated microgravity and the Moon conditions compared with the 1*g* control. However, it is not significantly decrease on Mars condition. So, the impact of hypergravity is not enough to alter the nucleolus area compared with the 1*g* control.

1.4. CHAPTER 1: RESULTS SUMMARY

Table 6: Chapter 1: results summary in a comparison with 1*g* control. Using of the pipette clinostat and the magnetic levitation as a microgravity simulators. Results summary reveal that, simulated microgravity (Clinorotation) alters the distribution of the cell cycle in mid-term experiments. While short term is not enough to alter the cells. Internal 1*g* control is not valid to be used, as the cell viability is reduced due to the nutrients lack.
Simulated microgravity induced by the magnetic levitation alters the nucleolar activity and reduces the mitotic index.

	Short term (3 hours)			**Mid-term (14 hours)**		
Pipette clinostat	Cell cycle	Nucleolar activity	Cell viability	Cell cycle	Nucleolar activity	Cell viability
Clinorotation µ*g*	=	=	=	alter	--	=
Internal 1*g*	=	=	=	alter	=	--
Magnetic levitation	Cell cycle	Nucleolar activity	Mitotic index	Cell cycle	Nucleolar activity	Cell viability
1*g**	=	=	=			
0.37*g**	=	=	=			
0*g**	=	--	--			
Levitation 0*g**	=	=	--			

Table 7: Chapter 1: Results Summary. **A)** Validation the use of different mode of operation to induce partial gravity. It is noticed that, there is no significant difference of the use of the hardware or software in the Moon gravity simulators, while it was difference on the Mars conditions. **B)** Altered gravity has an influence on the cell proliferation and cell growth through the exposure time. Cell cycle is altered significantly on the mid and long term experiments. While 24 hours is enough to reduce the nucleolar activity significantly in the hypogarvity levels. In particular; increase the exposure time, increase the influence of the altered gravity.

	Short term (3 hours)		**Mid-term (14 hours)**		**Long term (24 hours)**	
A) RPM^{HW} *VS* RPM^{SW}	Cell cycle	Nucleolar Activity	Cell cycle	Nucleolar Activity	Cell cycle	Nucleolar Activity
The Moon	=	=	=	=	=	=
Mars	=	=	alter	=	=	alter
B) Altered gravity levels *VS* 1*g*	Cell cycle	Nucleolar Activity	Cell cycle	Nucleolar Activity	Cell cycle	Nucleolar Activity
Sim µ*g* RPM	=	=	alter	=	alter	--
0.17*g* the Moon	alter	=	alter	=	alter	--
0.37*g* Mars	alter	=	alter	--	alter	--
2*g* LDC	=	=	alter	=	alter	=

RESULTS

CHAPTER 2: *ALTERED GRAVITY EFFECTS ON ARABIDOPSIS CELL CULTURES PROLIFERATION AND GROWTH*

2.1. Reduced Gravity Levels Increase The Subpopulation Of Cells Replicating DNA (*Rapid Detection Of S Phase Using EdU Labelling Assay*)

2.2. Nucleolus Structure And Activity Is Influenced By The Gravitational Alteration

2.3. Altered Gravity Influence at the Protein Expression Level

2.4. Altered Gravity Influence at The Gene Expression Level

2.5. Altered Gravity Disrupts Co-localization Of Our Marker Proteins; Analysis of Multicolor Confocal Immunofluorescence Microscopy Images

CHAPTER 2: ALTERED GRAVITY EFFECTS ON ARABIDOPSIS CELL CULTURES PROLIFERATION AND GROWTH

Once established the usefulness of the immobilization procedure to provide a system compatible with the altered gravity facilities, but the limited success in the observation of cell growth and cell proliferation rates with our lab classical approaches, we decided to use more elaborated techniques with the pretested conditions. *Arabidopsis* cell culture will be exposed to different RPM operation modes (simulated microgravity (μ*g*), the Moon (0.17*g*) condition using RPM^{SW} (RPM operated by software), Mars (0.37*g*) condition using RPM^{HW} (RPM operated by hardware)) and LDC (hypergravity (2*g*)) to be compared with 1*g* control. ***Experiment 3*** and ***Experiment 4*** were performed for 3 (short term), 14 (mid-term), and 24 hours (long term experiments):

- To investigate the impact of altered gravity levels on *Arabidopsis* cell proliferation.
- To investigate the impact of altered gravity on *Arabidopsis* cell growth.
- To investigate the impact of altered gravity on the epigenetic modifications; DNA methylations and histone H4 acetylation.

2.1. REDUCED GRAVITY LEVELS INCREASE THE SUBPOPULATION OF CELLS REPLICATING DNA (RAPID DETECTION OF S PHASE USING EDU LABELLING ASSAY)

Using EdU ¨5-ethynyl-2´deoxyuridine¨ labelling assay is a rapid and robust assay for detection of S phase, a superior alternative to other existing S phase assays including the indirect flow cytometry determination by DNA content (cells neither in G1 nor G2/M periods by DAPI staining) performed earlier. Under ***Experiment 4*** conditions, cells were incubated in EdU labeling assay for 2 hours before the end of each experiment (by stopping the machines no more than 2 min to add the drug). Samples were collected and frozen for the chemical click reaction of the EdU assay.

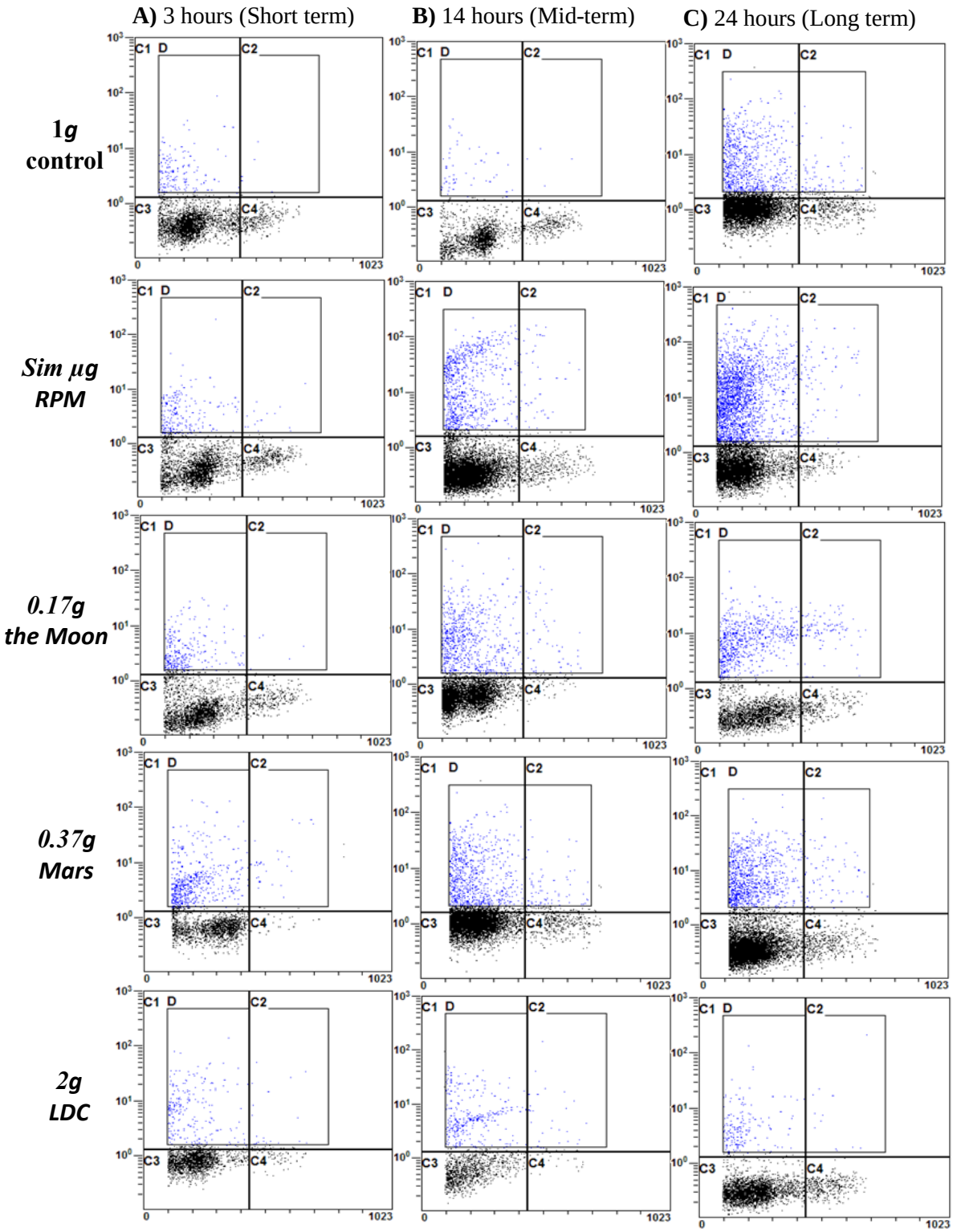

Figure 35: Cell cycle analysis with EdU labelling using flow cytometry. Effect of altered gravity levels; simulated µ*g*/RPM, the Moon, Mars and hypergravity on *Arabidopsis* proliferating cells (EdU labelling for S-phase detection) during **A)** 3, **B)** 14, and **C)** 24 hours experiment, compared with 1*g* control. Biparametric dot-plot analysis of Alexa Fluor 488-EdU intensity (logarithmic scale) versus DNA content (DAPI intensity). Background signal was sited (C3, and C4). Labeled cells sited in Blue, and the Non-labeled cells in Black. Scatter D represents all cells labeled with Edu

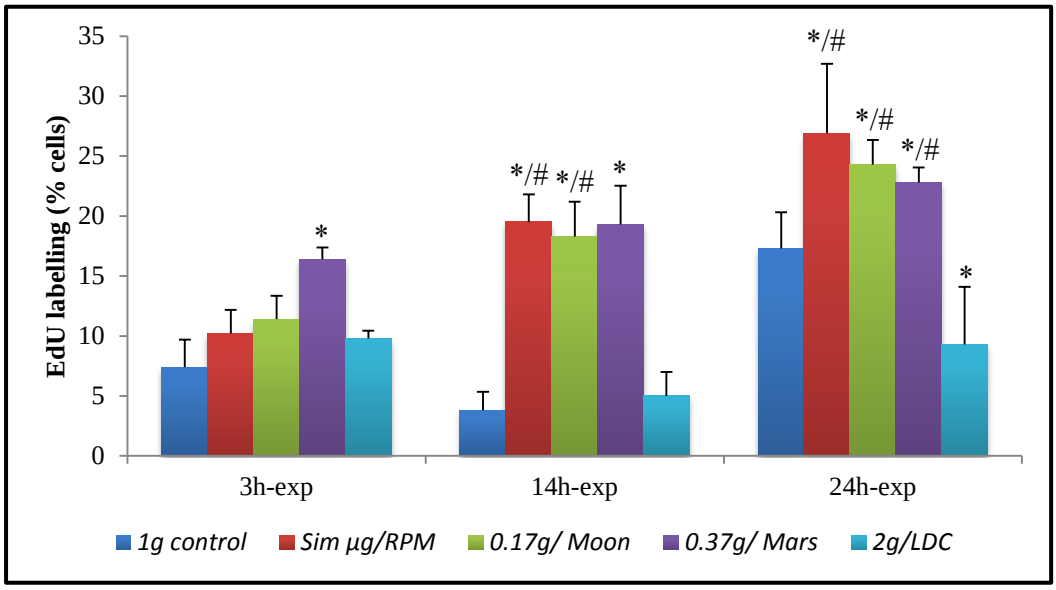

Figure 36: Precise determination of S phase cell subpopulation after short, mid and long-term exposures to altered gravity. EdU labelling (S phase labelling) percentage (Cells labelled in D plot in the bio-parametric dot plot analysis). Cells were exposed to different altered gravity level; 1*g* control, Sim µ*g*/RPM, 0.17*g*/Moon, 0.37*g*/Mars, and 2*g*/LDC for three exposure durations 3 (short term), 14 (mid-term), and 24 hours (long term). Significant variations by gravity level (P-Value < 0.05, ***** versus 1*g* control at the same exposure experiment) and by exposure time (**#,** versus same gravity level at short-term experiment) are shown.

Results show an increase in the S phase subpopulation of cells through the exposure time. **Figures 35, 36A** represent increments on the percentage of cells under replication after short term exposure to different altered gravity level, simulated microgravity, the Moon, and Mars conditions, whereas the percentage of labelled cells is significantly increased only under Mars conditions compared with the 1*g* control. By increasing the exposure time, the significance of the differences is increased in all the reduced gravity samples (simulated microgravity, the Moon and Mars conditions) compared with the 1*g* control during both mid- and long-term experiments and significantly compared with the same conditions after the short term (3 hours). Hypergravity samples show little variations on the number of replicating cells at any time, only appearing a significantly decrease in the long term experiment (24 hours) compared with the 1*g* control.

2.2. NUCLEOLUS STRUCTURE AND ACTIVITY IS INFLUENCED BY THE GRAVITIONAL ALTERATION

Different structural models for proliferating cells nucleolus in *Arabidopsis* cell cultures were proposed; vacuolated, compacted and fibrillar nucleolus in decreasing order of activity **(Figure 12)** (Manzano 2011). When easily determined nucleolus size does not provide consistent data ***(chapter 1)***, nucleolar activity is strictly correlated to the distribution of nucleolar structure models and supports the relation between cell proliferation and ribosome biogenesis under the gravitational alteration.

In ***Experiment 3***, the distribution of the nucleolus models varies under the influence of the gravitational alteration through the exposure time. Results **(Figure 37)** reveal that exposing cells to short term gravitational alteration reduces the percentage of nucleolus structural models of higher activity. Compacted nucleolus is the major structural model distributed in the cell population under 1g control and the other gravity levels. The Moon condition enhances the percentage of the vacuolated nucleolus distribution compared with the 1g control. Gravitational alterations decrease the nucleolar activity, it is noticed that, the inactive nucleolus distribution is increased under the gravitational alteration; hypogravity and hypergravity compared with the 1g control.

Furthermore, in the mid-term samples the effects are deeper, especially in the simulated microgravity and hypergravity samples **(Figure 38).** Results reveal that gravity alterations increase the distribution of the inactive nucleolus models significantly compared with the 1g control accompanied with a low level of vacuolated nucleolus. This alteration is maximized after long term exposure **(Figure 39)**, when more than half of the nucleolus shows a fibrillar/inactive structure with almost no vacuolated nucleolus in altered gravity samples.

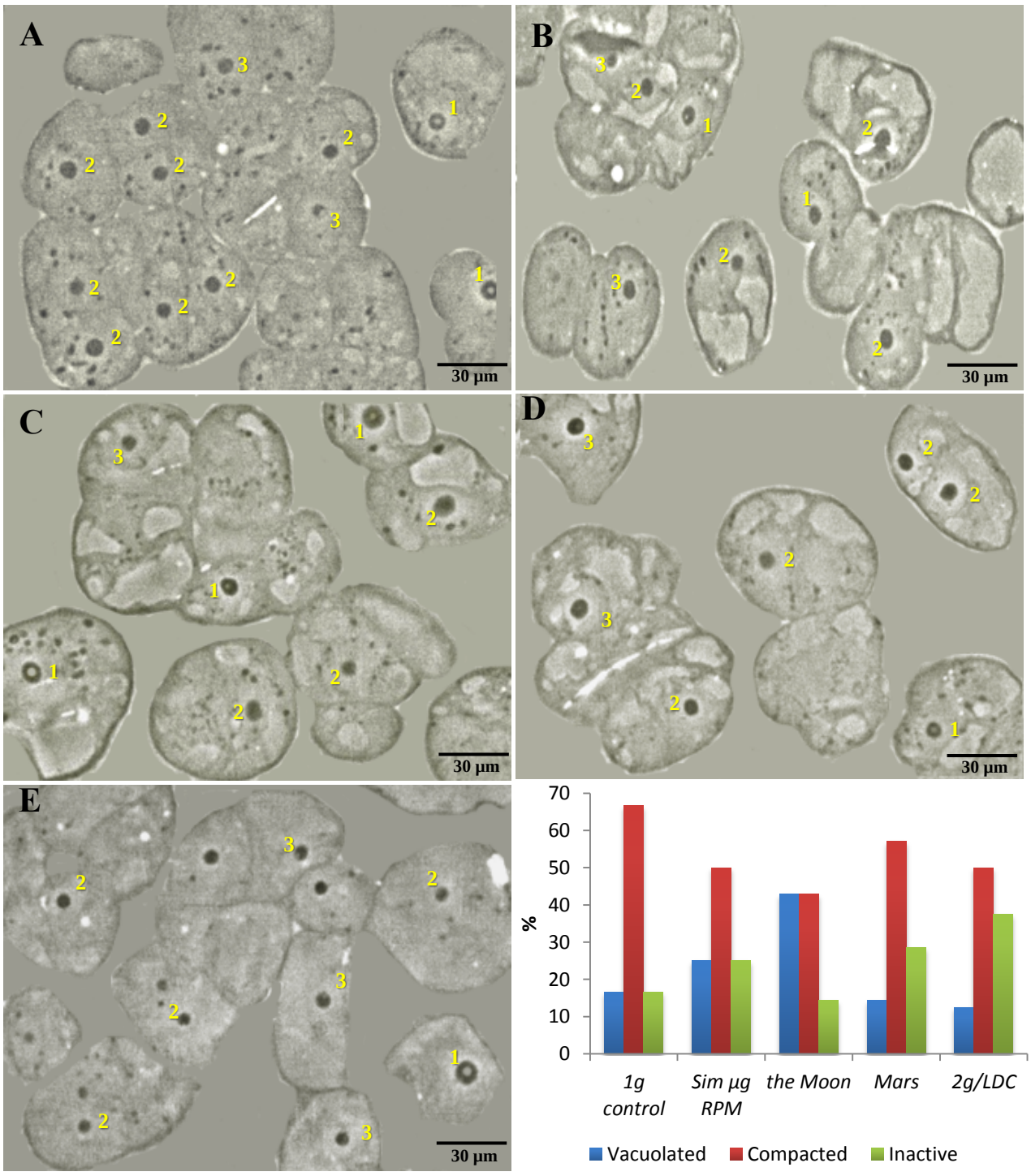

Figure 37: Gravity alteration on the nucleolus structure models distribution for the short term exposure (3 hours). A) 1*g* control, **B)** Sim µ*g* RPM, **C)** the Moon, **D)** Mars, **E)** 2*g* LDC. Nucleolus structure models are observed using the microscope in the contrast phase as defined by (Manzano et al In Press), (1) Vacuolated, (2) Compacted, (3) Inactive. Cells were expose to different. % of the nucleolus model distribution is estimated according to the total number of the nucelolus observed.

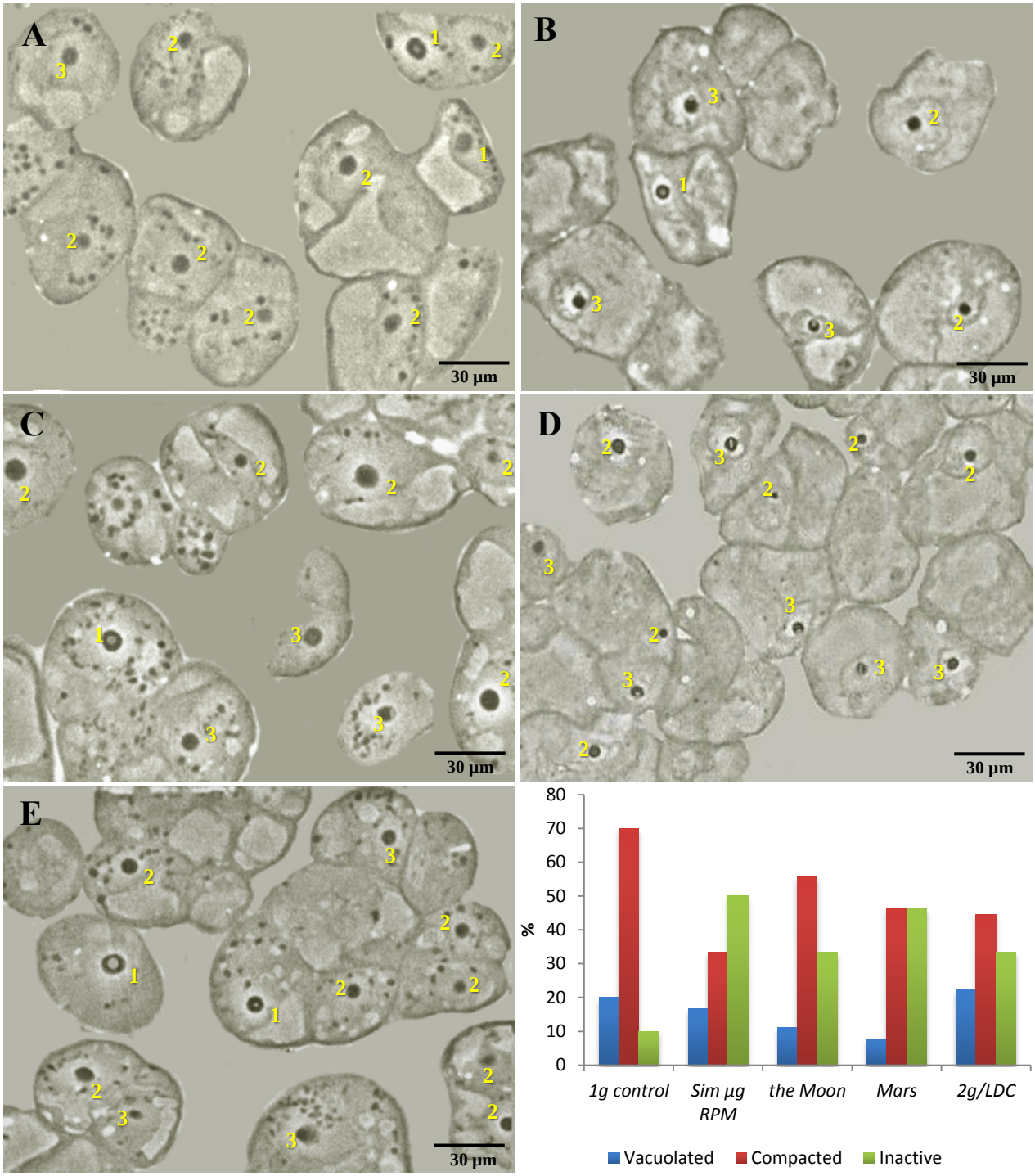

Figure 38: Gravity alteration on the nucleolus structure models distribution for the mid-term exposure (14 hours). A) 1*g* control, **B)** Sim µ*g* RPM, **C)** the Moon, **D)** Mars, **E)** 2*g* LDC. Nucleolus structure models are observed using the microscope in the contrast phase as defined by (Manzano et al In Press), (1) Vacuolated, (2) Compacted, (3) Inactive. Cells were expose to different. % of the nucleolus model distribution is estimated according to the total number of the nucelolus observed.

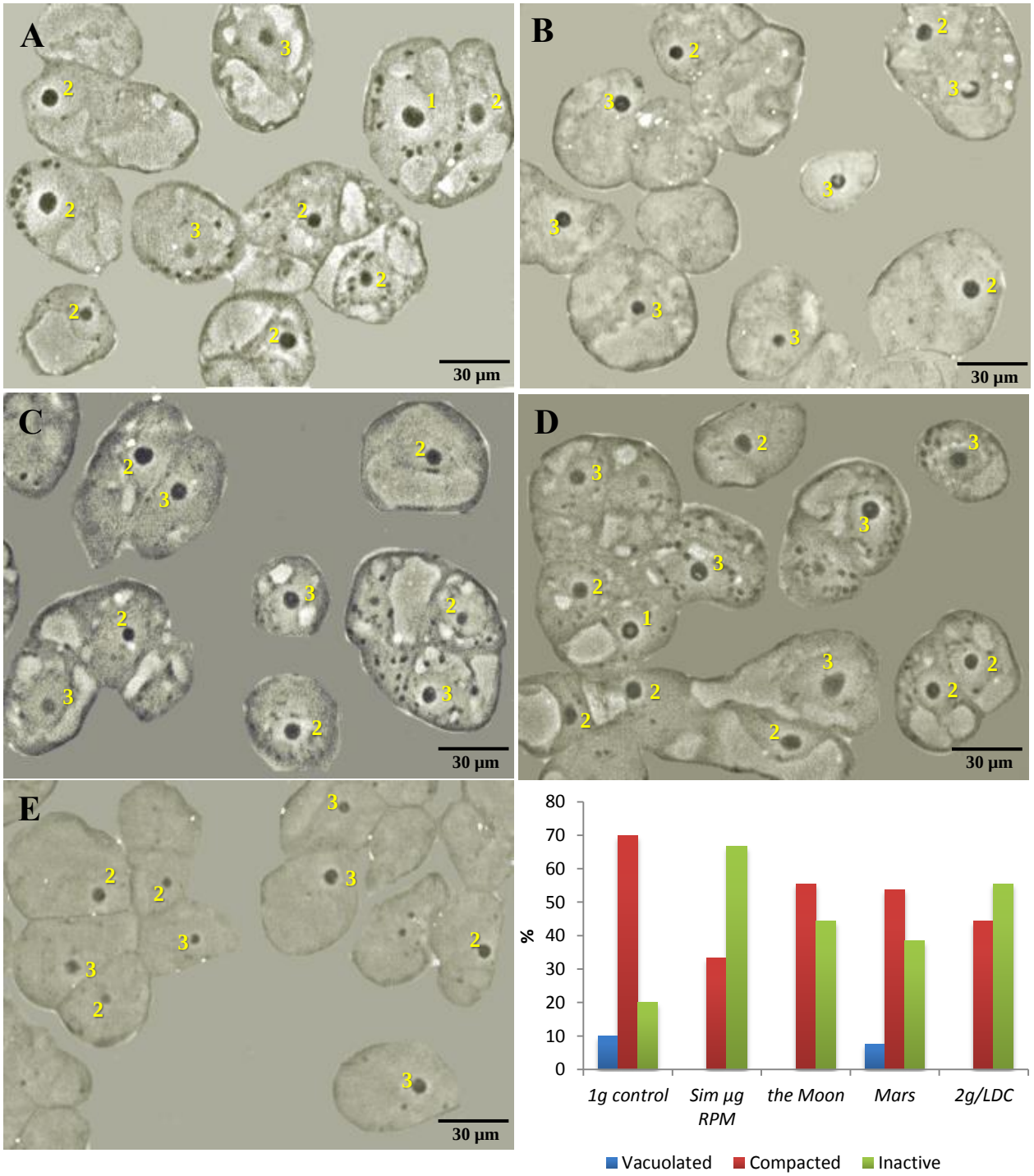

Figure 39: Gravity alteration on the nucleolus structure models distribution for the long term exposure (24 hours). A) 1*g* control, **B)** Sim µ*g* RPM, **C)** the Moon, **D)** Mars, **E)** 2*g* LDC. Nucleolus structure models are observed using the microscope in the contrast phase as defined by (Manzano et al In Press), (1) Vacuolated, (2) Compacted, (3) Inactive. Cells were expose to different. % of the nucleolus model distribution is estimated according to the total number of the nucelolus observed.

2.3. ALTERED GRAVITY INFLUENCE AT THE PROTEIN EXPRESSION LEVEL

2.3.1. Ribosome Biogenesis Proteins Expression Is Reduced By Altered Gravity Levels

As a support to previous findings, quantitative evaluation of certain protein markers level was determined by immunofluorescence by flow cytometry analysis. Ribosome biogenesis was evaluated using specific antibodies to detect nucleolin (AtNucL1) and fibrillarin (AtFIB1) proteins in ***Experiment 3.***

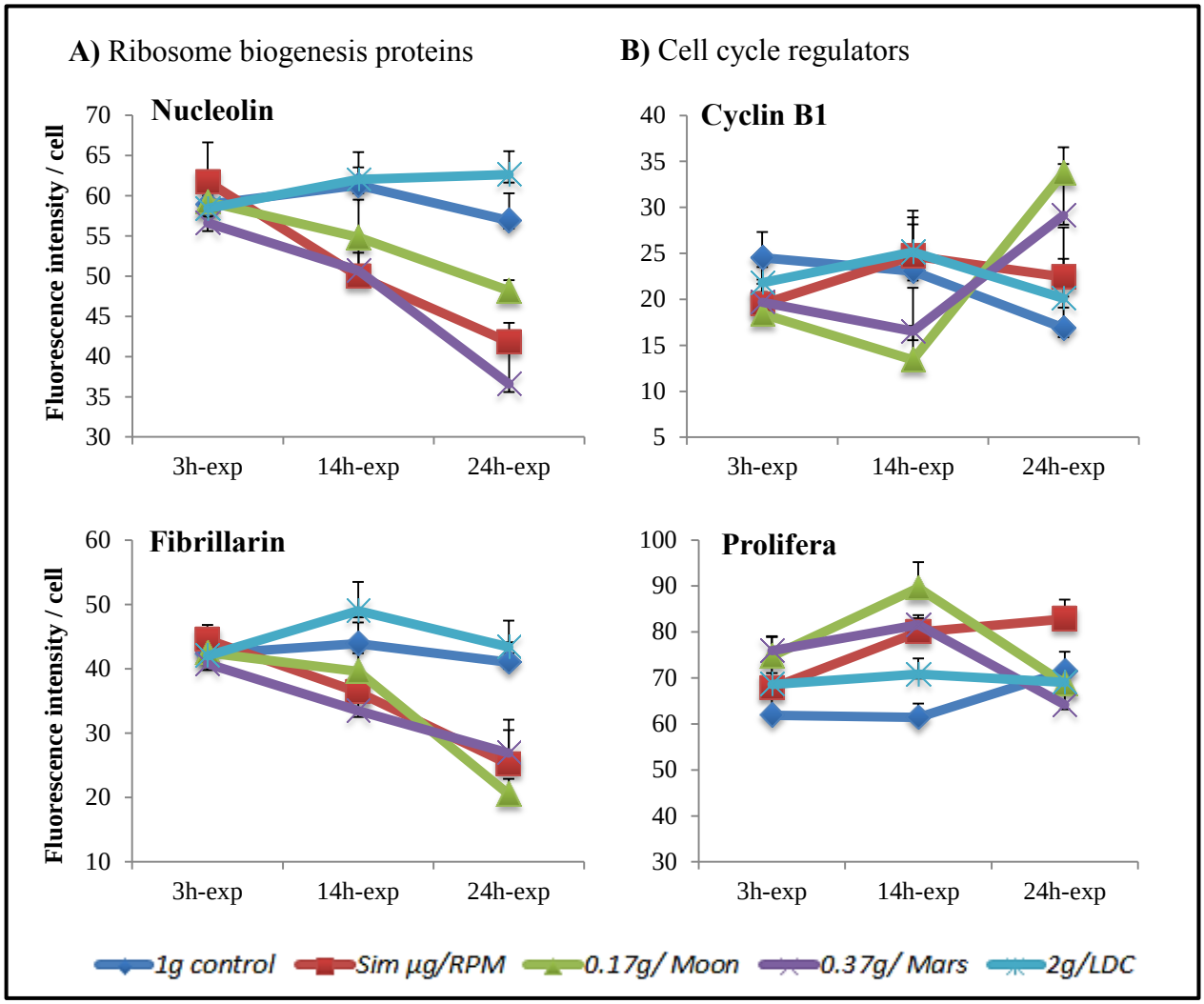

Figure 40: Mean fluorescence intensity per cell using specific ribosome biogenesis (Nucleolin and Fibrillarin) and cell cycle regulators antibodies (CyclinB1 and Prolifera) under altered gravity conditions. Cells are exposed to different gravity level; 1*g* control, Sim µ*g*/RPM, 0.17*g*/Moon, 0.37*g*/Mars, and 2*g*/LDC for three exposure durations 3 (short term), 14 (mid-term), and 24 hours (long term). Protein expression level is evaluated using specific fluorescent antibodies. Fluorescence intensity per each cell was quantified using flow cytometry on 10000 cells labelled with each specific antibody. P-Value < 0.05.

Short term exposure is not enough to alter the nucleolin fluorescence intensity **(Figure 40A)**. However, increasing the exposure time to mid-term shows a significance depression on the nucleolin expression in reduced gravity conditions compared with the 1g control. This influence becomes clearly significant after the long term exposure. Hypergravity shows a moderate and opposite influence on the nucleolin expression. It is being significantly influenced after long term exposure, in which the nucleolin expression was increased versus 1g control.

As nucleolin, fibrillarin is considered one of the most important ribosome biogenesis proteins related to cell growth. Simulated microgravity, the Moon and Mars conditions show a similar significance reduction on the fibrillarin expression **(Figure 40A)** after mid-term exposure and strongly after the long term exposure compared with the 1g control. Hypergravity condition also moderately enhances the fibrillarin expression reaching significance after mid-term but not after the long term experiment compared with 1g control.

2.3.2. Cell Cycle Regulators Proteins Are Affected By Altered Gravity Levels

Previous results support *Arabidopsis* cell cycle phases are disrupted by altered gravity levels. Cell cycle regulators protein expression studies should lead us to a reliable conclusion. Cyclin B1 which, relate to the regulation of G2/M phase and Prolifera which relate to G1/S phase were studied by the fluorescence intensity estimation using the flow cytometry approach.

Short term exposure is not enough to disrupt the Cyclin B1 expression levels **(Figure 40B)**. Although, simulated microgravity and hypergravity have no influence after mid-term exposure, it is found a significant depression influenced by the Moon and Mars condition. Comparison among 1g control condition through the exposure durations, it is shown that, there are significant depressions after long term exposure experiment compared with short and mid-term experiment. Complementing to this disruption on the long term experiment, it is found an irregular increases under the Moon and Mars condition compared with the mid-term experiment. Simulated microgravity and hypergravity show insignificance decreases after the long term exposure compared with mid-term experiment. During the long term experiment, it is found that simulated microgravity, the Moon and Mars condition have significance increments compared with the 1g control.

Prolifera fluorescence intensity shows a rapid alteration after short term exposure **(Figure 40B)**, including significant increments influenced by the Moon and Mars conditions. Prolifera expression is later tremendously increased under the simulated microgravity, the Moon and Mars conditions significantly compared with the 1g control after mid-term experiment. But later than that, Prolifera expression is depleted by the Moon and Mars conditions after long term exposure compared with the mid-term exposure experiment. However, simulated microgravity has a significant increment compared with the 1g control. 1g control shows a significant increase after long term compared with short and mid-term exposure. Not surprisingly, hypergravity has low influence on the Prolifera expression even within longer exposure times.

2.3.3. Epigenetics are Impacted By Altered Gravity Influences

Since chromatin regulation through epigenetic mechanisms is a rapid and reversible response to different environmental stresses (Jaskiewicz et al 2011, Luo et al 2012a), we decided to add a DNA methylation protein marker in our study. Methylcytidine base was detected using the previous flow cytometry approach. Hypermethylation pattern accumulates due to longer exposures to altered gravity levels **(Figure 41A)**. Short term exposure is just enough to alter DNA methylation under simulated microgravity; while increased exposure times up 14 hours (mid-term) induces a significant hypermethylation under all reduced gravity conditions, confirmed in the 24 hour samples. Hypergravity samples show the same pattern only after long term exposure compared with 1g control.

Since histone modification is another epigenetic mechanism involved in the plant stress response, a marker of histone acetylation was assay under the studied gravity levels **(Figure 41B)**. Histone acetylation is quickly disrupted by altered gravity conditions, showing significant alterations in the short term (except in the simulated microgravity sample compared with 1g control). These significantly depletions reach the maximum in all the altered gravity conditions in the mid-term and are maintained at the long term exposure compared with 1g control. Moreover, it is noticed that the Moon gravity induced a particularly strong depletion on the histone acetylation in both, the mid and long term exposure.

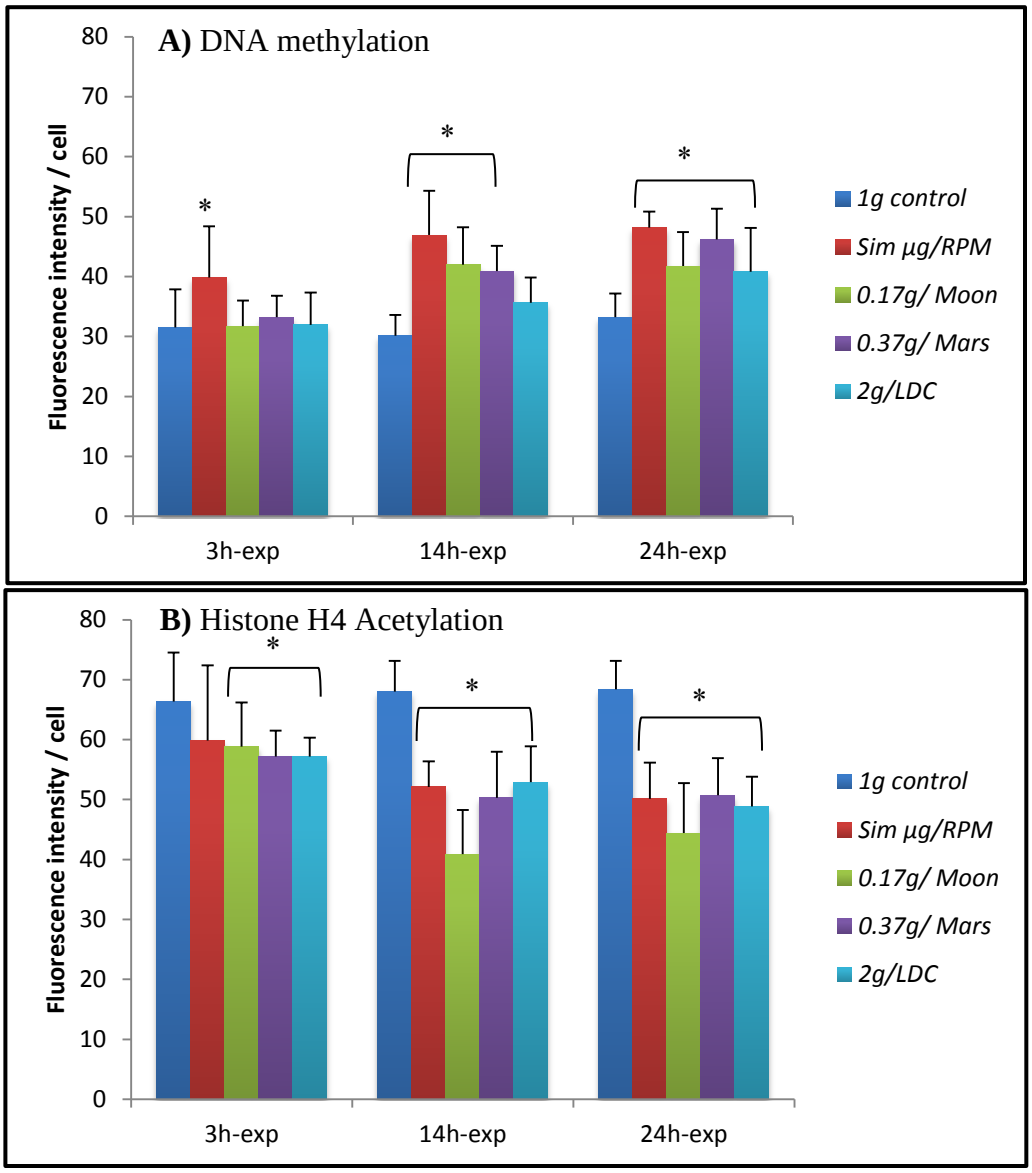

Figure 41: Relative protein expression level of epigenetic markers under altered gravity exposure. Epigenetic elements; **A)** DNA methylation (5mdc) **and B)** Histone H4 Acetylation (AcH4) were quantified using flow cytometry approach**.** Cells are exposed to different altered gravity level; 1*g* control, Sim µ*g*/RPM, 0.17*g*/Moon, 0.37*g*/Mars, and 2*g*/LDC for three exposure durations; 3 (short term), 14 (mid-term), and 24 hours (long term). Protein expression level was evaluated in 10000 cells by flow cytometry using specific fluorescent antibodies. P-Value < 0.05. (*) is used in a comparison with 1*g* control in the same GBF. (—) is used to refer for significance for all the under covered conditions.

2.4. ALTERED GRAVITY INFLUENCE AT THE GENE EXPRESSION LEVEL

To confirm previous results we analyzed the impact of gravity alteration of the same essential processes at the gene expression level, such as, ribosome biogenesis (AtNucL1), cell proliferation (Prolifera) and epigenetic modifications (MET1) **(Figure 42).**

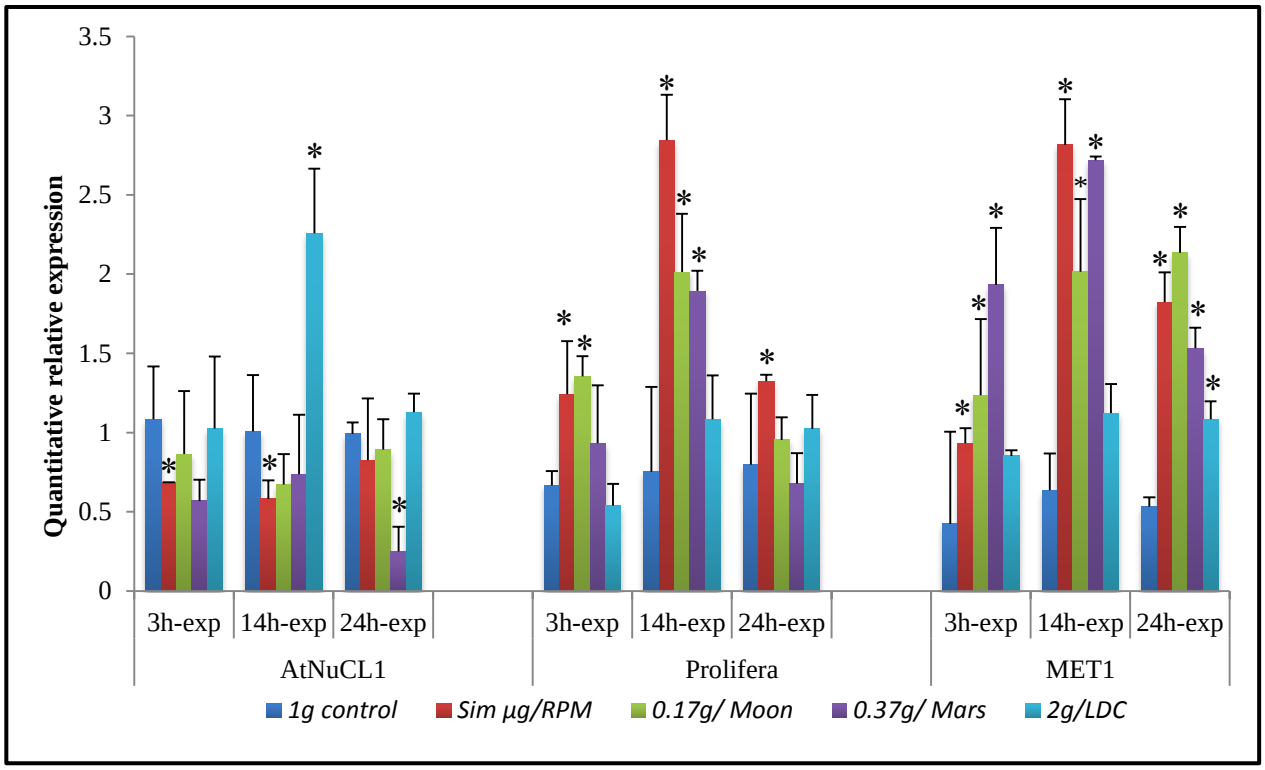

Figure 42: Relative gene expression (qPCR) of ribosome biogenesis (AtNucL1), cell proliferation (Prolifera), and epigenetic modifications (DNA methyltransferase) markers under altered gravity. Cells were exposed to different altered gravity level; 1*g* control, Sim µ*g*/RPM, 0.17*g*/Moon, 0.37*g*/Mars, and 2*g*/LDC for three exposure durations 3 (short term), 14 (mid-term), and 24 hours (long term). Relative gene expression is evaluated using qPCR analysis. P-Value < 0.05. (*) is used in a comparison with 1*g* control in the same experimental conditions.

Nucleolin expression, as cell growth related marker, is significantly decreased after short and mid-term exposure to simulated microgravity compared with the 1*g* control. This alteration is not observed for the long exposure. Furthermore, partial gravity alteration shows depletion on the expression levels, but only reaching significant levels in the Mars long term exposure. Contrary, hypergravity environment leads to particularly high nucleolin levels after 14 hour exposure. Furthermore, Prolifera expression level, as a cell proliferation indicator, shows a rapid increase under reduced gravity conditions. Significance is reached in the short term and enhanced after 14 hours exposure, while this alteration is lost after long term experiments. Prolifera expression level is not clearly affected by hypergravity. Epigenetics marker, particularly, DNA Methyltransferase expression is increased significantly under hypogravity conditions; gradually, a rapid alteration appears in the short-term, that peaks at mid-term and is later reduced in the long term. Slower effect is observed in the hypergravity conditions, in which the significant alteration is reached after long term exposure.

2.5. ALTERED GRAVITY DISRUPTS CO-LOCALIZATION OF OUR MARKER PROTEINS; ANALYSIS OF MULTICOLOR CONFOCAL IMMUNOFLUORESCENCE MICROSCOPY IMAGES.

2.5.1. Ribosome Biogenesis Proteins (Nucleolin and Fibrillarin) Colocalization Inside The Nucleolus Is Altered By The Gravitational Alteration

As an additional proof of the alterations in cell growth and cell proliferation processes, colocalization of the two major ribosome biogenesis proteins (Nucleolin and Fibrillarin) was studied with the samples of ***Experiment 3.*** Double fluorescence was imaged using excitation of a laser at the wavelength of 488 (green-nucleolin) and 561 (red-fibrillarin). Double-stained images were obtained by sequential scanning for each channel to eliminate the cross-talk of chrompohores and to ensure the reliable quantification of colocalization (Demandolx & Davoust 1997). As a first look, confocal immunofluorescence microscopy images confirm that both, nucleolin and fibrillarin are expressed inside the nucleolus **(Figure 43)**. Images were acquired and processed as described in Methods, Pearson´s correlation coefficient (PCC) and colocalization coefficient (m1 and m2) were examined.

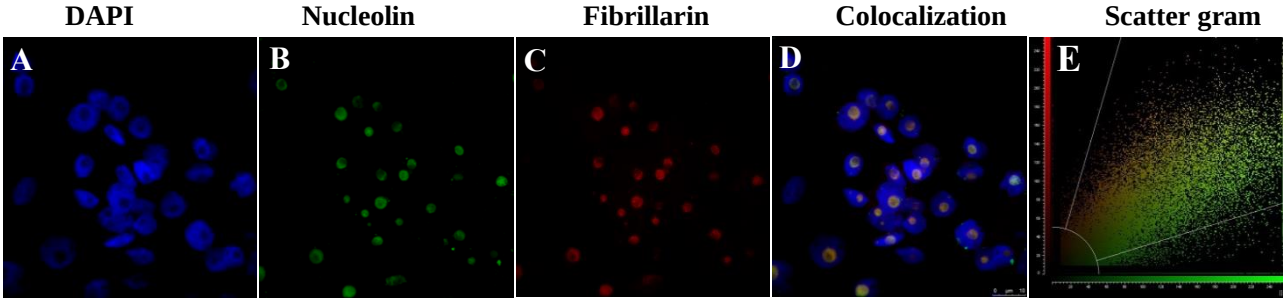

Figure 43: Confocal immunofluorescence images analysis of the ribosome biogenesis major proteins, Nucleolin and fibrillarin corresponding to be colocalized inside the nucleolus. A) Chromatin staining using DAPI to define the nucleolus. **B)** Nucleolin staining fluorochrome using Alexa 488 in a laser line 488 nm (**Green**). **C)** Fibrillarin staining using Alex 548 in a laser line 561(**Red**). **D)** Colocalization of Nucleolin and Fibrillarin through the overlaps of the signals resulting in yellow staining. **E)** Scatter gram produced by the colocalization analysis software. It shows the distribution of pixels in images according to selected pair of channels (Channel 1 (**Green**), and Channel 2 (**Red**)). Colocalized yellow pixels are located along the diagonal. Black areas along X and Y axis indicates removed pixels of the background to ensure reliability of the colocalization coefficients calculations.

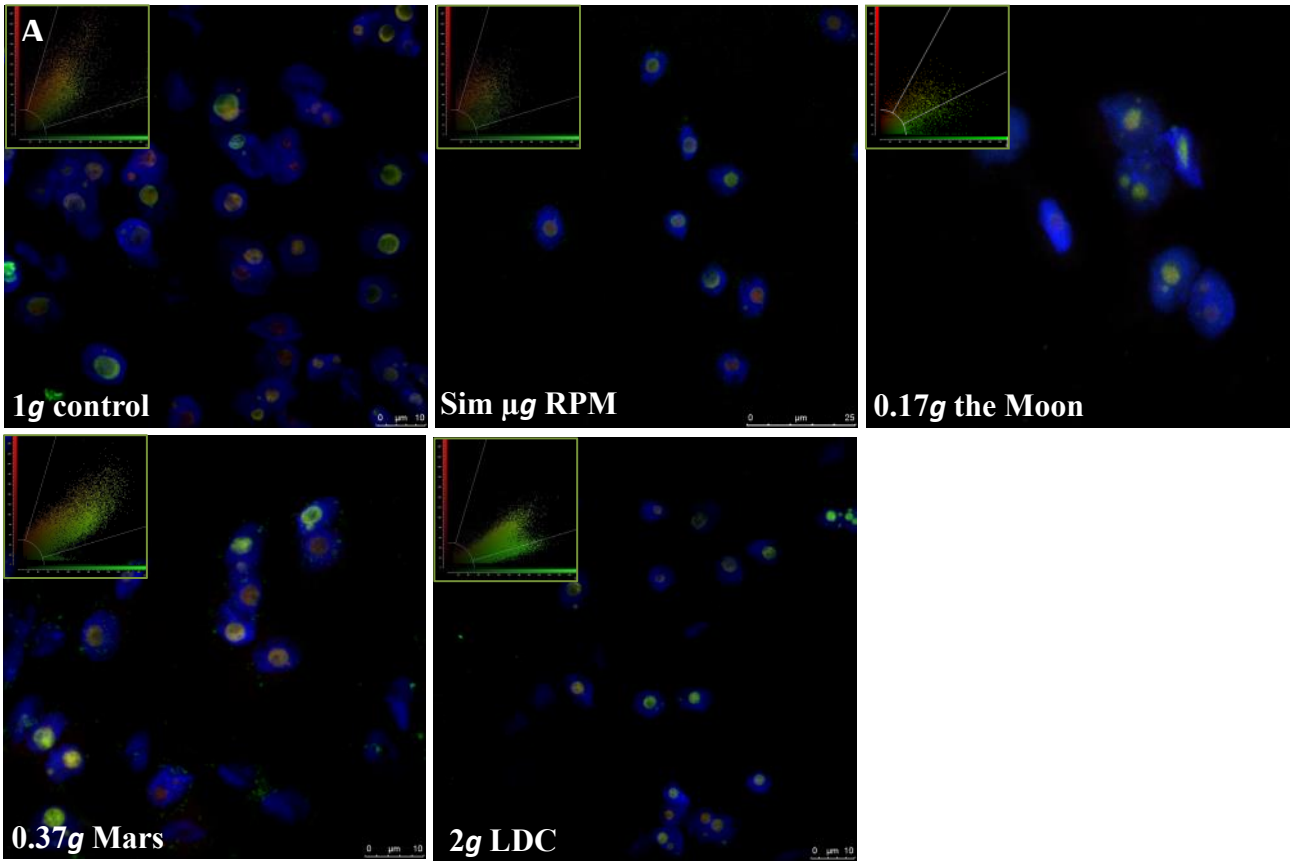

Figure 44A: Mid-term altered gravity disrupts Nucleolin-Fibrillarin immunofluorescence colocalization levels. Cells were expose to 1*g* control, Sim µ*g* RPM, 0.17*g* the Moon, 0.37*g* Mars and 2*g* LDC for mid-term (14 hours). Confocal images showing colocalization of Nucleolin (green) and Fibrillarin (Red) in the nucleolus. Embedded scatter gram in the upper left corner of the image estimates the amount of each detected antigen based on colocalization of Nucleolin (green, y-axis) and Fibrillarin (red, x-axis). Colocalized pixels of yellow color are located along the diagonal of the scatter gram.

Nucleolin-Fibrillarin colocalization is disrupted by the gravitational alteration for mid-term **(Figure 44A)** and long term **(Figure 44B).** Due to the insignificant alterations of the protein levels in the short term exposure and the limitation in the amount of the samples, this analysis was not performed for the short term. Nucleolin and fibrillar immunofluorescence were detected inside the nucleolus but colocalization rate was reduced proportionally to the reduction in the gravity level **(Figure 45).**

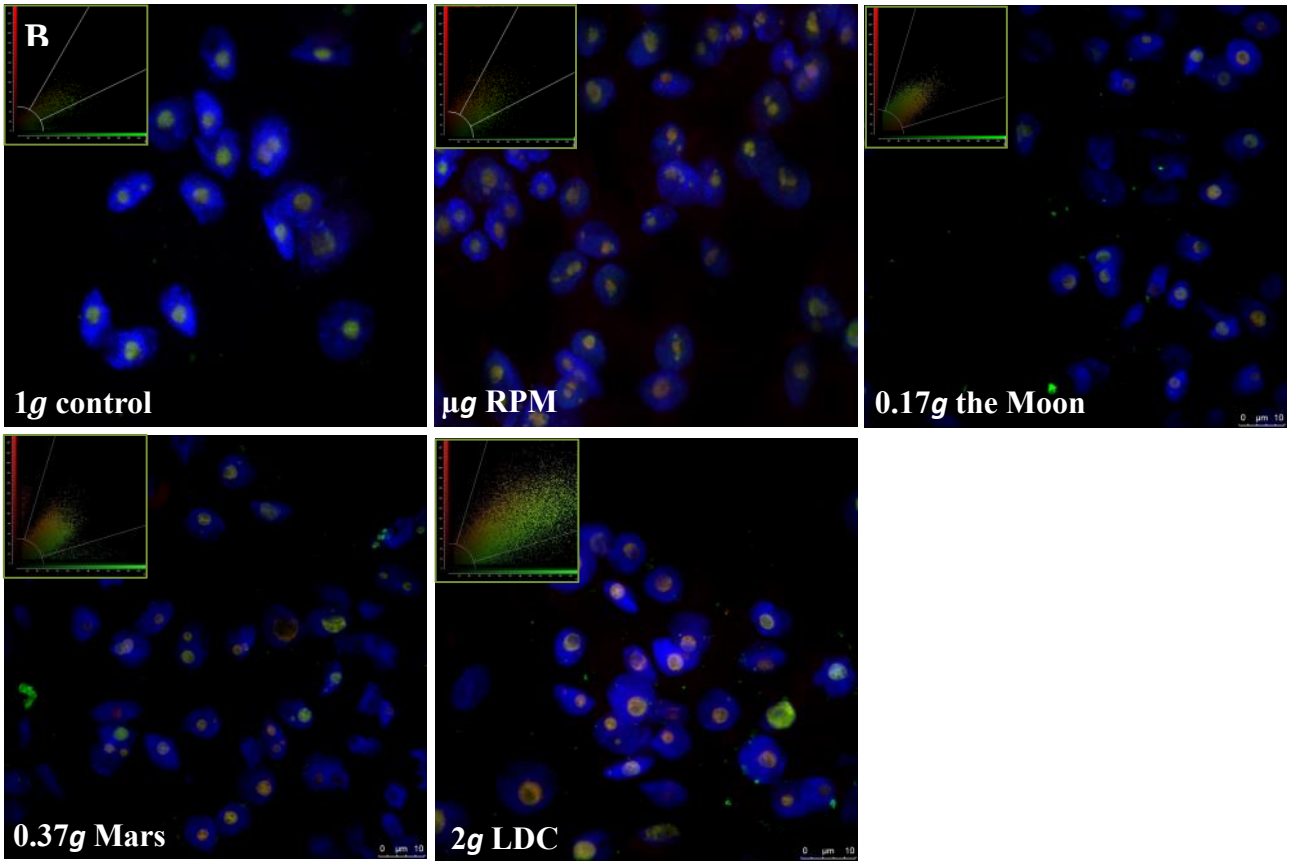

Figure 44B: Long term altered gravity disrupts Nucleolin-Fibrillarin immunofluorescence colocalization levels. Cells were expose to 1*g* control, µ*g* RPM, 0.17*g* the Moon, 0.37*g* Mars and 2*g* LDC for long term (24 hours). Confocal images showing colocalization of Nucleolin (green) and Fibrillarin (Red) in the nucleolus. Embedded scatter gram in the upper left corner of the image estimates the amount of each detected antigen based on colocalization of Nucleolin (green, y-axis) and Fibrillarin (red, x-axis). Colocalized pixels of yellow color are located along the diagonal of the scatter gram.

Quantitative colocalization analysis using PCC demonstrate a similar high degree of colocalization in 1*g* control (0.86, 0.84) and hypergravity (0.91, 0.86) samples, slightly decreasing with *g* reduction, from Mars (0.74, 0.77) to the Moon (0.67, 0.75) *g* levels and peaking simulated microgravity significant decrease (0.42 and 0.58) in both mid and long term exposure respectively.

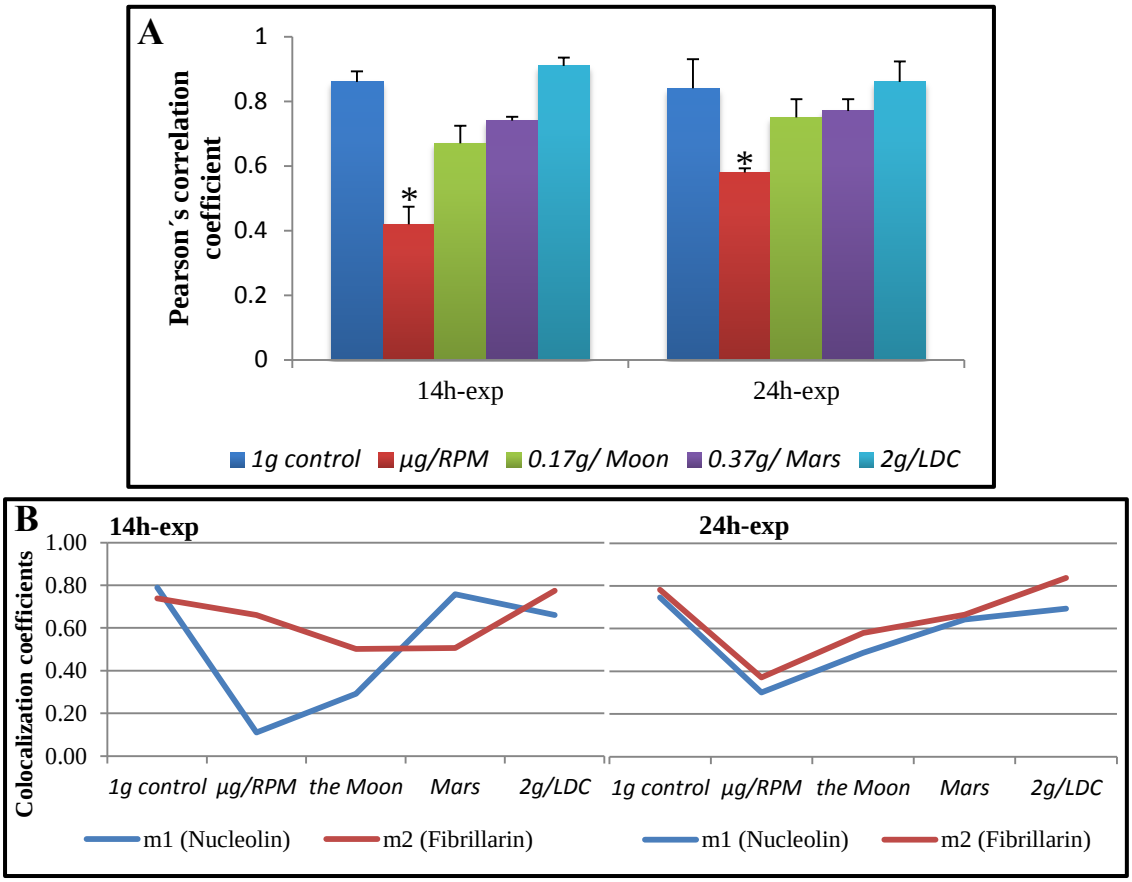

Figure 45: Quantifications of Nucleolin-Fibrillarin colocalization coefficients under gravitational alteration. Leica software was used to quantify the colocalization. A) Pearson's correlation coefficient (PCC). B) Colocalization coefficients m1 (Nucleolin) and m2 (fibrillarin). An average of coefficients of three replicates was calculated. P-Value < 0.05. (*) is used in a comparison with 1*g* control in the same experimental conditions.

Calculation of a complementary colocalization coefficients m1 and m2 is useful to describe the contribution of each protein on the colocalization levels. It is provide knowledge about the individual expression of each protein. Under 1*g* control conditions, both of nucleolin and fibrillarin are colocalized in an 80% of the total protein expressions **(Figure 45)**. The contribution of the nucleolin in the colocalization (m1) is significantly decreased by simulated microgravity and the Moon conditions for the mid-term exposure. This depletion is less clear after long term exposure, but it is still significant compared with 1*g* control. Little influence is noticed under Mars and hypergravity conditions. On other hand, fibrillarin colocalization coefficient (m2) is decreased under reduced gravity conditions not so importantly as nucleolin except in the case of Mars. This data is consistent with the low PCC under simulated microgravity conditions due to the low level of nucleolin-fibrillarin contribution on the colocalization.

2.5.2. Epigenetic Modifications; DNA Methylation Dynamic and Histone H4 Acetylation Changes Influenced by the Gravitational Alteration

The aptitude of chromatin regulation through epigenetic status to be altered rapidly and reversibly could be an important cellular dynamics for the different environmental cue response (Bruce et al 2007, Jaskiewicz et al 2011, Luo et al 2012a). Epigenetic modifications, and in particular DNA methylation, and histone acetylation might have a crucial impact on the plant response mechanism against stresses such as the gravitational alteration.

The 5-methyldeoxycytidine (5mdc) localization to reveal *in situ* dynamics of DNA methylation chromatin pattern under altered gravity

To investigate alterations in the global DNA methylation dynamics during the gravitational alteration, the pattern of nuclear methylated cytidines was determined by immunolocalization of the distribution of 5-methyldeoxycytidine (5mdc) in genomic DNA.

Confocal analysis of 5mdc immunolocalization showed a differential pattern of methylated cytidine by 14 hours gravitational alteration (mid-term) **(Figure 46)**. Cells exposed to reduced gravity contain larger and more abundant fluorescent spots, indicating a higher presence of 5mdc in nuclei compared with 1*g* control conditions. This alteration is maximized under simulated microgravity conditions, while hypergravity shows not significant alteration on the distribution of 5mdc compared with 1*g* control. This observation is supported by the immunofluorescence quantifications, in which, hypogravity conditions (simulated microgravity and partial gravity) show significant higher level of 5mdc intensity level compared with 1*g* control **(Figure 48)**.

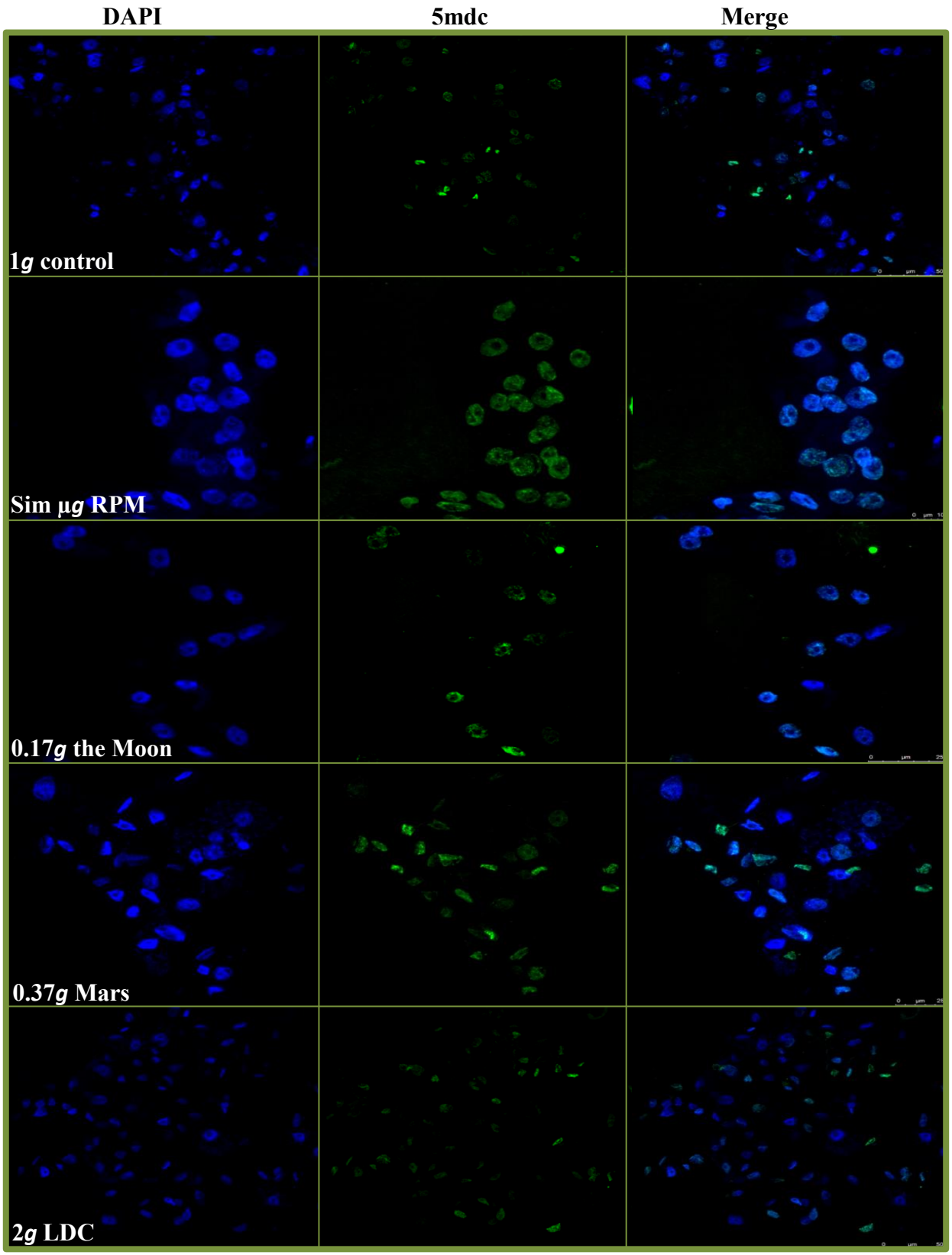

Figure 46: DNA methylation (5mdc) immunofluorescence patterns under altered gravity. Cells were expose to gravitational alteration; 1*g* control, Sim µ*g* RPM, 0.17*g* the Moon, 0.37*g* Mars and 2*g* LDC for 14 hours (mid-term). Confocal images showing immunolocalization of 5mdc (green) in the chromatin pattern (DAPI) and the merged images.

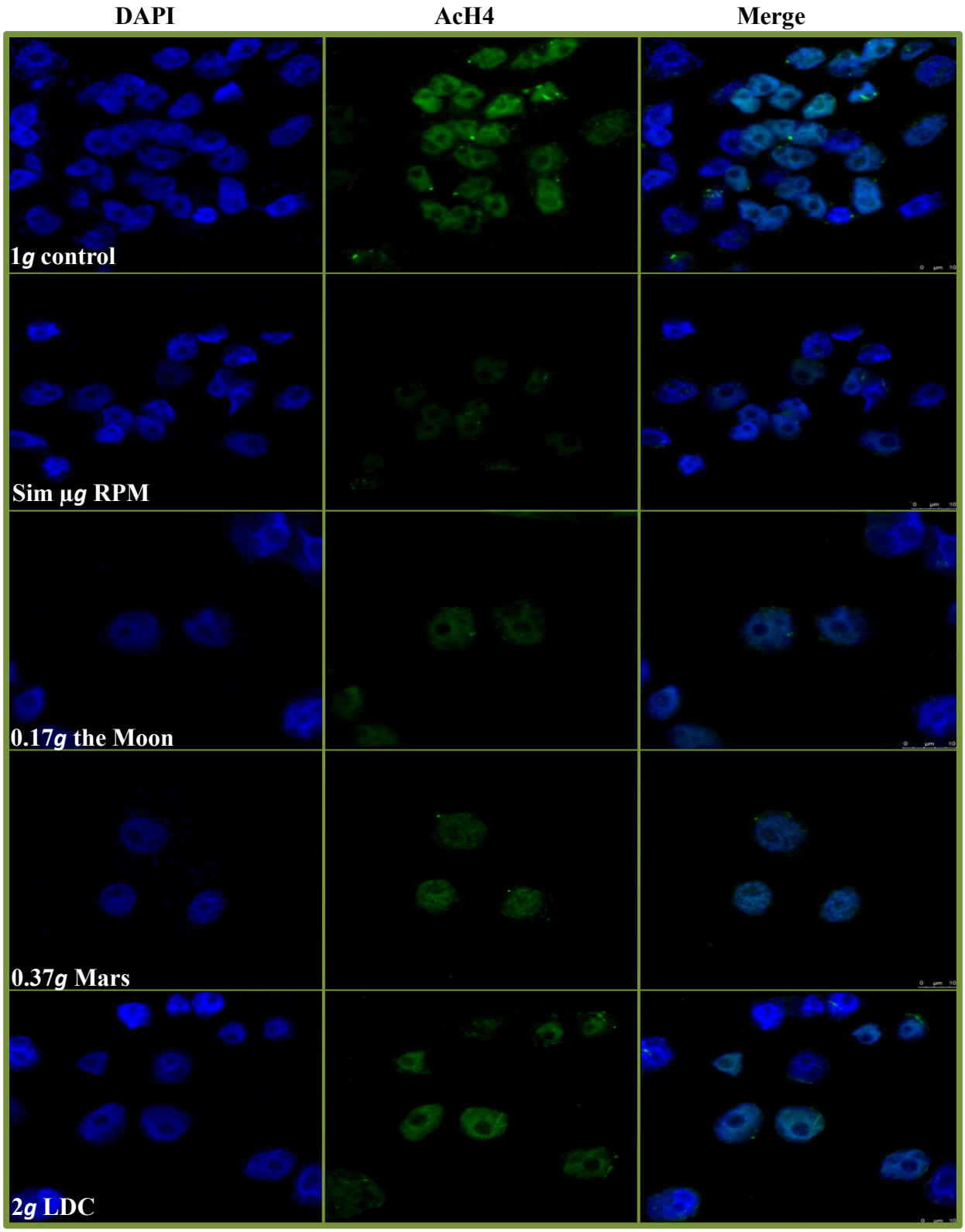

Figure 47: Histone H4 Acetylation (AcH4) immunofluorescence presence patterns under altered gravity. Cells were expose to gravitational alteration; 1*g* control, Sim µ*g* RPM, 0.17*g* the Moon, 0.37*g* Mars and 2*g* LDC for 14 hours (mid-term). Confocal images showing immunolocalization of histone acetylation (green) in the chromatin pattern (DAPI) and the merged images.

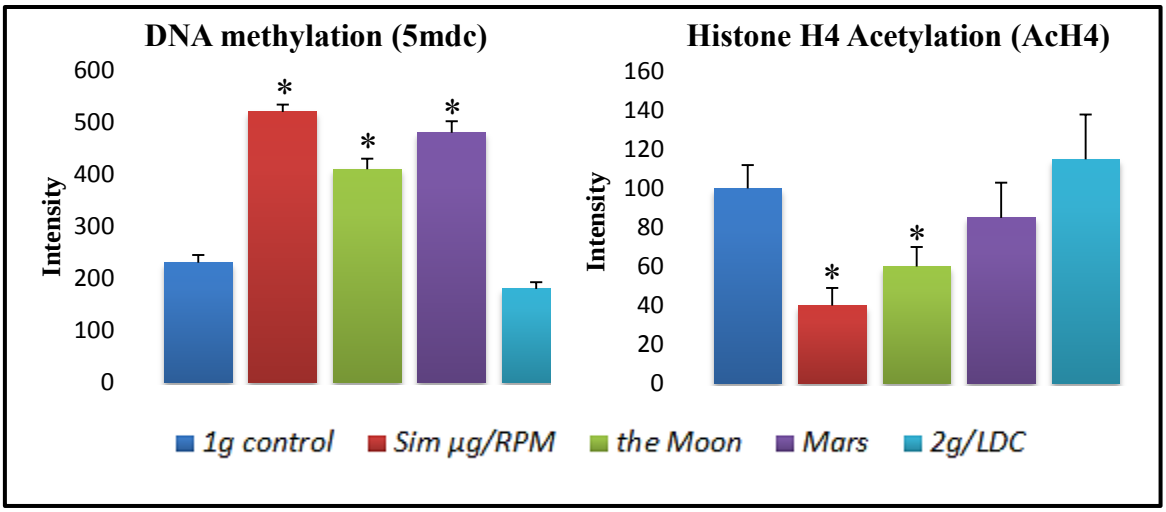

Figure 48: Quantification of DNA methylation (5mdc) and Histone H4 Acetylation (AcH4) fluorescence intensity levels. Cells were expose to gravitational alteration; 1*g* control, µ*g* RPM, 0.17*g* the Moon, 0.37*g* Mars and 2*g* LDC for 14 hours (mid-term). Quantitative fluorescence intensity level was determined using Leica confocal software in each individual cell to detect the green signal intensity. Averages of 100 cells were calculated in three different biological replicates. P-Value < 0.05. (*) reveal significant comparisons versus 1*g* control.

Gravity alteration influences the distribution pattern of the histone H4 acetylation

The immunolocalization of AcH4 is altered by the gravitational alteration compared with the control conditions for 14 hours exposure (mid-term) **(Figure 47).** It is observed that AcH4 immunofluorescence pattern show an opposite layout relative to 5mdc influenced by the different gravity alteration. The presence of AcH4 in the chromatin is depleted under hypogravity conditions compared with the 1*g* control. This low presence is significantly observed under simulated microgravity conditions, while hypergravity show no changes. The quantitative analyses of the immunofluorescence intensity support the disruption on the presence of AcH4 during the gravitational alteration. Results **(Figure 48)** reveal that AcH4 immunofluorescence intensity level is clearly depleted under hypogravity conditions, while significance is lost on Mars conditions. On the other hand, the impact of hypergravity is not strong enough to alter the AcH4 intensity compared with 1*g* control.

2.6. Chapter 2: Results Summary

Results summary of this chapter, which present the impact of the gravitational alteration on the *Arabidopsis* cell cultures process, cell proliferation, cell growth and the chromatin organization mechanisms **(Table 8)** concludes that, gravity alteration has a significant impact on growth and proliferation processes of the *Arabidopsis* cells through different exposure durations. The short exposure usually is not enough to alter most of the parameters, while most alterations become significant for the mid and long term exposure. Furthermore, hypergravity lead to weak, and sometimes opposite alterations than those caused by the hypogravity environment.

Cell cycle is altered by the gravitational alteration. On the level on the cell cycle regulators, Cyclin B1 is depleted due to the gravitational alteration, while the Prolifera is increased. Beside the cell cycle regulators alterations, the number of proliferating cells on S phase is increased due to the hypogravity alteration. Finally, using cell cycle analysis approach depending on DNA content only, it is not reliable enough to confirm an increasing or decrease cell proliferation rate. So on we are going to search for alternative methods or a direct approach for the cell cycle acceleration modifications. On the other hand, the ribosome biogenesis is decreased as reported by the nucleolin and fibrillarin levels, beside the increment of the inactive nucleolus. This alteration is companied with the epigenetic dynamics responding to the gravitational alteration, increasing the DNA methylation with depletion on the histone acetylation levels.

Table 8: Chapter 2: Results summary: Impact of various altered gravity levels on *Arabidopsis* cell cultures						
			µ*g* RPM	**0.17*g* Moon**	**0.37*g* Mars**	**2*g* LDC**
Short term (3 hours)	**Cell cycle**	Cell cycle	=	alter	alter	=
		EdU (S phase)	=	=	++	=
		Cyclin B1	=	=	=	=
		Prolifera	=	=	=	=
	Ribosome biogenesis	Nucleolin	=	=	=	=
		Fibrillarin	=	=	=	=
	Epigenetic	DNA methylation	++	=	=	=
		Histone acetylation	=	--	--	--
	Nucleolus	Nucleolar Models	compacted	compacted	compacted	compacted
		Nucleolar area	=	=	=	=
Mid-term (14 hours)	**Cell cycle**	Cell cycle	alter	alter	alter	alter
		EdU (S phase)	++	++	++	=
		Cyclin B1	=	--	--	=
		Prolifera	++	++	++	=
	Ribosome biogenesis	Nucleolin	--	--	--	=
		Fibrillarin	--	--	--	++
	Epigenetic	DNA methylation	++	++	++	=
		Histone acetylation	--	--	--	--
	Nucleolus	Nucleolar Models	inactive	compacted	inactive	compacted
		Nucleolar area	=	=	--	=
Long term (24 hours)	**Cell cycle**	Cell cycle	alter	alter	alter	alter
		EdU (S phase)	++	++	++	=
		Cyclin B1	--	++	++	=
		Prolifera	++	=	=	=
	Ribosome biogenesis	Nucleolin	--	--	--	++
		Fibrillarin	--	--	--	=
	Epigenetic	DNA methylation	++	++	++	++
		Histone acetylation	--	--	--	--
	Nucleolus	Nucleolar Models	inactive	compacted	compacted	Inactive
		Nucleolar area	=	--	--	=

RESULTS

CHAPTER 3: *CELL CYCLE PROGRESSION RATE UNDER DIFFERENT ALTERED GRAVITY CONDITIONS*

3.1. *Arabidopsis* Cell Cycle Progression for 72h after aphidicolin Block/Release under 1*g* control condition

3.2. Cell Cycle Progression for 72h after aphidicolin Block/Release under Simulated Microgravity (Sim µ*g* RPM) condition

3.2. Cell Cycle Progression for 72h after aphidicolin Block/Release under the Moon Condition (0.17*g*/ RPM^{SW})

3.4. Cell Cycle Progression for 72h after aphidicolin Block/Release under Mars Condition (0.37*g*/ RPM^{HW})

3.5. Cell Cycle Progression for 72h after aphidicolin Block/Release under Hypergravity Condition (2*g*/ LDC)

3.6. Cell Cycle Progression Varies in Opposite Ways under Hypo and Hypergravity Conditions

CHAPTER 3: CELL CYCLE PROGRESSION RATENDER DIFFERENT ALTERED GRAVITY LEVELSCONDITIONS

Once established the comparability between the seedlings and cell culture systems results in terms of cell growth and proliferation markers, we should use the cell system to investigate the plant cell proliferation disturbance using a more direct approach, in order to obtain a clear view about the impact of different altered gravity levels on *Arabidopsis* cell cycle progression. In this chapter, we are going to use aphidicolin synchronization approach to appraise the cell cycle progression rates.

Cell cycle synchronization with aphidicolin is a powerful tool to investigate cell cycle progression by arresting cells in late G1/S under different altered gravity conditions. The cells were then immobilized by embedding on agarose during the GBF experiments as a simulation requirement (***Experiment 5***). Sampling at different times allows isolation of different cell cycle phase enriched populations.

3.1. *Arabidopsis* Cell Cycle Progression through 72h after aphidicolin Block/Release Under 1*g* Control Condition

The distribution of cell cycle phases was determined by DAPI staining of the DNA using the flow cytometry analysis under 1*g* control condition as a reference. **Figure 49** shows that, after the release the aphidicolin block (T0), cell cycle progresses synchronously under 1*g* control conditions through a 72 hours experiment. Aphidicolin synchronizes the cell cycle by arresting approximately 2 out of 3 cells in the late G1/S phase at T0. The peak of synchronized cells corresponding to S phase is obtained after 2 hours (T2=65.2%). Through 10 hours, T10 sample shows the maximum peak for G2/M subpopulation of cells reaching 69%. These cells need 6 hours more to divide through G2/M phase and enter to a new cell cycle beginning with G1 phase (T16 sample represents G1 subpopulation peak (68.5% of cells in G1)). During the second cell cycle, synchronization is partially preserved. T28, T32, T44 shows the peaks of S-phase (34.4%), G2/M (38.55%), and G1 (59.5%), respectively. It must be cited that, this partial synchronization of 2/3 of the population is considered normal and it is better than the one obtained by sucrose starvation (Menges & Murray 2002).

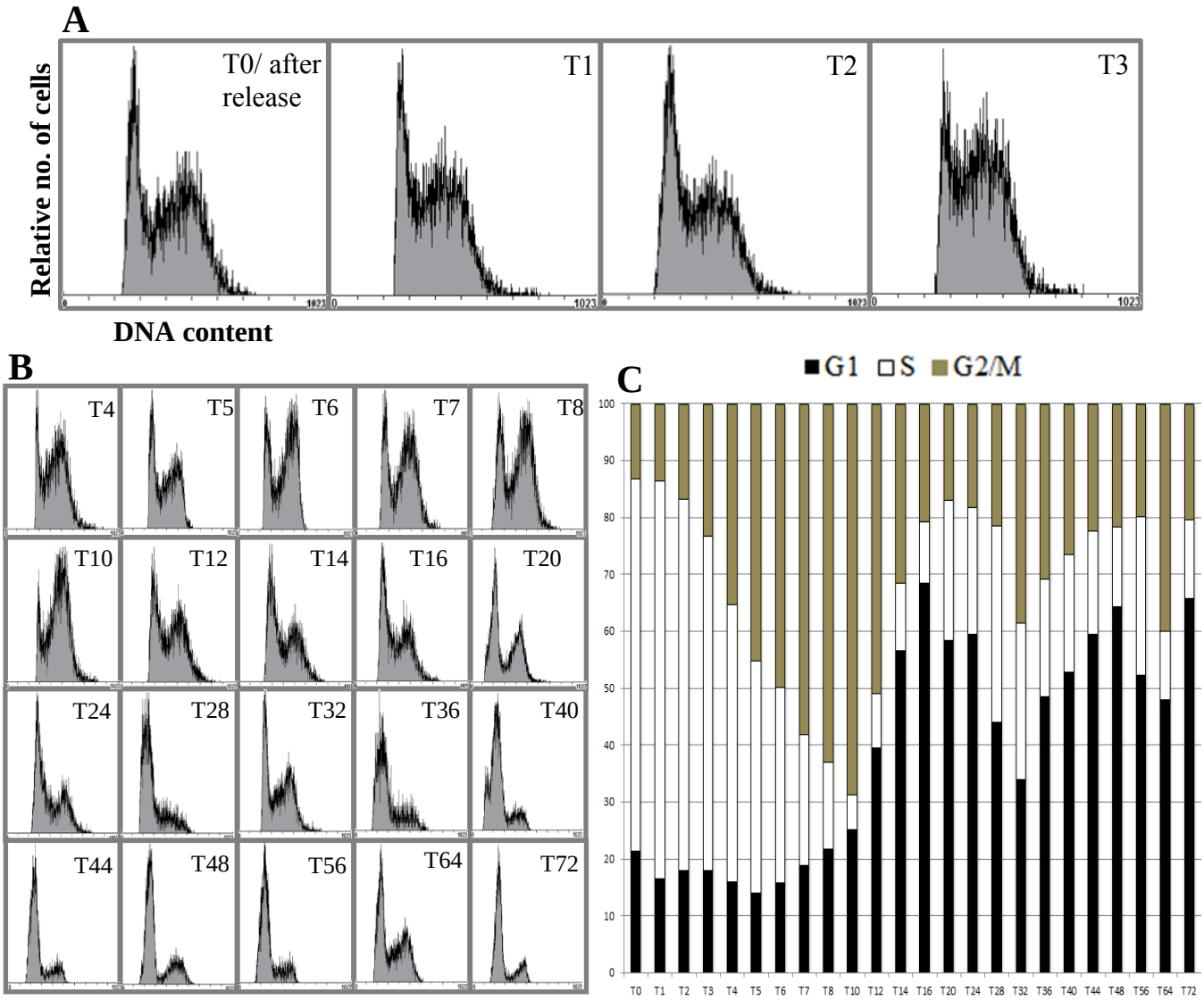

Figure 49. Cell cycle progression for 72h after aphidicolin block/release of *Arabidopsis* cell line MM2d immobilized in 1*g* control condition. **(A&B)** Distribution of cell cycle phases by flow cytometry analysis (DAPI) regarding to the DNA content corresponding to the relative number of cells**.** Samples taken at different times after the release of aphidicolin block in late G1/early S phase (T0). Each block represents a sample taken at a certain time from t=0 to t=72 hours. Sampling was performed every 1, 2, and 4 hours in the first, second, and the third day respectively. **(B)** DNA histogram of flow analysis results show the distribution of cells by DNA content corresponding to cell cycle phases G1 (Black), S-phase (White) and G2/M (Brown).

Synchronization is progressively lost in the third cell cycle up to 72 hours, in which the maximum peak of cells in S phase is shown after 56 h (T56 = 27.95%), G2/M population peak after 64 h (T64 = 40.05%) and G1 population peak after 72 hours (T72 = 65.8%). This data is consistent with a 26 hours length of the first cell cycle after synchronization (between the maximum proportion of cells in S phase at T2 up to the next S phase peak at T28). In this cell cycle, cells need 8h to proliferate from S phase (T2) to G2/M (T10) and 6 hours to reenter to G1 (T16). Second and third cell cycles durations cannot be accurately estimated because of synchronization lost together with a less frequent sampling. But the duration of the second cell cycle was similar, roughly 24h (between T28 and T52).

3.2. Cell cycle Progression through 72h after aphidicolin Block/Release under Simulated Microgravity (Sim µ*g* RPM) Condition

Similar approach was performed under simulated microgravity using the RPM (µ*g*/RPM) after aphidicolin block **(Figure 50A)**. First S phase peak is shown after 2 hours (T2 = 65.9%) as expected, but the cell cycle progression and entry into G2/M phase occurred at T7 (65.9% of cells in G2/M), 3 hours earlier than 1*g* control. G1 phase population peak of the new cell cycle after mitosis division is observed after 14 hours (T14 = 61.4%), 2 hours earlier than 1*g* control. For the second cycle, a good degree of synchrony is shown. At T28 a peak of cells in S phase is shown 56.5%. Then cells accumulate in G2/M phase after 36 hours (T36 = 60.95%). Next G1 peak occurs after 48hours by detecting 65% of proportion of cells in G1. For the third cell cycle, some synchronization is preserved yet. T56, T64, and T72 shows the peaks of S phase (34%), G2/M (37%), and G1 (60%) respectively.

Consequently, cell cycle synchronization is better preserved under simulated microgravity. It is maintained in 2 out of 3 cells for the first and second cell cycle and begins to desynchronize at the third cell cycle. The first cell cycle duration is predicted around 26 hours according the S phase peaks (T2 and T28). Cells need only 5 hours to accumulate at G2/M after S phase peak and other 7 hours to renter to G1 phase. The second cell cycle takes around 24 hours by T52 as predicted. Compared with the 1*g* control, a significant increase on the duration of the G1 phase (around 12 hours) is required to compensate the quicker G2 phase. Third cell cycle duration is not clear to be estimated because of lower synchronization and disperse sampling.

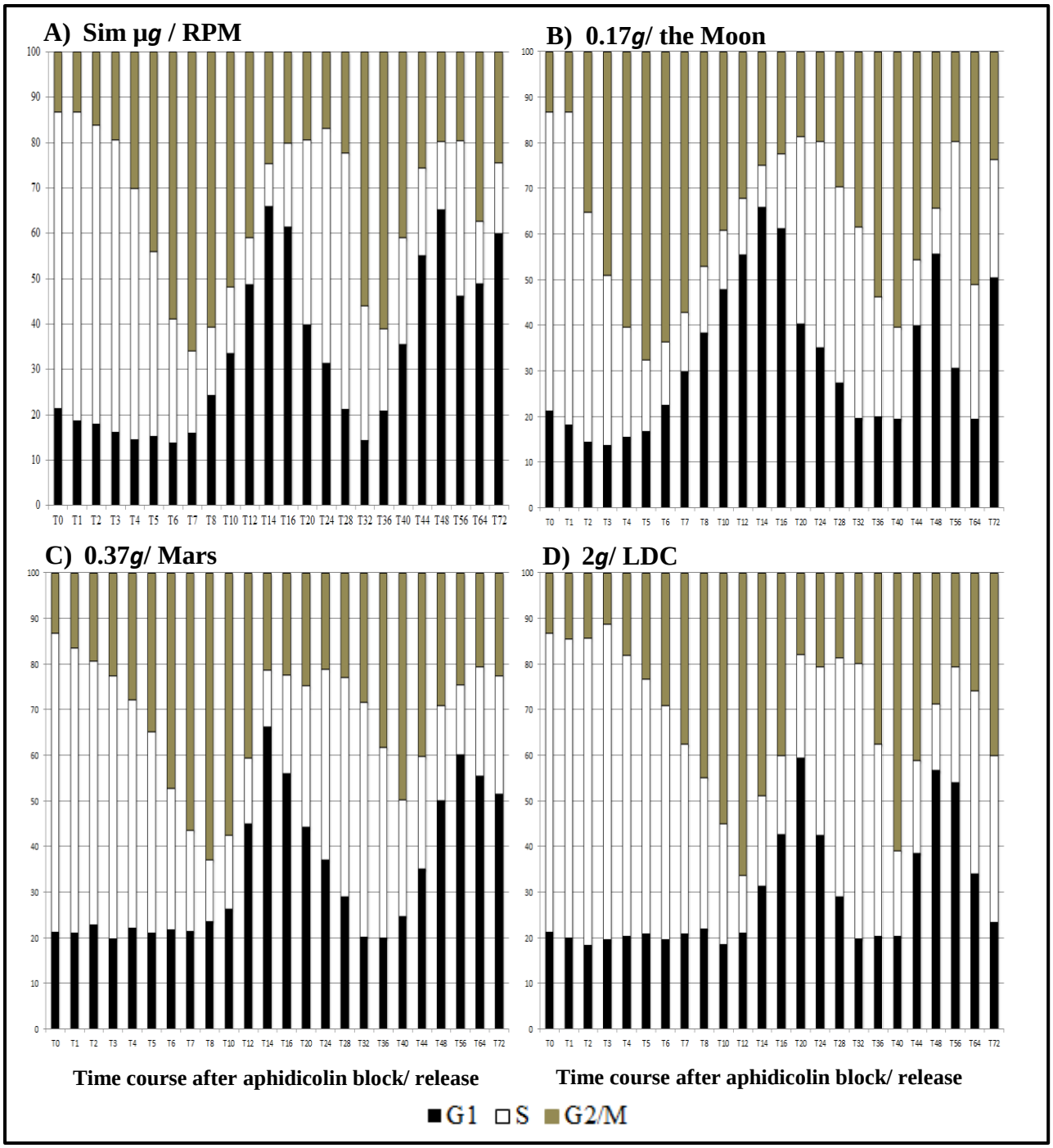

Figure 50. Cell cycle progression for 72h after aphidicolin block/release of *Arabidopsis* cell line MM2d immobilized under different gravity levels. **A) Simulated Sim µ*g*/ RPM conditions. B) 0.17*g*/ the Moon. C) 0.37*g*/ Mars. D) 2*g*/LDC.** DNA histograms of the cell cycle phases distribution by flow cytometry analysis (DAPI) regarding to the DNA content**.** Samples are taken at different times after the release of aphidicolin block in late G1/early S phase (T0) from t=0 to t=72 hours. 100% of the DNA content distributed among the cell cycle phases G1 (Black), S-phase (White) and G2/M (Brown). Source data on the distribution of the cell cycle (complete flow cytometry analysis as shown in **Figure 49A&B**) is displayed in the supplementary data **(Figure S1, S2, S3, and S4)**

3.3. Cell Cycle Progression through 72h after aphidicolin Block/Release under The Moon condition (0.17*g*/RPM^{SW})

Similar approach was performed under simulated Moon gravity conditions (0.17*g* by using RPM^{SW}). After release of the aphidicolin arrest, successive S phase peaks appear at T1 (68.45%), T24 (45.25%), and T56 (49.6%) respectively **(Figure 50B)**. G2/M peaks are observed at T5 (67.4%), T40 (60.3%), and T64 (51%). Cells are accumulated at G1 phase at T14 (65.9), T48 (55.7%), and T72 (50.5%). It seems that synchronization is well preserved, even in the third cycle. First cell cycle duration is around 23 hours (T1 to T24). In this cycle, cells progress rapidly from S phase to G2/M (4 hours, even shorter than in simulated microgravity), it takes 9 hours to reenter to G1 phase. Second cycle seems to be slightly wider; it is estimated up to 28-32 hours. Cells spend 15 hours to enter to G2/M and 8 hours to start a new cell cycle in the G1 phase. The third cycle is well observed also, although the difference between each cell cycle phases peaks is hard to estimate due to sparse sampling.

3.4. Cell Cycle Progression through 72h after aphidicolin Block/Release under Mars condition (0.37*g*/RPM^{HW})

Cell cycle phases through a similar 72 hours experiment performed at Mars gravity level (0,37*g* simulated in the RPM^{HW} facility) are monitored by observing the peaks of each phase **(Figure 50C).** S phase peaks reflecting the maximum proportion of cells in S phase, with 57.7% and 51.3% are found at T2 and T32 respectively. This data suggests that the first cell cycle duration is longer than normal, about 30 hours. Cells accumulate at G2/M phase for both, first and second cell cycle at T8 (62.7%), and T40 (49.7%). The duration of entering G2/M form S phase is closely similar 6, and 8 hours. Reentering a new cell cycle in G1 is observed in the first cell cycle at T14 (66.2%) and in the second at T56 (60.2%). The time from mitosis division to the next G1 peak is variable between the first and second cell cycle. It takes only 6 hours in the first cycle to renter into a new cell cycle in G1 compared with up to16 hours in the second one. A clear conservation of the synchronization up to T56 is observed, probably up to T72, although this is hard to say due to the unusually longer second cell cycle duration.

3.5. Cell Cycle Progression through 72h after aphidicolin Block/Release under Hypergravity Condition (2*g*/LDC)

Similar sampling approach was performed for 72h after release the drug under hypergravity(2*g*) condition provided by the LDC, showing even better preservation of the synchronization percentages through the three cell cycles **(Figure 50D).** The first cell cycle is predicted to start with the peak of S phase (T2 = 67.2%), passing the cells through G2/M (T12 = 66.1%) in a duration of 10 hours, opposite trend to the one observed under micro- and partial gravity samples. Cells need 8 hours more to reach the G1 peak (T20 = 59.5%). The first cell cycle is consequently longer than usual, approximately 30 hours were required to detect the second S phase peak (T32 = 60.1%). Through the second cell cycle (Start from T32 up to T60 as predicted the S phase peaks) cells spend 8 hours to enter to G2/M (T40 = 60.7%) compared with 10 hours in the first cycle, and another 8 hours to renter to G1 (T48 = 56.7%) as the same in the first cell cycle. The second cell cycle duration is around 28 hours. Due to the delayed cell cycles, we could not detect the third cell cycle beyond the 72 hours study time limit. But it can be estimated that S phase is around T60. Again suggesting a longer than expected cell cycle duration.

3.6. Cell Cycle Progression Varies in Opposite Ways under Hypo and Hypergravity Conditions

Here we are going to recapitulate and compare the first cell cycle phases durations for 24 hours in each altered gravity condition compared with 1*g* control. **Figure 51** shows the differential cell cycle progression starting from T0 release in each case. Different colored diagrams reveal the sampling times.

In each experimental condition, we choose the sample in which the different subpopulation peaks have been reached (S phase, G2/M phase and G1 phase), representing the previous sampling times by colors. Cell cycle progression rate is higher under simulated hypogravity by RPM (simulated microgravity, the Moon and Mars) compared with the 1*g* control respectively according to the acceleration rate. The cell cycle is 5, 3, and 2 hours shorter respectively (the Moon, simulated microgravity and Mars conditions), being the Moon condition the more intensively affected. On clear opposition, cell cycle duration expands under hypergravity conditions (2*g*/LDC). The cell cycle duration is 3-4 hours longer in hypergravity compared with the 1*g* control.

Figure 51. *Arabidopsis* cell line MM2d first cell cycle progression after aphidicolin release. A) 1*g* control. B) Sim µ*g*/RPM. C) 0.17*g*/the Moon. D) 0.37*g*/Mars. E) 2*g*/LDC. Distribution of cell cycle phases by flow cytometry analysis (DAPI) regarding to the DNA content. First peak (2n) reveals to G1 phase and the second peaks (4n) reveals to G2/M phase**.** Each colored block represents a sample taken at a certain time after aphidicolin release, Red color = T0, blue color = T1, pink color = T2, lime color = T5, cyan color = T7, orange color = T8, purple color = T10, green color = T12, yellow color = T14, olive color = T16, and turquoise color = T20.

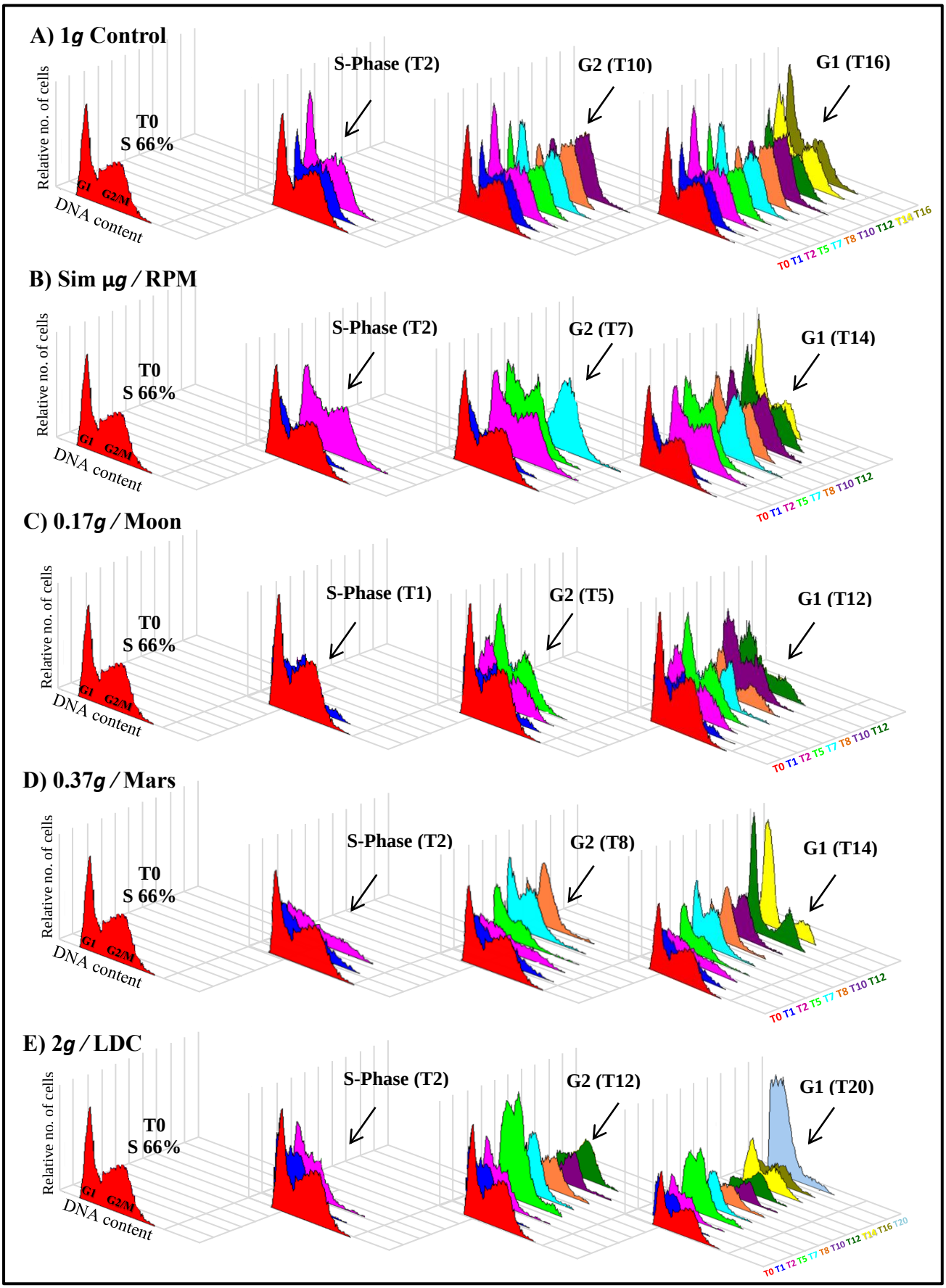
A) 1g Control
Relative no. of cells
DNA content
G1
G2/M
T0
S 66%
S-Phase (T2)
G2 (T10)
G1 (T16)
T0 T1 T2 T5 T7 T8 T10 T12 T14 T16
B) Sim µg / RPM
Relative no. of cells
DNA content
G1
G2/M
T0
S 66%
S-Phase (T2)
G2 (T7)
G1 (T14)
T0 T1 T2 T5 T7 T8 T10 T12
C) 0.17g / Moon
Relative no. of cells
DNA content
G1
G2/M
T0
S 66%
S-Phase (T1)
G2 (T5)
G1 (T12)
T0 T1 T2 T5 T7 T8 T10 T12
D) 0.37g / Mars
Relative no. of cells
DNA content
G1
G2/M
T0
S 66%
S-Phase (T2)
G2 (T8)
G1 (T14)
T0 T1 T2 T5 T7 T8 T10 T12
E) 2g / LDC
Relative no. of cells
DNA content
G1
G2/M
T0
S 66%
S-Phase (T2)
G2 (T12)
G1 (T20)
T0 T1 T2 T5 T7 T8 T10 T12 T14 T16 T20

RESULTS

CHAPTER 4: *CHARACTERIZATIONS OF SIMULATED MICROGRAVITY (μg RPM) DIFFERENTIAL EFFECTS ON ARABIDOPSIS CELL CYCLE PHASES SUBPOPULATIONS*

4.1. Defining The Sampling Reference Time For Each Cell Cycle Phase Subpopulation

4.2. Characterization Of Cell Cycle Phases Under 1*g* Control And Simulated Microgravity

4.2.1. Differential Nucleolar Structure and Activity during Each Cell Cycle Phases

4.2.2. Simulated Microgravity Effects on Nucleolar Ultrastructure at Cell Cycle Subpopulations

4.2.3. Simulated Microgravity Effects on Nucleolar Activity in Different Cell Cycle Phases

4.2.4. Simulated Microgravity Effects at the Protein & Gene Expression Levels in Different Cell Cycle Phases

4.2.5. Simulated Microgravity Modifies the Chromatin Organization and RNA Polymerase II activity through the cell cycle progression

4.2.6. Simulated Microgravity Modify DNA Methylation and Histone H4 Acetylation Patterns through the Cell Cycle Phases

CHAPTER 4: CHARACTERIZATIONS OF SIMULATED MICROGRAVITY (μg RPM) DIFFERENTIAL EFFECTS ON ARABIDOPSIS CELL CYCLE PHASES SUBPOPULATIONS

Any alteration on cell proliferation will lead to the establishment of alterations in the cell cycle progression. The cellular mechanisms regulate cell growth and proliferation and consequently, cell cycle progression affect the regulation of all the basic cellular process such as ribosome biogenesis. Furthermore, cell cycling activity and regulation has a strong influence on the definition of the development patterns (Beemster et al 2003, Gutierrez 2005) as well as the chromatin organization and epigenetic mechanisms varies through the cell cycle phases. So on, characterization of our study parameters in the different *Arabidopsis* cell cycle phases subpopulations defined at ***Chapter 3*** is important to understand the influence of simulated microgravity on plant cell, and even more to follow the regulation of the cell cycle and its effect on the other cellular process. In order to isolate each cell cycle phase subpopulation, synchronization was applied as described in the previous chapter under simulated microgravity compared with the 1*g* control to characterize the pattern of:

- Nucleolus structure and activity through different cell cycle phases
- Ribosome biogenesis and transcriptional activity through the cell cycle
- Chromatin organization controlled by epigenetic modifications through cell cycle phases

4.1. DEFINE THE SAMPLING REFERENCE TIME FOR EACH CELL CYCLE PHASE SUBPOPULATION

4.1.1. Using Cell Cycle Synchronization to Localize the Cell Cycle Phases under 1*g* Control and Simulated Microgravity

As described in the previous chapter, *Arabidopsis* cell cycle was synchronized using Aphidicolin block/release. Cell cycle progresses through the time course. Samples are collected for the flow cytometry analysis, in which we can determine the percentage of the proportion of cells in each cell cycle phases, G1, S, and G2/M. Results obtained from **figure 51A and B** show the different

cell cycle subpopulation peaks under 1*g* control and simulated microgravity. Under 1*g* control conditions, T2, T10, and T16 are referenced to S, G2/M, and G1 phase, in which more than two thirds of the cells are synchronized. Similarly, T2, T7, and T14 are referenced to S, G2/M and G1 sampling times respectively under the simulated microgravity conditions. The 6 reference sampling times (T0, T2 as common points and the 4 specific G2/M and G1 points) were used in both 1*g* and simulated microgravity samples.

4.1.2. Use Specific Cell Cycle Regulators markers to verify Cell Cycle Progression

As a first check that the sampling times have been properly chosen, we used a flow cytometry determination of some cell cycle proteins such as, Cyclin B1 in the control of G2/M transition (Breyne & Zabeau 2001, Mironov et al 1999, Potuschak & Doerner 2001), and Prolifera (Mcm7) protein which accumulates in the nucleus of recently divided cells during G1 phase (Springer et al 2000). This check is mandatory due to the partial (2/3) synchronization level.

Frozen aliquots of the same samples used in ***Experiment 5*** were used to validate the cell cycle references samples. Samples were stained with the specific antibodies for each protein. Quantity analysis was performed using flow cytometry approach.

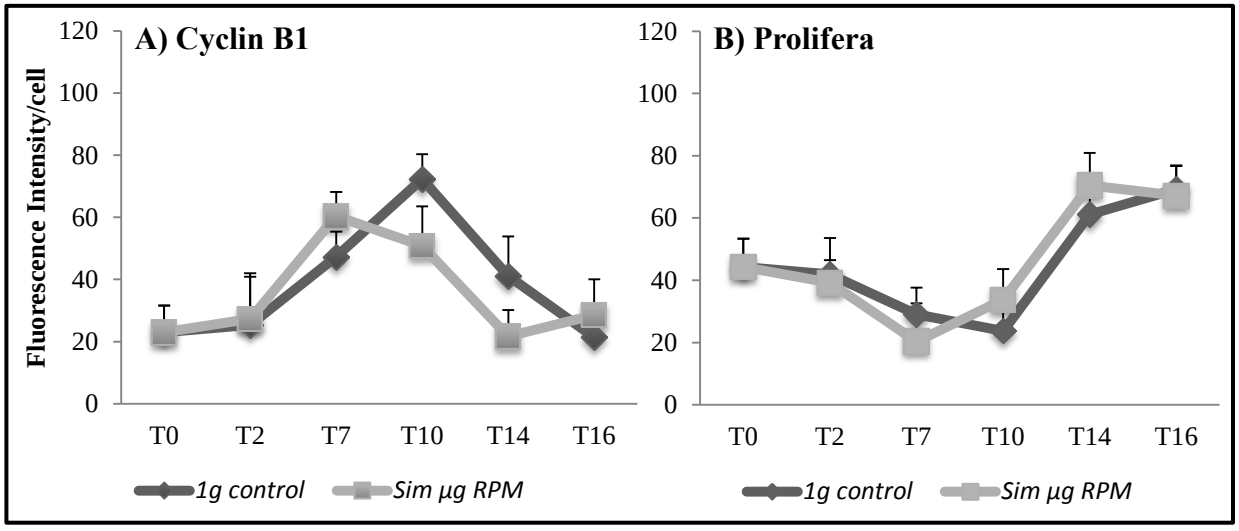

Figure 52: Cell cycle regulators (CyclinB1 and Prolifera) used as cell cycle phases markers. Cells are exposed to different gravity level; 1*g* control, Sim µ*g*/RPM after release the Aphidicolin block/release (T0) for ***Experiment 5***. Protein expression level is evaluated by quantifying fluorescence intensity in 10000 cells using specific fluorescent antibodies by flow cytometry.

Cyclin B1 level (fluorescence intensity) is used as G2/M Marker. Cyclin B1 levels, detected by estimating the protein fluorescent intensity using the flow cytometry approach, reaches the maximum values at T10 and T7 under $1g$ control and simulated microgravity respectively **(Figure 52A)**. So on, T10 and T7 reference samples correlates to G2/M phase under $1g$ control and simulated microgravity respectively. Cyclin B1 levels remains lower in other samples through the time course.

Prolifera level (fluorescence intensity) is used as G1 marker. Prolifera level quantification using the fluorescent intensity **(Figure 52B)** maximum peaks appear after T16 and T14 under $1g$ control and simulated microgravity respectively, correlating with the G1 phase as expected.

Coalescing the previous results; under $1g$ control, it is noticed that, T2, T10, and T16 refer to S, G2/M, and G1 respectively, while it is referenced under simulated microgravity up to T2, T7, and T14 respectively.

4.2. CHARACTERIZATION OF CELL CYCLE PHASES UNDER $1g$ CONTROL AND SIMULATED MICROGRAVITY

4.2.1. Differential Nucleolar Structure and Activity during Each Cell Cycle Phases

As described in other plant systems (Gonzalez-Camacho & Medina 2006, Manzano 2011) a link between nucleolar morphology and cell cycle phases exits. We extended this study to the system of cell culture synchronization after the aphidicolin block/release. However, since the aphidicolin synchronization reaches only 70%, a possibility of confusing results could exist if a nucleolus belonging to a non-synchronic cell is accidentally selected as representative of the period corresponding to the sample taken at the reference time. In order to minimize this possibility of confusion, we have first counted the different structure models on the level of contrast phase microscope to have a the general view and count the different structure models of the nucleolus under $1g$ conditions, and then extended the ultrastructure study to nucleoli showing the typical nucleolar of each cell cycle phase under control and simulated microgravity conditions.

Samples from ***Experiment 6*** were prepared as semi-thin to quantify in the contrast phase microscope the different nucleoli models which described by (Manzano 2011), **Figure 12**) for the selected referenced times after synchronization (T2, T7, T10, T14, T16).

Under 1*g* control conditions **(Figure 53);** the major nucleolus model is the compacted one (65%) at T2 compared with vacuolated and inactive/fibrillar models. At T7, an increment on the percentage of vacuolated nucleolus model (40%) due to a reduction on the compacted model (40%) occurs. These effect is deeper at T10, the major nucleolus model corresponding to T10 is the vacuolated (65%) compared with 30% of the compacted model and virtually none inactive nucleolus. At T14 and T16 the pattern is very similar, 80% of the nucleolus population belongs to the compacted model with a less than 10% of each vacuolated and fibrillar models.

Thus, these nucleolar models are coherent with the expected cell nucleolus activity in the different cell cycle phases. S phase period is referenced by T2 in which compacted nucleolus model is present. Vacuolated nucleolus models are maximized at the T10, the reference time for the G2/M period. Furthermore, T16 is characterized by compacted nucleolus models that are more frequent at G1 phase.

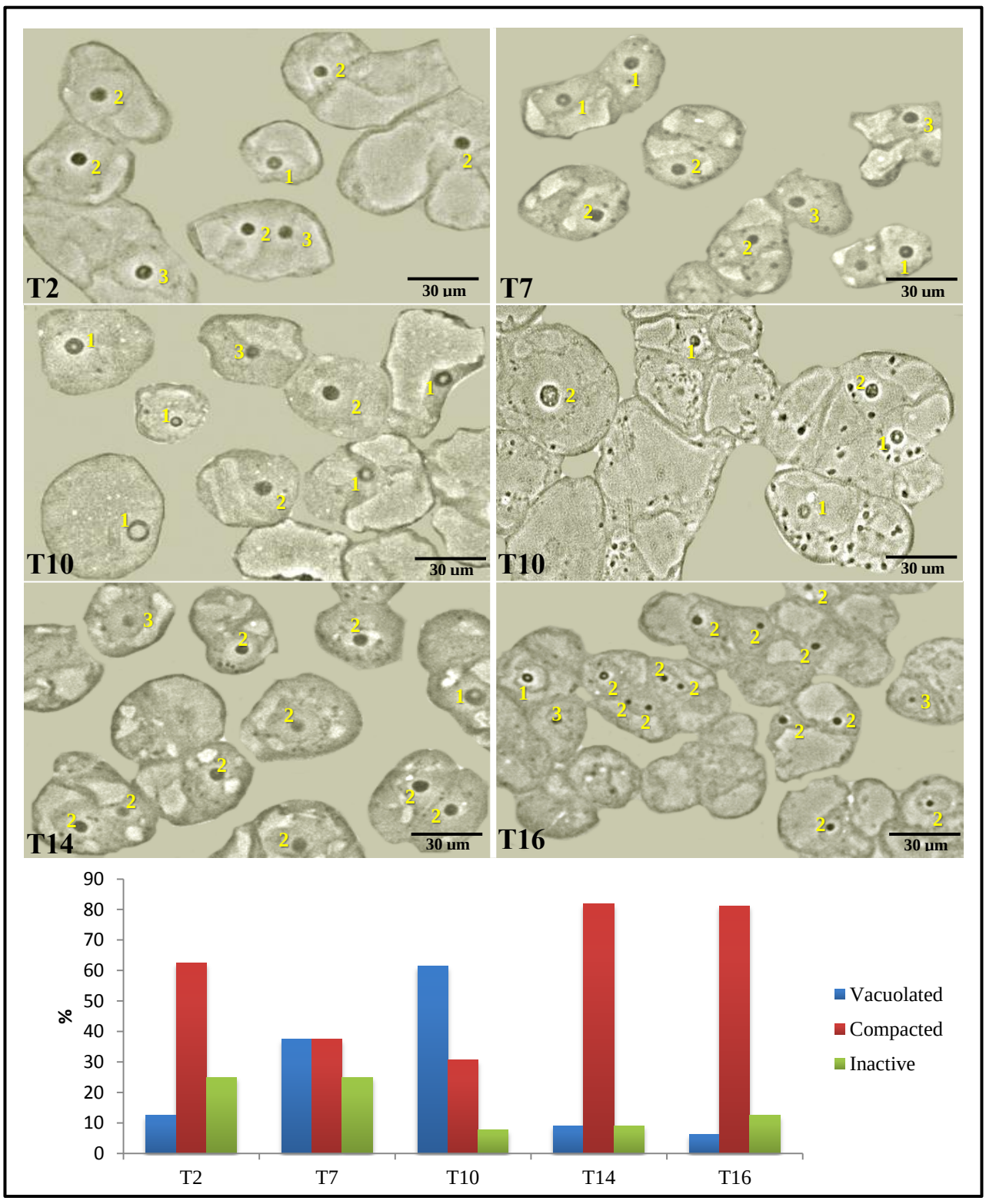

Figure 53: Nucleolus structure models distribution through the cell cycle progression after synchronization under 1*g* control conditions (T2, T7, T10, T14, and T16). Nucleolus structure models are observed using the microscope in the contrast phase to visualize the 3 different models which defined by (Manzano 2011); (1) Vacuolated, (2) Compacted, (3) Fibrillar. % of the nucleolus model distribution is estimated according to the total number of the nucleolus observed.

4.2.2. Simulated Microgravity Effects on Nucleolar Ultrastructure at Cell Cycle Subpopulations

Nucleoli were selected as representative of each specific cell cycle phases attending to the nucleolar morphology and size. Then they were analyzed ultrastructurally in conventionally fixed (Glutaraldehyde/LRW) cross-sections at the electron microscope. Depending on the previous results, compacted nucleolus models is associated to G1 phase and other compacted larger associated to S phase, and the vacuolated one associated to G2 phase.

In the G1 phase **(Figure 54A)**; the compacted nucleolus is constituted practically exclusively by a dense fibrillar component. It shows abundant DFC (70%) with a lower level of GC (20%) and a complete absence of a nucleolar internal space which called nucleolar vacuoles. Fibrillar centers (FCs) occupied a 10% of the total nucleolar area **(Table 9)**. Interestingly, G1 nucleolus has no vacuole models in *Arabidopsis*, while it is observed in onion (Gonzalez-Camacho & Medina 2006). G1 compacted nucleolus is the smallest one among the different cell cycle models. Moreover, G1 phase nucleolus structure and organization is altered by simulated microgravity; it shows increases on the nucleolar vacuoles to 5% embedded in the DFC with increment on the FCs distribution up to 15%. Furthermore, this gravitational alteration is not produce significantly different nucleolar size.

In the S phase, the nucleolus is double sized compared with the compacted nucleolus in the G1 phase **(Table 9)**. This increment is accompanied with the changes on the ultrastructure features which appeared conspicuously changes **(Figure 54B)**. The lower level of GC in the G1 phase is compensated by its thickness and distribution, appearing in the S phase as a more abundant component (60%). Consequently, the mass of DFC was reduced with small vacuoles areas.

Nevertheless, the relative organization of the DFC and GC was conserved oppositely in the S phase than the G1. Moreover, within the DFC region, FCs are observed higher and bigger than in G1 but in a small numbers. Morphometrically, the relative abundance of the DFC was reduced in the S phase to one-third of that shown in G1, whereas the GC was more than three times the one in G1 **(Table 9)**. S phase associated nucleolus structure and size is altered by the simulated microgravity alteration.

The nucleolar size is not significant affected, but the distribution of the nucleolar component is significantly different than the 1*g* control. DFC is increased significantly to be abundant mass of the nucleolus (65%). This increment on DFC is compatible with the depletion on the distribution of the GC (13%). Interestingly, it is observed an increment FCs size, it becomes connected and larger and decreased in the number compared with the 1*g* control conditions.

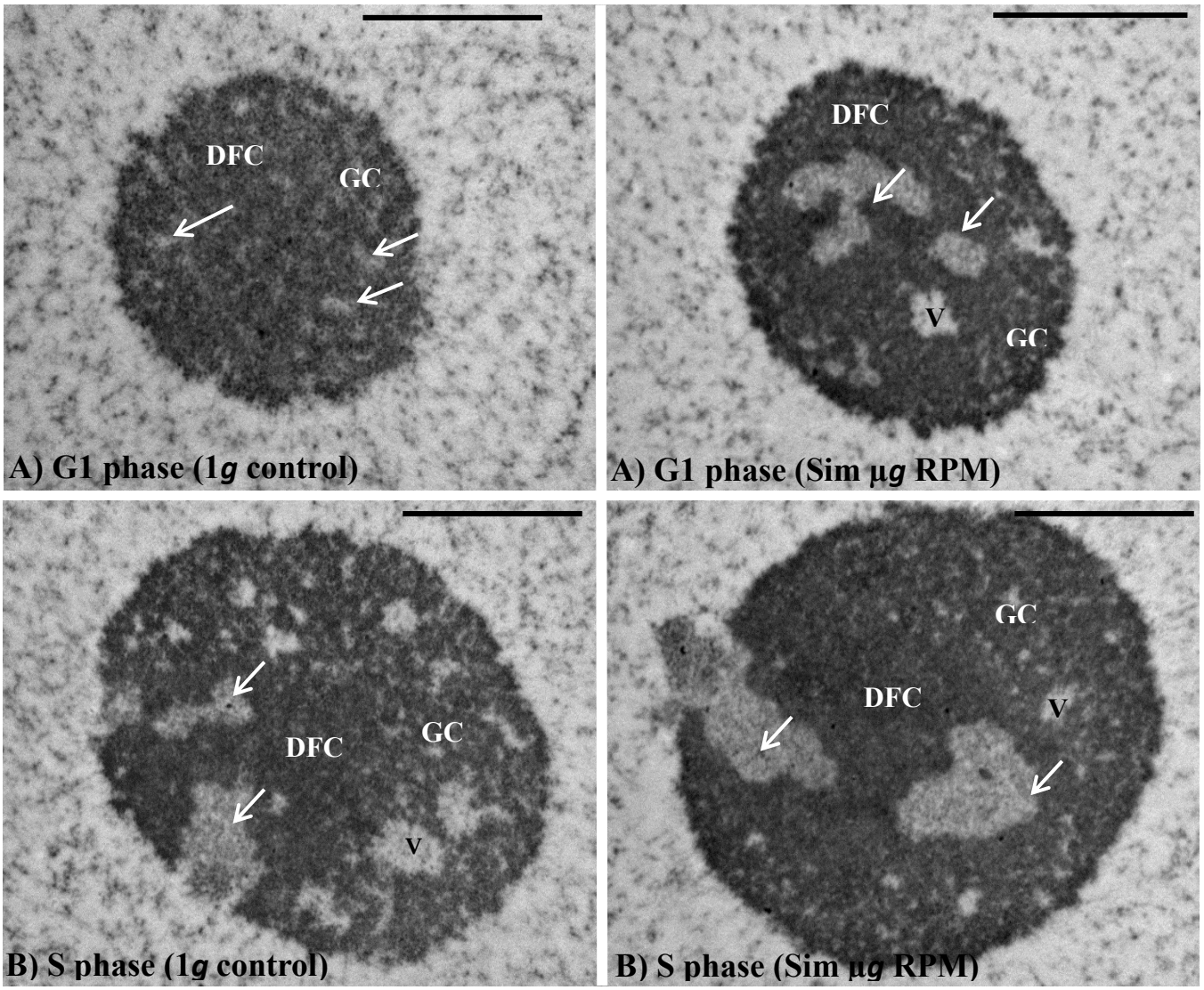

Figure 54: Ultrastructure of nucleoli in synchronized cells associated with different cell cycle phases (G1 and S phase) under 1*g* control and simulated microgravity. A) Compacted nucleolus associated to G1; samples were taken after 14 and 16 hours of synchronizations in 1*g* control and simulated microgravity respectively. B) Compacted nucleolus associated to S phase, samples were taken after 2 hours of synchronizations in both 1*g* control and simulated microgravity. DFC refers to the dense fibrillar centers. GC refers to the granular component. V refers to the clear space ¨nucleolar vacuole¨. The arrows refer to the fibrillar centers (FCs).

In the G2 phase. Two types of the nucleolus models are associated to the G2 phase, depending on the presence of a large central nucleolar vacuole **(Figure 55)**. Enough structural differences were observed between the two types to discard the possibility that being the same nucleolus models sectioned at different levels. The ¨no vacuolated¨ model is similar to the one in S phase but with a large distribution of the fiber centers (50%) surrounded by the DFC with a slightly increased distribution of the GC (25%).

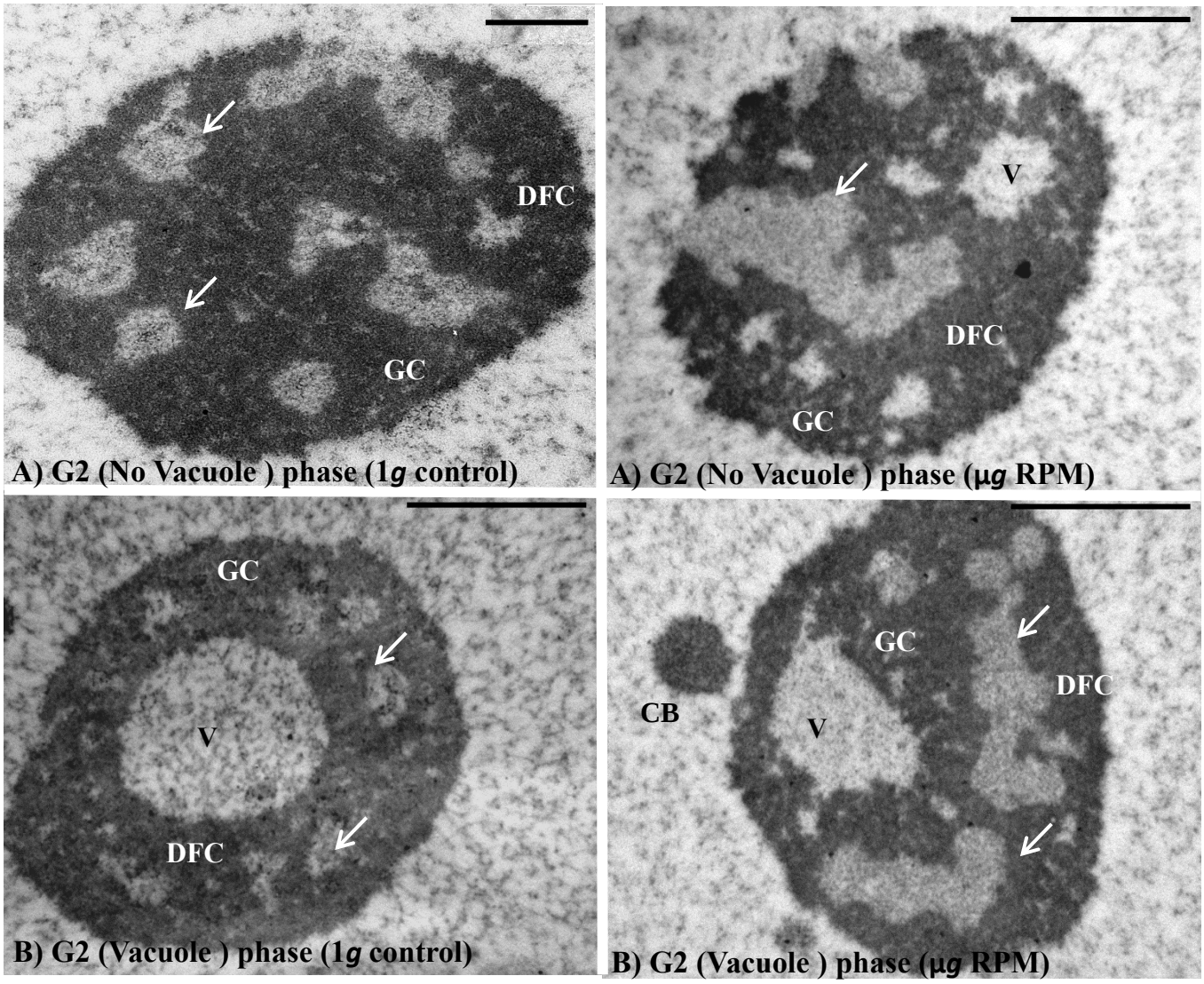

Figure 55: Ultrastructure of nucleoli in synchronized cells associated with different cell cycle phases (G2 phase) under 1*g* control and simulated microgravity. A) No vacuole nucleolus associated to G2; samples were taken after 7 and 10 hours of synchronizations in 1*g* control and simulated microgravity respectively. B) Vacuole nucleolus associated to G2 phase, samples were taken after 7 and 10 hours of synchronizations in 1*g* control and simulated microgravity respectively. DFC refers to the dense fibrillar centers. GC refers to the granular component. V refers to the clear space ¨nucleolar vacuole. The arrows refer to the fibrillar centers (FCs). CB refers to cajal bodies.

The ¨vacuolated¨ model contains a large central space ¨vacuole¨ (50%) surrounded by a thin layer of the GC (20%) and FCs (20%). Moreover, it is observed that this vacuole is not linked structurally to any FCs. The number of fiber centers on the vacuolated is lower than in the no vacuolated model. Cajal bodies are associated with G2 phase. This observation is noticed also in the optical microscope in T7 and T10 (**Figure 53**). Morphometrically, there are no substantial differences between the two structural models, except for the presence of the vacuole. The GC accounts 20-25% of the nucleolar area, and the highest value of the fibers centers through the cell cycle periods appear in the no vacuolated G2 associated nucleolus, beside the number of these FCs is higher than the rest of the cell cycle phase **(Table 9).**

Simulated microgravity produces important effects in the nucleolar structure during G2 phase **(Figure 55)**. One the one hand, the number of inactive nucleolus is increased, on the other both two G2 phase models show larger amount of the DFC through the nucleolus counted more than 50% of the nucleolar area with a significant increment on the distribution of the FCs which connected the small spots in a large regions through the nucleolar area compared with the 1*g* control. Furthermore, the G2 nucleolus under the alteration of the simulated microgravity is significant smaller than the 1*g* control one **(Table 9)**.

Table 9: Nucleolar size and structure (distribution of the nucleolar components) for the different nucleolar models associated to the cell cycle phases under 1*g* control and the simulated microgravity conditions.

Data were obtained from the electron microscope images, FCs (Fibrillar centers), DFC (dense fibrillar centers), GC (granular component), V (vacuole), No-Vac (no vacuole model), Vac (vacuole model)

Phase	Nucleolar Size (μm^2) (Mean ±STD)	Nucleolar Component (%)			
		FCs	DFC	GC	V
1*g* Control					
G1	10.34 ± 1.37	10.2	69.8	20	0
S	25.50 ± 0.69	14.2	22.1	57.8	5.9
G2 (No-Vac.)	46.06 ± 0.99	49.6	18.3	25	7.1
G2 (Vac.)	48.19 ± 1.03	20.3	15	20.2	44.5
μ*g* RPM					
G1	13.84 ± 0.82	14.3	61.4	19.1	5.2
S	28.54 ± 1.11	17.1	65.6	13	4.3
G2 (No-Vac.)	39.12 ± 2.45	27.7	42.6	18.3	11.1
G2 (Vac.)	37.09 ± 0.75	28.2	51.6	7.4	12.8

4.2.3. Simulated Microgravity Effects On Nucleolar Activity in Different Cell Cycle Subpopulations

Nucleolar activity, estimated by the average nucleolar area in each cell cycle phase reference sample, remains constant through G1 and S phases, and is significantly doubled in G2/M phase in both 1*g* control and simulated microgravity conditions **(Figure 56).** On other hand, the normal G2/M nucleolus increase in size observed in 1*g* control is significantly reduced under simulated microgravity, while microgravity effect is barely observed on G1 and S phases' nucleolus.

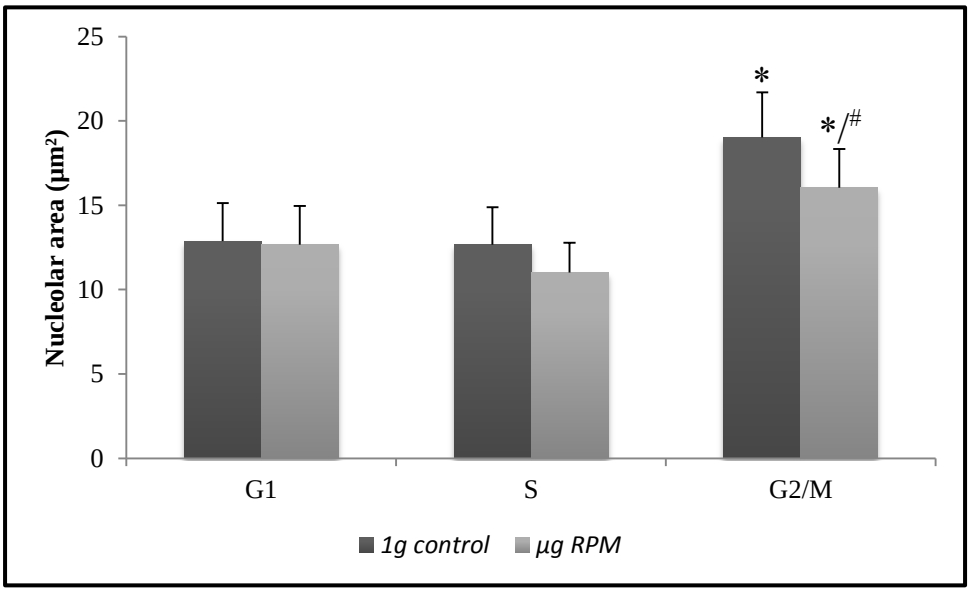

Figure 56: Nucleolar area through *Arabidopsis* cell cycle phases under 1*g* control and simulated microgravity (µ*g RPM*). More than 50 nucleolus area (α-nucleolin staining) of *Arabidopsis* cells were measured for each experiment conditions. P-Value < 0.05 is shown for significant differences calculated within cell cycle phases (without changing *g* level, *) or simulated microgravity versus 1*g* control (without changing cell cycle phase, #).

4.2.4. Simulated Microgravity Effects at the Protein & Gene Expression Levels in Different Cell Cycle Subpopulations

Effects on Ribosome biogenesis markers (Nucleolin and Fibrillarin). Using the flow cytometry approach, nucleolin level is increased significantly (doubled) in S phase conditions compared with G1 **(Figure 57)**. These increments are increased even more (tripled) under G2/M phase. Regarding the impact of the simulated microgravity, it is noticed that the cell cycle variations are reduced; nucleolin protein expression is decreased significantly in G2/M phase

compared with G2/M in 1*g* control conditions, while this alteration is not enough within other phases. This result is compatible with the nucleolin gene quantitative gene expression analysis **(Figure 58)**, in which the level of the gene expression is increased significantly in both, S and G2/M phase (triple amount) under 1*g* control conditions, and significantly reduced in G2/M phase under simulated microgravity. Interestingly, under simulated microgravity the level of nucleolin is significantly higher in S phase conditions compared with 1*g* control.

Fibrillarin protein level show a significant increase on G2/M phase compared with G1 and S phase in both, 1*g* control and simulated microgravity **(Figure 57)**. As Nucleolin, the G2/M phase increase is smaller in the case of the simulated microgravity. Fibrillarin gene expression is also compatible with the protein level analysis **(Figure 58)**. It is found a significant increment on G2/M phase compared with G1 and S phase. Moreover, there is a significant depletion on G2/M influenced by the simulated microgravity compared with 1*g* control.

Effects on Cell cycle regulators markers (Cyclin B1 and Prolifera). Flow cytometry analyses confirmed **(Figure 57)** that cyclin B1 is a specific G2/M phase expressed protein compared with G1 and S phases. Under simulated microgravity a significant lower increase on the cyclin B1 levels was observed in comparison with 1g control on G2/M phase. Contrary, the level of cyclin B1 mRNA peaks significantly on our S phase samples compared with G1 and G2 phases in both 1*g* control and simulated microgravity. Surprisingly, this level is completely decreased on G2/M phase subpopulation **(Figure 58)**.

Prolifera role as G1 phase marker is confirmed, along with a significant decrease on S and G2/M phases **(Figure 57)**. This observation is supported by the gene expression analysis with an up regulation is shown under simulated microgravity **(Figure 58)**. Prolifera mRNA levels are altered, showing a significant up regulation in all the phases.

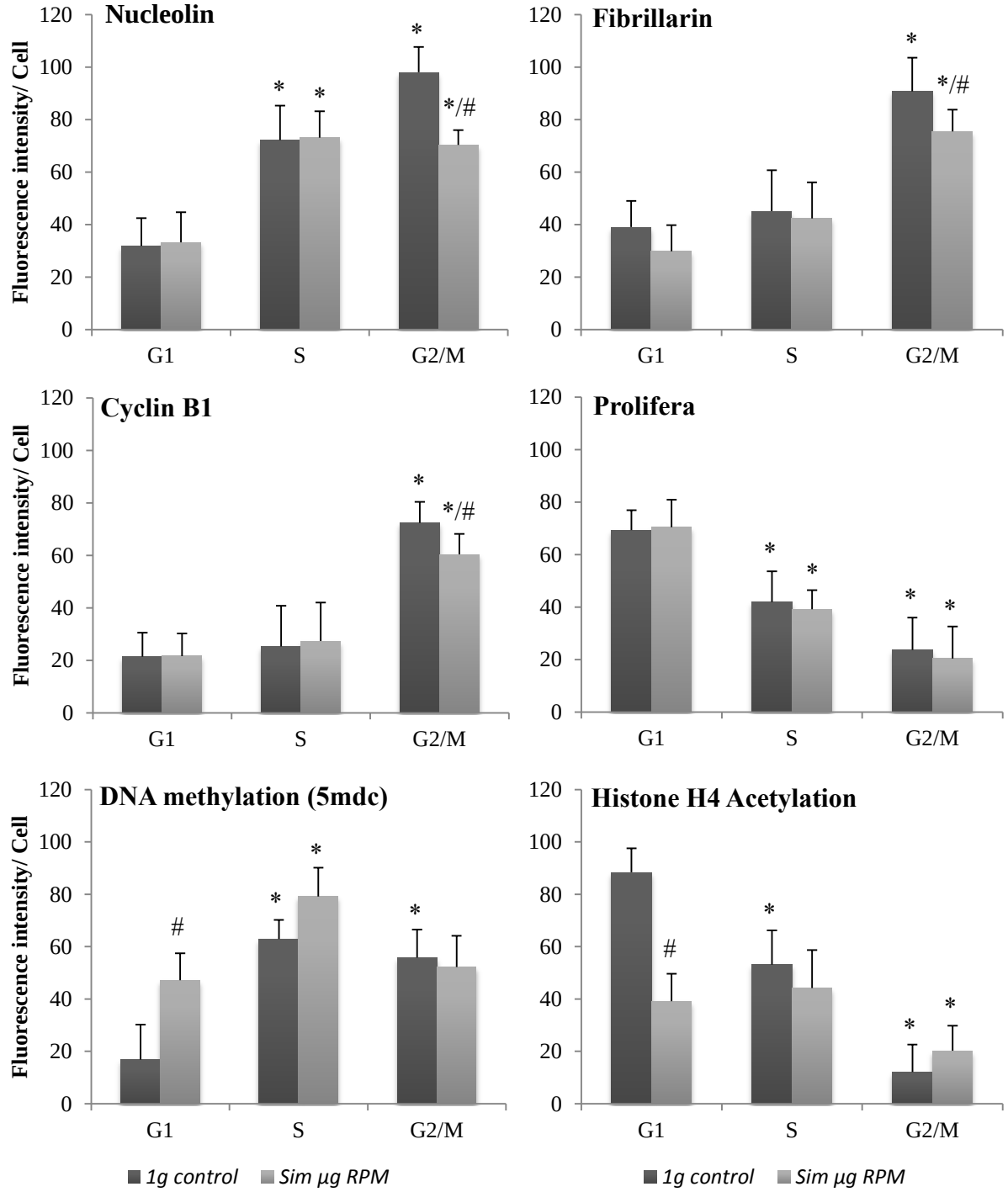

Figure 57: Flow cytometry determination of *Arabidopsis* proteins levels; ribosome biogenesis (Nucleolin and Fibrillarin), cell cycle regulators (Cyclin B1 and Prolifera), and epigenetic modifications (DNA methylation and histone 4 acetylation) markers through the cell cycle phases in 1*g* control and simulated microgravity (Sim µ*g* RPM) condition. P-Value<0.05 is shown for significant differences calculated within cell cycle phases (without changing *g* level, *) or simulated microgravity versus 1*g* control (without changing cell cycle phase, #).

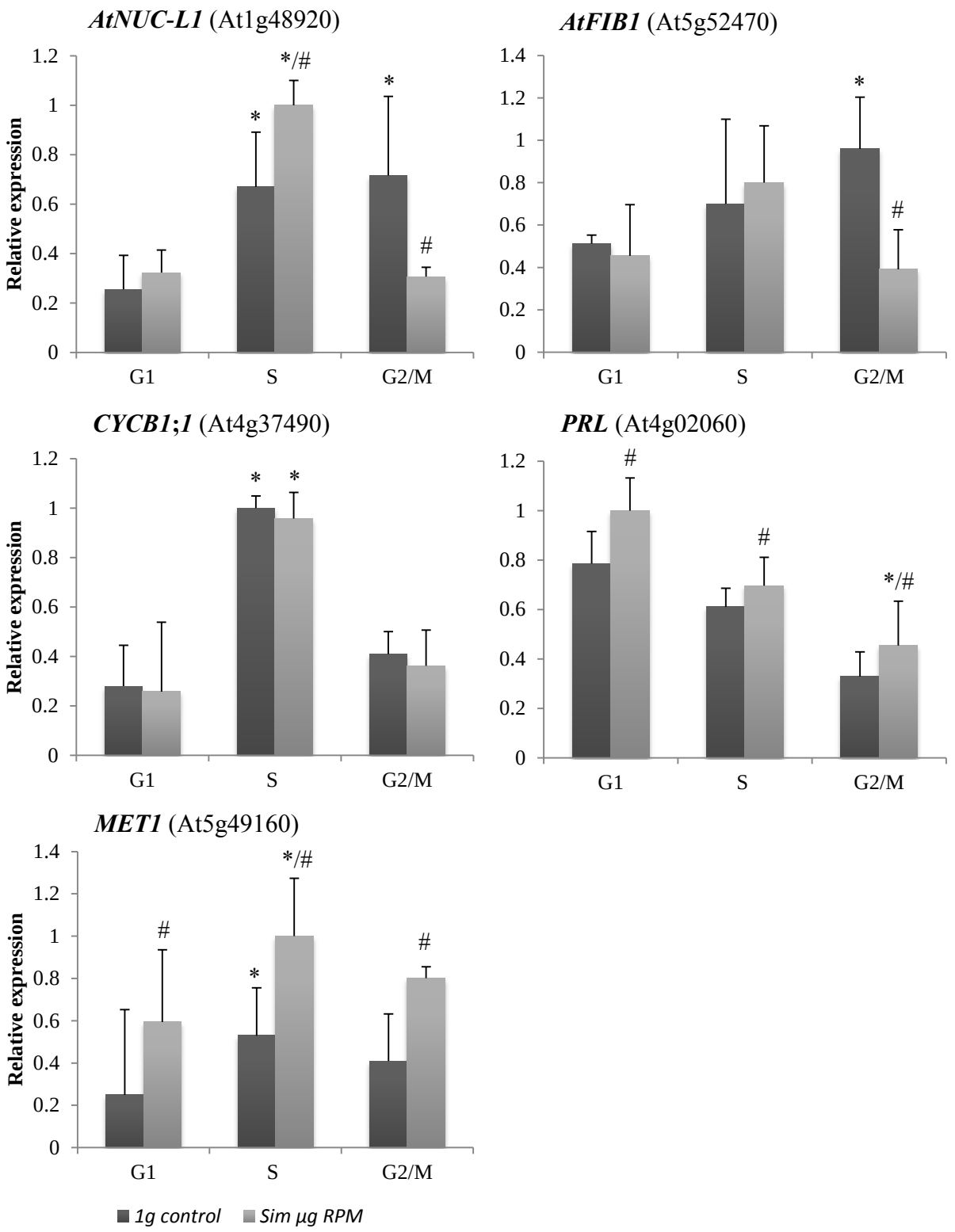

Figure 58: *Arabidopsis* cells relative gene expression (qPCR) for ribosome biogenesis (Nucleolin (AtNucL1) and Fibrillarin (AtFIB1)), cell cycle regulators (Cyclin B1 (CycB1;1) and Prolifera (PRL)) and epigenetic related genes (DNA methylation (MET1)) through the cell cycle phases in 1*g* control and simulated microgravity (Sim µ*g* RPM) condition. P-Value <0.05 is shown for significant differences calculated within cell cycle phases (without changing *g* level, *) or simulated microgravity versus 1*g* control (without changing cell cycle phase, #).

Effects on Epigenetic Modifications Dynamics (DNA Methylation and Histone H4 Acetylation). Chromatin reveals as a highly dynamic and major player in cell cycle regulation, not only owing to the changes that occur as a consequence of cell cycle progression but also because some specific chromatin modifications are crucial to move across the cell cycle such as DNA methylation and histone H4 acetylation.

Methylated cytidine (5mdc) fluorescent intensity **(Figure 57)** suggests DNA is significantly more methylated on S and G2/M phase compared with G1 in which a lower level of DNA methylation is observed under 1*g* control conditions. Under simulated microgravity, methylation activity is similar on S and G2/M phases but significantly higher on G1 also. This alteration is strongly supported by DNA methyltransferase gene expression **(Figure 58)**, which increase significantly not only on G1 but on all the cell cycle phases compared with 1*g* control and significantly high expressed on S phase compared with G1 and G2/M in both 1*g* control and simulated microgravity.

On the other hand, acetylated Histone H4 is inversely correlated with the methylation marker. G1 phase peak observed under 1*g* control **(Figure 57)** is lost under simulated microgravity conditions.

4.2.5. Simulated Microgravity Modifies The Chromatin Organization And RNA Polymerase II Activity Through The Cell Cycle Phases

Since RNA polymerase II is responsible for the synthesis of mRNA from protein-coding genes, it has been the focus of most studies of transcription in eukaryotes (Roeder 1996), and it has been used by us as a global marker of the transcriptional activity during cell cycle progression. ***Experiment 6*** samples were analyzed by confocal immunofluorescence with anti-RNAPolII and DAPI (anti-DNA) double staining. Under 1*g* control conditions, the organization of the chromatin mass and the distribution of the RNA polymerase transcription is similar during the cell cycle phases reference samples **(Figure 59A)**, while, the level of the RNA polymerase transcription fluorescence intensity is altered by the cell cycle progression **(Figure 60).**

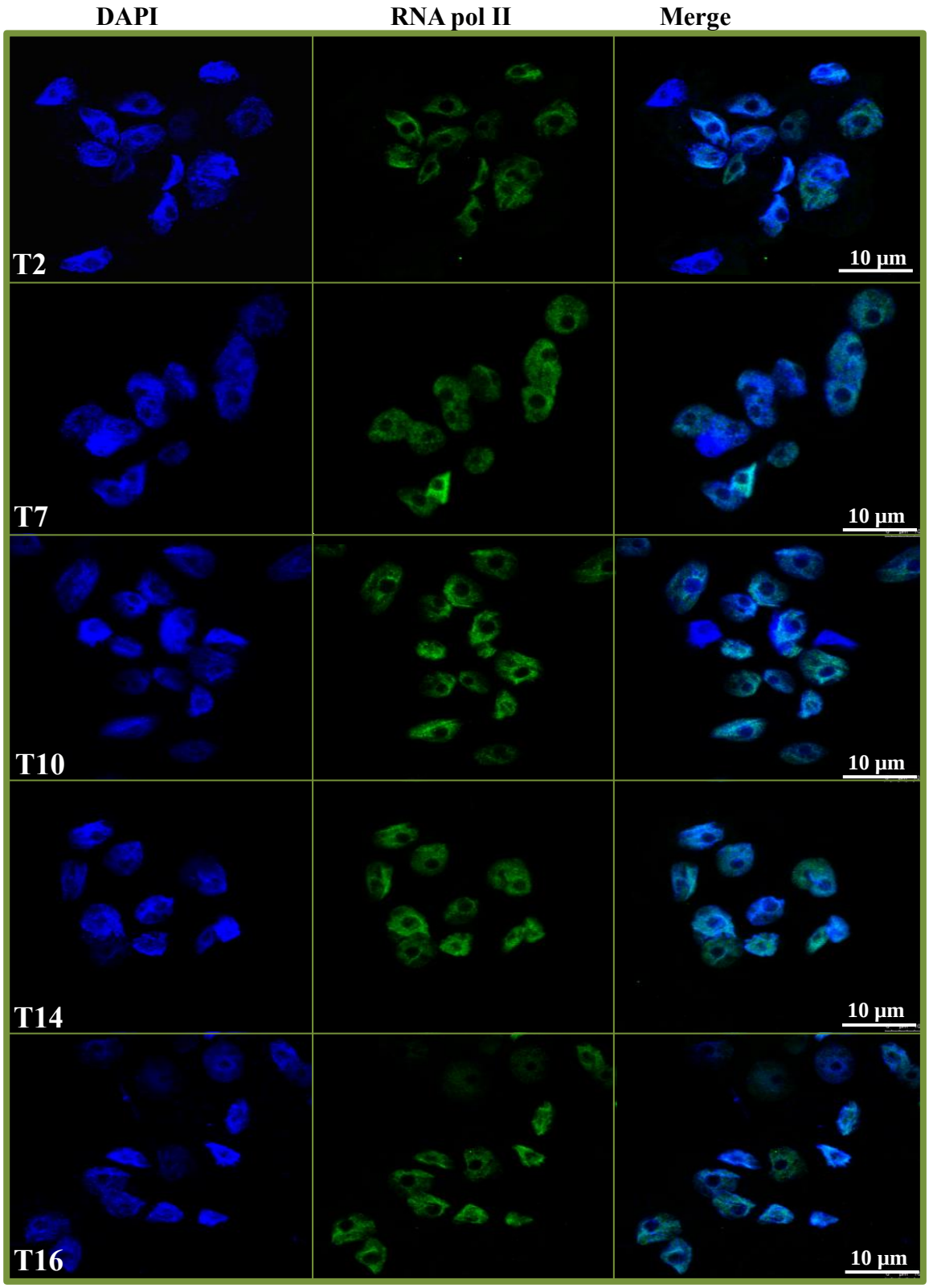

Figure 59A: pre-mRNA (extranucleolar) transcription (immunostaining by α-RNA pol II through *Arabidopsis* cell cycle progression under 1*g* control in the reference cell cycle time course after synchronization. A) Chromatin structure pattern, detected by DAPI staining (blue). **B)** Transcriptional levels estimated by α-RNA polymerase II immuno staining of nuclei (green). C) Confocal merges immunofluorescences images.

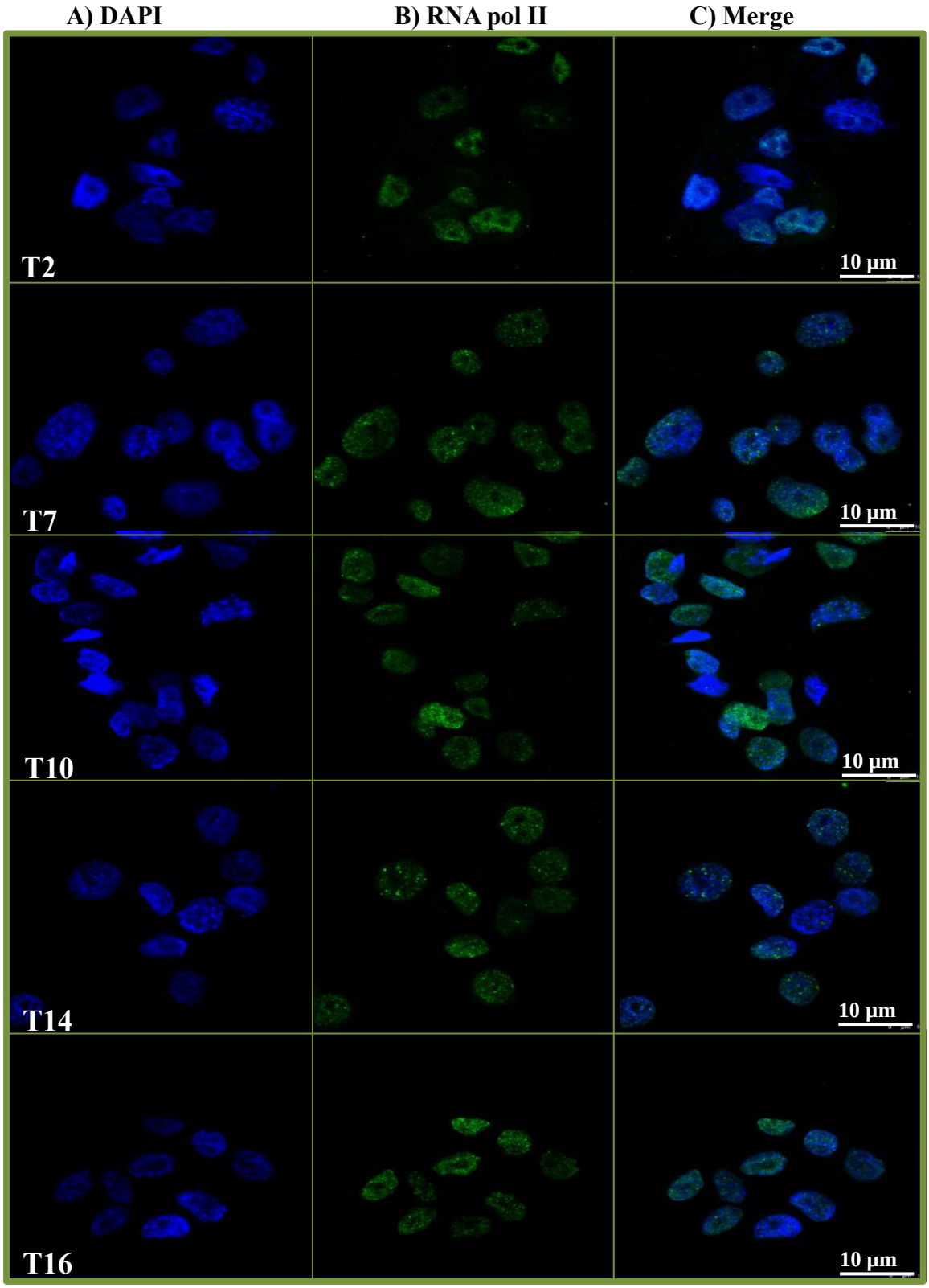

Figure 59B: pre-mRNA (extranucleolar) transcription (immune-staining by α-RNA pol II through *Arabidopsis* cell cycle progression under simulated microgravity exposure in the reference cell cycle time course after synchronization. A) Chromatin structure pattern, detected by DAPI staining (blue). **B)** Transcriptional levels estimated by α-RNA polymerase II immune-staining of nuclei (green). **C)** Confocal merges immunofluorescences images. Magnification was 63x (10 µm).

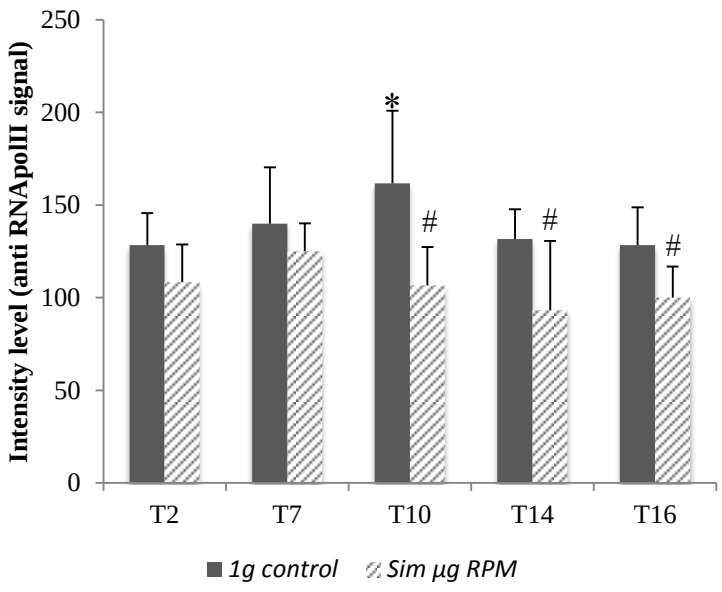

Figure 60: Pre-mRNA (extranucleolar) transcription level determined by immunofluorescence anti-RNA-polII under simulated microgravity alteration through the cell cycle progression. Cells were expose to simulated microgravity (Sim µ*g* RPM) and 1*g* control conditions after Aphidicolin block/release (T0) for 16 hour time reference time. Quantitative fluorescence intensity level was determined using Leica confocal software in each individual cell to detect the green signal intensity. An average of 100 cells was measured in three different biological replicates. P-Value < 0.05 is shown for significant differences calculated within cell cycle phases (without changing *g* level, *) or simulated microgravity versus 1*g* control (without changing cell cycle phase, #).

It is noticed a gradual increase on the intensity levels until become significantly increased at T10 (G2 reference time) and then reduced gradually until returning to original S phase values at T16 (G1 reference time) **(Figure 60)**.

Under simulated microgravity, the alteration on the distribution of the RNA polymerase transcription, the chromatin mass organization, and the level of the fluorescence transcription intensity is remarkable **(Figure 59B)**. On the one hand, the distribution of the chromatin mass by the DAPI staining goes from even distribution of the chromatin masses in the 1*g* control to the appearance of small spots with a high intensity level of DAPI fluorescence. This observation is accompanied with the changes on the distribution of the RNA polymerase transcription regions in the chromatin. This effect seems to be cumulative with simulated microgravity exposure regardless to the cell cycle progression. It is already significant at T7 while T2 (2 hours of the gravitational alteration) is not enough to alter the chromatin organization and the RNA polymerase transcription. On the other hand, simulated microgravity also significantly reduces the level of the extranucleolar transcription fluorescence intensity from T10 up to T16 samples **(Figure 60)**.

4.2.6. Simulated Microgravity Modify DNA Methylation and Histone H4 Acetylation Patterns Through The Cell Cycle Phases

As a logical next step after the chromatin differential transcriptional patterns was the evaluation of epigenetic mechanisms markers with a similar approach. DNA methylation (5mdc **(Figure 61)**) and histone H4 acetylation **(Figure 62)** markers antibodies were used for immunofluorescence staining analysis to detect the alteration through the chromatin mass and the level of the intensity of each one in different cell cycle phases under 1*g* and simulated microgravity conditions.

DNA methylation confocal immunofluorescence was performed by double staining with 5mdc antibody to detect the methylated cytidine and DAPI **(Figure 61).** DNA methylation is modified by the cell cycle progression under the 1*g* control conditions as previously shown **(Figure 57)**. A few methylated cytidine sites are associated to G1 phase, slightly increasing in S phase and being significantly observed in G2 phase in which DNA is highly methylated. This observation is supported by the quantification of the fluoresce intensity of the methylated sites **(Figure 63A).** Results reveal that the intensity of the methylated DNA varies among the cell cycle progression under 1*g* control conditions. It is increased doubled level on G2/M phase compared with the G1 and S phase. On the other hand, expose to the simulated microgravity has reinforced the DNA methylation dynamics compared with the 1*g* control **(Figure 61)**. This alteration is also clear on the fluorescence intensity quantification in which, significant increases are observed in all the cell cycle phases versus 1*g* control conditions **(Figure 63A)**.

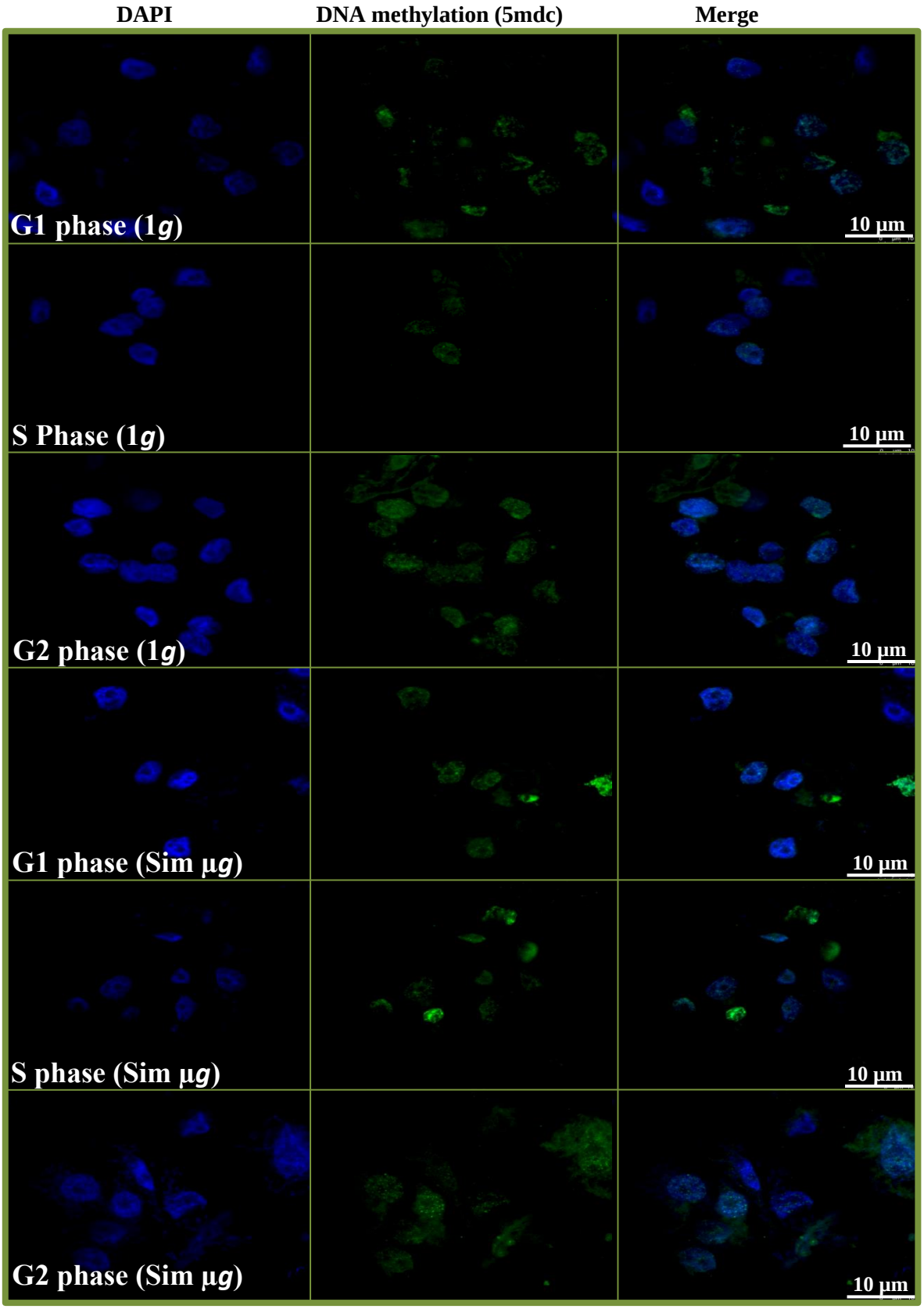

Figure 61: DNA methylation (5mdc) immunofluorescence patterns through *Arabidopsis* synchronic cell cycle phases under 1*g* control and simulated microgravity (µ*g* RPM). Confocal images showing immunolocalization of 5mdc (green) in the chromatin pattern (DAPI) and the merged images. Magnification was 63x (10 µm).

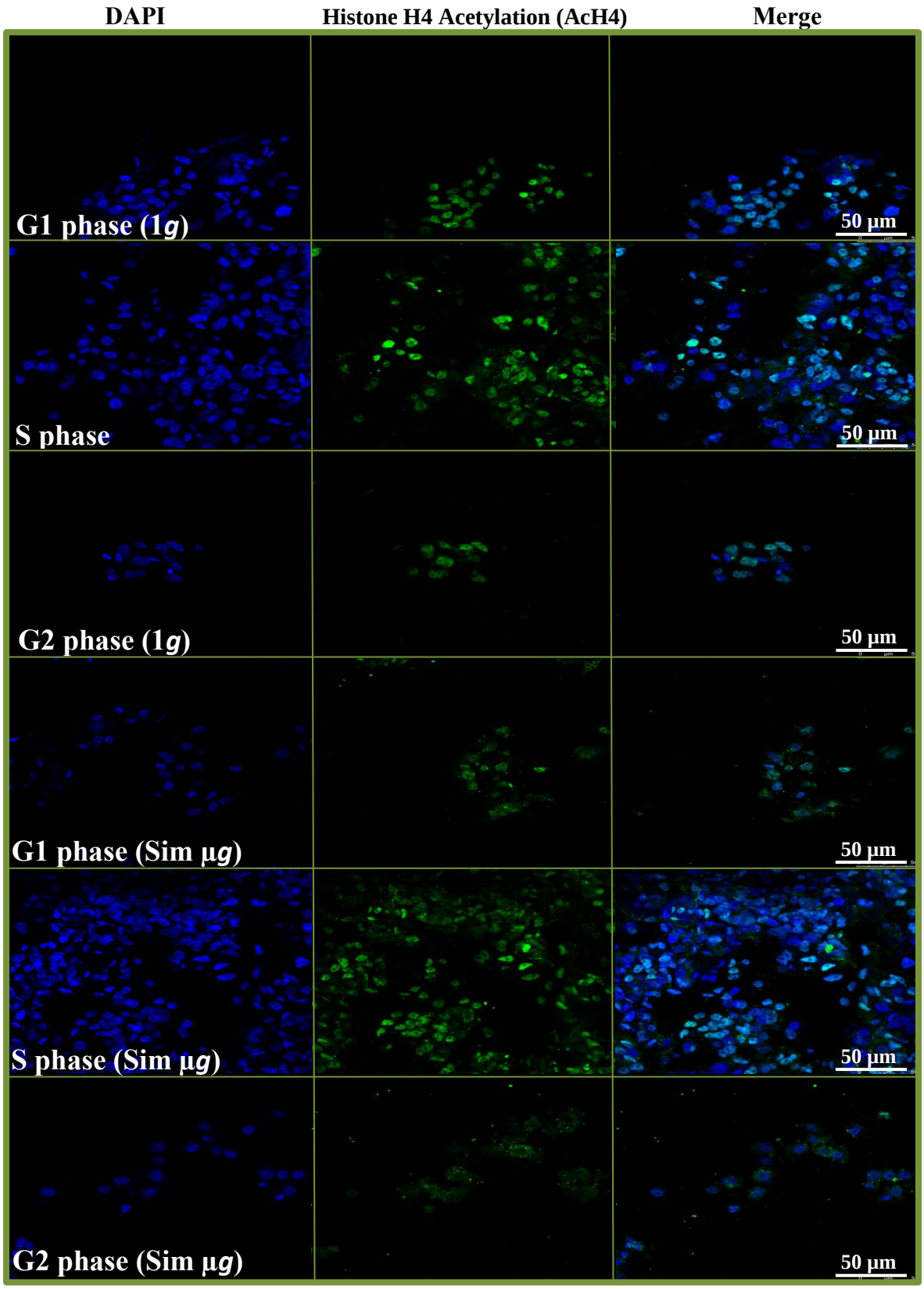

Figure 62: Histone H4 Acetylation (AcH4) immunofluorescence patterns through *Arabidopsis* synchronic cell cycle phases under 1*g* control and simulated microgravity (µ*g* RPM). Confocal images showing immunolocalization of AcH4 (green) in the chromatin pattern (DAPI) and the merged images. Magnification was 10x (50 µm).

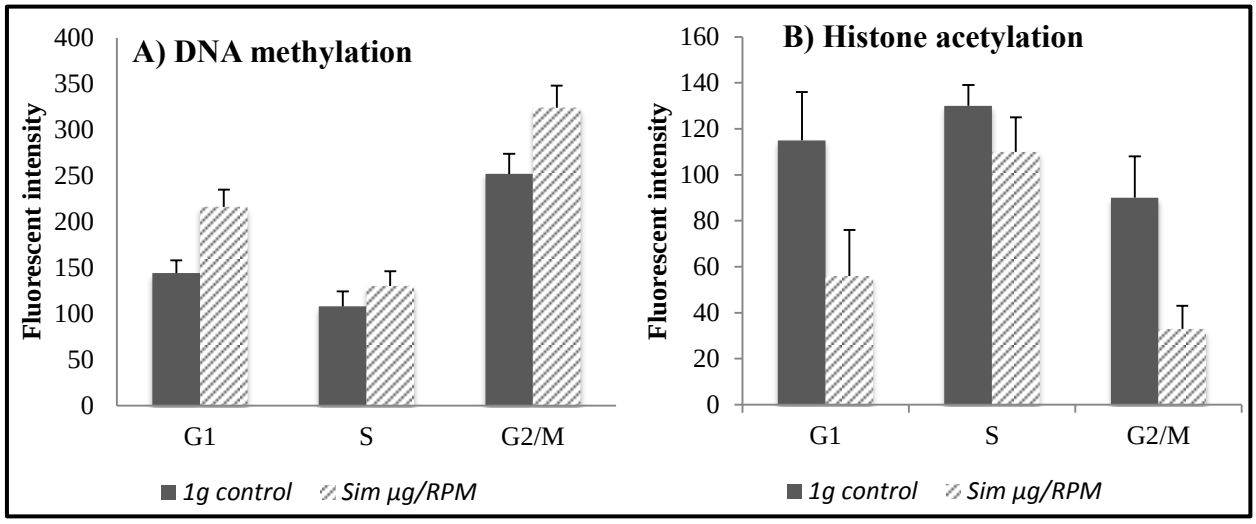

Figure 63: Quantification of epigenetic modifications (DNA methylation (5mdc) and Histone H4 Acetylation (AcH4) fluorescence intensity levels) through *Arabidopsis* synchronic cell cycle phases under 1*g* control and simulated microgravity (µ*g* RPM). Quantitative fluorescence intensity level was determined using Leica confocal software in each individual cell to detect the green signal intensity. Statistical analysis is not performed as this results obtained form only one experimental samples (Standard deviation estimated by counting 50 cells in the same sample)

On the other hand, immunofluorescence image analysis for the acetylated histone H4 reveals a similar but inverted effect than the methylation one **(Figure 62).** It is observed that, S phase is characterized by highly acetylation levels in the 1*g* control conditions being reduced by the progression to G2/M phase and later gradually increased when in G1 phase. This observation is accompanied with the quantification analysis **(Figure 63B)**, which reveals that, under 1*g* control condition, the level of the histone acetylation fluorescence intensity is reduced significantly under G2 control compared with G1 and S phase. Under simulated microgravity, histone H4 acetylation is reduced aggressively on G2 phase and G1 phase, while S phase has not been affected enough maybe due to short time exposure **(Figure 62)**. Moreover, the level of the fluorescence intensity is altered by the gravitational alteration. It is noticed a significant depletion on G2/M and G1 phases compared with 1*g* control **(Figure 63B)**.

RESULTS

CHAPTER 5: *SIMULATED MICROGRAVITY EFFECTS ON THE OVERALL GENOME TRANSCRIPTIONAL PROFILE ON ASYNCHRONIC AND SPECIFIC CELL CYCLE PHASES (G1 AND G2/M) SYNCHRONIC CELL CULTURES*

5.1. Global Transcriptome Analysis In *Arabidopsis in vitro* Cultures (Synchronous/Asynchronous) Under Simulated Microgravity Conditions

5.2. Differential Effects of Simulated Microgravity in Gene Expression through the Cell Cycle Progression (Synchronous G2/M and G1)

5.3. Global Analysis of the Core Cell Cycle Regulators Expression in *Arabidopsis* i*n vitro* Culture (Synchronous/Asynchronous) under Simulated Microgravity

5.4. Chromatin Dynamics and Remodeling Gene Expression in *Arabidopsis* i*n vitro* Culture (Synchronous/Asynchronous) under Simulated Microgravity

5.5. Abiotic Stress Related Genes in *Arabidopsis in vitro* Culture (Synchronous/Asynchronous) under Simulated Microgravity

5.6. Linking Genes of Unknown Function with the Simulated Microgravity Alteration in *Arabidopsis* i*n vitro* Culture (Synchronous/Asynchronous) Responsive System

5.7. Array Data Validation by Specific Genes Expression qPCR Analysis

CHAPTER 5: SIMULATED MICROGRAVITY EFFECTS ON THE OVERALL GENOME TRANSCRIPTIONAL PROFILE ON ASYNCHRONIC AND SPECIFIC CELL CYCLE PHASES (G1 AND G2/M) SYNCHRONIC CELL CULTURES

Studying the genomic alterations caused by simulated microgravity in *Arabidopsis* proliferating cells (*in vitro* culture) depending on exposure time and cell cycle progression will help to provide further support to the previous chapters findings in terms of cell proliferation, cell growth and epigenetic mechanisms affected. Three different samples coming from ***Experiment 6*** were used in this genome level analysis; synchronous cultures enrich in G1 phase subpopulation (14 h RPM/ 16 h 1*g* control), synchronous cultures enrich in G2/M phase subpopulation (7h RPM/ 10h 1*g* control) and asynchronous culture exposed to similar time than G1 phase simulated microgravity sample (14 h RPM/ 14 h 1*g* control). Two different biological replicates with 2 technical replicates were used to perform a comprehensive study conducting the whole genome level in order to study the gene expression in the different experimental samples subjected to simulated microgravity alterations using hybridization of total RNA with full transcriptome microarray (CATMA*v6.2* array based on Roche-NimbleGen technology, *See material and methods 4.4*). Microarray results were analyzed statistically using a FDR analysis (P-value ≤ 0.05). Different bioinformatics analyses were applied to get a clear idea about the alteration on the transcriptome analysis using different bioinformatics tools.

5.1. GLOBAL TRANSCRIPTOME ANALYSIS IN *ARABIDOPSIS IN VITRO* CULTURES (SYNCHRONOUS/ASYNCHRONOUS) UNDER SIMULATED MICROGRAVITY CONDITIONS

5.1.1. GEDI Whole-genome Transcriptional Status of the Different Samples Exposed to Simulated Microgravity

As a first attempt to enter into the global and integrative transcription analysis of the data, synchronic cell cultures at G1 (14h RPM/ 16h 1*g*) and G2/M (7h RPM/ 10h 1*g*) together with asynchronic cell culture global expression pattern were calculated **(Figure 64)** using the GEDI *v2.1* program analysis ¨*The Gene Expression Dynamics Inspector*¨ (Eichler et al 2003).

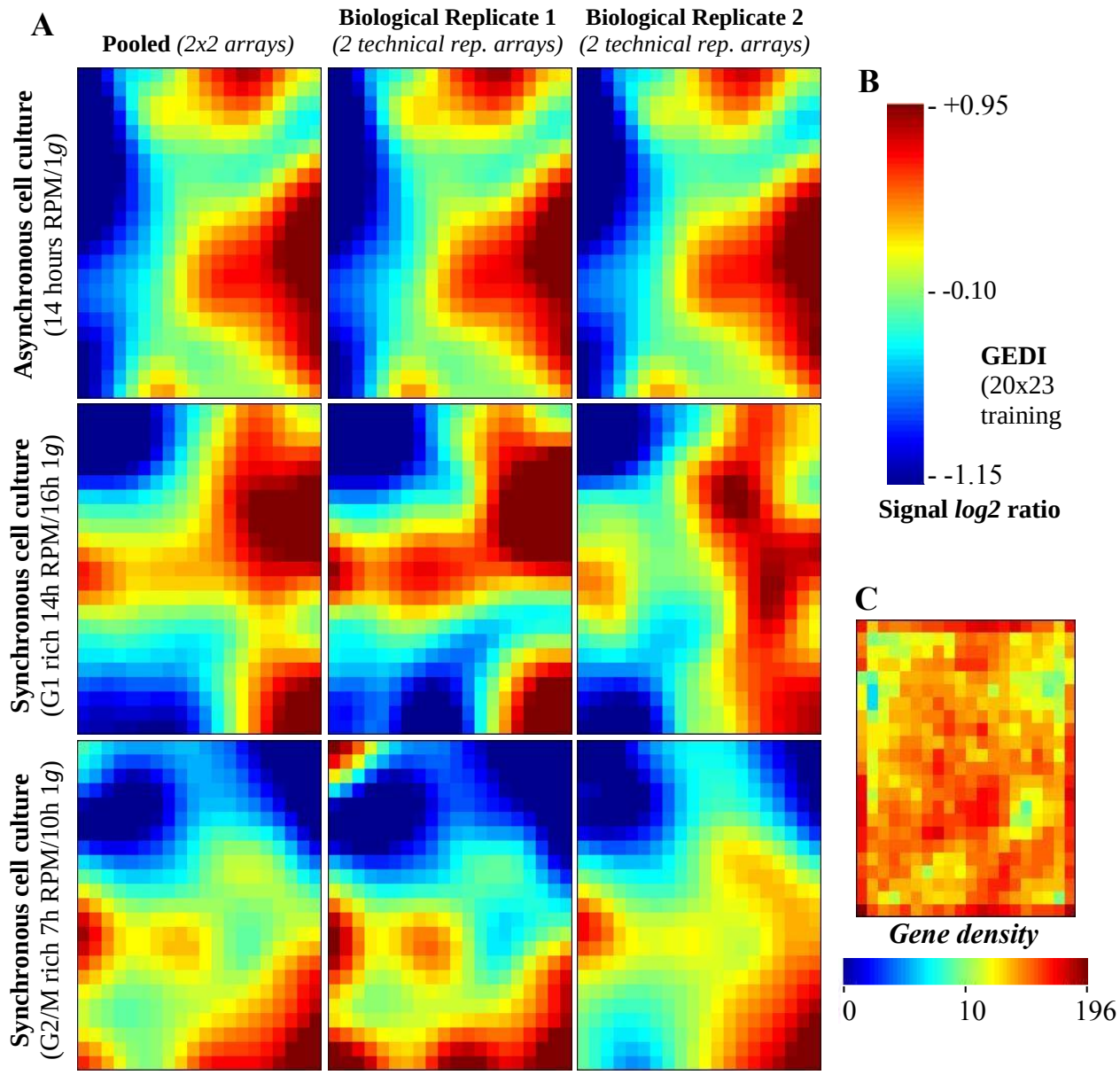

Figure 64: GEDI whole-genome transcriptional status of synchronous cell culture (Cell cycle phases; G1 and G2/M) and Asynchronous cell culture (14 hours) under the simulated microgravity alteration. **A)** A 20 x 23 clustering analysis of the transcriptome graphic presents each condition with 2 different biological replicates and the pooled final analysis. Profile of each condition in the gravitational alteration compared with 1*g* control is shown graphically. **B)** Average signal log_2 ratio of each cluster (each pixel signal) compared with 1*g* control, in an average from red to blue in different colors. **C)** Gene density map in each single pixel. Image frame shows the number of genes that are considered in each cluster/pixel (average number of probes per cluster is = 46).

It is used a clustering algorithm to present the global gene induction or repression profile in each condition and the similarities between them from the quantitative point of view of each individual gene. GEDI profile allows the visualization of the gene expression across the transcriptome generating a mosaic image or dot matrix, consisting of 20 x 23 pixels (average of <46 probe sets/tile) using the self-organizing maps algorithm and standard setting of the software (Eichler et al 2003) using the signal log_2 ratio of the selected probe sets through using the 20961 probes with any significant change in expression from the total of 73229 probes included on the CATMA arrays. Each pixel on the figure represents a group or cluster of genes that behave similarly in all the experimental conditions. Each pixel will have a different color that reflects the average expression of the genes included in the cluster for each experimental condition compared to 1*g* control. The GEDI program firstly decides which genes should be included in each cluster and then places similar clusters in nearby area of the mosaic, creating an image and allowing global transcriptome analysis as a single entity for display in different gravitational conditions.

The global transcriptional profiles comparison of the different conditions versus 1*g* control **(Figure 64)** corroborates firstly, that the pattern between the two different biological replicates is similar for every pair of samples, but clearly different in the case of the synchronous cells (G1 and G2/M). Secondly, when comparing the three different conditions pattern, shows that the synchronous G1 is closely related to the asynchronous cells (expected due to the high percentages of G1 cells in the asynchronous culture, *see external control (shaking standard conditions)* **(Figure 24 in *Chapter 1***) with a slightly changes in a side pattern it is upregulated in the synchronous one. Thirdly, transcriptome pattern on the synchronous G2/M is varying compared with the other conditions in the opposite behavior. It is observed that some gene clusters are expressed or depressed oppositely to the other two conditions with an observation of the repressed genes clustering pattern.

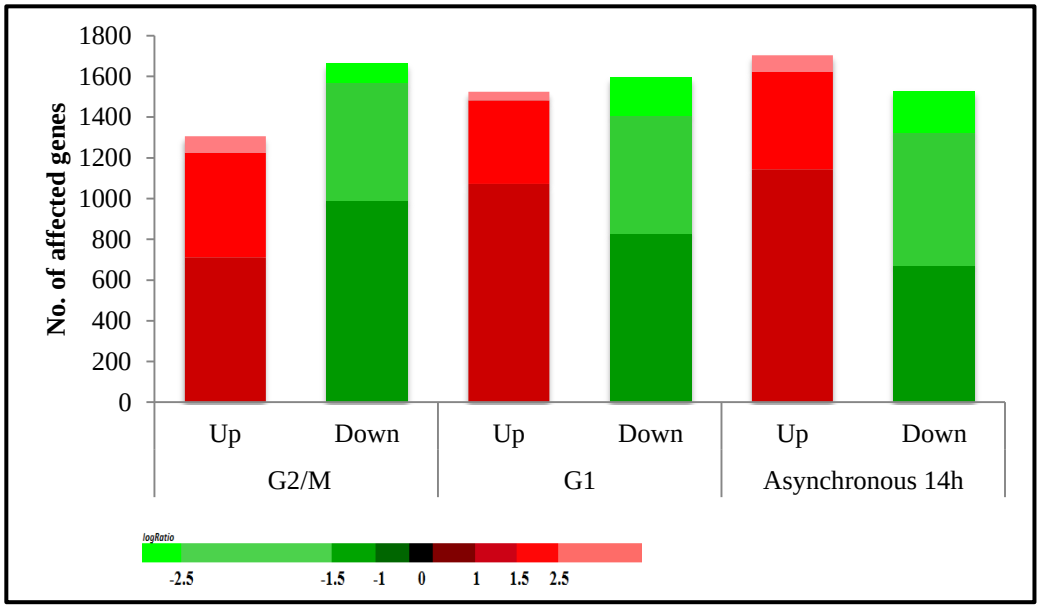

Figure 65: Total number of altered genes (Upregulated/ Downregulated) for synchronous cell culture (Cell cycle phases; G1 and G2/M) and Asynchronous cell culture (14h) under the simulated microgravity alteration compared with 1*g* control. Genes are altered by the microgravity alteration by upregulated or downregulated according to the *log2 ratio* of each gene value. Red range color refers to the upregulated genes and green range color refers to the downregulated genes.

5.1.2. Number of Genes Shown Altered Expression (Up- or Downregulation) under Simulated Microgravity

The total number of altered genes (induced/repressed) varies among the different three samples **(Figure 65).** Altered genes were filtered according to the FDR p-value <0.05 for the statistical meaning and more than a 2 fold change (*log2ratio*>1) for the biological meaning in each individual experimental sample, in order to optimize the robustness of the results.

While in the overall analysis **(Figure 64)** there is more downregulated than upregulated genes (the axis indicates that the mean change in expression level is -0.1), this property is not evenly distributed in the three samples. After 7 hours of exposure to simulated microgravity, the number of the repressed genes on the synchronous G2/M samples is clearly higher than the induced genes, while the alteration after 14 hours in both synchronous G1 and asynchronous culture is similar on the level of induced/repressed genes. Furthermore, if we consider the genes with changes in expression higher than 1.5 *log2ratio*, the effect is inverted in the 14 hours, appearing more downregulated than up-regulates genes.

5.1.3. Gene Ontology Analysis of the Genes with Altered Gene Expression under Simulated Microgravity

Gene ontology was analyzed using the simulated microgravity affected genes in the synchronous (G2/M and G1) and asynchronous cultures through using the gene ontology tool provided by TAIR database. **Figure 66** shows the upregulated and downregulated biological processes, including in all samples a similar high percentage of genes included in the unspecific group of "other cellular/metabolic processes".

The major specific upregulated biological function **(Figure 66A)** are related with cellular response to stress and biotic or abiotic stimulus related genes, upregulated in G2/M (30% of the affected genes belong to this group) compared with 20% in G1 and asynchronous culture. A similar 30% of unknown biological process related genes is upregulated in all the samples. Interestingly, a remarkable number of genes belonging to the developmental process, cell organization and biogenesis, and DNA metabolism groups are upregulated in G1.

In terms of downregulated biological processes (**Figure 66B**), the unknown biological processes group is downregulated (40% of the downregulated genes belong to this group). A larger number of cell organization and developmental process appears downregulated in G2/M compared with G1 and asynchronous cultures. Furthermore, it is noticed that, protein metabolism (20% of the related genes) is also downregulated in all the samples as well as the transcription and DNA dependent (15% of the altered genes). Remarkably, response to stress and abiotic or biotic stimulus appears also as a downregulated function, affecting a similar 20% of the genes upregulated and downregulated in G1 and the asynchronous cultures compared with less than 15% of genes downregulated in G2/M (versus the 40% enrichment in the upregulated list).

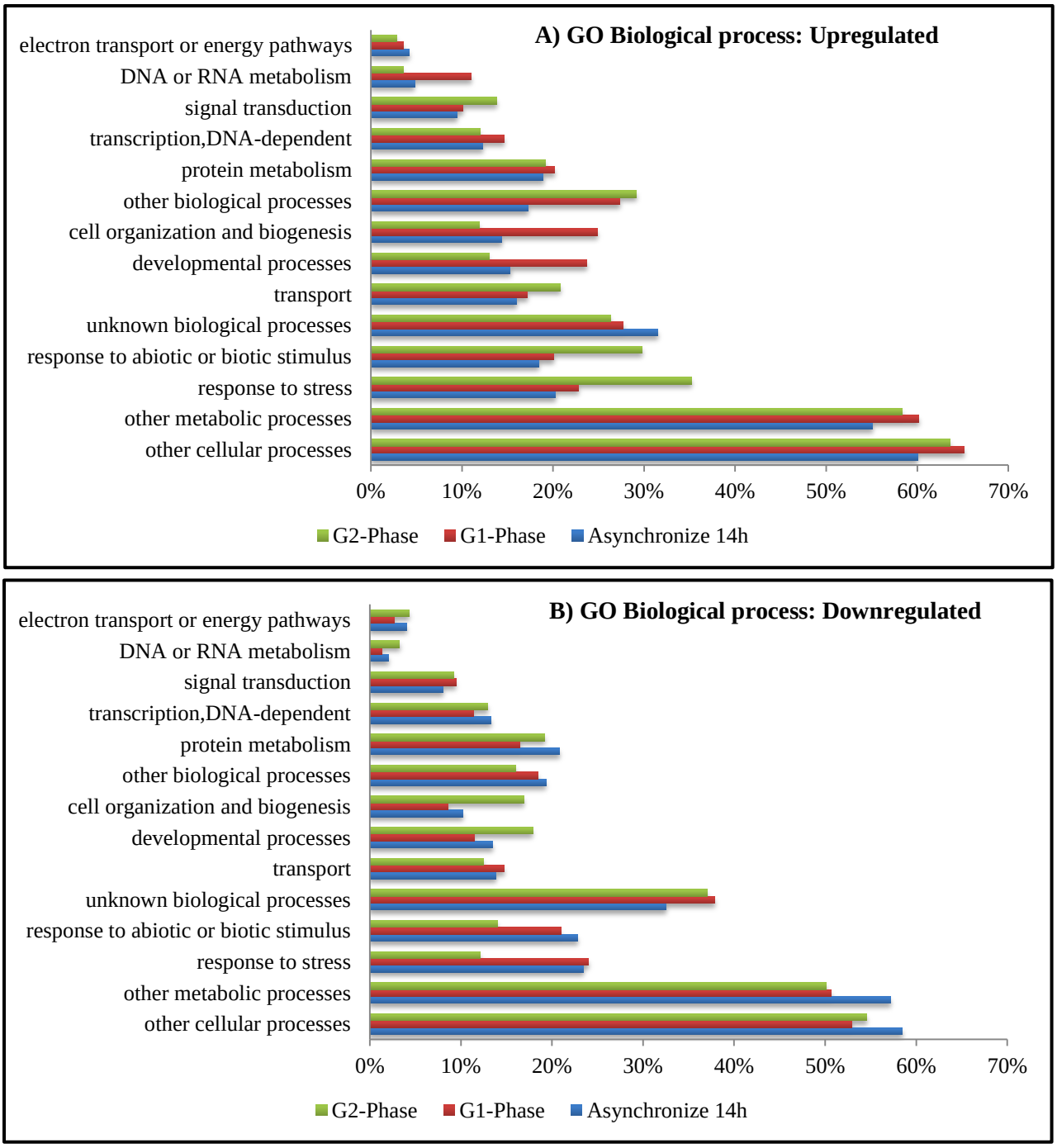

Figure 66: Analysis of enriched GO Biological process groups (TAIR ONTOLOGY) related with the genes showing significant altered expression in *Arabidopsis* cell cultures (synchronous/asynchronous) under simulated microgravity. A) GO Biological process of the genes showing a significant upregulation (>2 fold). **B)** GO Biological process of the genes showing a significant downregulation (<-2 fold).

5.1.4. Common Effects of the Simulated Microgravity Environment in all cell cycle Subpopulation Samples

In order to locate the key genes responding to the microgravity environment we compared the list of genes altered similarly in the three cell suspension culture subpopulations. **Figure 67** reflects the number of common up- and downregulated genes in the three experimental samples. A similar number of upregulated (73) and downregulated (83) common genes is found. Minor variations have been found in the GO biological processes affected in both groups and versus individual analysis, but GO cellular component shows alterations due to the simulated microgravity stimulus, including a high number of upregulated genes related to the mitochondria (24% versus 5% in the downregulated list) at the expenses mainly of the nucleus related genes (22% in the downregulated list versus 14% in the upregulated list). Moreover, 15% of the common upregulated genes and 12% of the downregulated genes is associated to the membranes, beside to 5-3% is associated to cell wall. This finding can be related with the graviresistance mechanism. It has been reported also that a number of membrane-linked proteins of *Arabidopsis* are up-/downregulated by real microgravity in a previous study performed on board the International Space Station (GENARA A) using *Arabidopsis* seedling (Mazars et al 2014a, Mazars et al 2014b)

More than that, simulated microgravity alters some specific molecular function GO domains in all the three different experimental conditions; synchronous/asynchronous cultures **(Table 10)**. Significant up regulation of the NADH activity related genes is observed together with other mitochondria related functions as cellular respiration, oxidative activity, NADH dehydrogenase activity and the mitochondria components complex. In terms of downregulated genes gene ontology, it is noticed that ribosome activity and the photosynthesis related functions are downregulated significantly by the simulated microgravity alteration. **Table 10** shows that, plastid and organellar ribosome activity are significantly downregulated as well as, the photosynthesis, photosystem, and chloroplast component related functions.

Figure 67: Gene ontology analysis of the common altered expression genes in *Arabidopsis* synchronous (G2/G1) and asynchronous 14h under simulated microgravity. A) Venn diagram showing the common upregulated genes (73). **B)** Venn diagram showing the common downregulated genes (83). **C)** Analysis of enriched GO cellular component groups in the up- and downregulated common genes. **D)** Analysis of enriched GO Biological process groups in the up- and downregulated common genes.

A) Common Genes: Upregulated

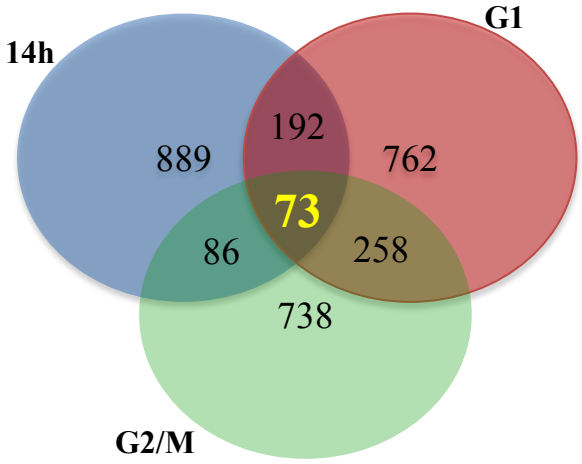

B) Common Genes: Downregulated

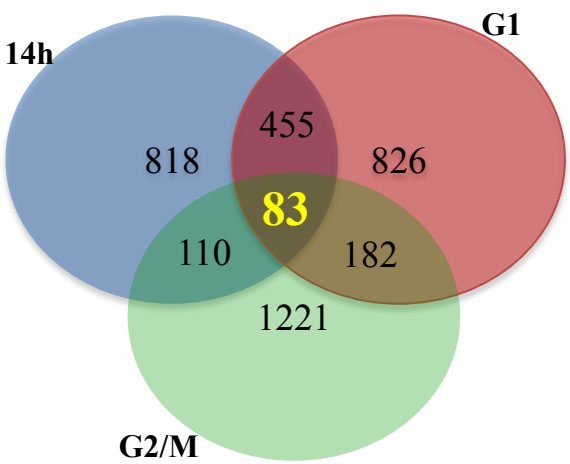

C

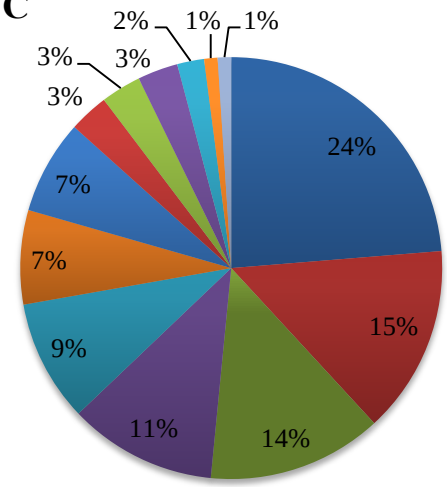

GO Cellular component: Upregulated

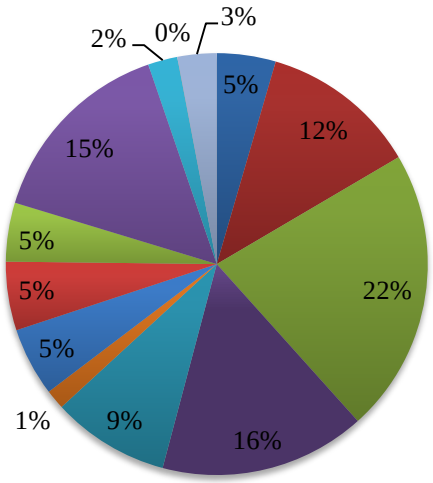

GO Cellular component: Downregulated

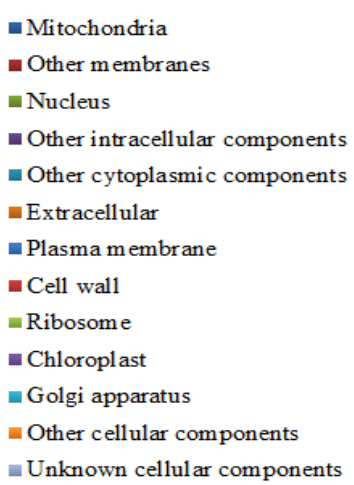

D

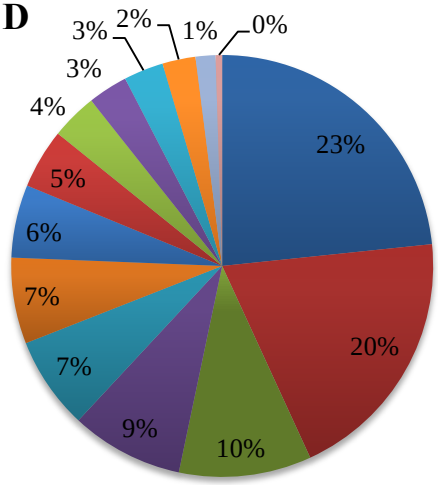

GO Biological process: Upregulated

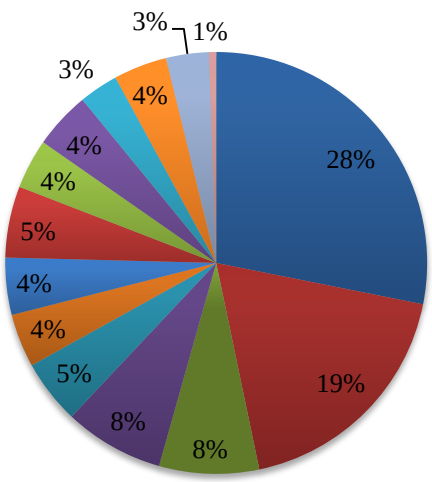

GO Biological process: Downregulated

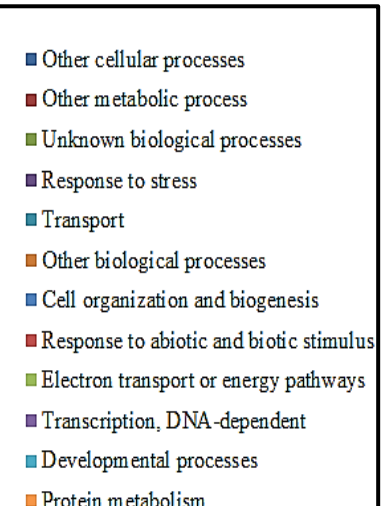

Table 10: Analysis of enriched GO groups (Molecular Function) in common genes with altered expression in all the experimental conditions. The following GO groups are significantly enriched (in the Up or Downregulated lists) commonly in all the samples as determined using GeneMANIA with default setting using FDR rankprod p value. Coverage refers to the number of genes in the network with a given function/ all genes in the genome with the function.

Molecular Function (Upregulated)	FDR	Coverage
Oxidoreductase activity, acting on NAD(P)H	4.39e-10	10 / 77
NADH dehydrogenase activity	8.14e-10	8 / 35
Cellular respiration	1.76e-5	7 / 79
Energy derivation by oxidation of organic compounds	1.76e-5	7 / 79
Mitochondrial respiratory chain complex I	9.7e-5	6 / 60
NADH dehydrogenase complex	1.03e-4	6 / 64
Respiratory chain complex I	1.03e-4	6 / 64
Generation of precursor metabolites and energy	3.16e-4	8 / 199
Mitochondrial respiratory chain	4.77e-4	6 / 86
Respiratory chain	6.43e-4	6 / 92
Oxidoreductase complex	1.28e-3	6 / 105
Oxidation-reduction process	2.47e-3	7 / 192
Mitochondrial inner membrane	2.47e-3	7 / 192
Mitochondrial membrane	4.72e-3	7 / 214
Mitochondrial envelope	5.27e-3	7 / 222
Mitochondrial membrane part	5.27e-3	6 / 142
Organelle inner membrane	7.84e-3	7 / 238
Mitochondrial part	1.1e-2	7 / 253
NADH dehydrogenase (quinone) activity	1.53e-2	3 / 16
NADH dehydrogenase (ubiquinone) activity	1.53e-2	3 / 16
Oxidoreductase activity, acting on NAD(P)H, Quinone or similar as acceptor	3.95e-2	3/22
Molecular Function (Downregulated)	**FDR**	**Coverage**
Plastid ribosome	3.43e-6	63 / 25
Organellar ribosome	3.43e-6	6 / 27
Photosynthetic membrane	3.15e-4	10 / 292
Oxidoreductase activity, acting on NAD(P)H	9.24e-4	6 / 77
Chloroplast thylakoid membrane	9.24e-4	9 / 275
Plastid large ribosomal subunit	9.24e-4	4 / 16
Organellar large ribosomal subunit	9.24e-4	4 / 17
Plastid thylakoid membrane	9.24e-4	9 / 277
Photosystem	9.86e-4	5 / 45
Photosynthesis	1.03e-3	7 / 144
Thylakoid membrane	1.03e-3	9/290

5.2. DIFFERENTIAL EFFECTS OF SIMULATED MICROGRAVITY IN GENE EXPRESSION THROUGH THE CELL CYCLE PROGRESSION (SYNCHRONOUS G2/M AND G1)

To distinguish the effects of simulated microgravity in each cell cycle phase, a GEDI clustering analysis was performed using the lists of genes with altered expression (up regulation/down regulation) significantly more than 2 fold under G2/M synchronous subpopulations and significantly altered in the G1 phase subpopulation. As shown in **Figure 68**, genes were not evenly distributed by the GEDI algorithm, in fact not all combinations expected by the clustering algorithm found genes to be included within (for example, there are not genes greatly upregulated in G2 with no variation in G1, as shown in the empty spaces between List 7 and 8) strengthening the clustering value of the tool. Similar clusters of genes behaving similarly and differentially through the progression of the cell cycle phases were distributed in 8 different lists of genes as indicated in **Figure 68**; list 1 includes the clusters of genes (large number of genes in these clusters as indicated by the brown color) downregulated in the synchronous G2/M and clearly upregulated in the synchronous G1 phase, list 2 includes the repressed genes in G2/M and weakly induced in G1, list 3 refers to the repressed genes in G2/M which are weakly repressed in G2, list 4 refers to the barely repressed genes in G2/M and more significantly downregulated in G1, list 5 refers to similarly upregulated genes in G2/M and G1, list 6 refers to the upregulated genes in G2 and less induced in G1, list 7 refers to the strongly upregulated genes in G2/M and significantly less in G1, and list 8 which refers to the induced genes in G2/M and repressed significantly in G1.

Interestingly, analysis of gene ontology with GeneMANIA with these lists produced significant results in only 4 of them **(Table 11)**. GO biological processes enriched groups in gene list1 (significant down regulation in G2/M and significant up regulation in G1) reveal that the cell cycle regulation functions is downregulated in G2/M and upregulated in G1 under the simulated microgravity conditions, as well as the hydrolase activity (including the microtubule motor activity), photosynthesis and chloroplast (including the anchored and intrinsic to the plasma membrane). Plastid ribosome, organellar ribosome and photosystem are the biological functions repressed in G2 phase and weakly repressed in G1 altered by the simulated microgravity (list 3).

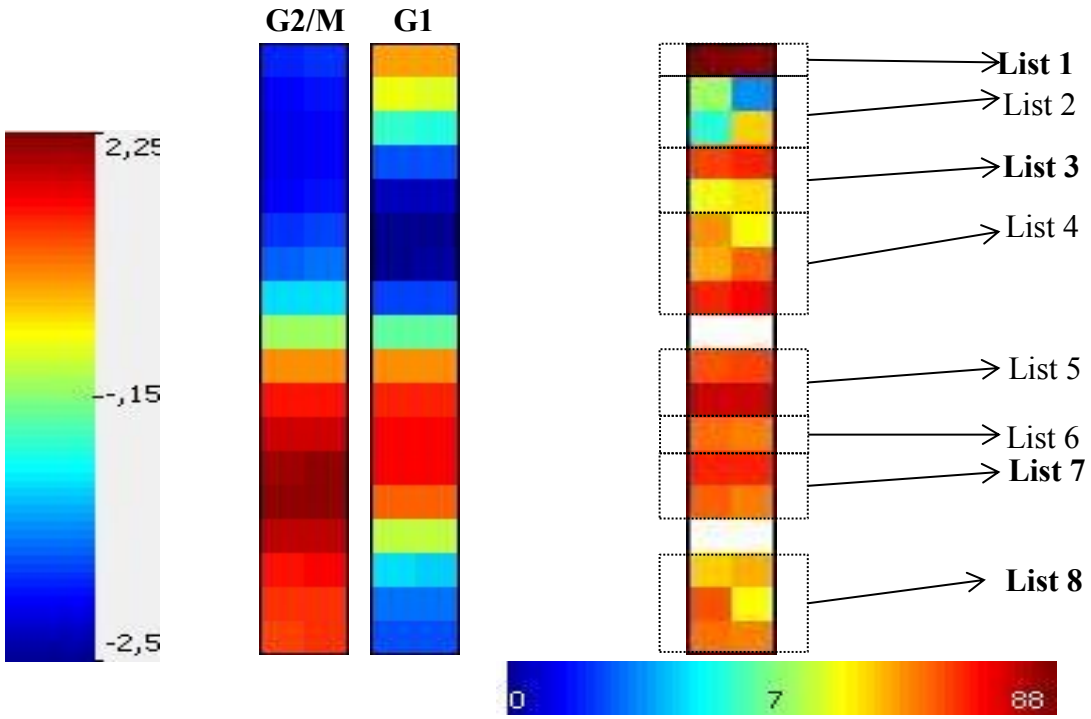

Figure 68: GEDI study of differential synchronous cell cycle phases gene expression (G2/M and G1 phases) under simulated microgravity. Clustering analysis of the 993 genes changing expression under G2/M and G1 phases under simulated microgravity visual presents each cluster average gene expression variation using the scale on the left (significant *Log2 ratio*>1). On the right, the density map has been used to indicate the group of genes included in any of the 8 lists behaving with a differential pattern in G2/M and G1 phases. Lists in Bold will offer significant GO function studies in **Table 12**.

List 7 gene ontology analysis for strongly upregulated genes in G2/M and less also upregulated in G1 refers to functions correlated to mitochondrial NADH dehydrogenase, ATP biding/ Kinase activity (defense response apoptosis) and the phosphoglycerate dehydrogenase biological process. Finally, list 8 is enriched in heat shock response and the hydrolase activity (oxidative stress response) components, which are significantly upregulated in synchronous G2/M and downregulated significantly in G1.

Table 11: Analysis of enriched GO groups in genes showing significant altered expression in G2/M and G1. The following GO groups are significantly (Up or Downregulated) commonly in all the samples as determined using GeneMANIA with default setting using FDR rankpord p value.

Function description	FDR
List 1 : Downregulated in G2 → Increased significantly → Upregulated in G1	
Cyclin-dependent protein serine/threonine kinase regulator activity	2.09e-5
Microtubule motor activity	2.09e-5
Kinase regulator activity	3.42e-5
Motor activity	3.42e-5
Protein kinase regulator activity	3.42e-5
Cell cycle	3.42e-5
Regulation of cell cycle	6.06e-5
Anchored to plasma membrane	9.25e-4
Intrinsic to plasma membrane	1.65e-3
List 3 : Downregulated in G2 → Decreased significantly → Downregulated in G1	
Plastid ribosome	5.95e-4
Organellar ribosome	1.26e-3
Photosystem	1.12e-3
List 7 : Upregulated in G2 → Decreased significantly → Upregulated in G1	
Oxidoreductase activity, acting on NAD(P)H	6.58e-21
NADH dehydrogenase activity	4.66e-17
NADH dehydrogenase (quinone) & (ubiquinone) activity	1.08e-12
Oxidoreductase activity, acting on NAD(P)H, quinone or similar compound as acceptor	1.94e-11
Respiratory chain complex I & NADH dehydrogenase complex	4.47e-10
Respiratory chain	1.46e-8
Oxidation-reduction process	1.58e-7
Cellular respiration	1.72e-7
Energy derivation by oxidation of organic compounds	1.72e-7
Mitochondrial respiratory chain complex I	1.39e-6
Generation of precursor metabolites and energy	5.18e-6
Mitochondrial respiratory chain	1.75e-5
Oxidative phosphorylation	9.32e-5
Mitochondrial ATP synthesis coupled electron transport	9.32e-5
Electron transport chain	1.1e-4
Respiratory electron transport chain	2.07e-4
Mitochondrial membrane part	2.66e-4
List 8 : Upregulated in G2 → Decreased significantly → Downregulated in G1	
Response to heat	1.91e-39
Response to high light intensity	2.92e-17
Response to hydrogen peroxide	1.99e-16
Response to light intensity	2.3e-13
Response to reactive oxygen species	2.82e-12
Response to oxidative stress	9.7e-12
Heat acclimation	1.63e-6

5.3. GLOBAL ANALYSIS OF THE CORE CELL CYCLE REGULATORS EXPRESSION IN *ARABIDOPSIS IN VITRO* CULTURE (SYNCHRONOUS/ASYNCHRONOUS) UNDER SIMULATED MICROGRAVITY

After completing the overall study of the arrays data, we decided to focus in the genes related with the biological functions particularly addressed on this thesis. *Arabidopsis* has over 81 genes (CDK, CKL, cyclin, CYL and other cell cycle regulators included in the CATMA array) encoding conserved and plant-specific core regulators of the cell cycle that were analyzed transcriptionally under the microgravity alteration in both asynchronous and synchronous cell culture samples.

CDKs (CDK and CKL genes) expression is disrupted by simulated microgravity. All CDK and CKL genes expression data was extracted from the CATMA arrays for the three different cell cycle subpopulations. Heat map visualization (R software) was used to represent the expression of the whole family of CDK and CKL proteins (only significant expression changes are shown, **Figure 69**). On the one hand, CDK genes are unevenly affected by altered gravity in the different cell cycle phases; CDKB2;1 and CDKB2;2 are downregulated in G2/M and upregulated in both G1 and asynchronous culture, while CDKE;1 shows the opposite trend and CDKD;1 is downregulated in all the conditions under simulated microgravity. On the other hand, CKL genes are generally upregulated in all the conditions under simulated microgravity, but CKL3 is downregulated in G2/M and asynchronous culture, CKL10 in G1 and asynchronous, and CKL7 show an erratic pattern.

Cyclins expression is disrupted by simulated microgravity. Global transcriptome analysis for the cyclins (A-B-C-D-H) and CYL1 **(Figure 70)** reveals that, the expression of the CYCA family is altered by the simulated microgravity and generally upregulated in all the experimental conditions, with the exception of a great down regulation of CYCA;1;1 in G2/M. Whereas, CYCBs are altered by the simulated microgravity and the cell cycle progression. General down regulation of CYCB in the synchronous G2/M and up regulation in G1 is observed, while the alteration is not clear in the asynchronous cultures.

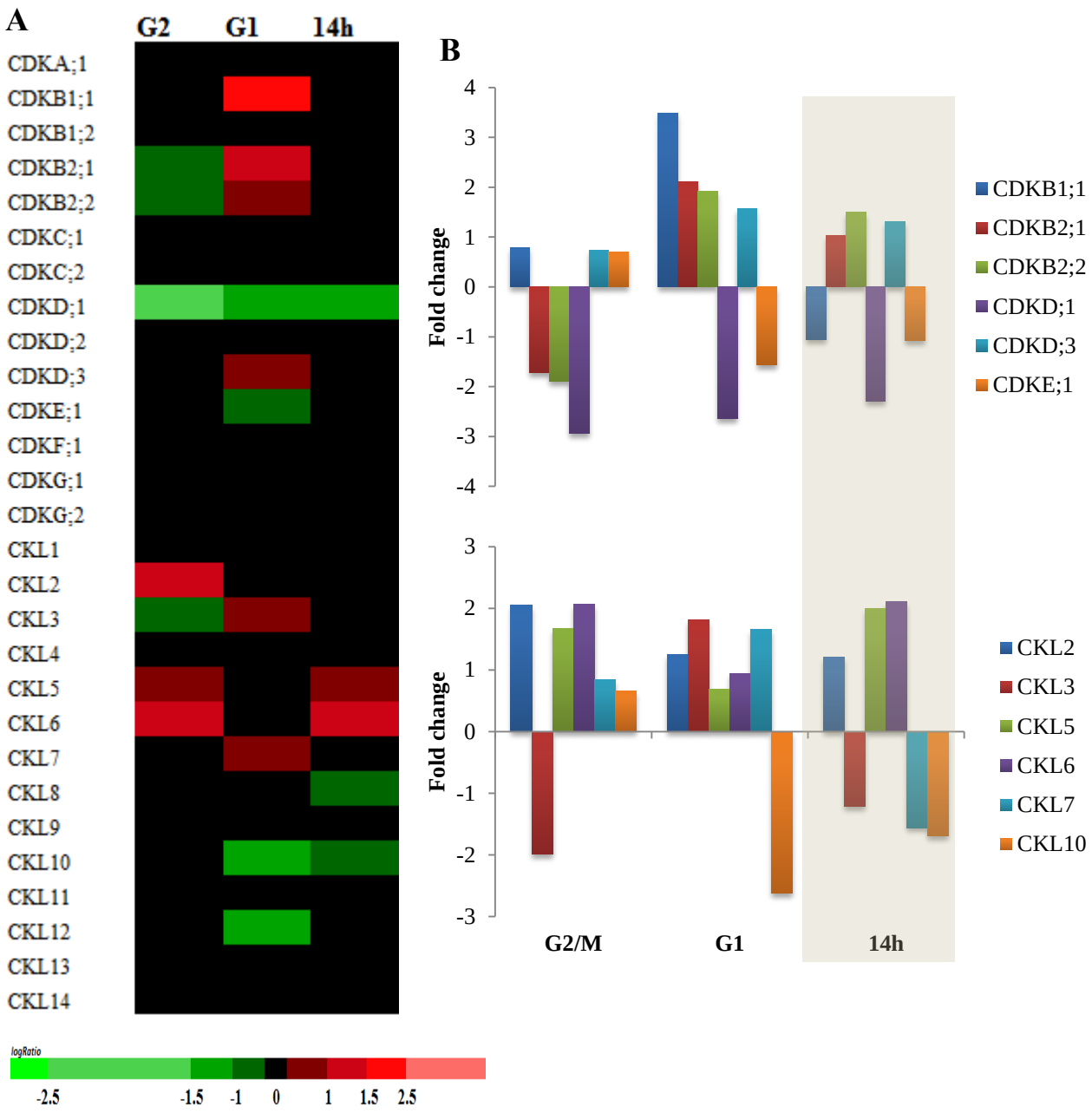

Figure 69: CDK and CKL kinases gene families' expression analysis in *Arabidopsis* synchronous (G2/M and G1 rich phase) and asynchronous cultures (14h) under simulated microgravity versus 1*g* control. A) Heat map generated using R software refers to the transcriptome expression of the whole gene family showing in color as indicated in the lower *log2ratio* scale. **B)** Fold change expression data of the significantly up-/downregulated CDK/CKL genes (FDR P-value <0.05).

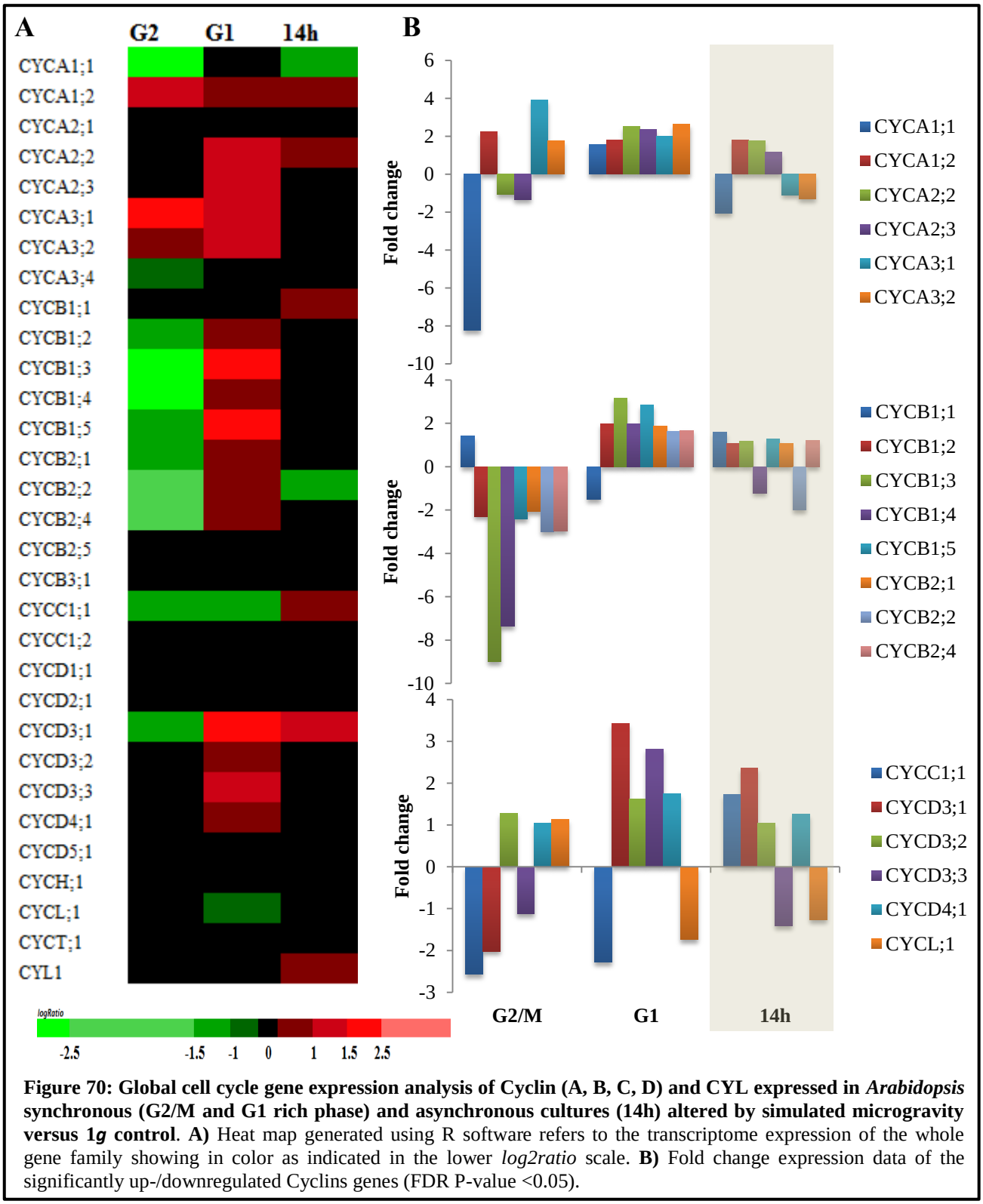

Figure 70: Global cell cycle gene expression analysis of Cyclin (A, B, C, D) and CYL expressed in *Arabidopsis* synchronous (G2/M and G1 rich phase) and asynchronous cultures (14h) altered by simulated microgravity versus 1*g* control. **A)** Heat map generated using R software refers to the transcriptome expression of the whole gene family showing in color as indicated in the lower *log2ratio* scale. **B)** Fold change expression data of the significantly up-/downregulated Cyclins genes (FDR P-value <0.05).

CYCC and CYCD are not clearly altered except CYCC1;2, CYCD3;1 and CYCD3 are altered in the three different samples; upregulated in G1 and asynchronous and downregulated in G2/M.

One by one, CYCA are upregulated significantly in the synchronous G1. CYCA1;1, CYCA2;2, and CYCA2;3 show a repression in G2/M, but CYCA1;1 shows high level of repression, while CYCA1;2, CYCA3;1, and CYCA3;2 are upregulated significantly. Under the microgravity alteration in the asynchronous cultures, Cyclin A is less altered compared with the synchronous cultures.

CYCBs show a high level of repression in the synchronous G2/M except the expression of CYCB1;1. Moreover, CYCB1;3 and CYCB1;4 are the more affected genes. On the other hand, an opposite expression is detected in G1, a general induction of the CYCB in G1 except the repression of CYCB1;1. In the asynchronous cultures, CYCB is generally expressed less than the other conditions, except the repression of the CYCB1;4 and CYCB2;2.

CYCC1;1 is downregulated in the synchronous cultures and upregulated in the asynchronous significantly. Furthermore, CYCD is induced in G1 and asynchronous except the repression of CYCD3;3 in asynchronous cultures, while the expression is different in G2/M; CYCD3;1 and CYCD3;3 is repressed and CYCD3;2 and CYCD3;4 is induced. Moreover, it is noticed a repression of CYCL;1 in G1 and asynchronous with an upregulation in G2/M.

Other core cell cycle regulators expression is altered significantly after 14 hours exposure in synchronous and asynchronous cultures. It is identified other core cell cycle regulators genes expressed differentially under simulated microgravity and through the synchronous/asynchronous cultures **(Figure 71)**. Little variations are observed in the T7 exposure in synchronous G2/M cultures, while they are disrupted in the G1 and asynchronous culture after 14 hours of microgravity exposure. Slightly repression of WEE1 is observed in G2/M, while it is induced significantly in G1 and asynchronous culture. In G1, KRP CDK inhibitors show a downregulation level in G1 and asynchronous cultures, except KRP3 which repressed significantly in the asynchronous cultures. CKS family (CKS1-2) and E2F/DEL families show an upregulation in both, G1 and asynchronous culture. Other regulators such as SIM; are downregulated in G1 and induced in the asynchronous cultures.

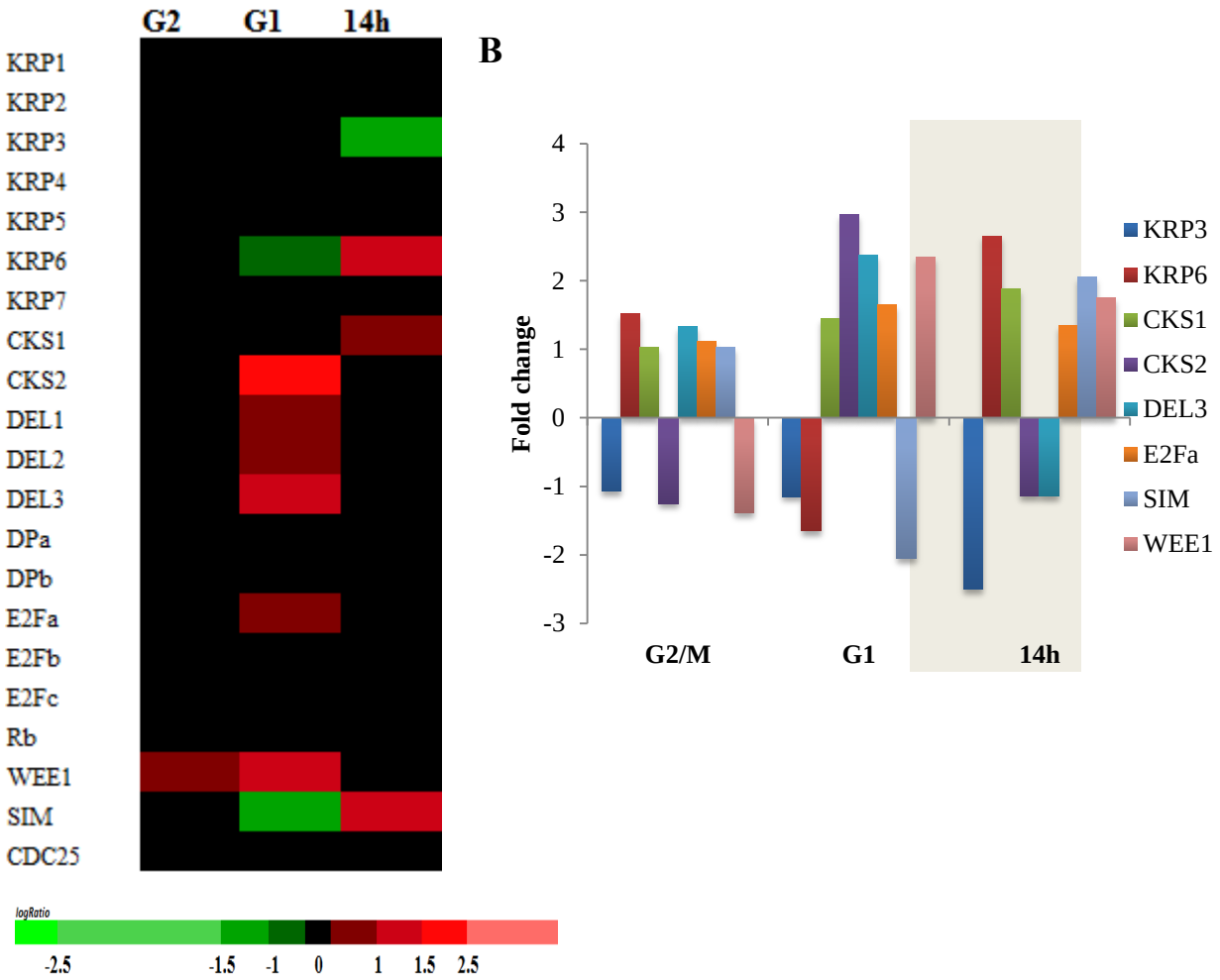

Figure 71: Global cell cycle gene expression analysis of other core cell cycle regulators expressed in *Arabidopsis* synchronous (G2/M and G1 rich phase) and asynchronous cultures (14h) altered by simulated microgravity versus 1*g* control. **A)** Heat map generated using R software refers to the transcriptome expression of the whole gene family showing in color as indicated in the lower *log2ratio* scale. **B)** Fold change expression data of the significantly up-/downregulated genes (FDR P-value <0.05).

5.4. CHROMATIN DYNAMICS AND REMODELING GENE EXPRESSION IN *ARABIDOPSIS IN VITRO* CULTURE (SYNCHRONOUS/ASYNCHRONOUS) UNDER SIMULATED MICROGRAVITY

Cell cycle progression depends on a highly regulated series of events of which transcriptional control plays a major role (Sanchez et al 2008). The accessibility of specific chromatin sites to the transcription machinery is favored by the chromatin remodeling complexes, DNA methylation and histone modifications (Kouzarides 2007, Weber & Schubeler 2007). These dynamics have to be studied under the simulated microgravity condition through the cell cycle progression. As performed for the cell (cycle) proliferation genes, we have performed a deep analysis on the expression patterns of the epigenetic regulators based on the CATMA arrays.

DNA methylation related genes expression is altered by simulated microgravity. DNA methylation genes; MET1 and CMT3, are upregulated in the different samples. This hypermethylation is constant with the previous proteomic/genomic results in asynchronous cultures **(*Results Chapter 2*)**. Furthermore, the alteration in the synchronous cell cycle phases is higher than in the asynchronous cultures **(Figure 72)**. MET1 and CMT3 are significantly upregulated in G2/M phase more than the expression level in G1 as obtained in the specific analysis of the cell cycle phases **(*Results Chapter 4)***. While, this alteration is lower on the asynchronous culture. Moreover, it is noticed that the CMT3 is repressed in the asynchrony cultures after 14 hours of the microgravity alteration.

Histone modification gene expression is altered by simulated microgravity. Another parameter that it is upregulated in direct correlation with the exposure time is Histone H4 expression **(Figure 72)**. Moreover, covalent histone modifications, in many cases reversible carried out by specific enzymes show a similar exposure related effect in the synchronous cultures form 7 hours (G2/M phase) to 14 hours (G1 phase). In the G2/M synchronous culture, histone kinase (AUR1-3 kinase family) activity is upregulated, while the activity of methylases is repressed. These changes could correlate with the histone acetylases (slightly up-regulation) and deacetylases (mostly downregulated) activity. Exceptions are HDA18, histone deacetylases of the RPD3/HDA1 family, that it is greatly upregulated in opposition to the similar down-regulation of histone deacetylases HD2 family (HDT1-4). Since the reversible nature of the histone modifications, G1 synchronous and asynchronous samples exposed for 14 hours show a

different picture. The histone kinase activity is repressed as well as the activity of the histone deacetylases and methylases families. Moreover, the histone modifications alterations on the asynchronous cell culture are observed **(Figure 72)**. Histone methylases enzyme SUVH1 is repressed while the SUVH3 is induced. This alteration is not clear in the histone kinase and acetylases activity. Furthermore, Histone deacetylases HDT4 is repressed in a high level, while the other family group HDA18 is expressed.

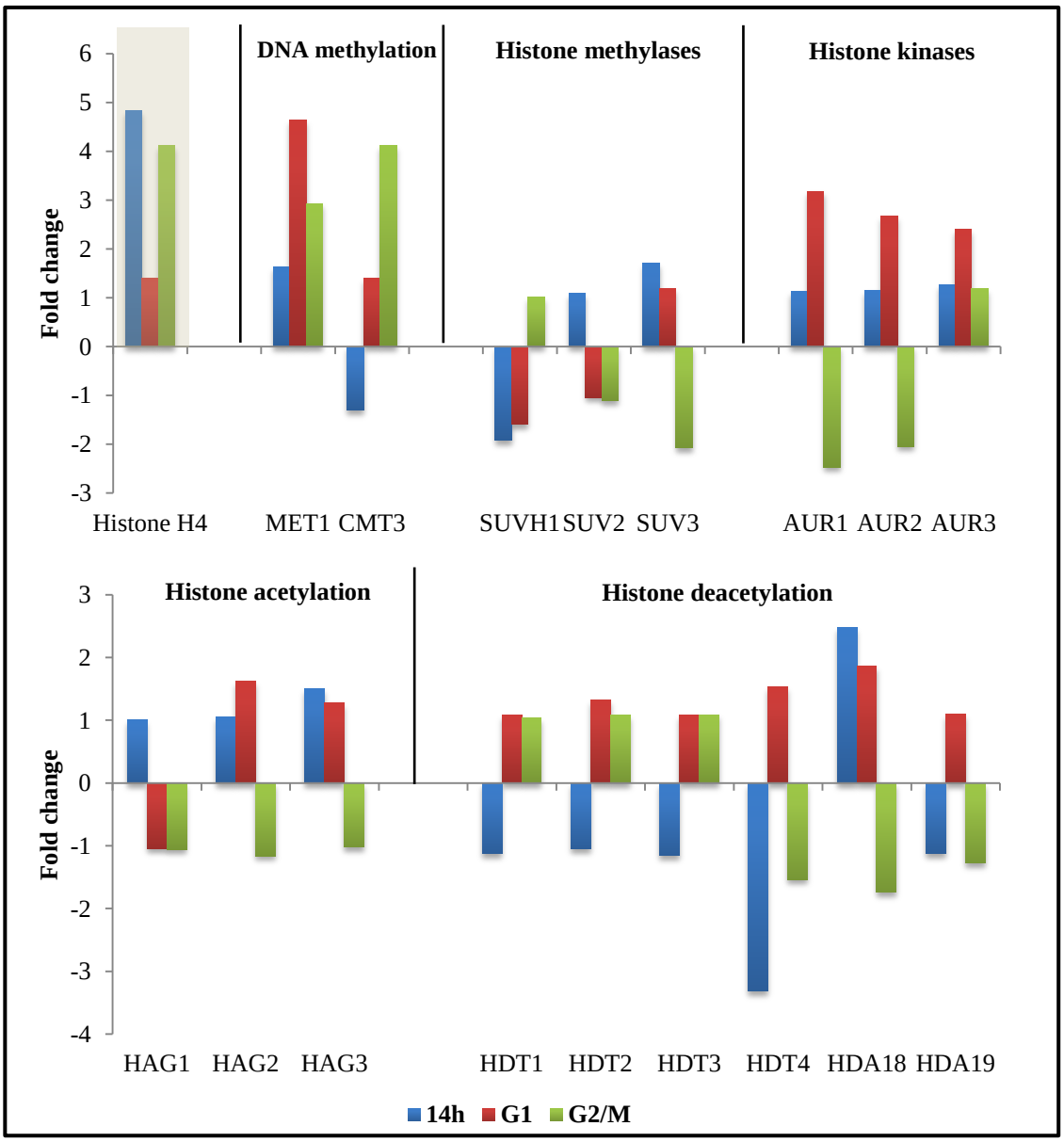

Figure 72: Gene expression changes in histone and DNA modification genes in *Arabidopsis* synchronous (G2/M and G1 rich phases) and asynchronous (14 hours) cultures under simulated microgravity. Fold change expression of the MET1, DNA methyltransferase; CMT3, Chromomethylase; SUVH1-3, suv homologue 1-3; AUR1-3, Aurora kinases 1-3; HAG1-3, histone acetylases 1-3 of the GNAT family; HDT1-4, histone deacetylases 1-4 of the HD2 family; HDA18-19, histone deacetylases of the RPD3/HDA1 family. The pattern of H4 expression has been included as a reference for a well-characterized gene upregulated at the G1/S transition under simulated microgravity.

5.5. ABIOTIC STRESS RELATED GENES IN *ARABIDOPSIS IN VITRO* CULTURE (SYNCHRONOUS/ASYNCHRONOUS) UNDER SIMULATED MICROGRAVITY

As a result of the findings of a large number of stresses related genes affected by our treatment **(GO results, Figure 66 and 67),** we decided to perform a deep analysis of these gene family. On this study, we aim to follow how the plant will use mechanisms evolved to cope with other abiotic stresses to deal with simulated microgravity in synchronous and asynchronous cell cultures.

Stress Responsive Transcription Factor Database (STIFD *v2.0* (***http://caps.ncbs.res.in/stifdb2/index.html***) was used in our study. It is a comprehensive collection of biotic and abiotic stress responsive genes in *Arabidopsis thaliana* (Naika et al 2013, Shameer et al 2009, Sundar et al 2008) that includes 3999 abiotic stress related genes identified in the response to UV-B, Heat, Osmotic, Iron, Aluminum, Wounding, ABA, Cold, Drought, Light, NaCl, Oxidative and/or Dehydration stresses **(Table 12)**, that was determined in our three gravitational stress samples **(Figure 73)**.

Table 12: Content of the Stress responsive transcription factor database including number of genes related to each abiotic stress group. ***Note some of the genes appear in more than 1 group***

Stress Signal	No. of Responsive Genes
UV-B	91
HEAT	45
OSMOTIC	44
IRON	108
ALUMINIUM	24
WOUNDING	39
ABA	570
COLD	890
DROUGHT	691
LIGHT	558
NaCl	836
OXIDATIVE-STRESS	32
DEHYDRATION	71

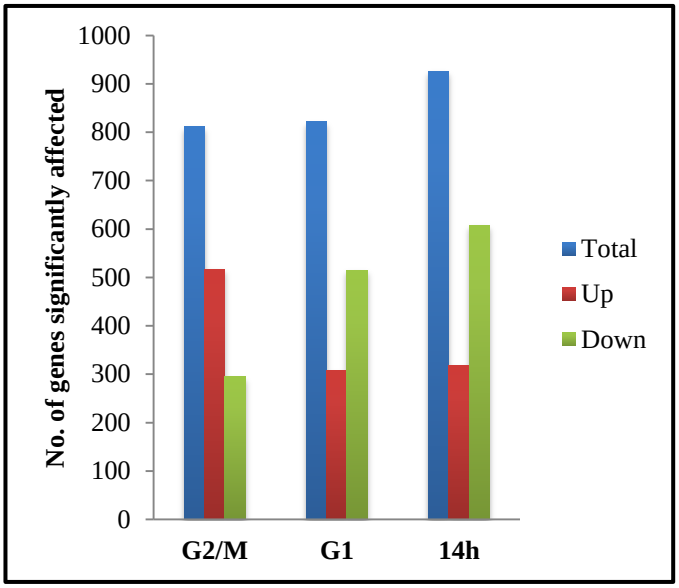

Figure 73: Abiotic stress related genes groups significantly Up-or downregulated (Fold change >2) in *Arabidopsis* synchronous (G2/M and G1 rich phase) and asynchronous cultures (14h) under simulated microgravity versus 1*g* control (CATMA array).

Figure 73 reflects the number of abiotic stress related genes significantly altered (fold change >2) by simulated microgravity in different experimental conditions. It is noticed that, the total number of the altered genes is approximately 20-23% of the total number of abiotic stress described genes. As already observed in gene ontology results, there is a differential behavior of these genes in our samples. Expose to synchronous G1 or G2/M samples affects a similar number of genes (approx. 20%) but the number of upregulated genes is 2/3 of the total in G2 and the opposite is observed in G1 (2/3 of downregulated genes). Furthermore, asynchronous 14 hours sample show slightly higher effects than synchronous G1 cultures.

To determine the contribution of each specific abiotic stress to this picture, a heat map was created using R program according to the significant altered expression genes in each experimental conditions **(Figure 74A)**. In synchronous G2/M, it is found that, 25% of the total related genes of UV-B, Heat, Osmotic and Wounding are upregulated under simulated microgravity, while this percentage drop to 10-15% in other abiotic stress groups **(Figure 74B)**. Furthermore, according the number of the genes involved in the simulated microgravity response, the high number of related genes belongs to drought, NaCl, light and cold stresses.

After 14 hours in synchronous and asynchronous cultures, the UV-B, Heat, Osmotic and Wounding (the four abiotic stresses which upregulated in G2/M) are generally repressed; around 20% of the genes related in each abiotic stresses group.

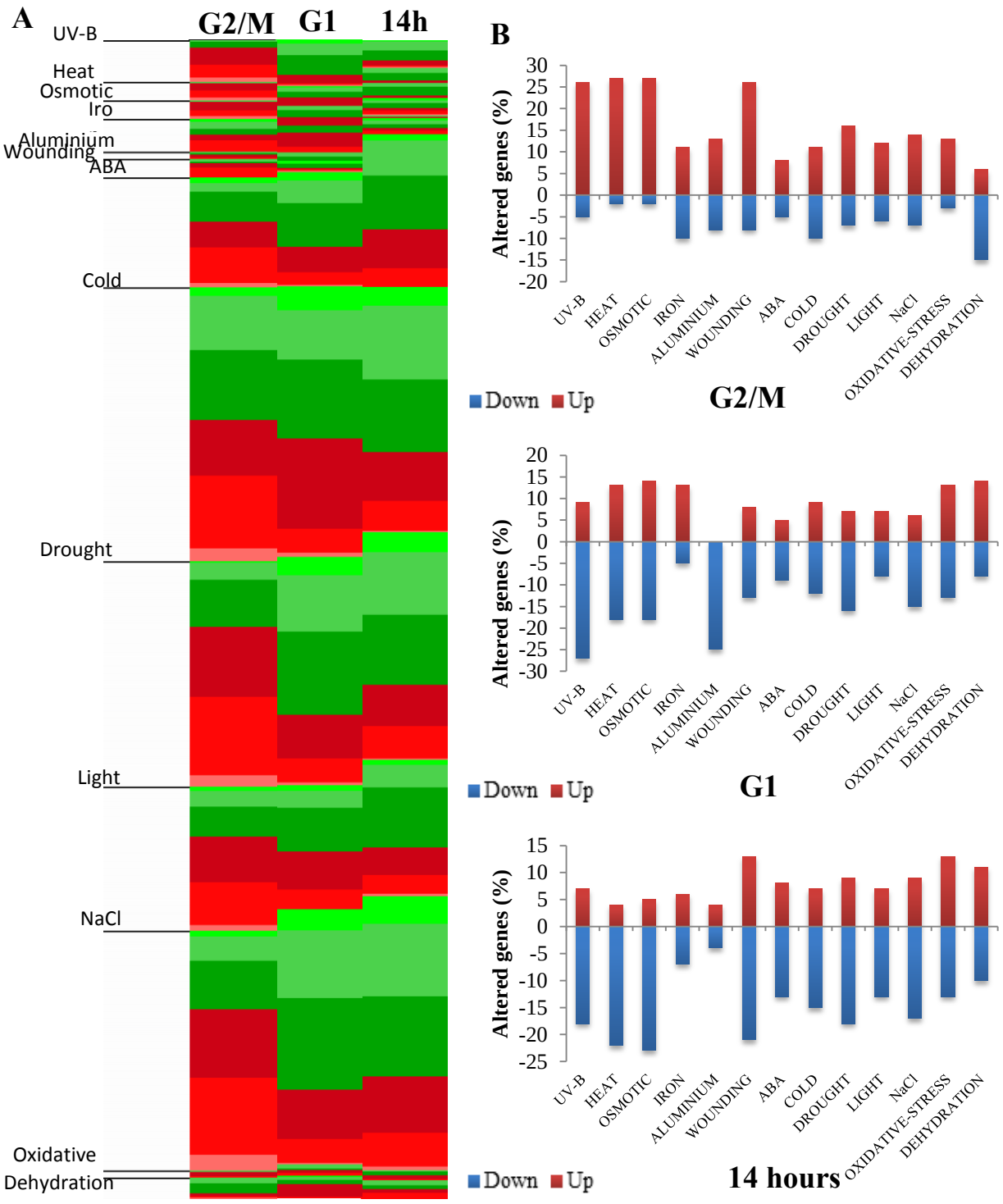

Figure 74: Abiotic stress related genes groups significantly down-or upregulated in *Arabidopsis* synchronous (G2/M and G1 rich phase) and asynchronous cultures (14h) altered by simulated microgravity versus 1*g* control. A) Heat map generated using R software refers to the transcriptome expression of the abiotic stress related genes altered significantly (list of genes are filtered significantly altered according to (FDR p-value <0.05)) showing in colored representation across different experiments samples. A predominantly green color refers to the repressed significantly genes and red represent upregulated. **B)** Percentage of altered genes significantly in each abiotic stress group for the total number of related genes (Red refers to upregulated and blue refers to down regulated).

5.6. LINKING GENES OF UNKNOWN FUNCTION WITH THE SIMULATED MICROGRAVITY ALTERATION IN *ARABIDOPSIS IN VITRO* CULTURE (SYNCHRONOUS/ASYNCHRONOUS) RESPONSIVE SYSTEM

Another group of genes overrepresented in our arrays results is the Unknown function genes **(Figure 66).** Over 13% of all genes in the *Arabidopsis thaliana* genome encode for proteins classified as having a completely unknown function, with the function of >30% of the *Arabidopsis* proteome poorly characterized (Luhua et al 2013). So on, we aim to characterize some of these unknown genes as simulated microgravity related. Unknown genes which altered expression under simulated microgravity were 260, 300 and 323 in G2/M, G1 and asynchronous cultures respectively, but only 20 unknown genes were detected in all the conditions **(Table 13)**. From these common genes, 16 genes corresponding to unknown biological and molecular functions and the other 4 genes are poorly characterized to be linked to response to mechanical stimulus (2 genes), carboxylesterase activity (1 gene) and chromosome organization (1gene). Furthermore, GO cellular component analysis reveal that, 11 genes related to mitochondria, 5 genes to the nucleus, 3 genes to plasma membrane and 1 gene related to the cell wall.

An effort of further characterization of the unknown genes included a STRING program calculation to establish the network of genes responding to the microgravity alterations. Function network **(Figure 75A)** reveals that, among 16 unknown genes there is only one network established consists of four genes (At2G07728, At2G07674, ORF113 (ATMG01220), ORF114 (ATMG01000)). Moreover, increasing the scale of the network to detect more genes linked to our interested network, it is found that the network consists of the 4 unknown genes is part of a large ORF–Hypothetic proteins network which it is located in the mitochondria. This network is appearing to be an independent network located in the mitochondria **(Figure 75A)**. Furthermore, transcriptome analysis of this extended network genes member **(Figure 75B)** shows a significant up regulation in the expression of their members in all the experimental samples under simulated microgravity.

Table 13: Gene ontology (Function description) of the common upregulated unknown genes in Arabidopsis in vitro synchronous/asynchronous cultures altered by the simulated microgravity. Gene ontology for the list of the unknown genes was performed using TAIR database analysis showing GO Biological process, GO cellular component, Molecular function

Genes ID	Function Description		
	Biological	**Molecular**	**Cellular component**
AT1G06475	Unknown	Unknown	Membrane
AT1G19380	Unknown	Response to chitin, mechanical stimulus, wounding	Membrane
AT1G30135	Unknown	Ethylene biosynthetic process, response to jasmonic stimulus and wounding	Nucleus
AT2G46940	Unknown	Unknown	Nucleus
AT4G13690	Unknown	Unknown	Nucleus
AT4G26950	Unknown	Unknown	Nucleus
AT5G23100	Unknown	Unknown	Nucleus
AT5G23870	Unknown	Carboxylesterase activity	Extracellular region
AT3G60950	Unknown	Unknown	Plasma membrane (Cultured plant cell)
AT2G07728	Unknown	Unknown	Mitochondria (Cultured plant cell)
AT2G07775	Unknown	Unknown	Mitochondria
AT4G32295	Unknown	Unknown	Mitochondria
AT2G07674	Unknown	Unknown	Mitochondria
AT2G07702	Unknown	Unknown	Mitochondria
AT2G07722	Unknown	Unknown	Mitochondria
ATMG00320	Unknown	Unknown	Mitochondria
ATMG00630	Unknown	Chromosome regulation	Mitochondria
ATMG01000	Unknown	Unknown	Mitochondria
ATMG01220	Unknown	Unknown	Mitochondria
ATMG01350	Unknown	Unknown	Mitochondria

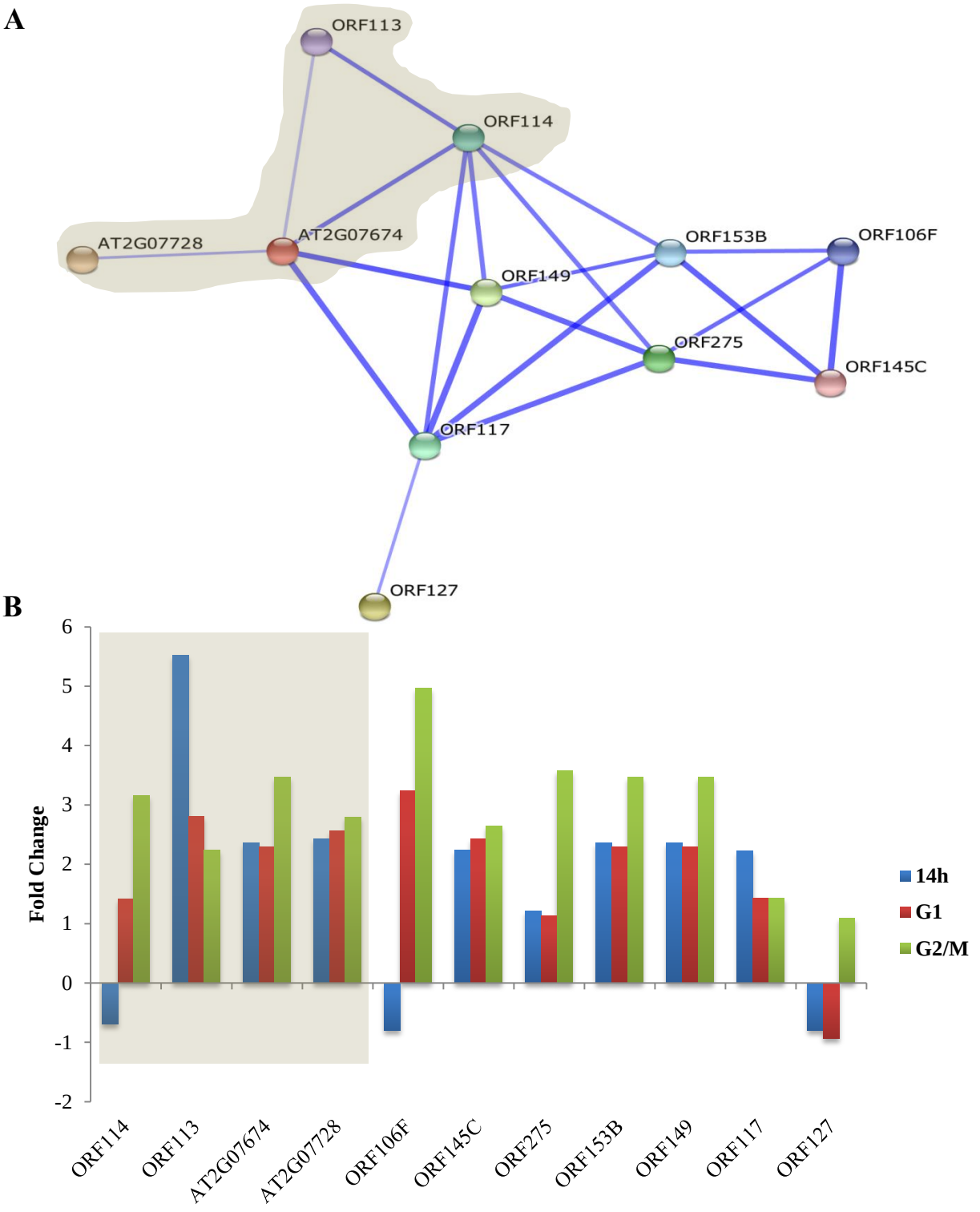

Figure 75: Network based on Unknown genes with upregulated gene expression under simulated microgravity (Protein-Protein interaction). Four unknown genes are observed to be linked in a network established using STRING v9.1 networks. **A)** A confidence network view, stronger associations are represented by thicker lines. Shadow determination shows the original 4 unknown altered gene in our study. **B)** Fold change expression of the network gene members using the array data analysis confirms a similar gene expression pattern for the whole network.

5.7. ARRAY DATA VALIDATION; SPECIFIC GENES EXPRESSION BY QPCR ANALYSIS

DNA microarrays provide an unprecedented capacity for whole genome profiling with relatively low amount of biological sample (a requirement in Space Research). However, the quality of gene expression data obtained from microarrays can vary greatly with platform and procedures used so a quantitative real-time PCR (qPCR) validation is needed. Here we are going to validate array based data by qPCR of specific genes expression variations under simulated microgravity. These genes include at least one member of the following processes: cell growth and ribosome biogenesis, cell cycle core regulators, epigenetic modifications, abiotic stress and ORF-hypothetical network related genes **(Table 14)**. Furthermore, actin housekeeping gene is used as internal standard (Thellin et al 1999). In a first global view, we can observe that qPCR confirms the significant changes in most of the microarray detected variations, being the amount of the change generally overestimated in the G2/M sample and underestimated in the asynchronous sample.

Ribosome biogenesis related genes validation using qPCR. Among the ribosome biogenesis related genes, Nucleolin and Fibrillarin were selected as the two abundant ribosome biogenesis genes **(Table 14)**. It is noticed that the quantitative relative expression analysis results are in agreement with the microarray results but the variation is underestimated in the array; being both Nucleolin are Fibrillarin repressed significantly in the synchronous G2/M and asynchronous culture.

Cell cycle regulators related genes validation using qPCR. To study the validation of the array analysis on the cell cycle core related genes expression, CYCB1;1, and Prolifera probe sets were used. **Table 14** reveals that the cell cycle related genes are validated by this qPCR approach in almost of the conditions. As general, insignificant variations is obtained in the CYCB1;1 expression in both platforms in the synchronous samples, while it reach a significant up regulation in the arrays supported with the insignificant upregulation of the quantitative expression.

Prolifera quantitative relative expression analysis results are in agreement with the microarray results. Significant up regulation in the synchronous G1 samples with in significant up regulation in the asynchronous. While the significant relative expression in G2/M sample linked to the insignificant variation in the array results.

Table 14: Relative expression (Ratio (μ*g* vs 1*g* control) validation (qPCR + Array) transcriptome analyses for specific genes show a significant alteration in different experimental samples. Significant variations mentioned in bold

Functions	Interested Genes	Synchronous G2/M		Synchronous G1		Asynchronous 14h	
		qPCR	Array	qPCR	Array	qPCR	Array
Ribosome biogenesis	***AtNUC-L1*** (At1g48920)	**0.427**	0.586	1.264	1.283	**0.300**	0.722
	AtFIB1 (At5g52470)	**0.408**	**0.486**	0.765	1.424	**0.299**	0.582
Cell cycle core	***CYCB1;1*** (At4g37490)	0.833	1.414	0.921	0.664	1.081	**1.602**
	Prolifera PRL (At4g02060)	**1.397**	0.807	**1.273**	**2.848**	1.147	1.007
Epigenetic	**MET1** (At5g49160)	**1.963**	**2.928**	**2.395**	**4.627**	0.810	**1.625**
	CMT3 (At1g69770)	**1.540**	1.141	0.915	**2.462**	**0.494**	0.768
	AUR2 (At2g25880)	0.549	**0.490**	**2.260**	**2.676**	0.670	1.149
Abiotic stress	**Unknown** (At2g20560)	1.117	**3.031**	0.712	0.547	**0.409**	**0.351**
	CYP71A12 (At2g30750)	**2.489**	**3.630**	**1.782**	**0.480**	1.071	0.785
Unknown /mitochondria	**ORF113** (Atmg01220)	0.736	**2.235**	1.297	**2.809**	0.685	**5.540**
	Unknown (At2g07728)	**1.682**	**2.789**	**2.788**	**2.567**	**2.979**	**2.428**
	Unknown (At2g07674)	0.879	**3.458**	0.793	**2.297**	**2.625**	**2.346**
	Unknown (At2g07702)	0.968	1.986	0.783	1.602	0.807	**4.199**

Epigenetic modifications related genes validation using qPCR. MET1 and CMT3 (DNA methyltransferase enzymes) and AUR2 (histone kinases) were selected to perform the quantitative relative expression analysis **(Table 14)**. Epigenetic modifications microarray expression values are validated to a great extent by qPCR results. Upregulation of MET1 is confirmed, but slightly overestimated, in both synchronous cultures.
Moreover, CMT3 up-regulation in G1 synchronous is not clear by qPCR but slight repression under asynchronous cultures is confirmed by the qPCR results. AUR2 shows confirmed down regulation in G2/M and up regulation in the synchronous G1.

Abiotic stress related genes validation using qPCR. As there is a general behavior on stress relating genes showing up regulation in synchronous G2/M and down regulation in G1 **(Figure 74)**, we decided to validate this effect using two different genes. At2g20560 is selected as a heat stress related gene **(Table 14)**. Quantitative relative expression is in agreement with the array results; up regulation in the synchronous G2/M (overestimated in the array results) and confirmed repression in 14 hours exposure (both the insignificant variations in synchronous G1 and significant variations in asynchronous). CYP71A12 is selected as an oxidative stress related gene **(Table 14)**. qPCR results are in agreement with CYP71A12 upregulation in the synchronous G2/M samples, while small variations changes detected after 14 hours exposure (G1 and asynchronous) were not consistent.

Unknown genes related to mitochondria (ORF network genes) validation using qPCR. As an important perspective to provide credibility to the functional link between unknown genes related to simulated microgravity **(Figure 75A)**, a validation study was performed including the four genes used to build the ORF network (all upregulated in all the experimental samples under simulated microgravity). As general the quantitative relative expression shows agreement with the array upregulation results or provides no significant different expression **(Table 14)**. At2g07728 significant up regulations in all the samples are confirmed by qPCR, as well as Atmg01220 upregulation expression in G1 synchronous, At2g07674 upregulations in asynchronous cultures.

RESULTS

CHAPTER 6: *NEW MATERIALS TO BE USED IN FUTURE SPACE RESEARCH: PRODUCTION OF TRANSGENIC CALLUS/CELL CULTURES FROM TRANSGENIC SEEDS/SEEDLINGS*

6.1. Successful Induction of Callus from Space Research Interesting Transgenic *Arabidopsis* Seedlings

6.2. Expose Transgenic CYCB1 Line:*uidA* (GUS) Callus to Altered Gravity

6.3. Expose Transgenic CYCB1:GFP and AtNUCL1:GFP Callus to Altered Gravity

CHAPTER 6: NEW MATERIALS TO BE USED IN FUTURE SPACE RESEARCH: PRODUCTION OF TRANSGENIC CALLUS/CELL CULTURES FROM TRANSGENIC SEEDS/SEEDLINGS

Using plant cell cultures in the plant space biology programs is important for the future investigations to detect the cellular response to the gravitational alteration. So on, providing a cellular biological system able to be analyzed "*in vivo*" with the microscopic techniques could be implemented in flight experiments to the International Space Station to enhance the scientific outcomes in the space biology programs.

Fluorescent imaging offers the ability to monitor biological functions, in this case biological responses to space-related environments. For plants, fluorescent imaging can include general health indicators such as chlorophyll fluorescence as well as specific metabolic indicators such as engineered fluorescent reporters.

Two reporter systems have been used extensively in the past decade. GUS reporter system (*GUS*: β-glucuronidase) is particularly useful in plant molecular biology (Jefferson et al 1987). This technique based on the histochemical analysis is used to monitor the activity of a promoter (in terms of expression of a gene its controls) either in a quantitative way or through visualization of its activity in different tissues. The technique is based on β-glucuronidase, an enzyme from the bacterium *Escherichia coli* (Blanco et al 1982). Green fluorescent protein (GFP) comes from jellyfish, *Aequoria victoria,* and its fluorescence was first used as a marker for gene expression to highlight sensory neurons in nematodes (Chalfie et al 1994). *GFP* gene has become a useful tool for making chimeric proteins that are linked to other proteins for use as fluorescent protein tags and the most common reporter gene used in plant cell biology (Dixit et al 2006, Haseloff & Siemering 2006, Leff & Leff 1996, Leffel et al 1997). Fluorescence was detected in *Arabidopsis* upon excitation with UV or blue light. This technique can be used to monitor the repaid gene expression alteration in the real time of the experiments and localized the protein expression by observing the GFP expression *in vitro* and for the step forward *in vivo* using a fluorescent microscope *in vivo* detection, whereas the fluorescent microscope become a recent advanced biotechnology technique in ISS (NASA 2014).

6.1. Successful Induced Callus from Space Research Interesting Transgenic *Arabidopsis* Seedlings

Arabidopsis semi-solid cultures (Callus) were successfully induced from the transgenic hypocotyl *Arabidopsis* lines established by (Manzano 2011) in our lab and described in material and methods (*see 1.4*). Transgenic CYCB1:*uidA* (GUS), NUCL1:mGFP and CYCB1;1:mGFP were induced form the specific hypocotyl lines **(Figure 76)** to be used under the gravitational alterations as indicated in Materials and Methods ***Experiment 7*** description as a primary step for the future use of the transgenic cell cultures for the microscopy observation on the International Space Station. Even more, the next results are just a primary steps for new techniques are going to be developed in the lab in the near future as a part of the future space flight preparation using plant cellular systems for deeply biological answers.

6.2. Expose Transgenic CYCB1 Line:*uidA* (GUS) Callus to Altered Gravity

Transgenic CYCB1 Line:*uidA* callus cultures were exposed to altered gravity (simulated microgravity using RPM and hypergravity using LDC) in a comparison with 1*g* control condition for two different exposure time, 4 and 6 days **(Figure 77)**. Cyclin B1 expression level was studied by quantify the distribution of the synthetic reporter construct with a CyclinB1 promoter driving β-glucuronidase activity. It is noticed that the use of the transgenic callus is successfully applied and altered. CyclinB1 expression distribution is altered by the gravitational effect through the different time compared with 1*g* control; significant decreases in the simulated microgravity after 4 days exposure, while it is increased significantly after 6 days. Hypergravity repressed the cyclinB1 expression after 6 days.

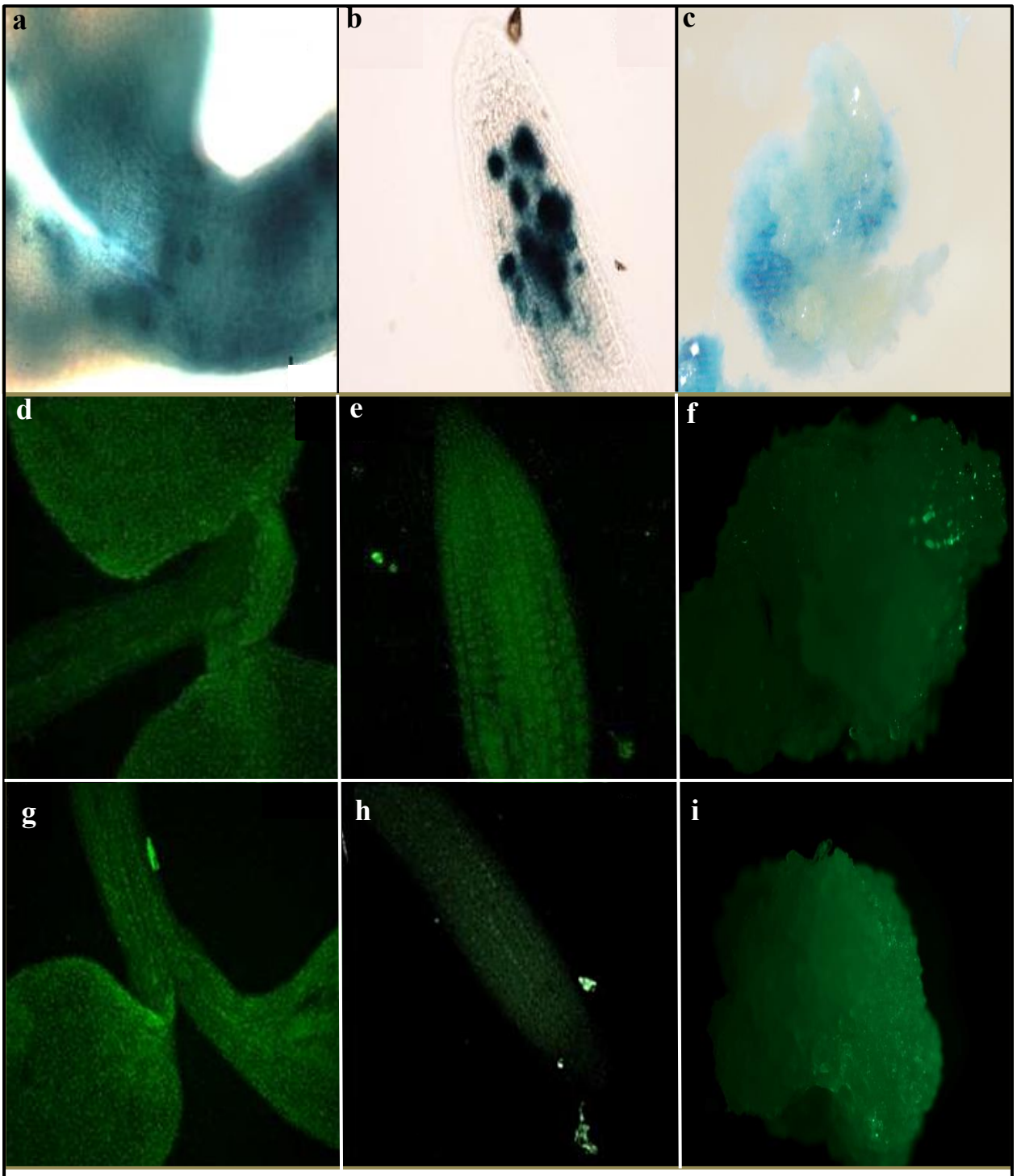

Figure 76: Induced callus semi-solid cultures form different *Arabidopsis* transgenic lines. Upper part presents the induced callus with CYCB1:GUS construction report gene using contrast microscope observation with the scale bar 50µm. **(a)** Hypocotyl **(b)** root tips in *Arabidopsis* seedlings **(c)** induced callus. **Lower parts** present the induced callus with the GFP transgenic lines under the fluorescent microscope observation with the scale bar 50µm. **(d)** Hypocotyl **(e)** root tips in *Arabidopsis* seedlings **(f)** induced callus with the construction of CYCB1:GFP. **(g)** Hypocotyl **(h)** root tips in *Arabidopsis* seedlings **(i)** induced callus with the construction of AtNUCL1:GFP. ***Note:*** Hypocotyl and root tips images obtained from (Manzano 2011) who prepared the original transgenic seedlings lines.

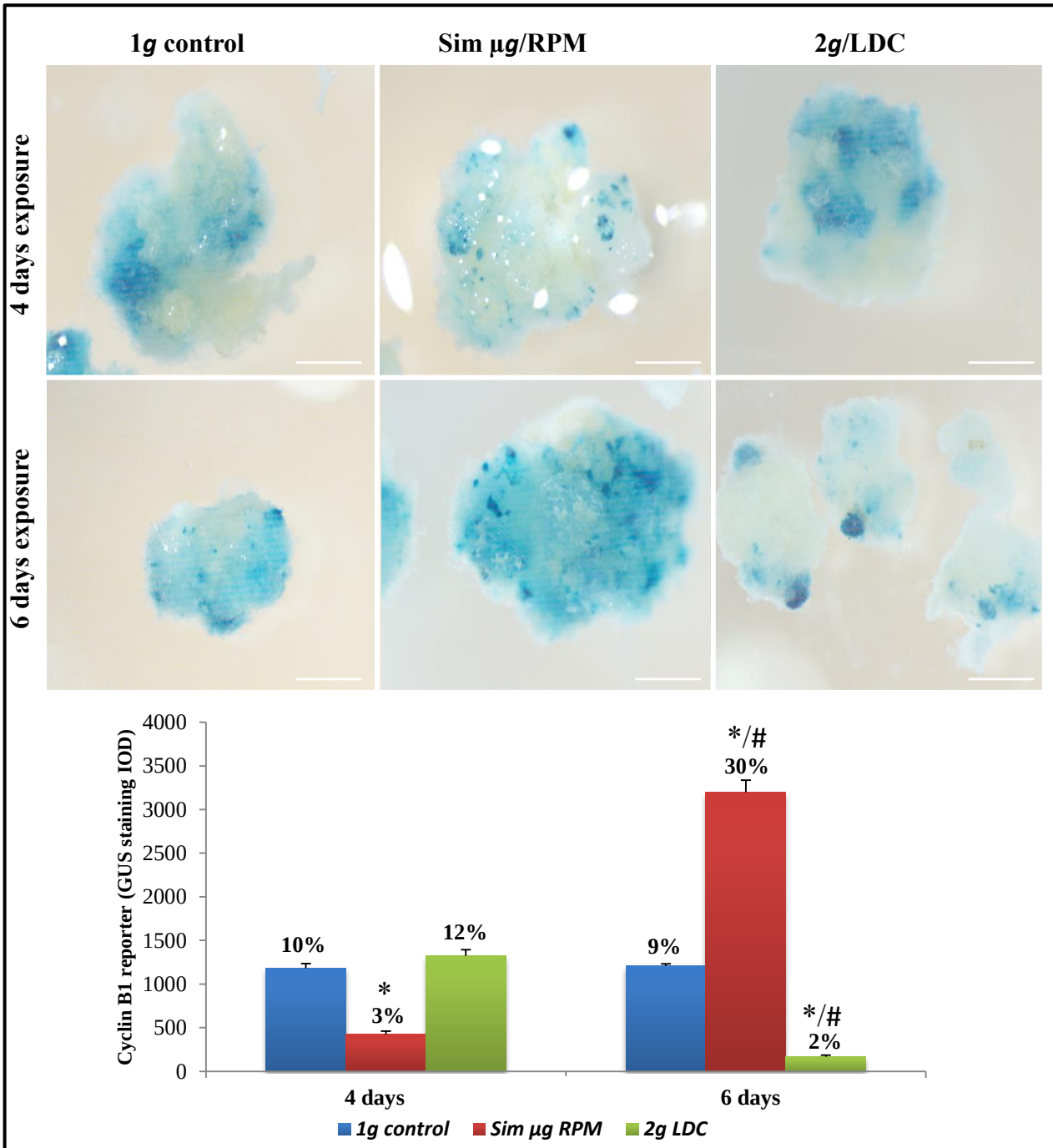

Figure 77. Cyclin B1 expression in *Arabidopsis* semi-solid callus cultures revealed by GUS staining. The use of the reporter gene line CYCB1:GUS allowed the microscopy visualization of the expression of the cyclin B1 gene. Whole mount preparation of the callus samples were stained and observed by optical microscopy using 1x magnification (scale bar 1cm). Callus cultures were exposure to different gravitational alteration; from left to right: 1*g* control, simulated microgravity (µ*g* RPM), and hypergravity (2*g* LDC) for different exposure duration. **A**) 4 days. **B)** 6 days. **C)** Quantitative study of the expression of the cyclin B1 gene by measuring the integrated optical density (I.O.D.) supplemented with the area stained percentage (%). P-Value <0.05, (#) used in a comparison with the same gravity level in different exposure time 4 days vs 6 days. (*) used in a comparison with 1*g* control in the same exposure experiment.

6.3. Expose Transgenic CYCB1:GFP and AtNUCL1:GFP Callus to Altered Gravity

CyclinB1 expression level (by detecting the GFP signal) is altered by the gravitational alteration under 4 and 6 days exposure **(Figure 78A).** Monitoring the level of the GFP reveals that simulated microgravity increases the cyclinB1 expression after 4 days of the gravitational alteration (simulated microgravity and hypergravity) compared with the 1g control. After 6 days of exposure, cyclinB1 expression is increased altered by the simulated microgravity, while hypergravity causes a repression on the cyclinB1 level.

AtNUCL1 expression was studied by the linking GFP promoter under the gravitational alteration **(Figure 78B)**. It is noticed a repression on the AtNUCL1 (GFP signal) due to the simulated microgravity alteration in both 4 and 6 days, while hypergravity increase the expression of the nucleolin levels.

Figure 78. CYCB1:GFP and AtNUCL1:GFP expression in *Arabidopsis* semi-solid callus cultures revealed by GFP signal levels. The use of the reporter GFP allowed the microscopy visualization of the expression of the cyclin B1 **(A)** and Nucleolin **(B)** genes. Whole mount preparation of the callus samples were fixed and observed by UV fluorescent microscopy using 1x magnification (scale bar 1cm). Callus cultures were exposed to different gravitational alteration; from left to right: 1g control, simulated microgravity (Sim µg RPM), and hypergravity (2g LDC) for two different exposure duration; 4 days and 6 days.

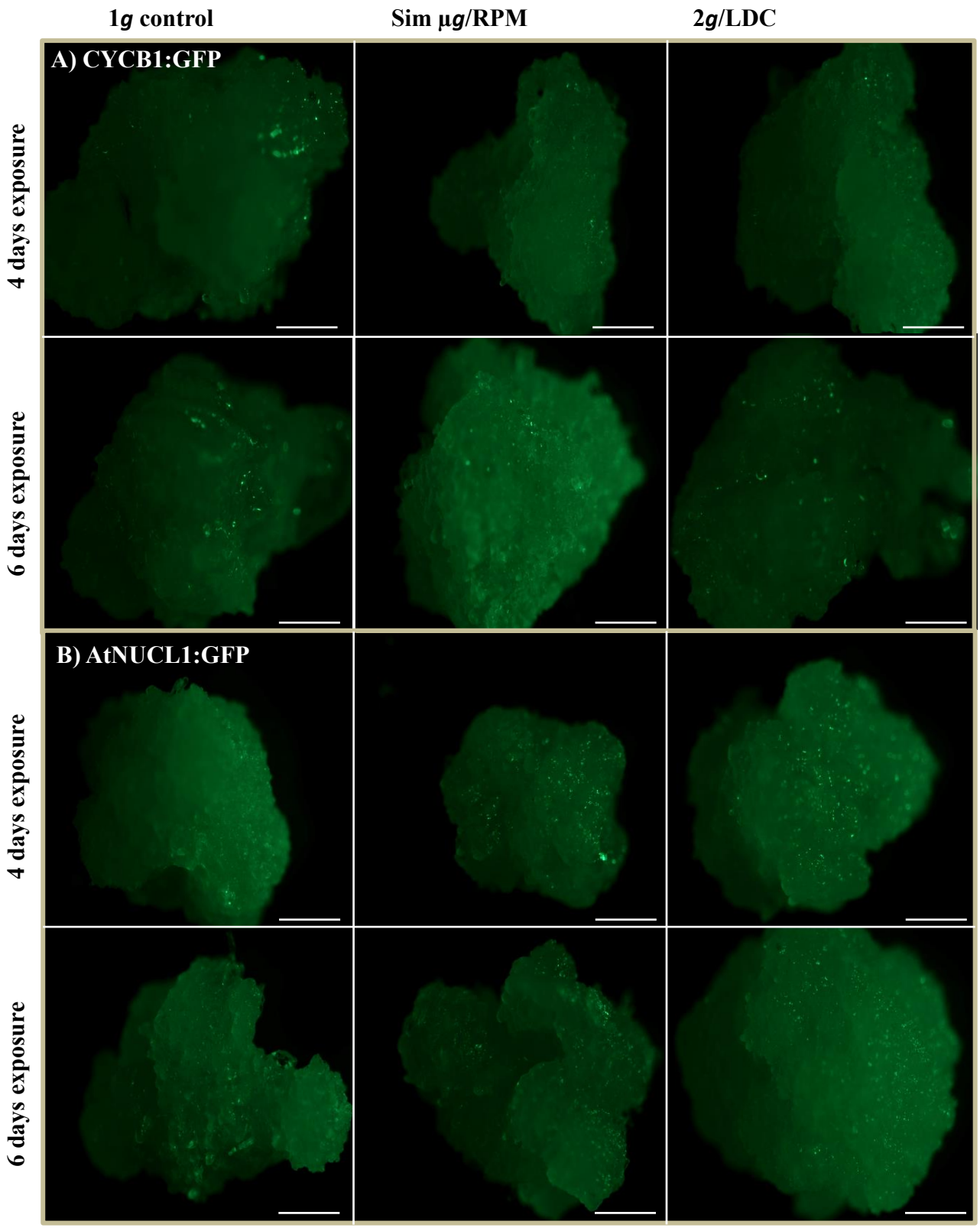
1g control
Sim µg/RPM
2g/LDC
A) CYCB1:GFP
4 days exposure
6 days exposure
B) AtNUCL1:GFP
4 days exposure
6 days exposure

Using immobilized cells in the RPM and LDC is the best method to simulate altered gravity environments. Cell developmental processes were altered as in root meristematic cells of seedlings even in the context of a system without known professional gravisensitive cells. Plants response to altered gravity relies in a complex and unique mechanism suggesting a synergistic effect. The implication of the results for life support systems in space and Earth is certain.

DISCUSSION

Revisiting the foundations of GBF on plant cells

Simulated microgravity alters cell developmental processes

Implications for space exploration

Implications for life on Earth

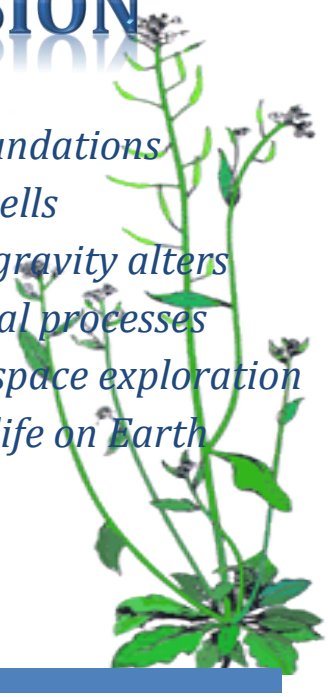

1. REVISITING THE FOUNDATIONS OF ALTERED GRAVITY SIMULATION AND FACILITIES. MODE OF OPERATION FOR THE PLANT CELL MODEL SYSTEMS

The first, classical and most extensively used GBFs for exposing biological materials to simulated microgravity are clinostats. In the specific case of the cell culture model systems, clinostats are still considered as proper facilities, together with magnetic levitation for partial gravity simulation (Herranz et al 2013a). Here we have found that immobilized cell cultures, used in Random Positioning Machines (RPMs) are better and more versatile alternatives, at least for relatively long-term studies. They serve as valuable tools for preparing spaceflight experiments and also allow stand-alone studies, thus providing additional and cost-efficient platforms for gravitational research. We will discuss thereof which ground based facilities might be most appropriate for different altered gravity experiments using plant cellular systems, as well as theorize about alternative modes of operation to allow proper use of the clinostat, RPMs or magnetic levitation facilities.

1.1. PROPER USE OF 1g CONTROLS IN SIMULATED MICROGRAVITY RESEARCH: THE CASE OF THE PLANT CELL SUSPENSION CULTURE USING 2D PIPETTE CLINOROTATION

To better decipher and interpret the effects of the altered gravity simulation in the conditions used in our experiments, we should discriminate and understand the forces acting on each one of the experimental conditions tested, including the reference controls **(Figure 79)**. Under real microgravity (a condition which has not been tested in this work, but it should be considered as the ideal condition for studying spaceflight biological effects) cells are supposed to be free floating in the culture medium, so they would remain in suspension without any mechanical force being present in the system **(Figure 79A)**. In the case of the internal (non-shaking) 1g control (***see Experiment 1 description in Methods***), the suspension of cells with a higher density than the surrounding medium will eventually sediment **(Figure 79D)**. Cells under this condition would be stressed by a lower availability of nutrients, resulting in synchronization by starvation.

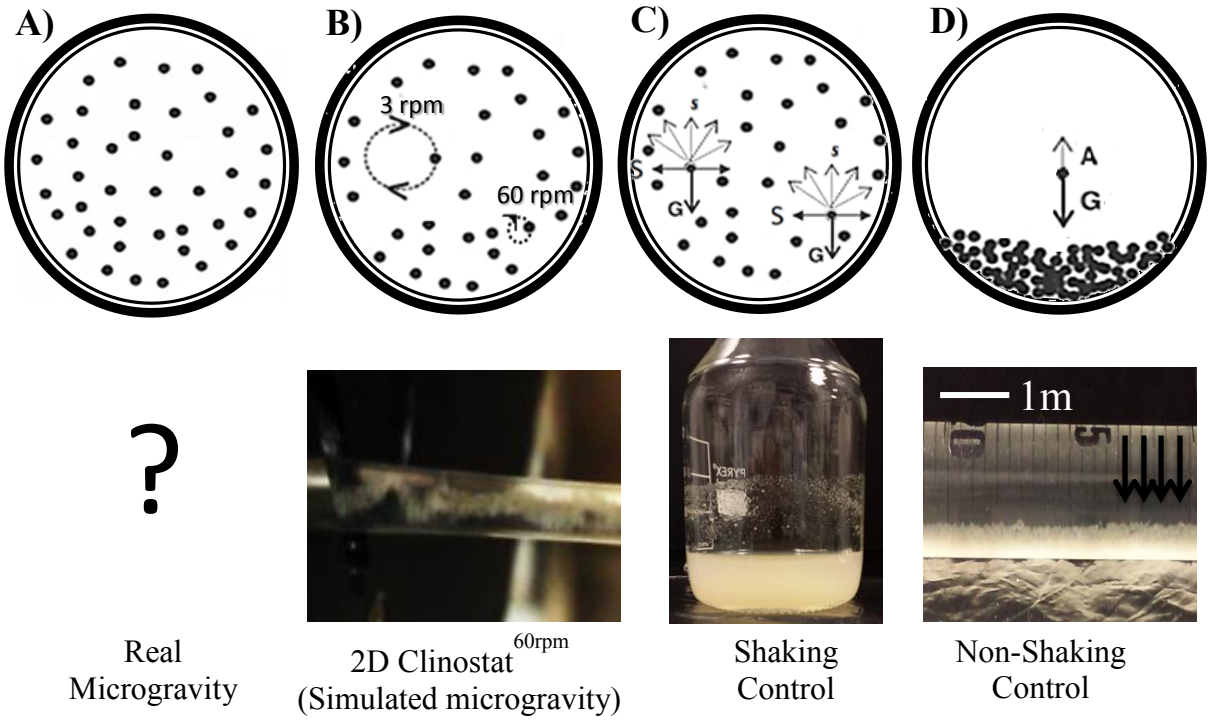

Figure 79: Mechanical explanation of the forces acting on the cells under different type of altered gravity conditions. A) We assume cells in real microgravity to be in a suspension, homogeneously distributed in the tube, free of mechanical stimulus. B) Pipette-2D-clinostat: under simulated microgravity, the cells distribute homogeneously due to the lack of sedimentation, the cells are forced on circular paths due to the clinostat rotation, whose radii are inversely proportional to the speed of rotation (3 rpm cause larger circular paths than 60 rpm). C) Shaking control; cells are affected by the gravity vector (G) inducing sedimentation and, at the same time, due to the shaking, the cells are exposed to shear forces (S). Cells remain in suspension depending on the speed of the shaking. D) Non-Shaking Control; under 1*g*, the cells in suspension sediment at the bottom of the tube, affected by the 1*g* force. The cell position depends on its weight (G) and buoyancy (A). Below each condition is exemplified by a real photograph of the cell culture behavior in the particular experimental condition (real microgravity is not included in this work, so a question mark has been added). Note the helix/coiled structure that appears in the 2D clinostat suggesting that fluid motions are disturbing the simulation experience. Schemes inspired from Figure 2.1 in (Häder et al 2005)

In fact, we observed an increase in the number of cells in S phase under the internal 1*g* control with a reduced fraction of cells in G1 in the long-term experiment, a result compatible with the arrest of cells in S phase, being unable of reaching G2/M, and also compatible with a decreased survival, as observed by Trypan blue staining. In contrast, external 1*g* (shaking) control shows a distribution of cells in suspension more similar to the one appearing under real microgravity conditions, but other additional stresses, related to shearing forces, could be produced **(Figure 79C)**. These forces, which are always present under the standard cell culture growth conditions, are reduced in simulated microgravity using a 2D clinostat, with the consequence of reducing this type of mechanical stress on the cells. However, cells under clinorotation are exposed to a randomized gravity vector but also to fluid motions shear, which depends on the rotational speed

(as observed by the coiled distribution of the cell culture near the center of the rotating pipette, **Figure 79B)** and it is practically impossible to differentiate the cell response to either of these two mechanical stimuli. The same is true for the utilization of rotating wall vessels to simulate microgravity (Kaysen et al 1999). As a summary, we can conclude that none of the two 1g controls is enough, on its own, to fulfill all the requirements of a true control, since both of them include different components of the forces acting on the clinorotation simulation.

A mandatory requirement for plant cell suspension cultures is that they should be permanently subjected to shaking, in order to prevent that the proliferating cells aggregate and then enter into the differentiation program by the formation of cell clusters (May & Leaver 1993, Menges & Murray 2002). However, this requirement does not exist in the case of animal cells, which can survive in culture without shaking. For this reason, there is a significant number of literature references using clinorotation with animal cell cultures. For example, human T lymphocytes were cultured into the same 2D Pipette clinostat as in our experiments, and 1g control were stored without shaking into a stable bag in some successful experiments (Thiel et al 2012). In our opinion, it is only possible to perform experiments using a 2D clinostat with plant cell suspensions if they remain short-termed. In order to circumvent the problems of the 1g control, the alternative would be to produce a 1g control in the pipette clinostat with similar forces than the clinorotated samples, but preventing sedimentation in a single point. This kind of alternative 1g control could be created by using a bigger 2D clinostat by increasing the rotation speed up to 160 rpm into a 3.3 cm diameter cylinder with a small central pipette. The samples in the internal pipette will be clinorotating (simulated microgravity) and the samples near the border of the cylinder will be clinorotating also and exposed to a 1g centrifugal force (1g normal gravity averaged), mitigating some of the problems of the non-shaking control **(Figure 80)**.

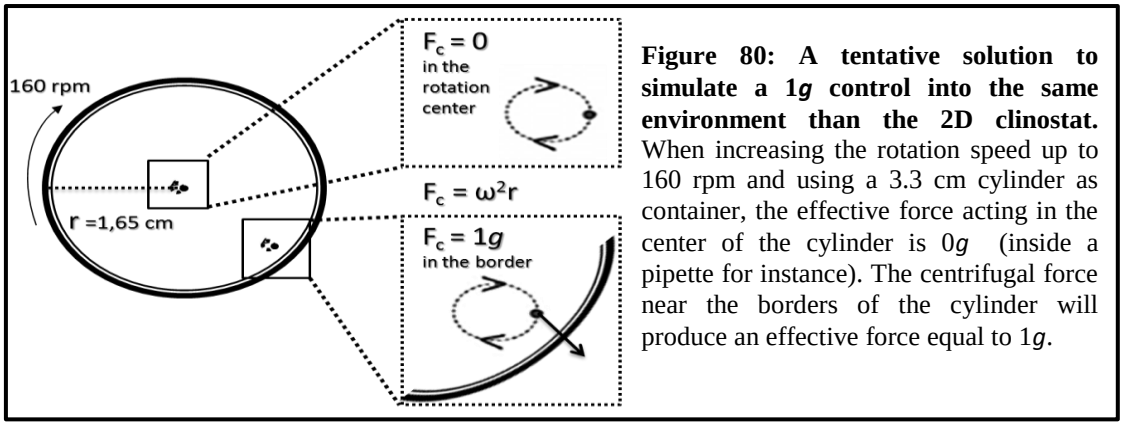

Figure 80: A tentative solution to simulate a 1g control into the same environment than the 2D clinostat. When increasing the rotation speed up to 160 rpm and using a 3.3 cm cylinder as container, the effective force acting in the center of the cylinder is 0g (inside a pipette for instance). The centrifugal force near the borders of the cylinder will produce an effective force equal to 1g.

1.2. ARE PLANT CELLS IN A SUSPENSION REALLY EXPOSED TO SIMULATED MICROGRAVITY WHEN EXPOSED TO DIAMAGNETIC LEVITATION?

It is particularly interesting to elaborate on the magnetic levitation effects at the cellular level. Can it be applied to individual cells in suspension within a levitating water droplet? In our experiments we used the diamagnetic force (13T with a strong gradient) required to compensate the weight of the cell suspension as a whole, but it was noticed that the cells inside the droplet sediment through the time due to the different densities and magnetic susceptibilities of components other than water. In the droplet experiment, the sedimentation occurs because the gravity force is higher than the magnetic force applied to the cells.

The reason is that the magnetic susceptibility is lower for the cells than for water, so that the magnetic field acting on the cells (F_m^{cells}) is lower than the one acting on the whole solution (F_m^{sol}), which is equal to the gravity force on the levitation point. Moreover, it is noticed that the cells cannot spear out of the water drop due to the surface tension force. Accordingly to the formula for diamagnetic levitation

$$F_m = xVB\frac{dB}{dZ}\mu_0^{-1}$$

Three scenarios can be used to levitate a cell suspension (as schemed in **Figure 81**):

- $0g^*$ stable levitation (for solution): It is the droplet experiment configuration. F_m^{sol} is equal to g in the center of the droplet that it is stabilized by a slightly lower F_m^{sol} in the top and slightly higher F_m^{sol} in the bottom of the drop. Empirical value of F_m^{sol} is quite similar to the calculated value of $F_m^{H_2O}$ for pure water. $F_m^{sol} > F_m^{cells}$, so sedimentation occurs.

- $0g^*$ unstable levitation (for solution): It is performed in the secondary $0g^*$ point in a non-levitation condition configuration. F_m^{sol} is still equal to g in the center of the sample but it is non-stable due to slightly higher, repealing F_m^{sol} both in the top and in the bottom of the cell culture facilitating the suspension to be expulsed. $F_m^{sol} > F_m^{cells}$, so sedimentation occurs.

- $0g^*$ "stable" levitation (for cells): It is a virtual experiment we have not attempted. Once the culture is tapped to prevent the liquid to escape, an increase in the magnetic field could produce that F_m^{cells} is equal to g in the center of the sample. $F_m^{sol} > F_m^{cells}$ so movements in the fluid will produce shear stress by fluid motions, but the cells will be "stabilized" in the center of the culture by slightly lower F_m^{cell} in the top and slightly higher F_m^{cell} in the bottom of the container.

Consequently, if the $B_z\, dB_z/dz$ conditions can be established considering the magnetic properties of the cells only, then the cells could be levitated inside a non-levitating solution, although we did not attempted to test this alternative. In fact, increasing the magnet force to 16T was enough to eliminate the water drop out of the levitation range without a cap. Consequently, the cells were exposed to low-gravity levels by the magnetic force but it is not enough to consider the results only relying on microgravity (as it will occur in a Spaceflight or a free-fall orbit).

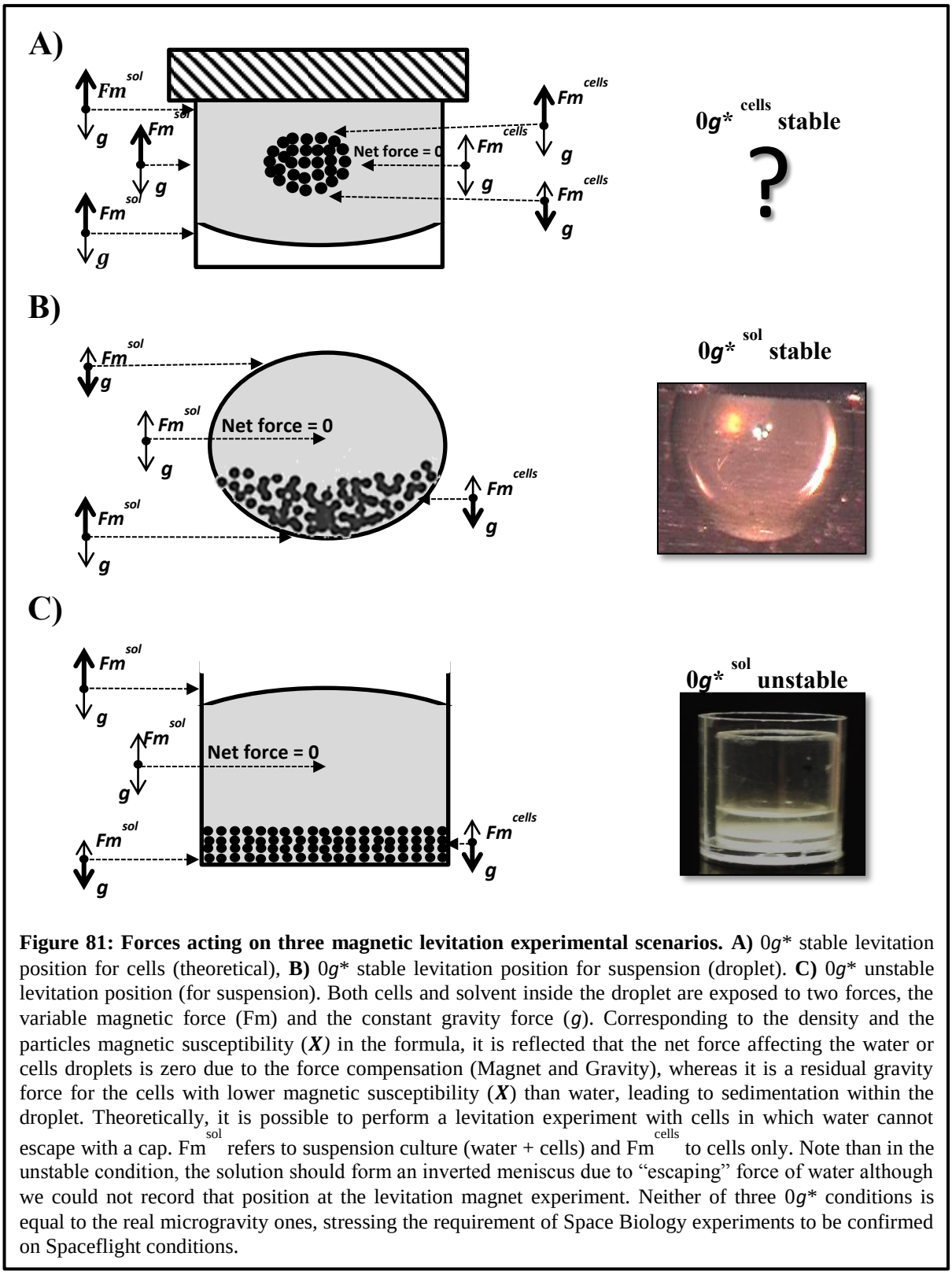

Figure 81: Forces acting on three magnetic levitation experimental scenarios. A) 0*g** stable levitation position for cells (theoretical), **B)** 0*g** stable levitation position for suspension (droplet). **C)** 0*g** unstable levitation position (for suspension). Both cells and solvent inside the droplet are exposed to two forces, the variable magnetic force (Fm) and the constant gravity force (*g*). Corresponding to the density and the particles magnetic susceptibility (***X***) in the formula, it is reflected that the net force affecting the water or cells droplets is zero due to the force compensation (Magnet and Gravity), whereas it is a residual gravity force for the cells with lower magnetic susceptibility (***X***) than water, leading to sedimentation within the droplet. Theoretically, it is possible to perform a levitation experiment with cells in which water cannot escape with a cap. Fm^{sol} refers to suspension culture (water + cells) and Fm^{cells} to cells only. Note than in the unstable condition, the solution should form an inverted meniscus due to "escaping" force of water although we could not record that position at the levitation magnet experiment. Neither of three 0*g** conditions is equal to the real microgravity ones, stressing the requirement of Space Biology experiments to be confirmed on Spaceflight conditions.

1.3. DEFINING PROPER CONTROLS AND MODE OF OPERATIONS WHEN USING RPM AND LDC FOR PLANT SUSPENSION CULTURES ON PARTIAL *g* OR HYPERGRAVITY RESEARCH

An alternative to clinostat/magnetic levitation that we have successfully used here is to immobilize the culture and use it as a solid object in other microgravity simulators, such as the Random Positioning Machine (RPM), or the conventional clinostats. These devices cannot be used for exposing to simulated microgravity cell suspensions in a liquid, since the fluid movements will greatly diminish the quality of the microgravity simulation (van Loon 2007). Such a solution will involve embedding cells in low-temperature gelling agarose to protect the flooding of cells in the absence of the shearing forces (Sieberer et al 2007, Sieberer 2009). We demonstrated that embedding cells in agarose does not alter the cell viability **(Figure 32)** compared with the standard shaking control.

The use of the RPM allowed us to simulate different partial gravity levels such as the Moon and Mars in addition to the simulated microgravity condition (real random mode). Two partial gravity paradigms were tested, one using software to modify the random speed and rotation angles, as called RPM^{SW} (operated by software) and the other using a centrifuge inside the RPM to create the partial gravity as called RPM^{HW} (RPM and centrifuge). Preliminary experiments using *Arabidopsis* cell culture (cell cycle distribution and nucleolar activity) reveal that there are no significant differences of using RPM^{HW} or RPM^{SW} for the Moon gravity level, while few differences appeared in the case of Mars ($0{,}37g$) RPM^{HW} simulations. Although more experiments should be done to completely discard any methodological effect on our data, due to the limited access to the GBF (not available in Madrid), we decided to exclude RPM^{HW} facility under Mars gravity, (we used the RPM^{SW} paradigm for Mars) and the available RPM^{HW} facility to recreate the Moon gravitational experience.

1.4. ADDITIONAL NOTES AND RECOMMENDATIONS ON THE USE OF ALTERED GRAVITY FACILITIES

It must be cited here that, despite the simulation artifacts already mentioned for the clinostat, magnetic levitation and partial *g* designs, which could reduce the quality and/or statistical meaning of the results, most of the experiments produced similar trends in terms of the decoupling of the cell growth and cell proliferation markers.

The use of clinorotation with *in vitro* cell cultures (cells in suspension) produced alterations in the cell proliferation and cell growth. While ribosome biogenesis (a marker of cell growth) was clearly downregulated by the clinorotation treatment, the interpretation of the increase in the proportion of cells at the G1 phase of the cell cycle is less clear. Accumulating cells in G1 could reflect a high rate of cell proliferation caused by an acceleration of mitosis and a quicker entry into the early G1 phase. This suggestion was supported with the low mitotic index value. On the other hand, the smaller nucleolus observed after 14h clinorotation is consistent with the decrease in the proportion of cells in G2 phase, which is known to have a large and active nucleolus (Gonzalez-Camacho & Medina 2006).

Magnetic levitation results are also complicated to interpret because of the unknown, but actual effects of the high magnetic field which is strongly acting on the samples (Manzano et al 2012c), even in the 1*g** internal control, and also due to the sedimentation of the cells which has been discussed above. Despite that, we have noticed decreases on the ribosome biogenesis (nucleolus area) and a decrease in the mitotic index. The impact on the cell cycle is not clear, due to the short term exposure.

Finally, RPM and LDC are validated as compatible with the use of plant cell suspensions, provided cells are immobilized by embedding in agarose. We obtained results consistent with previous root meristem and semi-solid culture (callus) data (Herranz et al 2013c, Manzano et al 2012a, Manzano et al 2012b, Manzano et al 2014, Manzano et al 2012c, Medina & Herranz 2010). This consistency of results has validated our system to further advance in the knowledge of the impact of gravity alteration on the functions of plant proliferating cells.

In summary, GBFs and simulated microgravity can be highly useful instruments to investigate the effective role of gravity on the biological systems. However, all these instruments involve the action of collateral forces (mechanical, magnetic) which overlap with the primary effect of simulating gravity alteration. The action of these forces synergizes with gravity alteration in the intensification of the gravitational stress condition to plant cells. Obviously, these additional stresses are not present in real microgravity conditions, in space (they actually exist, but causing by different factors). Although it may be difficult to exactly identify what effect is due to gravity alteration and what is due to collateral forces, the maximum effort should be made in this identification, in order to minimize the unwanted effects and to select the best procedures from this point of view. Investigations of purely microgravity effects should be performed in space, but mechanical and magnetic simulators could be used to study similar phenomena if we are able to distinguish the mechanical/magnetic effects from the gravitational effects in our biological systems.

A list of the capabilities of the different facilities to be used in plant biology experiments is summarized in **Table 15,** summarizing the different applicable use of the GBF simulators.

Table 15: Experimental design concerns and applicability of the Ground Based Facilities simulators. X means no available/compatible, + suboptimal use, ++ optimal use.

		Pipette clinostat	Magnetic levitation	RPM	Partial Gravity		LDC
					RPM^{SW}	RPM^{HW}	
Plant Biological materials	Plant Seedling	X	+	++	++	++	++
	Immobilized culture	X	+	++	++	++	++
	Suspension culture	+	+	X	X	X	X
Gravity level range		Sim µ*g*	0*g**-2*g**	Sim µ*g*	0*g*-1*g*		2*g*-*20g*
Other forces alterations		Shears Forces	Magnetic forces	Mechanical Forces		Mechanical/ Centrifugation	
1*g* control validation	External 1*g* control	+	++	++	++	++	++
	Internal 1*g* control	+	+	X	X	++	++
Exposure duration (Using plant cellular models)	Short-term (< 3h)	+	+	++	++	++	++
	Mid-term (3h < 14h)	X	+	++	++	++	++
	Long-term (> 24h)	X	X	++	++	++	++
Advanced implementation	Rapid Fixation	++	X	++	++	++	+
	Gas exchange	++	++	++	++	++	++
	Video record	X	+	+	+	+	++
	Microscope	X	X	X	X	X	++
	Incubators (various)	X	X	+	X	X	++
	Environmental control	+	+	++	+	+	++
Viability of use	BioLab nearby	++	X	++	++	++	++
	ESA Access	DLR	Radboud University	ESTEC-ESA	ESTEC-ESA	ESTEC-ESA	ESTE-ESA

2. SIMULATED MICROGRAVITY CAUSES CHANGES IN *ARABIDOPSIS* CELL DEVELOPMENTAL PROCESSES; CELL GROWTH, CHROMATIN ORGANIZATIONS, AND CELL PROLIFERATION

The use of immobilized cell cultures in RPM-based altered gravity conditions, combined with advanced flow cytometry techniques, have allowed us to confirm and extend previously described alterations in cell cycle and cell growth, crucial processes in plant physiology in space. Alterations in these processes caused by changes in the direction or the intensity of the gravity vector, as perceived by the plant, rely on mechanisms that take place at the cellular level. It is particularly remarkable the involvement of epigenetic mechanisms in the regulation of the changes induced by altered gravity on the processes of growth and development in plants (Ferl et al 2002, Herranz & Medina 2014, Medina & Herranz 2010, Perbal 2001).

2.1. PLANT CELL CYCLE PROGRESSION RATE IS INCREASED UNDER SIMULATED MICROGRAVITY CONDITIONS

After the description of the cell growth and proliferation uncoupling in the root meristem under spaceflight conditions (Matía et al 2010), a deeper analysis of the cell cycle perturbations in a large and homogeneous population of actively proliferating cells was pending. Here, we have adapted advanced flow cytometry techniques used in other biological model systems (Chehrehasa et al 2014, Li et al 2014, Mead & Lefebvre 2014, Spier 1991) to the *Arabidopsis* cell suspension cultures to study cell proliferation and cell growth in the absence of developmental and differentiation programs of seedlings. Cell cultures clearly represent a very useful system to investigate the cell cycle (Gould 1984), and its regulation under environmental cues. Their capability of synchronization allows us to better understand this process (Menges & Murray 2002, Menges & Murray 2006). Moreover, we combined DAPI staining of DNA during G1 or G2/M phases with an adapted reliable method for detection of the plant cells under DNA replicating phase (S phase) as a complementary useful method for determination of cell cycle status.

Preliminary experiments on asynchronous cell cultures showed that the distribution of cell cycle phases changes after mid- and long-term exposures to altered gravity. Results obtained from the distribution of the cell cycle population determined by means of flow cytometry reveal that cells are accumulated in S phase, passing to the G2/M gradually through the exposure time. Thus, a reduction on the population of cells in G1 is observed, probably because the cells are entering faster into the S phase **(Figure 33)**. Accumulating cells in S phase was confirmed by EdU labelling, suggesting a higher proliferation rate in simulated microgravity. These results are totally compatible with the acceleration of the cell cycle. However, it was noticed that this acceleration is accompanied with the disruption of some cell cycle regulators, such as cyclin B1. This alteration in the cyclin B1 is accompanied with the enhancement of the cell proliferation rate, which was also reported in *Arabidopsis* root meristematic cells (Manzano et al 2009, Manzano et al 2012c, Matía et al 2010) and in semi-solid cell cultures (Herranz & Medina 2014, Manzano et al 2014). Otherwise, increasing S phase subpopulation and decreasing the proportion of cells in G1 is totally compatible with the acceleration of the cell cycle, and it is also well-matched with a high level of the Prolifera antigen, expression (recorded both by quantitative estimation of the protein level and by the gene expression) through the progression of the exposure time. Up-regulation of Prolifera could accelerate the rate of cells passing through the G1/S transition, because Prolifera is an MCM complex protein which enters into the nucleus, binds chromatin and participates in the initiation of replication (Springer et al 2000). In fact, Prolifera is a homologue of Cdc47 (Mcm7) which is required for the initiation of DNA replication along with ORC (Origin Recognition Complex) during S phase (Dalton & Whitbread 1995). Cdc47 is the only MCM protein that interacts with the retinoblastoma (Rb) regulatory protein in human cells (Sterner et al 1998), suggesting that it plays a key regulatory role in G1/S transition (Tanaka et al 2007, Tsuji et al 2006).

More elaborated experiments, involving cell synchronization, were performed by arresting cells in late G1/S by a 24h treatment with aphidicolin. Sampling at different times during 72 hours after release of the drug allowed the isolation of different cell- cycle-phase-enriched populations to follow the progression of the cell cycle under simulated microgravity **(Figure 50)**.

In these synchronized cultures, increased cell cycle progression rate under simulated microgravity conditions was confirmed. First cell cycle was 3 hours shorter, due to the reduction

in the time required to reach the G2/M subpopulation peak (7 hours under simulated microgravity versus 10 hours under 1*g* control). Close examination of the microarray expression data for cell cycle core regulators of G2/M phase showed clear disruptions **(Figure 82)**. Cyclins B, which are thought to regulate the G2/M phase (Inze & De Veylder 2006, Menges et al 2002, Vandepoele et al 2002), showed a general downregulation while the alterations in cyclins A and D was not certain. Cyclins A/B/D associate with both CDKA and CDKB as part of the G2/M transition regulatory mechanism (Inze & De Veylder 2006). Downregulation of elements of the CDK-activating kinase pathway produces effects in controlling the activity of the distinct CDK/CYC complexes (Shimotohno et al 2004, Umeda et al 2005, Umeda et al 2000). Also, down-regulation of the WEE1 kinase, which is putatively involved in the inhibitory phosphorylation of CDKs (Sorrell et al 2002, Vandepoele et al 2002), promotes the acceleration of the G2/M transition; alternatively, the overexpression of WEE1 genes causes cell cycle arrest (Sorrell et al 2002, Sun et al 1999). Although cyclin B expression decrease is normally associated with a lower proliferation rate, our results showing enhanced proliferation rate with reduced levels of cyclin B can be interpreted by assuming that a shorter G2/M period will lead to less accumulation of the cyclin B messenger. Together with WEE1 expression, these data are supporting an "early" entry into M phase with the observed reduction in the cell growth.

On the other hand, an opposite alteration is observed in the G1 regulatory mechanism, where one hour is recovered compared with the control eventually producing a final delay of 2 hours in the entire duration of cell cycle **(Figure 82)**. Global analysis of the core cell cycle regulators in G1/S transition reflects a general upregulation of the D-type cyclins (CYCD) which are associated with the CDKA/CYCD complex through the G1/S transition (Inze & De Veylder 2006, Menges et al 2002, Vandepoele et al 2002), in contrast with the down-regulation observed in the G2/M subpopulation. The activation of the CDKA/CYCD complex requires the phosphorylation of the CYCD (Inze & De Veylder 2006) which it is upregulated by simulated microgravity suggesting a reinforcement in this G1/S transition checkpoint. This interpretation of the activation of the G1/S transition is supported by the upregulation of the E2F/DEL families which are associated with the S phase (del Pozo et al 2002, Menges et al 2005). Moreover, KRPs which can inhibit the activated CDK/CYCD complexes under stress (De Veylder et al 2001, Verkest et al 2005a, Verkest et al 2005b, Zhou et al 2003) are not altered under simulated microgravity in contrast with other types of abiotic stresses such as ABA and cold (Wang et al 1997).

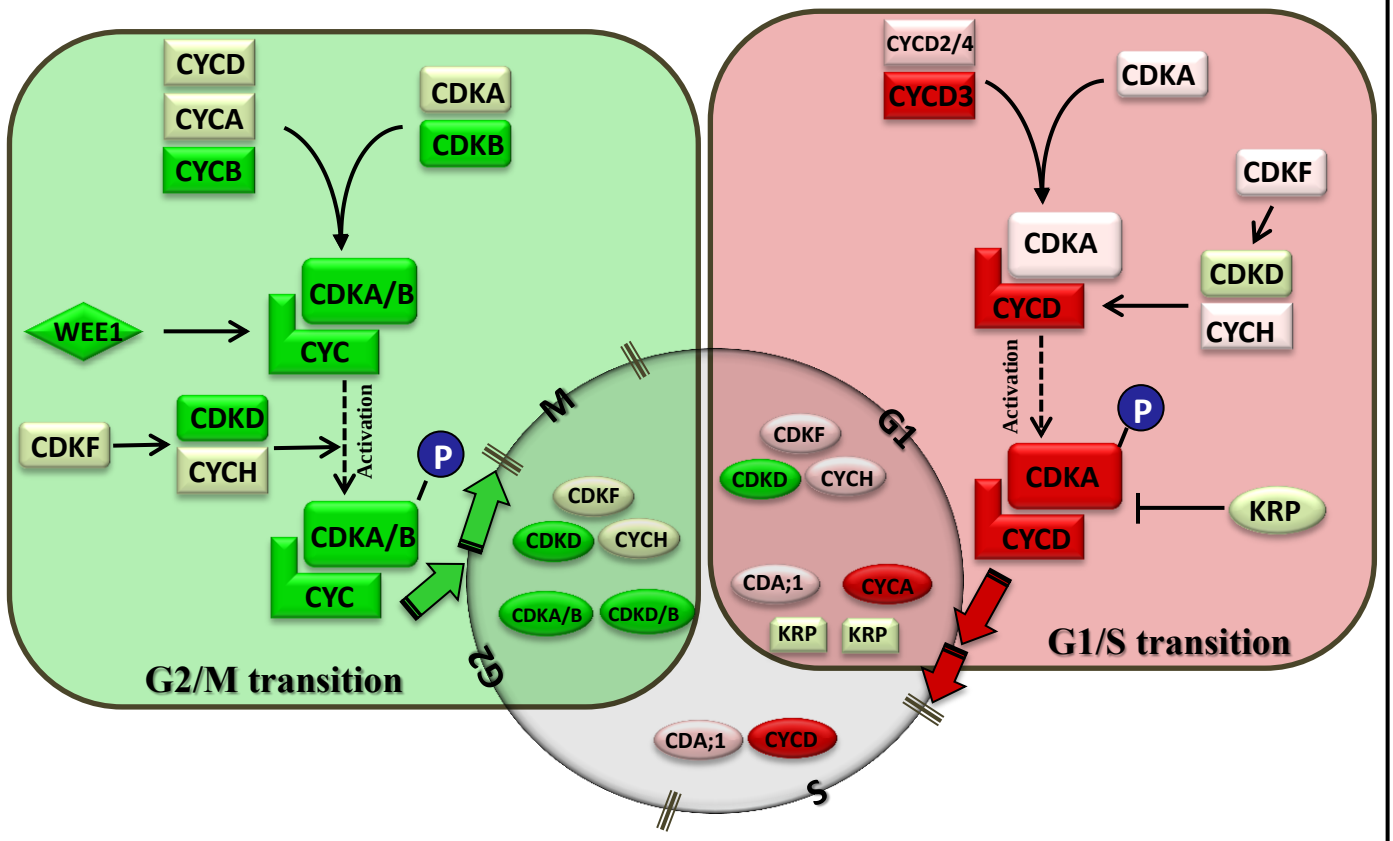

Figure 82: Schematic representation of the *Arabidopsis* cell cycle regulation under the simulated microgravity conditions based on the transcriptome data. Regulation of G2/M transition is disrupted under microgravity conditions: down regulations of the G2/M checkpoint regulators. During the G2 phase of the cell cycle, cyclins of the A, B, and probably D types (CYCA, CYCB, and CYCD) which associate with both CDKs of the A and B types (CDKA and CDKB) are downregulated. Therefore, the CDK-activating kinase pathway is negatively regulated, involving down regulation of the CDKF and CDKD associated with an H type cyclin (CYCH), disrupting the activity of the distinct CDK/CYC complexes. CDK activity can be negatively regulated by the WEE1 kinase, which is triggered upon loss of DNA integrity. On other hand, positively regulation of the G1/S transition regulators such as D type cyclins (CYCD) which associate with A-type CDK (CDKA), forming an inactive CDKA/CYCD complex. This complex is activated through the phosphorylation by the CDK-activating pathway, which involves CDKF and CDKD associated with CYCH support the positive control of the checkpoint. KRPs which can inhibit the activated CDK/CYD complexes is downregulated. Green color reflects the down regulation fold change, while, the red color reflects the up regulation gene expression. Green arrows refer to the acceleration speed through the checkpoints under the simulated microgravity conditions and in opposite the red arrow refer to the deceleration/checkpoint.

2.2. PLANT CELL GROWTH IS REDUCED BY SIMULATED MICROGRAVITY CONDITIONS

2.2.1. Revisiting the Relations between Nucleolus Morphology, Ribosome Biogenesis and Cell Growth under 1*g* Control

The nucleolus is a highly polymorphic structure, as it was classically described (Hadjiolov 1985, Smetana & Busch 1974). It has been largely established that the rate of ribosome biogenesis can be estimated throughout certain features of the molecular cytology of the nucleolus (Medina et al 2000, Sáez-Vásquez & Medina 2008, Shaw & Doonan 2005). In plants, different nucleolar morphofunctional models were identified for each one of the cell cycle phases in onions (Gonzalez-Camacho & Medina 2006). Here, we also defined different models corresponding to specific cell cycle phases in *Arabidopsis* taking the onion study as reference. Moreover, here we supported the correlation of the nucleolar morphology with the nucleolar activity, i.e. the rate of transcription and processing of ribosome precursors, taking advantage of characterized cell cycle phases. This has represented an advance in the nucleolus characterization as a reliable marker of cellular activities throughout different functional, (Goessens 1984, Hadjiolov 1985, Medina et al 2000, Risueño et al 1982, Scheer & Hock 1999, Shaw & Jordan 1995, Stepinski 2014).

Using selected subpopulations of cells from synchronous *Arabidopsis* cell cultures, it was noticed that different ultrastructural models for proliferating cells nucleolus could be associated with the cell cycle phases; G1 (compacted nucleolus model), S (double sized compacted nucleolus model) and G2 (triple sized vacuolated, and non-vacuolated models, **Figure 83)**. Furthermore, the usefulness of the adscription of the well-defined nucleolar structural patterns to each cell cycle phase (Grummt 2003, Klein & Grummt 1999, Kwiatkowska & Maszewski 1979, Raska et al 2004, Risueño & Medina 1986) allows a functional determination of the cell proliferation by nucleolus morphological features observed on the microscope.

- The nucleolus enlarges throughout interphase gradually, since the nucleolar size is double in S, and is almost tripled in G2 compared with the G1 size. This is different in onion, in which the nucleolar size is constant in G1 and S and almost doubled in G2 (Gonzalez-Camacho & Medina 2006). The main cause for the enlargement is the increase of the GC which grows first at the expense of diminishing DFC (in the S period) and then it grows to

becoming vacuolated (in G2). So on, enhanced nucleolar activity in S and G2 phases gradually correlated to the GC distribution (Hadjiolov 1985, Smetana & Busch 1974).

- The structure and morphometric parameters of FCs show a clear association with cell-cycle progression, which agrees exactly with the correlation of these features with nucleolar activity as previously defined (Medina et al 1983, Risueño et al 1982). As cell cycle progresses, the number of FCs increases and their individual size becomes smaller; structurally, heterogeneous FCs are present in G1 and they progressively disappear in S, so that the G2 nucleoli practically contains only homogeneous FCs.

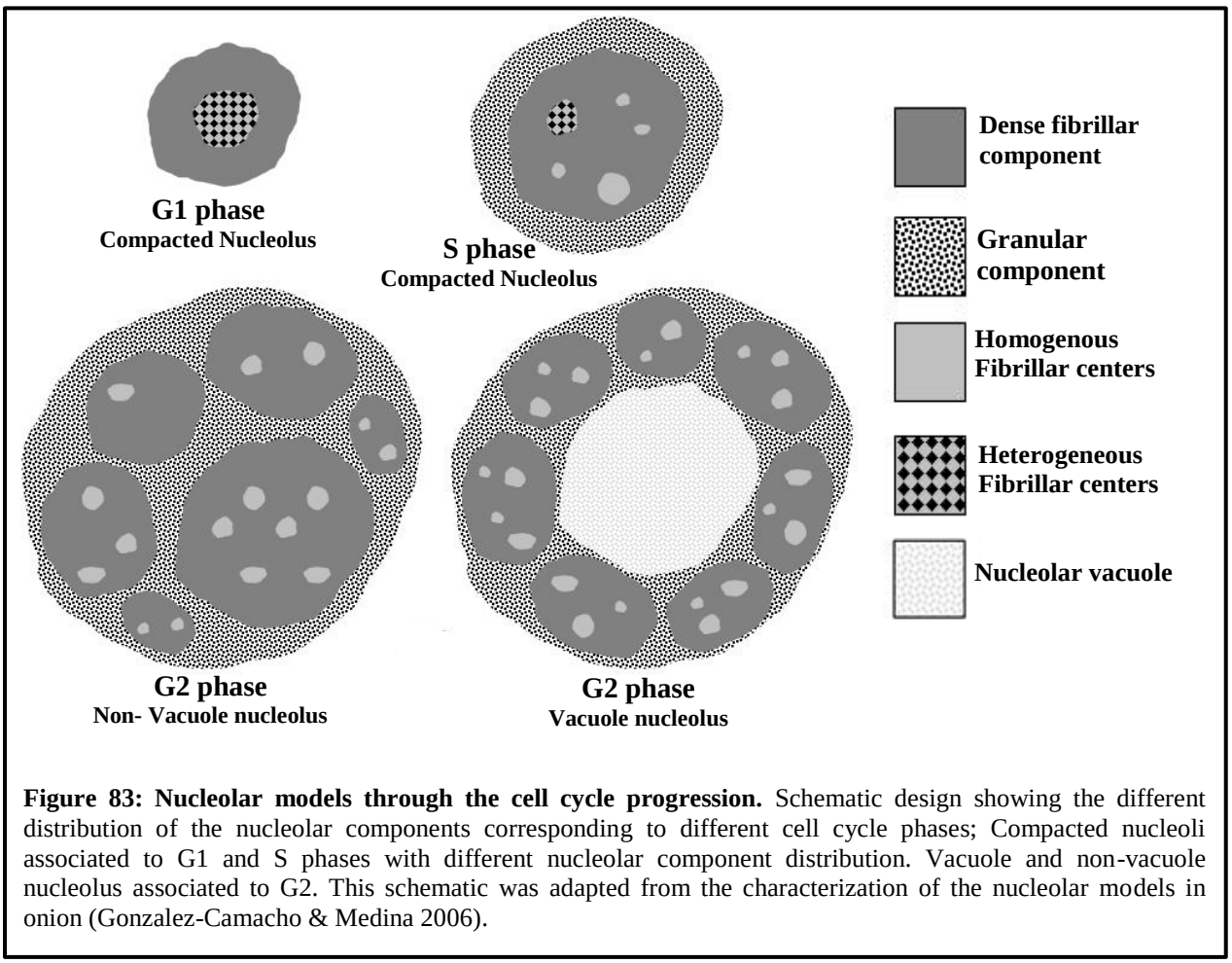

Figure 83: Nucleolar models through the cell cycle progression. Schematic design showing the different distribution of the nucleolar components corresponding to different cell cycle phases; Compacted nucleoli associated to G1 and S phases with different nucleolar component distribution. Vacuole and non-vacuole nucleolus associated to G2. This schematic was adapted from the characterization of the nucleolar models in onion (Gonzalez-Camacho & Medina 2006).

- Two different nucleolar models are characterized in the G2 phase, which is the most active phase: the vacuolated nucleoli, featuring a large clear internal space, or ‘‘nucleolar vacuole’’, and the non-vacuolated nucleolus. The G2 vacuole is large, regular in shape, disconnected from FCs, and containing granules either isolated or clustered. It is a structure closely associated with a high rate of nucleolar activity, as was demonstrated using functional tests (Morena-Dias de la Espina et al 1980). The non-vacuolated nucleolus contains a large amount of FCs among the other models in which related to the activity. Granules observed within the vacuole represent pre-ribosomes in the last stages of their maturation, ready to be exported to the cytoplasm.

In addition to the morphological characterization, the nucleolin and fibrillarin proteins have been quantified throughout the cell cycle to connect the models with the ribosome biogenesis **(Figure 57, 58)**. As expected for nucleolin, as a protein playing a crucial role in the nucleolus activity, the levels of this protein are increased gradually and significantly from G1 to S (double), and to G2/M (triple), similarly as described in onion (Gonzalez-Camacho & Medina 2006). However, the increments of the nucleolin level is S phase may be considered or linked to other cellular activities not related to the cell cycle progression (Durut & Sáez-Vásquez 2014, Srivastava & Pollard 1999). The same observation was noticed for the fibrillarin levels, which were constant in G1 and S phase and increased significantly three times in G2/M. Increments in the G2/M (the most active phase in the cell cycle) is correlated to the requirement of the cells in G2/M for an optimal protein synthetic activity in order to support cell proliferation (Srivastava & Pollard 1999), particularly the viability of the two daughter cells.

In summary, and pooling all the collected information about nucleolar activity, we present in **Table 16** the characterization of the cell cycle phases at 1*g* control conditions, confirming that the G2/M is the highest active phase in terms of cell growth through the cell cycle progression.

Table 16: Characterization of the cell cycle phases under 1*g* control conditions in terms of the nucleolar structure, ribosome biogenesis, and chromatin organization and Epigenetics. *(X) refers the same units in the comparison.*

	G1 phase	S phase	G2/M phase
Nucleolar Models	Compacted	Compacted	Vacuolated – non vacuolated
Nucleolar size	1X	2X	3X
Nucleolar activity	1X	2X	3X
Ribosome biogenesis (Nucleolin Level)	1X	2X	3X
Ribosome biogenesis (Fibrillarin Level)	1X	1X	3X
Chromatin remodeling	Decondensation	Decondensation	Condensation
DNA methylation	Lower	Lower	Hypermethylation
Histone acetylation	Acetylated	Acetylated	Deacetylated

2.2.2. Effects of Simulated Microgravity on Nucleolar Parameters

The nucleolar morphofunctional types described above, which were identified and characterized under the electron microscope in other plant cells (Manzano et al 2014, Stepinski 2014) could be easily identified by means of phase-contrast microscopy in samples exposed to simulated microgravity. A gradual effect was observed with the increase of the exposure duration to simulated microgravity; there was a strong significant decrease in the number of cells with vacuolated and compact nucleoli, at the expenses of an increase in the inactive fibrillar nucleoli, which was maximized after the long term experiment with the complete loss of vacuolated nucleoli compared to the 1*g* control **(Figure 37, 38, 39)**. These results are consistent with those reporting a decreased nucleolar area (using nucleolin staining as the major nucleolar protein); this parameter reached the strongest depletion after long term exposures, suggesting a decline in nucleolar activity due to gravitational stress **(Figure 34)**. These results are fully consistent with previous results of our laboratory using *Arabidopsis* semisolid cell cultures under simulated microgravity (Manzano et al 2014) and root meristems under real microgravity (Matía et al 2010, Matía et al 2005).

An additional value of our research work it is the applicability of our nucleolus morphofunctional model to the study of other environmental stresses. Multiple stressors often lead to reorganization of nucleolar architecture (Boulon et al 2010). The fast and detectable response of the nucleolus to changes in the cell condition is long known in different biological model systems, both animal and plant, and it is related to the key role played by the nucleolus in the functional activities of the cell (Raska et al 2006, Srivastava & Pollard 1999). In fact, the nucleolus and nucleolar activity have been identified as efficient and reliable indicators of cellular stress (Boulon et al 2010, Mayer & Grummt 2005). It is suggestive that the varied effects on ribosome subunit production and cell growth induced by different type of cellular stresses, such as microgravity conditions, are often accompanied by dramatic changes in the organization and composition of the nucleolus **(Table 17).**

Table 17: Nucleolus responses reported for several abiotic and biotic stresses			
Stress type	**Organ/tissue**	**Effect on Nucleolus**	**References**
Real microgravity	*Arabidopsis* seedling (Root meristem)	Changes in nucleolar morphology: small nucleoli, few large fibrillar centers Reduction in ribosomal biogenesis	(Manzano et al 2009, Matía et al 2010, Matía et al 2005)
Simulated microgravity (Magnetic levitation)	*Arabidopsis* seedling (Root meristem)	Small nucleolus size and changes in the nucleolar subcomponent	(Manzano et al 2013)
Simulated microgravity (Clinorotation)	*Lepidium sativum* seedling (Root meristem)	Nucleolar disruption and changes in proteome (NopA100 localization)	(Sobol et al 2005a, Sobol et al 2005b)
Simulated microgravity (RPM)	*Arabidopsis* callus cultures	Inactive nucleolus: small nucleoli with an increase in DFC with low FCs. Reduce ribosome biogenesis	(Manzano et al 2014)
Hypergravity (Magnetic levitation)	*Arabidopsis* seedling (Root meristem)	Small nucleolus size and changes in the nucleolar subcomponent	(Manzano et al 2013)
Hypergravity (LDC)	*Arabidopsis* callus cultures	Increase the nucleolar size with a general compacted nucleoli model	(Manzano et al 2014)
Salinity	Barley root	Nucleolar disruption: DNA degradation	(Katsuhara & Kawasaki 1996)
Heat shock	Animal cells	Nucleolar disruption with small nucleolus and CBs Reduction of rRNA transcription	(Handwerger et al 2002, Rubbi & Milner 2003)
Nutrient stress (Starvation)	Animal cells	Nucleolar disruption, Reduction in the ribosome biogenesis	(Hoppe et al 2009, Murayama et al 2008, Tanaka et al 2010)
Osmotic stress & UV alterations	Animal cells	Nucleolar is not altered, with a Cajal Bodies disruption	(Cioce et al 2006)
Hypoxia	Human & Animal cells	Nucleolar disruption, rRNA transcription reduction	(Mekhail et al 2006, Rubbi & Milner 2003)
Virus infection	Various plant viruses	Recruit nucleolar proteins such fibrillarin with re-organization of CBs	(Canetta et al 2008, Kim et al 2007a, Kim et al 2007b)

2.2.3. Ribosome Biogenesis is Disrupted by Simulated Microgravity

Regulation of ribosome biogenesis is specifically linked to factors controlling cell growth and proliferation, thus confirming that the major function of the nucleolus is the ribosome biogenesis (Medina & González-Camacho 2003, Volkov et al 2004). It should be reminded here that ribosome biogenesis it is also intimately related with cell growth, particularly in the case of actively proliferating cells in which most of the protein synthesis demands are related to the cell growth requirements to achieve a cell size compatible with cell division (Baserga 2007). In fact, it should not be confused the concept of cell growth when leading to cell division with the concept of cell enlargement as a cell differentiation requirement normally linked to extensive vacuolization (Doerner 2008, Li et al 2005).

In our experiments, quantitative analyses were performed to use nucleolin and fibrillarin as markers of ribosome biogenesis activity, using immunofluorescence approaches and qPCR for quantitative determination of the protein and gene expression respectively. In asynchronic cell cultures, nucleolin and fibrillarin protein levels remained constant under 1g but they decreased with the time-exposure to simulated microgravity **(Figure 40, 42)**. Moreover the alteration on nucleolin, with a wider range of known functions (Sáez-Vásquez & Medina 2008) is stronger than in the case of fibrillarin, with a more specific pre-rRNA processing role. The nucleolin protein decrease is supported by the significant downregulation of the AtNucL1 gene expression. Additionally, in this case, the alteration in the gene expression was quick, even in the short term experiment, compared with the reduction in the protein levels which reached significance only after 14 hours.

When using synchronic cultures and specific cell cycle phase subpopulations, it was found that G2/M phase subpopulation showed greater alterations under simulated microgravity. A depletion on the ribosome biogenesis proteins was noticed, expressed in the levels of nucleolin and fibrillarin. Neither S phase nor G1 phase subpopulations showed clear variations in the ribosome biogenesis maybe because of the short exposure to simulated microgravity of just 2h. Despite that, the low level of ribosome biogenesis was demonstrated by direct quantification of the nucleolar structural models, which detected an increase in the number of inactive nucleoli under simulated microgravity. Furthermore, this depletion on the ribosome biogenesis, whose levels are

correlated with the rate of functional activity of the nucleolus, was maximized in G2 phase of the cell cycle (Ginisty et al 1999, Gonzalez-Camacho & Medina 2006, Pontvianne et al 2007).

2.3. EPIGENETIC MODIFICATIONS IN THE CHROMATIN AS A PLANT SYSTEMIC RESPONSE TO SIMULATED MICROGRAVITY

2.3.1. Epigenetic Mechanisms of Plant Responses to Microgravity

The regulation of genes via cytosine methylation and histone modification is a well-recognized component of the plant responses to environmental stresses (Agius et al 2006, Chinnusamy et al 2008, Choi & Sano 2007, Zhu et al 2008). In our study using asynchronic *Arabidopsis* cell cultures, an increase in the overall cytosine methylation pattern was detected under simulated microgravity **(Figure 41, 42, 48)**. The results of DNA methylation, based on the immunofluorescence protein (flow cytometry and confocal microscopy) showed a quick and extensive hypermethylation of cytosine residues through different times of exposure to microgravity. This observation is consistent with the upregulation of DNA methyltransferase enzyme (MET1) expression detected in the microarray study, which is mainly involved in maintaining symmetric cytosine methylation and the plant specific CMT1 (Chromomethylase 1) **(Figure 72)**. This is in agreement with the reported DNA hypermethylation of tobacco and potato cell cultures in response to osmotic stress (Kovarik et al 1997, Sabbah et al 1995) as well as with the MET-1 upregulation in maize roots in response to cold stress (Steward et al 2000). Our interpretation is that DNA methylation could be involved in the regulation of gene expression in response to the gravitational stress as it happens, for example, with saline stress. It was reported that the hypersensitivity of *met1-3* to salt led to a massive failure in cytosine methylation at a putative small RNA target site. This subsequently led to lower expression of a sodium transporter gene (AtHKT1), which is essential for salt tolerance (Baek et al 2011).

Similarly, we analyzed histone acetylation, which was quickly disrupted by altered microgravity. The presence of the acetylated histone H4, estimated by quantitative analysis with the fluorescence microscope **(Figure 41, 48)** appeared depleted through the exposure time, thus indicating that simulated microgravity causes histone deacetylation. The involvement of plant

histone modifications in response to environmental stresses has been reported. Several studies from rice and *Arabidopsis* have shown that the histone is deacetylated under the drought and/or ABA stresses (Luo et al 2012b, Sridha & Wu 2006).

2.3.2. RNA Polymerase II Transcription as a Marker of Chromatin Remodeling

RNA polymerase II (RNA pol II), which is responsible for the synthesis of mRNA from protein-coding genes, has been the focus of most studies of transcription in eukaryotes (Roeder 1996). This active RNA pol II is recruited to gene promoters during transcription initiation and, consequently, its presence, detected at the microscope, only marks the areas of the chromatin that are active (decondensed). Immunofluorescence analysis, used to visualize and quantify the distribution pattern of the extranucleolar transcription by RNA pol II, showed an overall inhibition of transcription **(Figure 59)**. These results are compatible with the reduction of the cell growth activity and downregulation of the global transcription detected by microarrays under simulated microgravity **(Figure 60).** Moreover, inhibition of RNA pol II transcription is compatible with the disaggregation of the nucleolar structure (chromatin staining using DAPI fluorescence), chromatin condensation and dispersion of the chromosomal domains **(Figure 84)**. Thus, remodeling of the local chromatin, by means of changes between decondensed and condensed chromatin is associated with variations in RNA pol II transcriptional activity (Fedorova & Zink 2008, Naryshkin et al 2000, Sproul et al 2005, Van de Corput et al 2012, Wang et al 2014). This chromatin organization and remodeling, leading to condensation under microgravity conditions, is consistent with the observed epigenetic modifications; when the DNA is in a methylated state and histones are deacetylated as demonstrated above, chromatin is condensed (Phillips & Shaw 2008) **(Figure 84)**.

It must be noted that simulated microgravity is a unique and novel environmental alteration for cells, never faced before in the course of the history of evolution. As we have shown, the mechanism of transcription through chromatin remodeling, in response to environmental cues is disrupted in the case of the gravitational stress. Both, chromatin condensation and decondensation have been reported in the literature as components of the epigenetic responses to abiotic stresses: on the one hand, the chromatin containing the stress-responsive genes is decondensed, to facilitate the expression of these genes (Orphanides & Reinberg 2000); this is

also the case reported for low light (Cutler & Cheever 2000, van Zanten et al 2010, Yu et al 2009) and heat stress (Pecinka et al 2010, Santos et al 2011).On the other hand, the general epigenetic stress response of the most part of the genome involves gene silencing in a higher or lower degree, and this is correlated to chromatin condensation; for example, no chromatin decondensation was observed under freezing stress Thus, condensed chromatin due to the microgravity is consistent with the unique nature of the gravitational stress, and it is compatible with the low level of the ribosome biogenesis rate and the reduction of the global transcription.

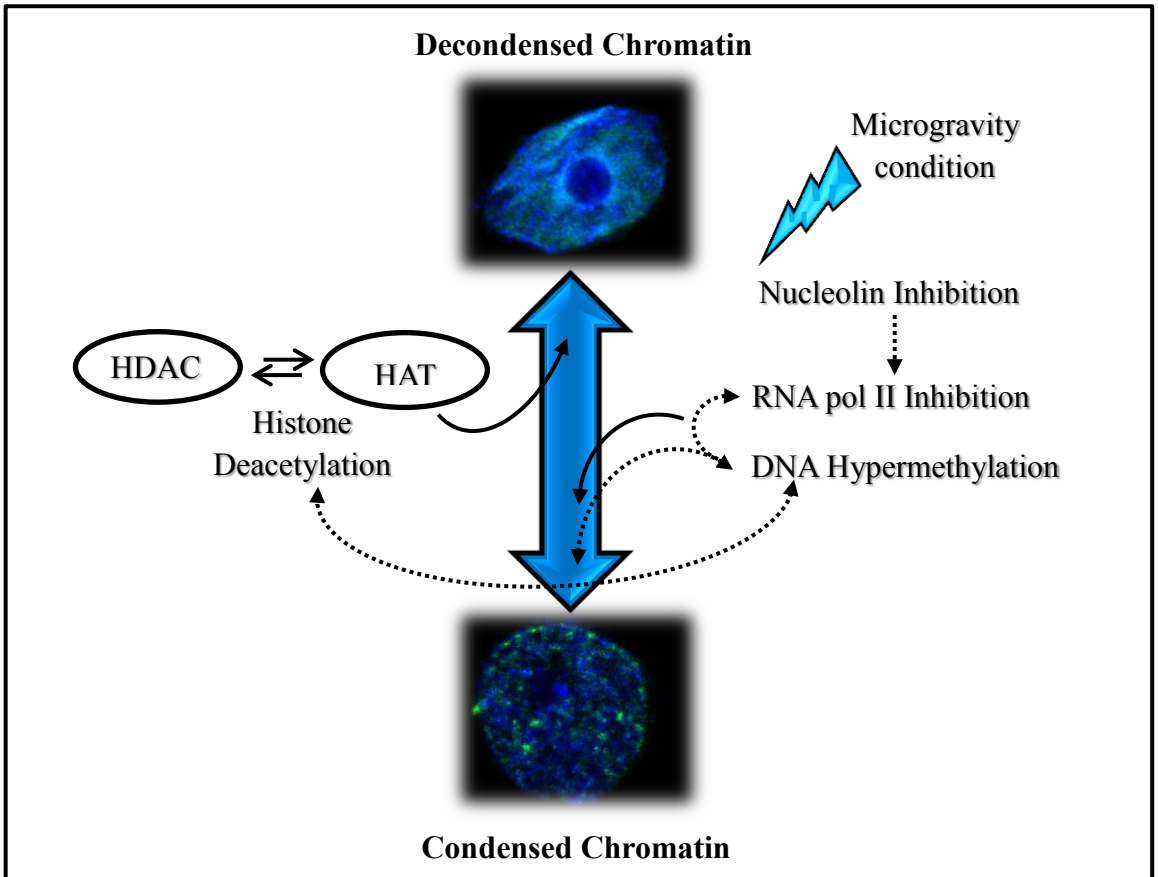

Figure 84: Schematic model for the mechanism of chromatin condensation and decondensation under simulated microgravity. Models for condensation and decondensation of chromatin, a determinant of transcriptional activity, involves enzymes for histone acetylation (HAT) and histone deacetylases (HDAC), DNA methylation, and RNA polymerase activity. Under simulated microgravity, DNA is hypermethylated and histone deacetylated in the presence of the low activity of the transcription through RNA polymerase II activity and altered with the nucleolin depletion lead to the chromatin condensation. This chromatin remodeling is reversible under changing environmental conditions.

2.3.3. A Chromatin Perspective of Plant Cell Cycle Progression

Cell cycle progression depends on a highly regulated series of events, of which transcriptional control plays a major role. In plant cells, in addition to the oscillating activity of various CDK-cyclin complexes (Inze & De Veylder 2006), more than one thousand genes show a cell cycle-dependent transcription profile (Menges et al 2003). This strongly suggested that transcriptional regulation is also of primary importance in plant cell cycle progression (Berckmans & De Veylder 2009).

As discussed in previous sections, changes in chromatin structure play a fundamental role in the regulation of transcription, since they control the accessibility of specific chromatin sites to the transcriptional machinery. As mentioned above, the major players of the changes in chromatin structure, responsible for the epigenetic regulation of gene expression are DNA methylation enzymes and histone modifications enzymes. Furthermore nucleolin depletion correlates with a low level of RNA polymerase I, since it is reported that depletion of nucleolin induces accumulation of RNA polymerase I at the beginning of the transcribed unit and reduction of the amount of UBF along the promotor and transcribed rDNA sequences (Cong et al 2012, Durut & Sáez-Vásquez 2014). Controlling nucleolin gene expression and association with rDNA chromatin (Pontvianne et al 2010, Pontvianne et al 2007) play a role in recruitment of chromatin remodeler activities that might activate or repress RNA polymerase transcription (Durut & Sáez-Vásquez 2014). Nevertheless, alterations in the nucleolin levels seems to be correlated with chromatin remodeling **(Figure 84)**, it is reported that Nuc1 mutant plants show rDNA chromatin decondensation (Durut et al 2014). Thus, nucleolin loss-function seems to trigger major changes in rDNA chromatin spatial organization, expression and trans-generational stability in plants (Durut & Sáez-Vásquez 2014).

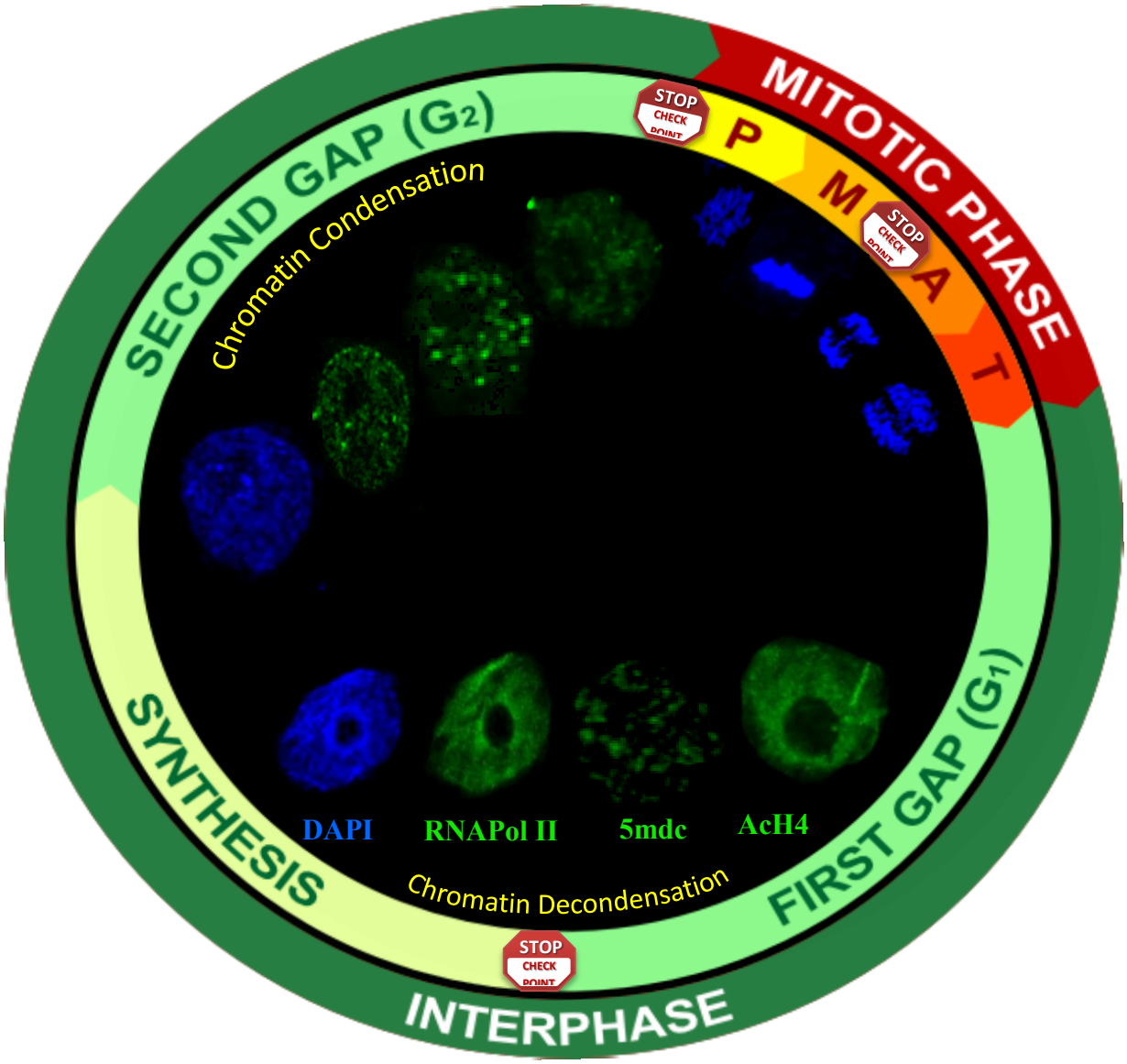

Figure 85: Interplay between chromatin remodeling and cell cycle progression. All steps of cell cycle progression from the initiation of DNA replication to mitosis depend on chromatin modifications. At the G1/S transition, histone acetylation is required for the specification and activation of replication origins with the active RNA polymerase II. During S phase, the chromatin structure has to be decondensed to allow fork progression, and to be reconstructed behind the fork. During the G2 phase, chromosome condensation is mediated by histone modifications such as deacetylation with the hypermethylation of DNA. This observation of the chromatin remodeling through the cell cycle is supported with the chromatin staining assay using DAPI staining. Examples of the chromatin status in a single cell at G1 and G2/M phases are extracted from our samples, as well as during Mitosis. Condensation/decondensation effects are even more visible under simulated microgravity.

We should raise the key question as to whether some of these chromatin changes can actually drive cell cycle transitions (Costas et al 2011, Sanchez et al 2008), as it has been shown in animal systems (Gondor & Ohlsson 2009, Liu et al 2010a, Probst et al 2009). In order to find an answer to this question, we pooled together the data from the immunofluorescence studies to visualize the chromatin patterns through the cell cycle phases subpopulations, namely DNA methylation (5mdc), Histone H4 Acetylation (AcH4), chromatin staining (DAPI) and the RNA polymerase II staining **(Figure 59, 61, 62)**, in addition to gene expression and protein levels during the cell cycle **(Figure 57, 58).** At 1*g* conditions, chromatin becomes locally decondensed in S phase, highly condensed during G2/M phase, and again decondensed before reentry into G1, as expected for the requirements of cell cycle phases **(Figure 85)**. Chromatin condensation during G2/M is temporally associated with a low level of histone H4 acetylation (Costas et al 2011, Green et al 2011, Xu et al 2009). On the contrary, the increments in the acetylation in G1 and G1/S transition cause chromatin decondensation. Otherwise, by means of the second epigenetic mechanism, heavily methylated regions of DNA are associated with chromatin condensation. This hypermethylation was noticed in G2/M and S phases, with a reduction in G1. Consistent with this, MET1 expression is upregulated at G1/S transition (Menges et al 2003). In an interestingly coordinated process, proteins that bind methylated DNA also form complexes with proteins involved in deacetylation of histones.

Under simulated microgravity, chromatin organization was severely affected through the cell cycle phases. Our first results with the asynchronic cell cultures demonstrated that chromatin was remodeled and specifically condensed in response to simulated microgravity. Consistent with this, MET1 expression is upregulated through the cell cycle progression, accompanied by a general downregulation of the Histone H4 acetylation over the cell cycle progression. The over-alteration was observed in the G1 phase, in which the microscope observation showed chromatin decondensation. Changes in histone modifications have been noticed to occur in G1 and G2/M under altered gravity, whereas histone kinases were increased in G1 and decreased in G2/M **(Figure 72).** The results of the genome-wide microarray experiment indicate that MET1, as well as the DNA methylation related CMT3 genes, are upregulated in both G1 and G2/M in conditions of simulated microgravity.

2.4. SIMULATED MICROGRAVITY DISRUPTS THE COORDINATION BETWEEN CELL PROLIFERATION AND RIBOSOME BIOGENESIS IN PROLIFERATING CELL SYSTEMS FROM BOTH SEEDLINGS (ROOT MERISTEMS) AND NON-DIFFERENTIATED CULTURE CELLS

Regulators of plant growth and proliferation are capable of activating key modulators of cell growth and cell division. Therefore, cell growth and cell proliferation are closely interconnected to one another in actively proliferating cells (Mizukami 2001). In this context, the effect of simulated microgravity on the *in vitro Arabidopsis* cell cultures has been demonstrated to be the disruption of the coordination between cell growth and cell proliferation; cell proliferation rate was enhanced, while the cell growth was depleted. The use of *in vitro* cell culture systems has several advantages in order to obtain a deep understanding of this phenomenon, such as the production of abundant biomass of proliferating cells, suitable for biochemical, genomic, and proteomic methods, in addition to the powerful flow cytometry applications, essential techniques for cell cycle studies, whose utilization is problematic in root meristems, where (especially in *Arabidopsis*) the number of proliferating cells is very limited.

It has been reported that the absence of gravity results in a similar uncoupling of cell growth and cell proliferation in seedling root meristems, which causes a disruption of the meristematic competence (Herranz & Medina 2014, Manzano et al 2012a, Manzano et al 2013, Matía et al 2010, Medina & Herranz 2010). It can be argued that the origin of this effect is the transduction of the gravitropic signal from the columella region, in the root tip, where it is sensed, to the elongation zone of the root, where the gravitropic stimulus results in the balanced or unbalanced elongation of cells. The mediator of the signal in the transduction process is the phytohormone auxin and the transduction pathway involves the root meristem **(Figure 86)**. For root gravitropism, gravity is sensed in specialized cells, called statocytes, through the movement of specialized amyloplasts called statoliths, according to the classical 'starch–statolith theory' proposed in 1928 (Cholodny 1928, Went 1928). Statoliths are capable of detecting magnitudes of the g vector lower than 10^{-3}. Under normal gravity conditions ($1g$), statoliths sediment in the bottom of the statocytes, indicating the direction of root growth. A change in the direction of the gravity vector leads to changing the root axis through the movement of the statoliths. If the gravity vector is absent (microgravity conditions) statoliths were observed to move towards the

central regions of the cell (Perbal et al 1987). Furthermore, in the case of starch-deficient mutants, lacking statoliths, they show a low level of gravitropism (Kiss et al 1998). The physical movement of the statolith sedimentation converts the mechanical signal into a chemical signal, capable of being transduced to the site where the gravity response is expressed. It was proposed that plant gravitropism is regulated through the statolith-actin cytoskeleton interaction (Blancaflor 2013, Kiss 2000, Nakashima et al 2014, Volkmann et al 1999), with the participation of mechanosensitive ion channels in the plasma membrane, especially Ca^{2+} (Baldwin et al 2013, Blancaflor & Masson 2003). Transduction of the mechanosignal involves the reorientation of auxin efflux carriers and subsequent redistribution of auxin streams in the distal regions of the root. These auxin changes were already proposed in the Cholodny-Went hypothesis. Furthermore, gravitational alterations produce inhibition of auxin polar transport with the consequent inhibition of growth and development (Miyamoto et al 1999a, Miyamoto et al 1999b, Muday & Haworth 1994, Oka et al 1995, Ueda 1999, Ueda et al 1999). Consequently, cell proliferation and cell growth alterations have been related with disturbances in auxin transport and distribution (Hoshino et al 2007, Medina & Herranz 2010, Miyamoto et al 2003, Shimazu et al 2003, Teale et al 2006), since auxin is an essential regulator of cell proliferation and cell cycle progression (Dudits et al 2011, Jiang & Feldman 2005, Jurado et al 2010, Magyar et al 2005).

Whereas a similar effect on cell growth and proliferation has been found in the root meristematic cells in seedlings and in cell cultures, it has to be noticed that *in vitro* cell cultures are not integrated into an organism possessing specialized mechanisms for gravity sensing. Therefore, the response to gravistimulus in cell cultures is autonomous in each individual cell, and it cannot be the result of the transduction of a signal from a more-or-less distant receptor organ (Herranz & Medina 2014, Herranz et al 2014). Thus, the gravity response in this system should rely on mechanisms compatible with the general properties of any cell in the plant. For example, graviresistance, the phenomenon that allows tree branches to support their own weight, has been considered to be based in cellular mechanisms including cell wall reinforcement in response to gravity. Unlike gravitropism, signal transduction in graviresistance does not involve different tissues or organs of the plant, but instead is intracellular. Thus, gravity resistance does not need to occur in specialized cells, but it may operate in several different cell types (Hoson et al 2005). The perception of gravity by this mechanism in the non-specialized cells is carried out through the gravitational pressure model of gravity sensing, using the mechanosensitive system located

on the plasma membrane (Staves et al 1997). Furthermore, reorientation of the cortical microtubules, which are responsible for structural stability of the cytoplasm and sustain various function of the cells, is involved in the graviresistance (Hoson et al 2010). Since there is physiological continuity between plasma membrane, cortical microtubules and cell wall, the signal transduction leads to an alteration in cell wall rigidity as final response. In parallel, signal transduction reaches the nucleus and induces the expression of different genes, influencing the structures and function of various membrane components (Hoson et al 2010, Hoson et al 2005).

Although the graviresistance mechanism is not experimentally supported to be responsible for the response of the *in vitro* cell culture to the gravitational alterations, causing disruptions in cell growth and proliferation, it is true that it is compatible with the results obtained in our study, especially in the absence of the gravitropism hypothesis. Actually, gravity resistance is a unique mechanism that is experimentally supported and provides an explanation for the detection, transduction and response to gravity signals of general application to all kinds of plant cells. Certainly, the gravity vector is an environmental factor of widespread influence in many cellular activities, apart from the direct effect that its absence or alteration may cause on specific processes such as those investigated in this work. It must be reminded here that cell polarization is an event influencing a plethora of cellular processes and the term "polarity" is intimately associated with the existence and influence of a gravity vector. Therefore, together with the known processes of gravity response, such as gravitropism and graviresistance, it cannot be excluded the existence of a general gravisensing mechanism, unknown at this moment, which could give account of all these cellular processes involving cell polarity in a higher or lower degree.

Therefore, since similar effects, recorded in both root meristematic and *in vitro* cultured cells, could be obtained via different mechanisms, including unknown ones, we are unsure about how much each one of the mechanisms is contributing to the final effect in each system **(Figure 86)**.

In this context, this research line seems to be exciting and very promising. Mechanisms of gravisensing and graviresponse in non-specialized cells must be experimentally demonstrated, and the differences and similarities with mechanisms supporting gravitropism, as well as the existence of possible synergies and crosstalks between the different pathways, should be investigated in the coming future.

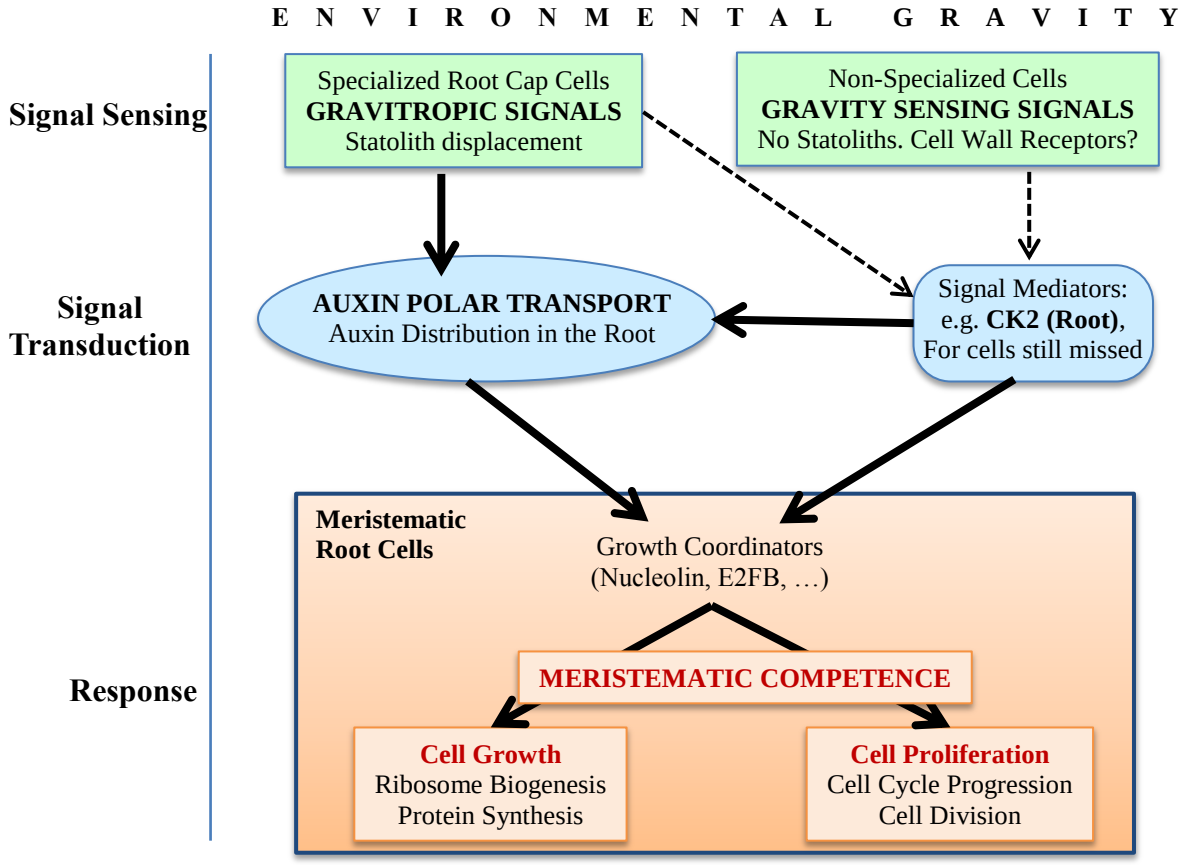

Figure 86: Schematic model of the main factors and functional processes playing a role in the regulation of the functionality of meristematic cells (meristematic competence, i.e., the coordination between cell growth and cell proliferation) by environmental gravity. Solid arrows represent experimentally supported connections, whereas dashed arrows indicate suitable processes, compatible with experimental data, but still pending of further investigation for their demonstration. The scheme is based on a previously published model (Medina & Herranz 2010). Sensing of the parameters of the gravity vector (magnitude, direction) may occur in different cellular types of the root by different mechanisms. In cells of the columella, in the root cap, gravity induces displacement (sedimentation) of statoliths, which is a requisite for establishing the gravitropic growth of the root. In fact, those environmental alterations which do not change the statolith position do not result in gravitropic changes. Gravitropic signals are transduced from the root cap to other regions of the root, resulting in alterations of the auxin polar transport. The mechanism of transduction of this signal is not totally understood and not all the mediators of this process have been experimentally identified. However, it is well known that the levels of auxin in root meristematic cells regulate the rates of cell growth and proliferation and establish the close coordination of these functions, that is, meristematic competence. In root cells other than columella cells, gravity can be sensed by mechanisms different from the statolith sedimentation. This alternative mechanism of gravity sensing can also be functional in proliferating *in vitro* cultured cells. Interestingly, in absence of statolith displacements, the effects of gravity alteration on cell growth and proliferation also produce the disruption of meristematic competence. Furthermore, this effect may occur in absence of any alteration of auxin levels, as it is the case of cells in culture. Whereas cell wall has been proposed as a gravity receptor (Hoson et al 2005), mediators of the transduction of gravity mechano-signal sensed in this way are experimentally unknown. The protein kinase CK2 is proposed as a candidate to be part of this scheme in view of the experimental findings that put it in close relationship with some physiological and cellular processes involved, such as auxin polar transport, ribosome biogenesis and cell cycle.

3. IMPLICATIONS OF THE ALTERATIONS OF CELL DEVELOPMENTAL PROCESSES IN *ARABIDOPSIS* FOR SPACE EXPLORATION

After previous sections of the discussion, which have been devoted to our contribution to proper use of simulated microgravity facilities for plant cell cultures, and to the basic science about the cell developmental processes affected by simulated microgravity respectively, we would like here to discuss the implications of our research for the development of the space exploration programs, either currently ongoing or projected at middle term. The most important of these programs deals with Mars exploration by the human being, including or not a previous step in the Moon. The main space agencies of the world have shown a great interest in this objective for the following decades. Therefore, it will become increasingly demanded to provide sustainable life support systems, including plants, not only as a source of food for space travelers, but also as a psychological reminder of the life on Earth. Our work will support these efforts by increasing our knowledge on plant responses and adaptation to spaceflight conditions (microgravity), but also to the gravitational loads expected to occur in the Moon ($0{,}17g$), Mars ($0{,}37g$) and even extrasolar planets more massive than the Earth (for example, $2g$).

3.1. ADAPTATION TO ALTERED GRAVITY CONDITIONS

Our preliminary experiments with asynchronous cultures included several exposures of different durations in the altered gravity environment in order to detect the minimum duration of the environmental disturbances capable of affecting the plant cell growth and/or cell proliferation functions. These experiments will also provide a preliminary approach to the process of adaptation to altered gravity in plants. Our results reveal that short term exposure (3 hours) is not enough to significantly alter the cell cycle, while mid- and long-term exposures produce increasingly important alterations affecting most of the observed parameters. Despite that, some exceptions have been found in which the long-term treated samples (24 hours) showed an effect weaker than those treated for 14 hours, suggesting that an adaptation process may appear as soon as one day after exposure to microgravity. The most clear example of these effects was observed in the transcriptomic study using synchronous cultures, that revealed a rapid response to

alterations on the synchronous G2/M samples after only 7 hours of exposure, while this alteration is less important on the 14-hour samples (synchronous G1 and asynchronous 14 hours), despite they have been primarily associated with G2/M greater sensibility to altered gravity. Furthermore, the large number of upregulated abiotic-stress-related genes in the synchronous G2 sample, which later appear downregulated in the 14-hour samples might support this idea of a preliminary abiotic stress response, followed by progressive cellular adaptation to changing environmental gravity.

3.2. RESPONSE UNDER PARTIAL GRAVITY (THE MOON AND MARS) CONDITIONS

Since international space agencies have declared the manned exploration of the Moon/Mars as one of their long-term goals, it is important to understand plant biology at the Moon ($0.17g$) and Mars ($0.37g$), as plants are likely to be a part of bio-regenerative life-support systems on these missions.

The results of our experiments using partial g RPM^{HW} ($0.17g$), RPM^{SW} ($0.37g$) have revealed that partial gravity conditions produce a decoupling of the cell growth and cell proliferation (depletion of cell growth and enhancement of cell growth). These alterations are similar to those of simulated microgravity, as a part of a common reduced gravity response. A disruption of the cell cycle progression has been demonstrated, according to the flow cytometry data **(Figure 33)**. It consisted of rapid increments in the S phase subpopulation in both the Moon and Mars conditions after short-term exposure, followed by a quick progression through G2/M phases. Otherwise, the decrease in the proportion of G1 cells is totally compatible with an accelerated cell cycle rate. These results are supported by the EdU labelling determination of S phase subpopulation, which showed significant increments in the proportion of cells in S phase **(Figure 35)**. Furthermore, in this context, it is noticed that the cell cycle regulator mechanisms are altered. Particularly, we found a decrease in cyclin B1 protein after mid-term experiment **(Figure 40)**, but, a clear increase was detected in the long- term experiments in both Mars and the Moon conditions. This increase in cyclin B1 levels was associated with the higher proportion of cells in G2/M in those samples. Furthermore, increased level of Prolifera is consistent with a cell proliferation enhancement and correlated with the increased proportion of cells in S phase.

Moreover, it is noticed that the level of Prolifera returns to normal values after the long-term exposures, suggesting the beginning of the adaptation process on the acceleration of the cell cycle after 24 hours.

Concerning partial gravity effects on the depletion on the cell growth, the expression levels of the ribosome biogenesis proteins, nucleolin and fibrillarin, showed a gradual depletion on the expression level, compared to the effect of longer exposures, reaching significance for nucleolin only after long-term exposures to Mars gravity. Nucleolar activity was progressively reduced (higher proportion of inactive and compacted nucleolus) with the exposure time, being consistent also with the observed progressively smaller size of the nucleolus. Moreover, it was observed a depletion of the proportion of vacuolated nucleoli, considered as the most active nucleoli (Gonzalez-Camacho & Medina 2006, Manzano et al 2014). Despite the higher proportion of cells in G2/M phase after long-term exposure, the proportion of vacuolated nucleoli (which is normally correlated to the rate of G2/M cells) was reduced under Mars conditions and even more severe effects were observed in the Moon gravity samples. These results support the existence of low-active nucleoli even it is located in G2/M phase, so suggesting a strong reduction in the cell growth activity despite the increased cell proliferation rate.

Regarding the chromatin organization and remodeling under partial gravity alterations, it was observed an increased DNA methylation activity with a reduction of the Histone H4 acetylation **(Figure 41, 46)**. These results are supported by the activity of the methyltransferase enzyme **(Figure 42)**. It seems that the chromatin is more condensed due to the partial gravity conditions, thus showing a lower level of transcription. This low level of transcriptional activity is also consistent with the reduced nucleolar activity and ribosome biogenesis.

3.3. RESPONSE UNDER EXOPLANETS HYPERGRAVITY CONDITIONS

Although a lot of research efforts have been dedicated to microgravity research, hypergravity is an avoidable partner in this endeavor. On the one hand, a space trip to other planet will involve a change from low gravity (spaceflight) to higher gravity conditions (0 to $0.37g$ at landing on Mars and 0 to $1g$ when returning to Earth, for example). On the other hand, several exoplanets compatible with human life could be more massive than Earth (for example, $2g$). Therefore, it is

highly advisable to b**e** capable of detecting the effect of hypergravity on the biological systems throughout the use of LDC (2g). In general, we have corroborated that the processes of cell growth and proliferation are altered under hypergravity conditions in the opposite direction and with lower intensities than under reduced gravity conditions including microgravity and partial gravity. The same effect of hypergravity was previously observed in both seedlings and semi-solid cell cultures (Manzano et al 2012a, Manzano et al 2014). Most of the alterations in the regulatory mechanisms of the cell cycle we have found are weak and not clear, cyclin B1 and Prolifera for example. Flow cytometry data shows a lower rate of the cell proliferation, increased cells in G1 phase with a reduction of cells in S phase supported by the EdU labelling cells. Moreover, EdU labelling S phase cells suggests a reduced subpopulation in S phase at any time, supporting the hypothesis of a decreased cell proliferation rate. Furthermore, flow cytometry data show expected results after mid-term exposure showing enhancement of S phase with a reduction of G1 phase.

The results on the expression levels of cell growth regulatory genes suggest an enhancement of the cell growth and ribosome biogenesis activity. Significant upregulation of the nucleolin gene and protein expression is accumulated with exposure time. The same results are confirmed by our second ribosome biogenesis marker, fibrillarin. This enhancement of the ribosome biogenesis activity is supported with increased frequency of vacuolated nucleolus after mid-term exposure followed by completely lost of the vacuolated nucleoli at the expenses of the compacted and inactive models later. Reduced G2/M subpopulation and enhancement of the G1 cells proportion was observed. Meanwhile, the nucleolar activity measured by the nucleolus area is not altered.

Furthermore, hypergravity conditions did not caused clear chromatin remodelling and epigenetic modifications. Immunofluorescence results reveal there are no alterations on the chromatin organizations. Furthermore, response of DNA methylation is not clear, despite of the hypermethylation observed after long term exposures, no accompanying reduction in histone acetylation was detected.

In conclusion, these results **(Table 18)** suggest that different altered gravity environments are a serious stress on the plant cell, capable of uncoupling cell proliferation and cellular growth which mandatory for the plant cell physiological processes in Earth.

Table 18: Summary of the results obtained in exposing *Arabidopsis thaliana* (cell cultures) to altered gravity as the one expected on Spaceflight (Microgravity), the Moon (0.17*g*), Mars (0.37*g*) and Exoplanet i.e. Tau Ceti e (Hypergravity, ~2*g*).




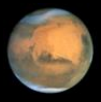
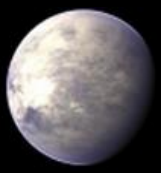

		Microgravity	The Moon	Mars	Tau Ceti e
Cell proliferation *(Enhanced)*	Cell cycle	**altered**	**altered**	**altered**	**altered**
	Cell proliferation rate	++	++	+	-
	S phase	++	++	++	-
	Cyclin B1	--	--	--	**no**
	Prolifera	++	++	++	**no**
Cell growth (Ribosome Biogenesis) *(Depleted)*	Nucleolar Models	**Inactive**	**Inactive**	**Inactive**	**compacted**
	Nucleolar Size	--	--	--	**no**
	Nucleolin Levels	--	--	--	+
	Fibrillarin Levels	--	--	--	+
Transcription *(Depleted)*		--	**Not applied**	**Not applied**	**Not applied**
Chromatin & Epigenetics *(Altered)*	Chromatin organization	**condensation**			
	DNA methylation	++	++	++	++
	Histone Acetylation	--	--	--	--

3.4. DEVELOPMENT OF NEW MATERIALS TO BE USED IN FUTURE SPACEFLIGHT EXPERIMENTS

There are strong scientific and engineering justifications for support the analysis of the effects of the spaceflight environment and the adaptation of biological systems in real time. New cellular materials allow the fluorescent imaging *in vivo*, which offers the ability to monitor biological functions, in this case biological responses to space-related environments. Particularly, we have used previously established transgenic lines that express a GFP protein under the control of AtNuc-L1 or Cyclin-B1 gene promoters to induce the formation of a cell callus with the same properties.

This methodological improvement will allow our lab in the future to provide a future cell culture experiment on Spaceflight using any mutant or GFP markers. More recently, modern molecular techniques have made available a range of fluorescent molecules that can be incorporated as genetic reporters of specific and wide ranging biological responses to stimuli/stress (Zhang et al 2002). These responses can be characterized and followed through the use of *in vivo* detection imaging and they are potentially usable in both simulated and real microgravity research.

4. IMPLICATIONS OF *ARABIDOPSIS* CELL DEVELOPMENTAL PROCESSES ALTERATIONS FOR LIFE ON EARTH

Since the developmental processes we are studying are fundamental to any cellular life, and animals and plants rely cell proliferation and cell growth control in similar mechanisms, we will try to elaborate in this final chapter the possible implications of our findings in other research fields. First of all, in the related field of sustainable agriculture under suboptimal (abiotic stress) conditions on Earth, secondly in the clinical area including pathological conditions as cancer or aging diseases.

4.1. CELL CULTURE SYNCHRONY, BY-PASS OF CHECK POINTS AND CANCER THERAPY

One of the most important results in this work is the finding of altered accelerated cell progression rate under reduced gravity conditions (Simulated microgravity, the Moon, and Mars), particularly during the G2/M phases of the cell cycle **(Figure 50)**. This was possible due to high quality synchronization using Aphidicolin and the validation of the synchronous cultures as a very useful system to investigate the cell cycle providing material representative of specific cell cycle phases (Gould 1984, Menges & Murray 2002). In opposition, we found that cells need more time to enter to the G2/M phase under hypergravity conditions compared with the control conditions. This acceleration on G2/M phase under hypogravity conditions is explained by a losing G2/M checkpoint control, as analyzed under microgravity conditions **(Figure 82)**. This data reveal that cell cycle is accelerated under hypogravity conditions providing high level of cell proliferation, while it is decelerated under hypergravity and become slowly providing a lower rate of cell proliferation. These results surely are connected with the requirements of cells growth a smaller size is required under reduced gravity and a larger size is shown under hypergravity.

More than that, we followed the second and third cell cycles to evaluate possible adaptations in the duration of the cell cycle and the subpopulation of cells synchronized **(Figure 87)**. It should remain clear that the reduced sampling and progressive desynchronization of the culture made obscure our data, nevertheless we estimated the cell cycle duration depending on the distance from first S phase peak to the following S phase peaks and the preservation of synchronization or the reduction in the percentage of cells synchronized in those peaks or the surrounding values.

Under 1*g* control conditions, the synchronization is quickly lost barely observable in the second S phase peak first cell cycle as expected from literature (Gould 1984, Menges & Murray 2002). This quick desynchronization could be related with a 2-3 hours delay imposed to different cells in the culture as a checkpoint requirement. Moreover, according to this quick desynchronization under control conditions, we extrapolate that the following cell cycles might be completely asynchronous.

Under simulated microgravity conditions, it is observed a gradual desynchronization. We suggest that there is a relaxation in the G2/M checkpoint after 7 hours of synchronization allowing the synchronous cells to define and enter into a new cell cycle rapidly, but with a lower size. So less delay at the checkpoint allows a high chance of preservation of the synchronous cells. These synchronous cells desynchronize slowly in any following cell cycle. Despite of the rapid acceleration of the cell cycle due to the disruption of the G2/M checkpoint, the duration of the cell cycle is similar compared with the control conditions. It is clearly supporting the idea of adaptation, in which cells extend the duration of G1 phase in the next cell cycle to allow a certain recovery of the size control, even more, up or down regulating the expression levels of the cell cycle controller genes at the checkpoints in comparison with the control condition.

Under the moon conditions we have detected the most severe effect, nearly complete preservation of the synchronization is noticed (exactly 45% of cells in the two sampling points surrounding the two S phase peaks, so we estimated that the peaks were just in the middle of the chosen sampling times, **Figure 87** dotted line peaks), due to the acceleration in the cell cycle rate. Moreover, cell cycle duration is similar to the control conditions but G2/M phase was even shorter than under simulated microgravity. We hypothesize that in this low gravity conditions the G2/M phase checkpoint is completely released, so there is not possibility of short term adaptation to the moon conditions, even if the G1 phase checkpoint delay the entry into S phase. Previous results of our group using 0.1*g** in magnetic levitation experiments already suggested that deeper effects could be expected, probably by a mixture of contradictory signals in the overlapping gravitropism (probably activated already) and graviresistance (probably deactivated yet), although this should be evaluated in seedlings. An alternative explanation is in connection with the complex forces and stresses acting on the cells under this partial g simulated conditions (RPM^{HW}) including centrifugation, mechanical forces, RPM rotation, in addition to the synchronization.

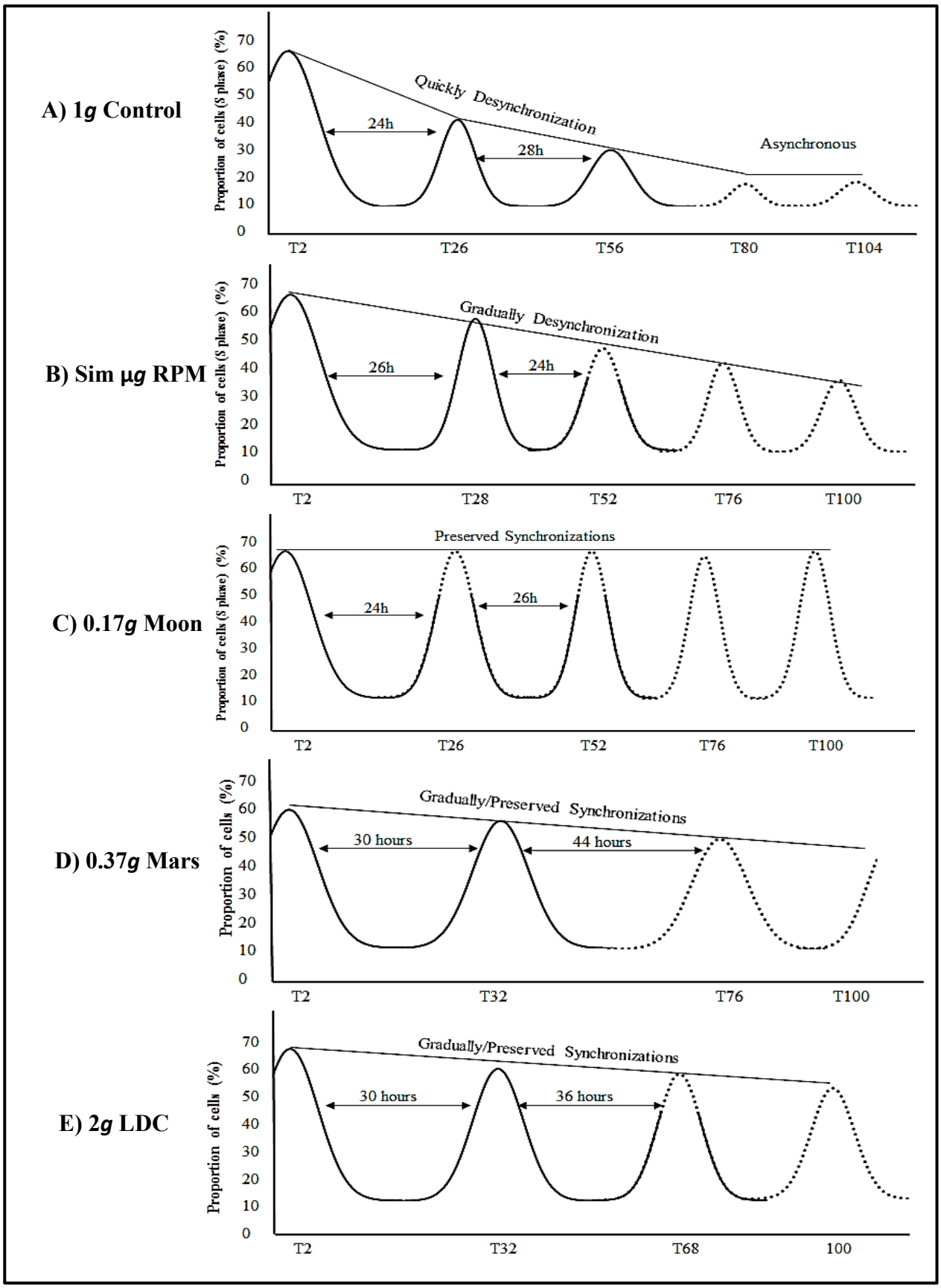
A) 1g Control
Proportion of cells (S phase) (%)
70
60
50
40
30
20
10
0
Quickly Desynchronization
24h
28h
Asynchronous
T2
T26
T56
T80
T104
B) Sim µg RPM
Proportion of cells (S phase) (%)
Gradually Desynchronization
26h
24h
T2
T28
T52
T76
T100
C) 0.17g Moon
Proportion of cells (S phase) (%)
Preserved Synchronizations
24h
26h
T2
T26
T52
T76
T100
D) 0.37g Mars
Proportion of cells (%)
Gradually/Preserved Synchronizations
30 hours
44 hours
T2
T32
T76
T100
E) 2g LDC
Proportion of cells (%)
Gradually/Preserved Synchronizations
30 hours
36 hours
T2
T32
T68
100

Finally, under Mars and hypergravity conditions, synchronization is partially preserved (similarly to the simulated microgravity samples) but a wide duration of the cell cycle phases is observed. Under hypergravity, the wide cell cycle could be easily associated to the long duration of the first cell cycle, so cells take more time to pass from phase to phase due to larger size observed. Precisely because there is a delay in the cell cycle progression forced by the additional requirements of cell growth, a higher synchronization should be lost in the long term. In contrast, the first cell cycle under mars conditions, display a short duration of the G2/M phase as expected for the acceleration on the cell cycle rate under reduced gravity, but the duration of the G1 phase to arrive next S peak seems to be extremely large, even larger in the second cycle versus the first one. Although it is very hard to provide an interpretation to this result, that will require additional experiments to be done and proper validation of the RPM^{HW} and RPM^{SW} facilities, it is clearly encouraging the increasingly use of the Mars conditions in future experiments. Apparently, a mixture of signals is completely confusing the cell cycle checkpoints, and consequently arresting as much as possible the cell cycle progression. But we still need more experiments focusing on the specific checkpoints samples in the successive cell cycles to distinguish the adaptation process, beside to extend the sampling time to recover the key samples.

The implications of our discoveries related to the study of the eukaryotic cell cycle in altered gravity conditions have the potential to be used on Earth in the treatment of cancer, and the cell cycle mechanisms can serve as targets in drug discovery (Blagosklonny 2001). Blocking a cell from passing through any of its phases will stop the cell from replicating. This is important in the study and treatment of cancer since it is desirable to find ways to block the replication of cancer cells without perturbing normal cells. In addition, meaningful representations of the data need to be extracted to facilitate the effective screening of different cell cycle inhibitors.

Figure 87. Representation of the differential preservation of synchrony during cell cycle progression (proportion of cells in S phase) under exposure to altered gravity for 72hours. **A)** 1*g* control, **B)** Simulated microgravity, **C)** the Moon, **D)** Mars, and **E)** 2*g* hypergravity. Baseline connecting the S phase peaks suggests differential desynchronization rates for each g level. Continuous line refers to the experimental data be are confident enough, while dotted line represents uncertainties due to disperse sampling or just extrapolation of the results (more than 72 hours). The estimated duration of the first two cell cycles (S to S peak) is shown.

Superficially, the connection between the cell cycle and cancer is obvious: cell cycle machinery controls cell proliferation, and cancer is a disease of inappropriate cell proliferation. Fundamentally, all cancers permit the existence of too many cells. However, this cell number excess is linked in a vicious cycle with a reduction in sensitivity to signals that normally tell a cell to adhere, differentiate, or die. This combination of altered properties increases the difficulty of deciphering which changes are primarily responsible for causing cancer. Clearly, the products of cell cycle regulatory genes are critical determinants of cancer progression.

On the other hand, researchers show that cancer cells which are aggressive on earth are considerably less aggressive in microgravity. Understanding the genetic and cellular processes that occur in space could allow the development of treatments that accomplish the same effect on Earth (Becker & Souza 2013, Ma et al 2014). Based in our results under microgravity conditions, it seems that the cell cycle control is nearly lost under altered gravity. Disruption on the cell cycle checkpoints regulators core is observed in cancer, allowing the cells to increase the replication rates such had occur under microgravity conditions (Collins et al 1997, Funk & Kind 1997). By understanding the genetic and cellular processes that occur in space loosing of the cell cycle controls to increase the cell proliferation rate, could we define the genetic changes that cooperate to accomplish the cancer cell's escape from the normal balance of cell growth?

4.2. UNIQUE RESPONSES TO A NOVEL SUBOPTIMAL ENVIRONMENT: SUSTAINABLE AGRICULTURE AND ABIOTIC STRESS

Another implication of our work to life on Earth is the use of a completely new, suboptimal environment to describe how plants can adapt themselves to an environment without this essential clue for their existence and survival on our planet. What happens at the molecular level in terms of transcriptional profile? Obviously, this includes the strategies and mechanisms of perception, response and adaptation to a wide range of abiotic environmental stresses in plants, potentially useful for sustainable agriculture requirements under suboptimal environments. Transcriptional profile of the abiotic stresses related genes was utilized in our study under the alterations of simulated microgravity using *Arabidopsis* cell cultures (Synchronous and Asynchronous) for different exposure time, whereas almost 4000 abiotic stresses related genes were examined **(Figure 73, 74)**. It is noticed that losing or alteration of the gravitational cue is

not only a stressful event by itself (in fact it can be understood as the "liberation" of the $1g$ stress already keeping cell proliferation under control), but will also alter the way in which organisms detect and respond to other environmental factors. Gene ontology data analysis reveals that 30% of the upregulated genes classified as associated to biotic and abiotic stress-responsive genes are affected. In particular, up-regulation of abiotic stresses related genes as a complex including more than 13 different type of abiotic stress gene specially UV-B, Heat, Osmotic, Wounding, Cold, Drought and NaCl stresses. Microgravity is unique in that it is a novel environment for plants; thus any response can provide insight into how eukaryotes cope with abiotic signals that lie completely outside their evolutionary experience. This unique mechanism of the gravity response suggests a synergistic effect that promotes a complex environmental stresses response, combining different abiotic stresses elements (Beckingham 2010, Herranz et al 2010). Moreover, the patterns of gene expression reflect adaptive strategies through the progression of the experimental exposure. It is noticed that the percentage of the upregulated stress-response genes is reduced in the 14 hours experiments (Synchronous/Asynchronous) compared with the 7 hours in the Synchronous G2/M samples. It is proposed that a rapid initial response to a new environment within the 7 hours experiment occurs, and patterns of gene expression change as a longer-term adaptive strategy. Future experiments should include additional exposure times to detect the initial response after minutes of the experiments accompanied with long term experiments.

In our data, the most dramatic response was UV and heat shock response which was also observed in the cell cultures responding to the spaceflight (Paul et al 2012, Zupanska et al 2013). Over than 25% of the genes encoding heat stress and UV were upregulated in a response to the simulated microgravity. Although our samples were no exposed to temperature differentials capable of promote a classical heat shock response, heat shock proteins were affected. This fact confirms signal transduction pathways overlapping and the role of heat shock proteins up-regulation to trigger tolerance for multiple environmental stresses (Swindell et al 2007).

Interestingly, a possible basis for many of these responses may be traced to a translation of changes in forces associated with the cytoskeleton and cell wall. A 25% of wounding related genes were upregulated, providing a very tightly connection to the gravitational response. In the tensegrity-based model of the gravisensing, an actin-based cytoskeletal network throughout the cytoplasm is coupled to stretch-sensitive receptor in the plasma membrane. Cytoskeletal actin

filaments attached to the plasma membrane have been postulated to participate in gravity-related signaling (Yoder et al 2001). Differentially regulated genes reflect categories of genes that are broadly associated with osmotic stresses including osmotic, ABA, Drought and NaCl stress and on other hand associated with the oxidative stresses, in spite of the well-controlled culture medium used in the experiment. Therefore, a direct and obvious relationship between the affected osmotic/oxidative genes and microgravity is missing (see next chapter). Moreover, the presence of these other stress-response genes is not related with the stimulus they used to detect, but rather included into a cross-linked unspecific/novel stress response pathway to counteract gravity changes.

Another approach to the biotic/abiotic stress topic is the role of Cyclin Dependent Protein Kinases. In our study, the main process inhibited impacted by the gravitational alterations is the cell cycle progression through the disruption of the cyclin dependent kinase (CDKs). This results is become supported by the array analysis of the cell cycle core and almost of the cell cycle core is inhibited and altered. Involvement of cyclin dependent kinase (CDKs) in the plant response machinery (Kitsios & Doonan 2011) and the well-known role of the CDKs in the animal cells response to genotoxic and other cell cycle specific stresses that cause DNA damage (Yata & Esashi 2009) is known, they can regulate the transcriptional response to a variety of stress conditions (Huang et al 2002) supporting our suggestion of the CDKs role in plant stress response. Furthermore, several protein kinases are involved in stress tolerance in plants, stimulated by ABA, a hormone with a well-documented role in stress response such as Ca^{+2}-dependent protein kinases (CDPKs), sucrose non fermentation 1 (SNF1)-related kinases (SnRKs) (Diedhiou et al 2008, Saijo et al 2000). Abiotic stress negatively affects CDK function by inhibit of CDK activity (De Veylder et al 2007). Additionally, it was reported that heat stress enhances inhibitory phosphorylation of CDKs and reduce the expression of cyclins, suggesting an alternative regulatory mechanism of CDK function (Nitta et al 1997, Rowley et al 1993). A common cellular response upon stress is the transient inhibition of cell cycle progression or even cell cycle exit. The signaling pathways that integrate abiotic stress with cell division control remains to be fully elucidated, but evidence suggests that post-transcriptional modulation of CDK kinase activity is important for transient inhibition. Other kinases including CDKs with functions other than cell cycle control also are crucial in the stress response. Such findings

suggest novel intrinsic functions for CDKs in the regulation of plant response upon biotic and abiotic stress (Burssens et al 2000, Kitsios & Doonan 2011, West et al 2004).

Taking into account all these results, microgravity conditions could provide us the way to improve our sustainable agriculture strategies to fight against both biotic and abiotic stresses, both on Earth and under space colonization agronomy/life support systems. It could be useful for this aim to study the behavior of the plant response to biotic/abiotic stress under the space conditions, particularly the synergies among multiple environmental stresses, and elaborate these mechanisms in crop plants farming strategies on earth to face the challenges raise due to the harmful and unavoidable climatic change on our planet.

4.3. CONSEQUENCES OF AN ENHANCED CELLULAR ACTIVITY UNDER SIMULATED MICROGRAVITY: UNKNOWN GENES, MITOCHONDRIA AND AGING

The more intriguing result arisen from our array analyses was the large number of unknown function genes affected by altered gravity. Over 13% of *Arabidopsis* thaliana genes encode for proteins classified as having a completely unknown function, while the function of >30% of *Arabidopsis* proteome are poorly characterized (Lamesch et al 2012). The expression of these unknown or poorly characterized genes, might be required for novel defense mechanisms or involved in critical signaling pathways (Gollery et al 2007, Luhua et al 2008), suggesting that genes of unknown function could play an important role in abiotic stress-response signaling or general acclimation mechanisms (Luhua et al 2008, Luhua et al 2013).

To test whether proteins of unknown or poorly characterized function play a role in the response of plants to the microgravity alterations, we focus on the 20 upregulated genes belonging to unknown GO biological function in all our experimental conditions. Among these unknown genes there is only one network established consisting in four genes (At2G07728, At2G07674, ORF114, ORF113) related to the hypothetic ORF protein network. Furthermore, ORF proteins are located into the mitochondria, suggesting a role of the mitochondria in the plant response to the gravitational alterations response.

Plants subjected to abiotic stress inevitably face a disruption of cellular homeostasis with inevitable consequences for the functioning of mitochondria, including their ability to adjust

cellular energy status to cope with adverse conditions and during recovery. Because of the crucial role of mitochondria in eukaryotic cells, one might expect that cells with compromised mitochondria should not be able to survive stress.

This is illustrated by the decisive role of mitochondria during cellular life switches in animal cells (Kakkar & Singh 2007) and by the primordial role of mitochondria in the autophagy process of cellular components in carbon deprived heterotrophic plant cells (Aubert et al 1996).

Here in our study, we consider whether mitochondrial function is adversely affected by changes associated with the microgravity conditions. Transcriptome results reveal that 24% of the upregulated genes altered by microgravity conditions in all the experimental samples associated to the mitochondria cellular components. These primary results suggest that plant mitochondrion may play a role during the microgravity alterations. The same link observed in other microgravity studies in drosophila (Herranz et al 2010), cultured human lymphocyte (Schatten et al 2001), human ocular tissue (Mao et al 2013), and plants (Sytnik & Popova 1998). Furthermore, recent studies support this role during abiotic/biotic stress response (Begcy et al 2011, Jacoby et al 2012, Jacoby et al 2011, Ruiz-Pesini et al 2007, Skirycz et al 2010).

Under microgravity conditions, mitochondria play an active role. This activation is achieved by the release of mitochondrial intermembrane space (IMS) proteins, in particular the electron transport chain (ETC). A distinct feature of plant mitochondria is the presence of several unique ETC component associated with Complex I (the rotenone-sensitive NADH dehydrogenase oxidizing matrix NADH) which increased under the microgravity conditions, besides increasing Complex I, the IMM contains alternative rotenone-resistance NAD(P)H dehydrogenase (Finnegan et al 2004, Rasmusson et al 2004) was increased **(Table 11)**. This suggests the respiration rate of the mitochondria can be significantly enhanced under the simulated microgravity. This suggestion support the unique alteration of the microgravity, as it was reported that biotic/abiotic stresses could impair the activities of NADH dehydrogenase (Complex I) and then a reduction on the respiration rate (Amirsadeghi et al 2007, Flagella et al 2006, Hamilton & Heckathorn 2001, Trono et al 2004).

On other hand, mitochondrial electron transport is associated with the generation of ROS such as superoxide and H_2O_2, which are referred as mitochondrial ROS (mROS). Microgravity elicits different transcriptional responses in a set of H_2O_2-responsive genes **(Figure 88).** Increased ROS production in synchronous G2/M (7 hours) is thought to be linked to the rapid response to the microgravity alterations, as well as to be a common effect of all abiotic stresses (Apel & Hirt 2004, Schwarzlander et al 2009). ROS are particularly important in the mitochondrial context because mitochondria generate a significant portion of cellular ROS mainly owing to leakage form ETC (Moller 2001).

This increase in the oxidative activity of the cells is very interesting for multiple reasons. First of all because it provide additional support and generality to aging related findings in other model systems exposed to real microgravity (flies) in which an accelerated aging connected with increased motility and redox activity was observed (Benguria et al 1996, de Juan et al 2007, Serrano et al 2010, Serrano et al 2013). Secondly, it justifies the use of plant and cell model systems as useful to solve basic science questions. And thirdly, as a reminder of the importance of microgravity and Space Biology research as a source of knowledge with unexpected and deep implications for life on Earth.

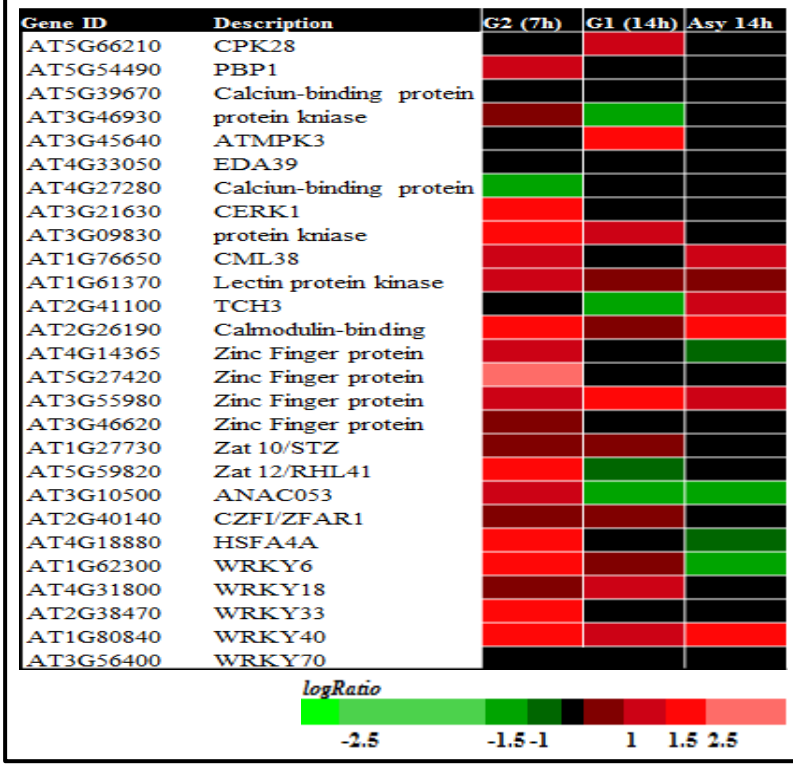

Figure 88: Changes in expression of hydrogen peroxide-responsive transcripts in *Arabidopsis* cell cultures (Synchronous/Asynchronous) exposed to simulated microgravity. The different hydrogen peroxide-responsive transcripts were identified in wild-type plants subjected to hydrogen peroxide treatments, as well as in knockout APX1 plants subjected to light intensity stress (Davletova et al 2005a, Davletova et al 2005b, Miller et al 2010). Red range color means upregulated genes and green range color downregulated genes in our array-based results.

CONCLUSIONS

1. We have found that the best method to expose a plant cell culture system to altered gravity environments, using ground based facilities, is the immobilization by agarose embedding. This method preserves cell viability, allows cell synchronization and avoids unwanted mechanical stimuli.

2. Using the biological system of in vitro plant cell culture, the best instruments to reproduce several altered gravity environments were the Random Positioning Machine (RPM), for simulated microgravity, the Large Diameter Centrifuge (LDC) for hypergravity, and the modified RPM, based on Hardware or Software modes of operation, for simulated partial *g*, i.e. levels of gravity between 0 and 1, comprising the Moon and Mars gravity conditions. In this latter case, further research is required to confirm their interchangeability. Other instruments tested have not given satisfactory results. The 2D Pipette Clinostat, often used for animal cellular systems, is not suitable, especially for long term experiments, due to technical problems in the 1*g* control samples (including cell viability issues). The magnetic levitation approach, while quite versatile in terms of partial *g* simulation, raises important concerns due to the high energy magnetic fields, and also to technical problems in the 0*g** alternative experiences.

3. Other important technical achievements have also resulted from the work with plant cell cultures under altered gravity conditions. These achievements include:
    a. The adaptation of powerful cell biology techniques to be used in our *Arabidopsis in vitro* model system for the first time: morphofunctional nucleolar models, EdU labelling assay, cell synchronization and quantitative colocalization techniques.
    b. The establishment of new transgenic cell cultures, which have been successfully derived from previously established mutant/marker lines.

4. Similarly to the effects observed in root meristematic cells of seedlings exposed to microgravity, either real ("Root" experiment performed in the ISS) or simulated, the coordination of fundamental plant cell developmental processes is disrupted under reduced gravity conditions (simulated microgravity and partial gravity - the Moon and Mars) in plant cell cultures, while hypergravity (2*g*) produces an opposite and weaker misbalance on the plant cell growth and proliferation equilibrium.

5. Cell cycle is accelerated under simulated microgravity and the Moon conditions, due to relaxation of the cell cycle checkpoints, particularly at the G2/M transition, resulting in a higher cell proliferation rate. This proliferation increase is accompanied by a reduced cell size, corroborated by a depleted nucleolar activity, taken as an estimation of cell growth.

6. Cell cycle is decelerated under hypergravity conditions, producing a significantly longer cell cycle. While cell size and some cell growth parameters are not significantly affected, an increase in the nucleolar activity is inferred from the analysis of nucleolar models.

7. Mars gravity conditions produce an intermediate effect: while cell proliferation is initially increased, due to a shorter G2/M phase, and cell growth is decreased (as in other reduced gravity conditions), G1 phase is particularly extended to produce a longer cell cycle, thus resembling the effect of hypergravity.

8. The effects of altered gravity on the plant cell culture *in vitro* should be explained in the context of a system without known professional gravisensitive cells, such as seedling statoliths. A likely interpretation should take into account the unspecific graviresistance mechanism, which involves gravity sensing by non-differentiated cells, but a universal, still unknown mechanism of gravity perception would also play a prominent role. The existence of this mechanism is supported by the plethora of known physiological processes which involve cell polarity or spatial organization of cells. The overlapping of different systems of graviperception could lead to "confusing" the system with contradictory signals, which could explain the results of the partial gravity simulation, somehow striking.

9. An extensive effect of simulated microgravity at the overall genome level has been differentially detected through the cell cycle phases. Transcriptomic responses have been confirmed by proteomic analyses and this is consistent with epigenetic modifications.

10. Epigenetic modifications, both hypermethylation of DNA and histone deacetylation, are a key component in the regulation of gene expression that allows the plant cells to cope with altered gravity environments. Chromatin modifications and remodeling effects are probably influencing the altered progression rates of *Arabidopsis* cell cycle, since variable condensed/decondensed chromatin states have been observed through the cell cycle.

11. Plant response to altered gravity, rather than being based in a small group of genes or transduction pathways, relies in a complex mechanism, characterized by a unique response against a novel environmental stress, suggesting a synergistic effect which combines elements of multiple abiotic stress pathways. The implication of these results for sustainable agriculture on Earth and in Life Support Systems in space is certain.

Supplementary Materials

The following supplementary figures and excel datasheets have been included in the attached CD-ROM for your reference together with the PDF version of the present Doctoral Thesis:

Figure S1. Extended version of the flow cytometry charts obtained for the cell cycle progression analysis for 72h after Aphidicolin block/release of *Arabidopsis* cell line MM2d immobilized **in Sim μ*g* RPM condition**.

Figure S2. Extended version of the flow cytometry charts obtained for the cell cycle progression analysis for 72h after Aphidicolin block/release of *Arabidopsis* cell line MM2d immobilized **in the Moon (0.17*g*) condition**.

Figure S3. Extended version of the flow cytometry charts obtained for the cell cycle progression analysis for 72h after Aphidicolin block/release of *Arabidopsis* cell line MM2d immobilized **in Mars (0.37*g*) condition**.

Figure S4. Extended version of the flow cytometry charts obtained for the cell cycle progression analysis for 72h after Aphidicolin block/release of *Arabidopsis* cell line MM2d immobilized **in hypergravity (2*g*/LDC) condition**.

Table S1: Extended analysis of enriched GO cellular component and molecular functions groups (TAIR ONTOLOGY) related with significantly **upregulated genes under simulated microgravity** in *Arabidopsis* cell cultures (synchronous/asynchronous).

Table S2: Extended analysis of enriched GO cellular component and molecular functions groups (TAIR ONTOLOGY) related with significantly **downregulated genes under simulated microgravity** in *Arabidopsis* cell cultures (synchronous/asynchronous).

Table S3: List of common up- and downregulated genes in the three simulated microgravity samples: *Arabidopsis* synchronous (G2/G1) and 14h asynchronous cultures.

REFERENCES

Agius F, Kapoor A, Zhu JK. 2006. Role of the *Arabidopsis* DNA glycosylase/lyase ROS1 in active DNA demethylation. *Proceedings of the National Academy of Sciences of the United States of America* 103: 11796-801

Amirsadeghi S, Christine AR, Vanlerberghe G. 2007. The role of the mitochondrion in plant responses to biotic stress. *Physiologia plantarum* 129: 14

Apel K, Hirt H. 2004. Reactive oxygen species: metabolism, oxidative stress, and signal transduction. *Annu Rev Plant Biol* 55: 373-99

Araki T. 2001. Transition from vegetative to reproductive phase. *Current opinion in plant biology* 4: 63-8

ASBiosciences. 2008. Epigenetic modification regulate gene expression. *COVER STORY: Epigenetics*

Aubert S, Gout E, Bligny R, Marty-Mazars D, Barrieu F, et al. 1996. Ultrastructural and biochemical characterization of autophagy in higher plant cells subjected to carbon deprivation: control by the supply of mitochondria with respiratory substrates. *The Journal of cell biology* 133: 1251-63

Aufsatz W, Mette MF, Matzke AJ, Matzke M. 2004. The role of MET1 in RNA-directed de novo and maintenance methylation of CG dinucleotides. *Plant molecular biology* 54: 793-804

Baek D, Jiang J, Chung JS, Wang B, Chen J, et al. 2011. Regulated AtHKT1 gene expression by a distal enhancer element and DNA methylation in the promoter plays an important role in salt tolerance. *Plant & cell physiology* 52: 149-61

Baldwin KL, Strohm AK, Masson PH. 2013. Gravity sensing and signal transduction in vascular plant primary roots. *American journal of botany* 100: 126-42

Banfalvi G. 2008. Cell cycle synchronization of animal cells and nuclei by centrifugal elutriation. *Nature protocols* 3: 663-73

Barneche F, Steinmetz F, Echeverria M. 2000. Fibrillarin genes encode both a conserved nucleolar protein and a novel small nucleolar RNA involved in ribosomal RNA methylation in *Arabidopsis thaliana*. *The Journal of biological chemistry* 275: 27212-20

Baserga R. 1984. Growth in size and cell DNA replication. *Experimental cell research* 151: 1-5

Baserga R. 2007. Is cell size important? *Cell Cycle* 6: 814-16

Becker JL, Souza GR. 2013. Using space-based investigations to inform cancer research on Earth. *Nature reviews. Cancer* 13: 315-27

Beckingham KM. 2010. Synergy between stresses: an interaction between spaceflight-associated conditions and the microgravity response. *Molecular ecology* 19: 4105-7

Beemster GT, De Vusser K, De Tavernier E, De Bock K, Inze D. 2002. Variation in growth rate between *Arabidopsis* ecotypes is correlated with cell division and A-type cyclin-dependent kinase activity. *Plant physiology* 129: 854-64

Beemster GT, Fiorani F, Inze D. 2003. Cell cycle: the key to plant growth control? *Trends in plant science* 8: 154-8

Begcy K, Mariano ED, Mattiello L, Nunes AV, Mazzafera P, et al. 2011. An *Arabidopsis* mitochondrial uncoupling protein confers tolerance to drought and salt stress in transgenic tobacco plants. *PloS one* 6: e23776

Benguria A, Grande E, de Juan E, Ugalde C, Miquel J, et al. 1996. Microgravity effects on Drosophila melanogaster behavior and aging. Implications of the IML-2 experiment. *J Biotechnol* 47: 191-201

Berckmans B, De Veylder L. 2009. Transcriptional control of the cell cycle. *Current opinion in plant biology* 12: 599-605

Bernstein KA, Baserga SJ. 2004. The small subunit processome is required for cell cycle progression at G1. *Mol. Biol. Cell* 15: 5038-46

Bernstein KA, Bleichert F, Bean JM, Cross FR, Baserga SJ. 2007. Ribosome biogenesis is sensed at the start cell cycle checkpoint. *Mol. Biol. Cell* 18: 953-64

Berry MV, Geim AK. 1997. Of flying frogs and levitrons. *Eur J Phys.* 18: 7

Binarova P, Dolezel J, Draber P, Heberle-Bors E, Strnad M, Bogre L. 1998. Treatment of Vicia faba root tip cells with specific inhibitors to cyclin-dependent kinases leads to abnormal spindle formation. *The Plant journal : for cell and molecular biology* 16: 697-707

Bird A. 2007. Perceptions of epigenetics. *Nature* 447: 396-8

Blagosklonny MV. 2001. Cell cycle checkpoints and cancer. *Landes Bioscience*

Blancaflor EB. 2013. Regulation of plant gravity sensing and signaling by the actin cytoskeleton. *American journal of botany* 100: 143-52

Blancaflor EB, Fasano JM, Gilroy S. 1998. Mapping the functional roles of cap cells in the response of *Arabidopsis* primary roots to gravity. *Plant physiology* 116: 213-22

Blancaflor EB, Masson PH. 2003. Plant gravitropism. Unraveling the ups and downs of a complex process. *Plant physiology* 133: 1677-90

Blanco C, Ritzenthaler P, Mata-Gilsinger M. 1982. Cloning and endonuclease restriction analysis of uidA and uidR genes in Escherichia coli K-12: determination of transcription direction for the uidA gene. *Journal of bacteriology* 149: 587-94

Blazquez MA, Weigel D. 2000. Integration of floral inductive signals in *Arabidopsis*. *Nature* 404: 889-92

Blow JJ, Dutta A. 2005. Preventing re-replication of chromosomal DNA. *Nature reviews. Molecular cell biology* 6: 476-86

Borst AG, van Loon JJWA. 2009. Technology and developments for the random positioning machine, RPM. *Microgravity Sci. Technol* 21: 6

Boulon S, Westman BJ, Hutten S, Boisvert FM, Lamond AI. 2010. The nucleolus under stress. *Molecular cell* 40: 216-27

Breyne P, Zabeau M. 2001. Genome-wide expression analysis of plant cell cycle modulated genes. *Current opinion in plant biology* 4: 136-42

Briegleb W. 1992. Some qualitative and quantitative aspects of fast-rotating clinostat as a research tool. *ASGSB bulletin : publication of the American Society for Gravitational and Space Biology* 5: 8

Brooks JS, Reavis JA, R. A. Medwood RA, Stalcup TF, Meisel MW, et al. 2000. New opportunities in science, materials, and biological systems in the low-gravity (magnetic levitation) environment (invited). *J Appl Phys* 87: 6

Brown JW, Shaw PJ, Shaw P, Marshall DF. 2005. *Arabidopsis* nucleolar protein database (AtNoPDB). *Nucleic acids research* 33: D633-6

Brown SE, Fraga MF, Weaver IC, Berdasco M, Szyf M. 2007. Variations in DNA methylation patterns during the cell cycle of HeLa cells. *Epigenetics : official journal of the DNA Methylation Society* 2: 54-65

Bruce TJA, Matthes MC, Napier JA, Pickett JA. 2007. Stressful "memories" of plants: Evidence and possible mechanisms. *Plant Sci* 173: 6

Buck SB, Bradford J, Gee KR, Agnew BJ, Clarke ST, Salic A. 2008. Detection of S-phase cell cycle progression using 5-ethynyl-2'-deoxyuridine incorporation with click chemistry, an alternative to using 5-bromo-2'-deoxyuridine antibodies. *BioTechniques* 44: 927-9

Burssens S, Himanen K, van de Cotte B, Beeckman T, Van Montagu M, et al. 2000. Expression of cell cycle regulatory genes and morphological alterations in response to salt stress in *Arabidopsis* thaliana. *Planta* 211: 632-40

Callan HG. 1986. Lampbrush chromosomes. *Molecular biology, biochemistry, and biophysics* 36: 1-252

Canetta E, Kim SH, Kalinina NO, Shaw J, Adya AK, et al. 2008. A plant virus movement protein forms ringlike complexes with the major nucleolar protein, fibrillarin, in vitro. *Journal of molecular biology* 376: 932-7

Cao X, Jacobsen SE. 2002. Locus-specific control of asymmetric and CpNpG methylation by the DRM and CMT3 methyltransferase genes. *Proceedings of the National Academy of Sciences of the United States of America* 99 Suppl 4: 16491-8

Cerdido A, Medina FJ. 1995. Subnucleolar location of fibrillarin and variation in its levels during the cell cycle and during differentiation of plant cells. *Chromosoma* 103: 625-34

Chaboute ME, Clement B, Philipps G. 2002. S phase and meristem-specific expression of the tobacco RNR1b gene is mediated by an E2F element located in the 5' leader sequence. *The Journal of biological chemistry* 277: 17845-51

Chalfie M, Tu Y, Euskirchen G, Ward WW, Prasher DC. 1994. Green fluorescent protein as a marker for gene expression. *Science* 263: 802-5

Chehrehasa F, Ekberg JA, St John JA. 2014. A novel method using intranasal delivery of EdU demonstrates that accessory olfactory ensheathing cells respond to injury by proliferation. *Neuroscience letters* 563: 90-5

Chen LT, Luo M, Wang YY, Wu K. 2010. Involvement of *Arabidopsis* histone deacetylase HDA6 in ABA and salt stress response. *Journal of experimental botany* 61: 3345-53

Chinnusamy V, Gong Z, Zhu JK. 2008. Abscisic acid-mediated epigenetic processes in plant development and stress responses. *Journal of integrative plant biology* 50: 1187-95

Choi CS, Sano H. 2007. Abiotic-stress induces demethylation and transcriptional activation of a gene encoding a glycerophosphodiesterase-like protein in tobacco plants. *Molecular genetics and genomics : MGG* 277: 589-600

Cholodny H. 1928. Beiträge zur hormonalen Theorie von Tropismen. *Planta* 6: 17

Christianen PC. 2010. Tuneable gravity using strong gradient magnetic fields. *News of elgra* 7: 4

Churchman ML, Brown ML, Kato N, Kirik V, Hulskamp M, et al. 2006. SIAMESE, a plant-specific cell cycle regulator, controls endoreplication onset in *Arabidopsis* thaliana. *The Plant cell* 18: 3145-57

Cioce M, Boulon S, Matera AG, Lamond AI. 2006. UV-induced fragmentation of Cajal bodies. *The Journal of cell biology* 175: 401-13

Clément G. 2005. Fundamentals of space medicine. *Space technology library* 23

Clément G, Slenzka K. 2006. Fundamental of Space biology; Research on Cells, Animals, and Plants in Space Series. *Space technology library* 18

Cockcroft CE, den Boer BG, Healy JM, Murray JA. 2000. Cyclin D control of growth rate in plants. *Nature* 405: 575-9

Coinu R, Chiaviello A, Galleri G, Franconi F, Crescenzi E, Palumbo G. 2006. Exposure to modeled microgravity induces metabolic idleness in malignant human MCF-7 and normal murine VSMC cells. *FEBS letters* 580: 2465-70

Collins K, Jacks T, Pavletich NP. 1997. The cell cycle and cancer. *Proceedings of the National Academy of Sciences of the United States of America* 94: 2776-8

Cong R, Das S, Ugrinova I, Kumar S, Mongelard F, et al. 2012. Interaction of nucleolin with ribosomal RNA genes and its role in RNA polymerase I transcription. *Nucleic acids research* 40: 9441-54

Coons AH, Kaplan MH. 1950. Localization of antigen in tissue cells. II. Improvements in a method for the detection of antigen by means of fluorescent antibody. *Journal of Exp Med* 91

Costas C, Desvoyes B, Gutierrez C. 2011. A chromatin perspective of plant cell cycle progression. *Biochimica et biophysica acta* 1809: 9

Crabbe A, De Boever P, Van Houdt R, Moors H, Mergeay M, Cornelis P. 2008. Use of the rotating wall vessel technology to study the effect of shear stress on growth behaviour of Pseudomonas aeruginosa PA01. *Environmental microbiology* 10: 2098-110

Cutler GJ, Cheever H. 2000. Shedding light on induced molting. *Journal of the American Veterinary Medical Association* 217: 8-11

Dalton S, Whitbread L. 1995. Cell cycle-regulated nuclear import and export of Cdc47, a protein essential for initiation of DNA replication in budding yeast. *Proceedings of the National Academy of Sciences of the United States of America* 92: 2514-8

Daneholt B. 1975. Transcription in polytene chromosomes. *Cell* 4: 1-9

Davletova S, Rizhsky L, Liang H, Shengqiang Z, Oliver DJ, et al. 2005a. Cytosolic ascorbate peroxidase 1 is a central component of the reactive oxygen gene network of *Arabidopsis*. *The Plant cell* 17: 268-81

Davletova S, Schlauch K, Coutu J, Mittler R. 2005b. The zinc-finger protein Zat12 plays a central role in reactive oxygen and abiotic stress signaling in *Arabidopsis*. *Plant physiology* 139: 847-56

de Juan E, Benguría A, Villa A, Leandro LJ, Herranz R, et al. 2007. The "AGEING" Experiment in the Spanish Soyuz Mission to the International Space Station. *Microgravity Sci Technol* 19: 170-74

De Veylder L, Beeckman T, Beemster GT, de Almeida Engler J, Ormenese S, et al. 2002. Control of proliferation, endoreduplication and differentiation by the *Arabidopsis* E2Fa-DPa transcription factor. *The EMBO journal* 21: 1360-8

De Veylder L, Beeckman T, Beemster GT, Krols L, Terras F, et al. 2001. Functional analysis of cyclin-dependent kinase inhibitors of *Arabidopsis*. *The Plant cell* 13: 1653-68

De Veylder L, Beeckman T, Inze D. 2007. The ins and outs of the plant cell cycle. *Nature reviews. Molecular cell biology* 8: 655-65

del Pozo JC, Boniotti MB, Gutierrez C. 2002. *Arabidopsis* E2Fc functions in cell division and is degraded by the ubiquitin-SCF(AtSKP2) pathway in response to light. *The Plant cell* 14: 3057-71

Demandolx D, Davoust J. 1997. Multicolour analysis and local image correlation in confocal microscopy. *j. Microsc* 185: 16

Dennis ES, Peacock WJ. 2007. Epigenetic regulation of flowering. *Current opinion in plant biology* 10: 520-7

Des Marais DJ, Nuth JA, 3rd, Allamandola LJ, Boss AP, Farmer JD, et al. 2008. The NASA Astrobiology Roadmap. *Astrobiology* 8: 715-30

Dewitte W, Murray JA. 2003. The plant cell cycle. *Annu Rev Plant Biol* 54: 235-64

Diedhiou CJ, Popova OV, Dietz KJ, Golldack D. 2008. The SNF1-type serine-threonine protein kinase SAPK4 regulates stress-responsive gene expression in rice. *BMC plant biology* 8: 49

Dixit R, Cyr R, Gilroy S. 2006. Using intrinsically fluorescent proteins for plant cell imaging. *The Plant journal : for cell and molecular biology* 45: 599-615

Doerner P. 2008. Signals and mechanisms in the control of plant growth In *Plant Growth Signaling*, ed. L Bögre, G Beemster, pp. 1-23: Springer Berlin / Heidelberg

Dolezel J, Cihalikova J, Weiserova J, Lucretti S. 1999. Cell cycle synchronization in plant root meristems. *Methods in cell science : an official journal of the Society for In Vitro Biology* 21: 95-107

Dudits D, Abraham E, Miskolczi P, Ayaydin F, Bilgin M, Horvath GV. 2011. Cell-cycle control as a target for calcium, hormonal and developmental signals: the role of phosphorylation in the retinoblastoma-centred pathway. *Annals of botany* 107: 1193-202

Durut N, Abou-Ellail M, Pontvianne F, Das S, Kojima H, et al. 2014. A duplicated NUCLEOLIN gene with antagonistic activity is required for chromatin organization of silent 45S rDNA in *Arabidopsis*. *The Plant cell* 26: 1330-44

Durut N, Sáez-Vásquez J. 2014. Nucleolin: Dual roles in rDNA chromatin transcription. *Gene*

Dutcher FR, Hess EL, Halstead TW. 1994. Progress in plant research in space. *Advances in space research : the official journal of the Committee on Space Research* 14: 159-71

Eichler GS, Huang S, Ingber DE. 2003. Gene Expression Dynamics Inspctor (GEDI): for integrative analysis of expression profiles. *Bioinformatics* 19: 2

Espunya MC, Combettes B, Dot J, Chaubet-Gigot N, Martinez MC. 1999. Cell-cycle modulation of CK2 activity in tobacco BY-2 cells. *The Plant journal : for cell and molecular biology* 19: 655-66

Esteller M. 2008. Epigenetics in cancer. *The New England journal of medicine* 358: 1148-59

Fedorova E, Zink D. 2008. Nuclear architecture and gene regulation. *Biochimica et biophysica acta* 1783: 2174-84

Feinberg AP, Tycko B. 2004. The history of cancer epigenetics. *Nature reviews. Cancer* 4: 143-53

Ferl R, Wheeler R, Levine HG, Paul AL. 2002. Plants in space. *Current opinion in plant biology* 5: 258-63

Ferreira PC, Hemerly AS, Engler JD, van Montagu M, Engler G, Inze D. 1994. Developmental expression of the *Arabidopsis* cyclin gene cyc1At. *The Plant cell* 6: 1763-74

Finnegan PM, Soole KL, Umbach AL. 2004. Alternative mitchondrial electron transport proteins in higher plants. *In: Day, D. A., Millar, A. H., Whelan, J. (eds) Plant Mitochondria: From Genome to Function. Kluwer Academic Publishers, Great Britain*: 68

Flagella Z, Laus MN, Trono D, Soccio M, Di Fonzo N, Pastore D. 2006. Seawater stress applied at germination affects mitochondrial function in durum wheat (Triticum durum) early seedling. . *Functional plant biology : FPB* 33: 10

Foucher F, Kondorosi E. 2000. Cell cycle regulation in the course of nodule organogenesis in Medicago. *Plant molecular biology* 43: 773-86

Franceschini A, Szklarczyk D, Frankild S, Kuhn M, Simonovic M, et al. 2013. STRING v9.1: protein-protein interaction networks, with increased coverage and integration. *Nucleic acids research* 41: D808-15

Francis D. 2007. The plant cell cycle--15 years on. *The New phytologist* 174: 261-78

Freed LE, Vunjak-Novakovic G. 2002. Spaceflight bioreactor studies of cells and tissues. *Advances in space biology and medicine* 8: 177-95

Funk JO, Kind P. 1997. [Cell cycle control, genetic instability and cancer]. *Der Hautarzt; Zeitschrift fur Dermatologie, Venerologie, und verwandte Gebiete* 48: 157-65

Garshnek V. 1994. The lunar environment as a fractional-gravity biological laboratory. *Acta astronautica* 33: 5

Geim AK, Simon MD, Boamfia MI, Helfinger LO. 1999. Magnet levitation at your fingertips. *Nature* 400: 2

Genschik P, Criqui MC, Parmentier Y, Derevier A, Fleck J. 1998. Cell cycle -dependent proteolysis in plants. Identification Of the destruction box pathway and metaphase arrest produced by the proteasome inhibitor mg132. *The Plant cell* 10: 2063-76

Ginisty H, Sicard H, Roger B, Bouvet P. 1999. Structure and functions of nucleolin. *Journal of cell science* 112 (Pt 6): 761-72

Glover PM, Cavin I, Qian W, Bowtell R, Gowland PA. 2007. Magnetic-field-induced vertigo: a theoretical and experimental investigation. *Bioelectromagnetics* 28: 349-61

Goessens G. 1984. Nucleolar structure. *Int Rev Cytol* 87: 107-58

Goldberg AD, Allis CD, Bernstein E. 2007. Epigenetics: a landscape takes shape. *Cell* 128: 635-8

Gollery M, Harper J, Cushman J, Mittler T, Mittler R. 2007. POFs: what we don't know can hurt us. *Trends in plant science* 12: 492-6

Gondor A, Ohlsson R. 2009. Replication timing and epigenetic reprogramming of gene expression: a two-way relationship? *Nature reviews. Genetics* 10: 269-76

Gonzalez-Camacho F, Medina FJ. 2006. The nucleolar structure and the activity of NopA100, a nucleolin-like protein, during the cell cycle in proliferating plant cells. *Histochemistry and cell biology* 125: 139-53

Gould AR. 1984. Control of the cell cycle in cultured plant cells. *CRC Crit. Rev. Plant Sci.* 1

Grafi G, Avivi Y. 2004. Stem cells: a lesson from dedifferentiation. *Trends in biotechnology* 22: 388-9

Green A, Sarg B, Green H, Lonn A, Lindner HH, Rundquist I. 2011. Histone H1 interphase phosphorylation becomes largely established in G1 or early S phase and differs in G1 between T-lymphoblastoid cells and normal T cells. *Epigenetics & chromatin* 4: 15

Groth A, Rocha W, Verreault A, Almouzni G. 2007. Chromatin challenges during DNA replication and repair. *Cell* 128: 721-33

Grummt I. 2003. Life on a planet of its own: regulation of RNA polymerase I transcription in the nucleolus. *Genes & development* 17: 1691-702

Guevorkian K, Valles JM, Jr. 2004. Varying the effective buoyancy od cells using magnetic force. *Appl. Phys. Lett* 84: 3

Gutierrez C. 2005. Coupling cell proliferation and development in plants. *Nature cell biology* 7: 535-41

Häder D-P, Hemmersbach R, Lebert M. 2005. *Gravity and the Behavior of Unicellular Organisms*. New York (USA): Cambridge University Press.

Hader DP, Rosum A, Schafer J, Hemmersbach R. 1995. Gravitaxis in the flagellate Euglena gracilis is controlled by an active gravireceptor. *Journal of plant physiology* 146: 474-80

Hadjiolov AA. 1985. The nucleolus and ribosome biogenesis. *Cell Biol Monogr* 12: 269

Halstead TW, Dutcher FR. 1987. Plants in space. *Annual review of plant physiology* 38: 317-45

Hamilton EW, 3rd, Heckathorn SA. 2001. Mitochondrial adaptations to NaCl. Complex I is protected by anti-oxidants and small heat shock proteins, whereas complex II is protected by proline and betaine. *Plant physiology* 126: 1266-74

Handwerger KE, Wu Z, Murphy C, Gall JG. 2002. Heat shock induces mini-Cajal bodies in the Xenopus germinal vesicle. *Journal of cell science* 115: 2011-20

Hannan RD, Rothblum LI. 1995. Regulation of ribosomal DNA transcription during neonatal cardiomyocyte hypertrophy. *Cardiovascular research* 30: 501-10

Harper JV. 2005. Synchronization of cell populations in G1/S and G2/M phases of the cell cycle. *Methods Mol Biol* 296: 157-66

Haseloff J, Siemering KR. 2006. The uses of green fluorescent protein in plants. *Methods of biochemical analysis* 47: 259-84

Hemmersbach R, von der Wiesche M, Seibt D. 2006. Ground-based experimental platforms in gravitational biology and human physiology. *Signal Transduction* 6: 381

Henderson IR, Dean C. 2004. Control of *Arabidopsis* flowering: the chill before the bloom. *Development* 131: 3829-38

Hendrickx L, De Wever H, Hermans V, Mastroleo F, Morin N, et al. 2006. Microbial ecology of the closed artificial ecosystem MELiSSA (Micro-Ecological Life Support System Alternative): reinventing and compartmentalizing the Earth's food and oxygen regeneration system for long-haul space exploration missions. *Research in microbiology* 157: 77-86

Herranz R, Anken R, Boonstra J, Braun M, Christianen PCM, et al. 2013a. Ground-based facilities for simulation of microgravity, including terminology and organism-specific recommendations for their use. *Astrobiology* 13: 1-17

Herranz R, Benguria A, Lavan DA, Lopez-Vidriero I, Gasset G, et al. 2010. Spaceflight-related suboptimal conditions can accentuate the altered gravity response of Drosophila transcriptome. *Molecular ecology* 19: 4255-64

Herranz R, Larkin OJ, Dijkstra CE, Hill RJ, Anthony P, et al. 2012. Microgravity simulation by diamagnetic levitation: effects of a strong gradient magnetic field on the transcriptional profile of Drosophila melanogaster. *BMC genomics* 13: 52

Herranz R, Larkin OJ, Hill RJ, Lopez-Vidriero I, van Loon JJWA, Medina FJ. 2013b. Suboptimal evolutionary novel environments promote singular altered gravity responses of transcriptome during Drosophila metamorphosis. *BMC evolutionary biology* 13: 133

Herranz R, Manzano AI, van Loon JJWA, Christianen PC, Medina FJ. 2013c. Proteomic signature of *Arabidopsis* cell cultures exposed to magnetically induced hyper- and microgravity environments. *Astrobiology* 13: 217-24

Herranz R, Medina FJ. 2014. Cell proliferation and plant development under novel altered gravity environments. *Plant Biol (Stuttg)* 16: 23-30

Herranz R, Valbuena MA, Youssef K, Medina FJ. 2014. Mechanisms of disruption of meristematic competence by microgravity in *Arabidopsis* seedlings. *Plant signaling & behavior* 9: e28289

Hill RJ, Larkin OJ, Dijkstra CE, Manzano AI, de Juan E, et al. 2012. Effect of magnetically simulated zero-gravity and enhanced gravity on the walk of the common fruitfly. *Journal of the Royal Society, Interface / the Royal Society* 9: 1438-49

Hoppe S, Bierhoff H, Cado I, Weber A, Tiebe M, et al. 2009. AMP-activated protein kinase adapts rRNA synthesis to cellular energy supply. *Proceedings of the National Academy of Sciences of the United States of America* 106: 17781-6

Hoshino T, Miyamoto K, Ueda J. 2007. Gravity-controlled asymmetrical transport of auxin regulates a gravitropic response in the early growth stage of etiolated pea (Pisum sativum) epicotyls: studies using simulated microgravity conditions on a three-dimensional clinostat and using an agravitropic mutant, ageotropum. *Journal of plant research* 120: 619-28

Hoson T, Kamisaka S, Buchen B, Sievers A, Yamashita M, Masuda Y. 1996a. Possible use of a 3-D clinostat to analyze plant growth processes under microgravity conditions. *Advances in space research : the official journal of the Committee on Space Research* 17: 47-53

Hoson T, Kamisaka S, Masuda Y, Yamashita M, Buchen B. 1997. Evaluation of the three-dimensional clinostat as a simulator of weightlessness. *Planta* 203 Suppl: S187-97

Hoson T, Matsumoto S, Soga K, Wakabayashi K. 2010. Cortical microtubules are responsible for gravity resistance in plants. *Plant signaling & behavior* 5: 752-4

Hoson T, Nishitani K, Miyamoto K, Ueda J, Kamisaka S, et al. 1996b. Effects of hypergravity on growth and cell wall properties of cress hypocotyls. *Journal of experimental botany* 47: 513-7

Hoson T, Saito Y, Soga K, Wakabayashi K. 2005. Signal perception, transduction, and response in gravity resistance. Another graviresponse in plants. *Advances in Space Research* 36: 1196-202

Huang D, Moffat J, Andrews B. 2002. Dissection of a complex phenotype by functional genomics reveals roles for the yeast cyclin-dependent protein kinase Pho85 in stress adaptation and cell integrity. *Molecular and cellular biology* 22: 5076-88

Inze D, De Veylder L. 2006. Cell cycle regulation in plant development. *Annual review of genetics* 40: 77-105

Ishii Y, Hoson T, Kamisaka S, Miyamoto K, Ueda J, et al. 1996. Plant growth processes in *Arabidopsis* under microgravity conditions simulated by a clinostat. *Uchu Seibutsu Kagaku* 10: 3-7

Jacoby RP, Li L, Huang S, Pong Lee C, Millar AH, Taylor NL. 2012. Mitochondrial composition, function and stress response in plants. *Journal of integrative plant biology* 54: 887-906

Jacoby RP, Taylor NL, Millar AH. 2011. The role of mitochondrial respiration in salinity tolerance. *Trends in plant science* 16: 614-23

Jaskiewicz M, Conrath U, Peterhansel C. 2011. Chromatin modification acts as a memory for systemic acquired resistance in the plant stress response. *EMBO reports* 12: 50-5

Jefferson RA, Kavanagh TA, Bevan MW. 1987. GUS fusions: beta-glucuronidase as a sensitive and versatile gene fusion marker in higher plants. *The EMBO journal* 6: 3901-7

Jenuwein T, Allis CD. 2001. Translating the histone code. *Science* 293: 1074-80

Jerzmanowski A. 2007. SWI/SNF chromatin remodeling and linker histones in plants. *Biochimica et biophysica acta* 1769: 330-45

Jiang K, Feldman LJ. 2005. Regulation of root apical meristem development. *Annual review of cell and developmental biology* 21: 485-509

Jones PA, Baylin SB. 2007. The epigenomics of cancer. *Cell* 128: 683-92

Joubes J, Chevalier C. 2000. Endoreduplication in higher plants. *Plant molecular biology* 43: 735-45

Jurado S, Abraham Z, Manzano C, Lopez-Torrejon G, Pacios LF, Del Pozo JC. 2010. The *Arabidopsis* cell cycle F-box protein SKP2A binds to auxin. *The Plant cell* 22: 3891-904

Kadonaga JT. 1998. Eukaryotic transcription: an interlaced network of transcription factors and chromatin-modifying machines. *Cell* 92: 307-13

Kakkar P, Singh BK. 2007. Mitochondria: a hub of redox activities and cellular distress control. *Molecular and cellular biochemistry* 305: 235-53

Katsuhara M, Kawasaki T. 1996. Salt Stress Induced Nuclear and DNA Degradation in Meristematic Cells of Barley Roots. *Plant & cell physiology* 73: 4

Kaysen JH, Campbell WC, Majewski RR, Goda FO, Navar GL, et al. 1999. Select de novo gene and protein expression during renal epithelial cell culture in rotating wall vessels is shear stress dependent. *The Journal of membrane biology* 168: 77-89

Kim SH, Macfarlane S, Kalinina NO, Rakitina DV, Ryabov EV, et al. 2007a. Interaction of a plant virus-encoded protein with the major nucleolar protein fibrillarin is required for systemic virus infection. *Proceedings of the National Academy of Sciences of the United States of America* 104: 11115-20

Kim SH, Ryabov EV, Kalinina NO, Rakitina DV, Gillespie T, et al. 2007b. Cajal bodies and the nucleolus are required for a plant virus systemic infection. *The EMBO journal* 26: 2169-79

King RW, Deshaies RJ, Peters JM, Kirschner MW. 1996. How proteolysis drives the cell cycle. *Science* 274: 1652-9

Kiss JZ. 2000. Mechanisms of the early phases of plant gravitropism. *Crit. Rev. Plant Sci.* 19: 551-73

Kiss JZ. 2014. Plant biology in reduced gravity on the Moon and Mars. *Plant Biol (Stuttg)* 16 Suppl 1: 12-7

Kiss JZ, Katembe WJ, Edelmann RE. 1998. Gravitropism and development of wild-type and starch-deficient mutants of *Arabidopsis* during spaceflight. *Physiologia plantarum* 102: 493-502

Kitsios G, Doonan JH. 2011. Cyclin dependent protein kinases and stress responses in plants. *Plant signaling & behavior* 6: 204-9

Klaus DM. 2001. Clinostats and bioreactors. *Gravitational and space biology bulletin : publication of the American Society for Gravitational and Space Biology* 14: 55-64

Klaus DM, Schatz A, Neubert J, Höfer M, Todd P. 1997. *Escherichia coli* growth kinetics: a definition of ¨functional weightlessness¨ and a comparison of clinostat and space flight results. *Naturwissenschaften* 143: 7

Klein J, Grummt I. 1999. Cell cycle-dependent regulation of RNA polymerase I transcription: the nucleolar transcription factor UBF is inactive in mitosis and early G1. *Proceedings of the National Academy of Sciences of the United States of America* 96: 6096-101

Kojima H, Suzuki T, Kato T, Enomoto K, Sato S, et al. 2007. Sugar-inducible expression of the nucleolin-1 gene of *Arabidopsis* thaliana and its role in ribosome synthesis, growth and development. *The Plant journal : for cell and molecular biology* 49: 1053-63

Kotogany E, Dudits D, Horvath GV, Ayaydin F. 2010. A rapid and robust assay for detection of S-phase cell cycle progression in plant cells and tissues by using ethynyl deoxyuridine. *Plant methods* 6: 5

Kouzarides T. 2007. Chromatin modifications and their function. *Cell* 128: 693-705

Kovarik A, Koukalova B, Bezdek M, Opatrny Z. 1997. Hypermethylation of tobacco heterochromatic loci in response to osmotic stress. *Theoretical and Applied Genetics* 95: 6

Kraft TF, van Loon JJWA, Kiss JZ. 2000. Plastid position in *Arabidopsis* columella cells is similar in microgravity and on a random-positioning machine. *Planta* 211: 415-22

Krikorian AD, Levine HG, Kann RP, O'Connor SA. 1992. Effects of spaceflight on growth and cell division in higher plants. *Advances in space biology and medicine* 2: 181-209

Kumagai-Sano F, Hayashi T, Sano T, Hasezawa S. 2006. Cell cycle synchronization of tobacco BY-2 cells. *Nature protocols* 1: 2621-7

Kwiatkowska M, Maszewski J. 1979. Changes in the activity of RNA polymerase detected in situ and the intensity of 3H uridine incorporation into the nucleolus and the nucleus of interphase cells in antheridial filaments of Chara vulgaris L. *Folia histochemica et cytochemica* 17: 275-86

Labra M, Ghiani A, Citterio S, Sgorbati S, Sala F, et al. 2002. Analysis of Cytosine Methylation Pattern in Response to Water Deficit in Pea Root Tips. *Plant Biol (Stuttg)* 4: 6

Labra M, Grassi F, Imazio S, Di Fabio T, Citterio S, et al. 2004. Genetic and DNA-methylation changes induced by potassium dichromate in Brassica napus L. *Chemosphere* 54: 1049-58

Lamesch P, Berardini TZ, Li D, Swarbreck D, Wilks C, et al. 2012. The *Arabidopsis* Information Resource (TAIR): improved gene annotation and new tools. *Nucleic acids research* 40: D1202-10

Larsen P. 1962. orthogeotropism in roots. *Encyclopedia of Plant Physiology, W Ruhland (ed) Springer, Berlin*: 7

Leff LG, Leff AA. 1996. Use of green fluorescent protein to monitor survival of genetically engineered bacteria in aquatic environments. *Applied and environmental microbiology* 62: 3486-8

Leffel SM, Mabon SA, Stewart CN, Jr. 1997. Applications of green fluorescent protein in plants. *BioTechniques* 23: 912-8

Leguy CA, Delfos R, Pourquie MJBM, Polema C, Krooneman J, et al. 2011. Fluid motion for microgravity simulation in a Random Positioning Machine. *Gravitational and Space biology* 25: 4

Lei M, Tye BK. 2001. Initiating DNA synthesis: from recruiting to activating the MCM complex. *Journal of cell science* 114: 1447-54

Li B, Zhao H, Rybak P, Dobrucki JW, Darzynkiewicz Z, Kimmel M. 2014. Different rates of DNA replication at early versus late S-phase sections: Multiscale modeling of stochastic events related to DNA content/EdU (5-ethynyl-2'deoxyuridine) incorporation distributions. *Cytometry. Part A : the journal of the International Society for Analytical Cytology* 85: 785-97

Li C, Potuschak T, Colón-Carmona A, Gutiérrez RA, Doerner P. 2005. *Arabidopsis* TCP20 links regulation of growth and cell division control pathways. *Proceedings of the National Academy of Sciences of the United States of America* 102: 12978-83

Lin L, Choudhary A, Bavishi A, Ogbonna N, Maddux S, Choudhary M. 2012. Use of the sucrose gradient method for bacterial cell cycle synchronization. *Journal of microbiology & biology education* 13: 50-3

Liu W, Tanasa B, Tyurina OV, Zhou TY, Gassmann R, et al. 2010a. PHF8 mediates histone H4 lysine 20 demethylation events involved in cell cycle progression. *Nature* 466: 508-12

Liu Y, Zhu D, Strayer DM, Israelsson UE. 2010b. Magnetic levitation of large water droplets and mice. *Advances in space research : the official journal of the Committee on Space Research* 45: 6

Luger K, Mader AW, Richmond RK, Sargent DF, Richmond TJ. 1997. Crystal structure of the nucleosome core particle at 2.8 A resolution. *Nature* 389: 251-60

Luhua S, Ciftci-Yilmaz S, Harper J, Cushman J, Mittler R. 2008. Enhanced tolerance to oxidative stress in transgenic *Arabidopsis* plants expressing proteins of unknown function. *Plant physiology* 148: 280-92

Luhua S, Hegie A, Suzuki N, Shulaev E, Luo X, et al. 2013. Linking genes of unknown function with abiotic stress responses by high-throughput phenotype screening. *Physiologia plantarum* 148: 322-33

Luo M, Liu X, Singh P, Cui Y, Zimmerli L, Wu K. 2012a. Chromatin modifications and remodeling in plant abiotic stress responses. *Biochimica et biophysica acta* 1819: 129-36

Luo M, Wang YY, Liu X, Yang S, Lu Q, et al. 2012b. HD2C interacts with HDA6 and is involved in ABA and salt stress response in *Arabidopsis*. *Journal of experimental botany* 63: 3297-306

Lurin C, Andres C, Aubourg S, Bellaoui M, Bitton F, et al. 2004. Genome-wide analysis of *Arabidopsis* pentatricopeptide repeat proteins reveals their essential role in organelle biogenesis. *The Plant cell* 16: 2089-103

Ma X, Pietsch J, Wehland M, Schulz H, Saar K, et al. 2014. Differential gene expression profile and altered cytokine secretion of thyroid cancer cells in space. *FASEB journal : official publication of the Federation of American Societies for Experimental Biology* 28: 813-35

Magyar Z, De Veylder L, Atanassova A, Bako L, Inze D, Bogre L. 2005. The role of the *Arabidopsis* E2FB transcription factor in regulating auxin-dependent cell division. *The Plant cell* 17: 2527-41

Manzano AI. 2011. Cambios funcionales en células prolifarantes de *Arabidopsis thaliana* crecidas en ambientes de gravedad alterada. *Tesis Doctoral, Departmento de Genética, Universidad Complutense de Madrid*

Manzano AI, González-Camacjo F, Carnero-Diaz E, van Loon JJWA, Dijkstra CE, et al. 2009. Germination of *Arabidopsis* Seed in Space and in Simulated Microgravity: Alterations in Root Cell Growth and Proliferation. *Microgravity Sci Technol* 21: 5

Manzano AI, Herranz R, van Loon JJWA, Medina FJ. 2012a. Cell growth and cell proliferation decoupling under hypergravity environments induced by centrifugation. *Microgravity Sci Technol* 24: 373-81

Manzano AI, Herranz R, van Loon JJWA, Medina FJ. 2012b. A hypergravity environment induced by centrifugation alters plant cell proliferation and growth in an opposite way to microgravity. *Microgravity Sci Technol* 24: 9

Manzano AI, Herranz R, van Loon JJWA, Medina FJ. 2014. Effects of altered gravity environment on plant cell growth and cell proliferation: Characterization of morphofunctional nucleolar models in an *Arabidopsis* cell culture system in vitro.

Manzano AI, Larkin OJ, Dijkstra CE, Anthony P, Davey MR, et al. 2013. Meristematic cell proliferation and ribosome biogenesis are decoupled in diamagnetically levitated *Arabidopsis* seedlings. *BMC plant biology* 13: 124

Manzano AI, van Loon JJWA, Christianen PC, Gonzalez-Rubio JM, Medina FJ, Herranz R. 2012c. Gravitational and magnetic field variations synergize to cause subtle variations in the global transcriptional state of *Arabidopsis* in vitro callus cultures. *BMC genomics* 13: 105

Mao XW, Pecaut MJ, Stodieck LS, Ferguson VL, Bateman TA, et al. 2013. Spaceflight environment induces mitochondrial oxidative damage in ocular tissue. *Radiation research* 180: 340-50

Maret G, Dransfeld K. 1985. Biomolecules and polymers in high steady magnetic fields topicsin. *Topics in Applied Physics* 57: 62

Martin M, Garcia-Fernandez LF, Diaz de la Espina SM, Noaillac-Depeyre J, Gas N, Javier Medina F. 1992. Identification and localization of a nucleolin homologue in onion nucleoli. *Experimental cell research* 199: 74-84

Mastroleo F, Monsieurs P, Leys N. 2010. Insight into the radiotolerance of the life support bacterium Rhodospirillum rubrum S1H by means of phenotypic and transcriptomic methods. *38th COSPAR Scientific Assembly.*

Matherly LH, Schuetz JD, Westin E, Goldman ID. 1989. A method for the synchronization of cultured cells with aphidicolin: application to the large-scale synchronization of L1210 cells and the study of the cell cycle regulation of thymidylate synthase and dihydrofolate reductase. *Analytical biochemistry* 182: 338-45

Matía I, Gonzalez-Camacho F, Herranz R, Kiss JZ, Gasset G, et al. 2010. Plant cell proliferation and growth are altered by microgravity conditions in spaceflight. *Journal of plant physiology* 167: 184-93

Matía I, Gonzalez-Camacho F, Marco R, Kiss JZ, Gasset G, Medina FJ. 2005. Nucleolar structure and proliferation activity of *Arabidopsis* root cells from seedling germinated on the international space station. *Advances in space research : the official journal of the Committee on Space Research* 36: 10

Matía I, Gonzalez-Camacho F, Marco R, Kiss JZ, gasset G, et al. 2007. Seed germination and seedling growth under simulated microgravity causes alterations in plant cell proliferation and ribosome biogenesis. *Microgravity Sci Technol* 21: 6

May MJ, Leaver CJ. 1993. Oxidative Stimulation of Glutathione Synthesis in *Arabidopsis* thaliana Suspension Cultures. *Plant physiology* 103: 621-27

Mayer C, Grummt I. 2005. Cellular stress and nucleolar function. *Cell Cycle* 4: 1036-8

Mazars C, Briere C, Grat S, Pichereaux C, Rossignol M, et al. 2014a. Microgravity induces changes in microsome-associated proteins of Arabi*d*opsis seedlings grown on board the international space station. *PloS one* 9: e91814

Mazars C, Briere C, Grat S, Pichereaux C, Rossignol M, et al. 2014b. Microsome-associated proteome modifications of *Arabidopsis* seedlings grown on board the International Space Station reveal the possible effect on plants of space stresses other than microgravity. *Plant signaling & behavior* 9

Mead TJ, Lefebvre V. 2014. Proliferation assays (BrdU and EdU) on skeletal tissue sections. *Methods Mol Biol* 1130: 233-43

Medina FJ, Camacho FG, Manzano AI, Manrique A, Herranz R. 2010. Nucleolin, a major conserved multifunctional nucleolar phosphoprotein of proliferating cells. *J App Biomed* 8: 10

Medina FJ, Cerdido A, de Carcer G. 2000. The functional organization of the nucleolus in proliferating plant cells. *European journal of histochemistry : EJH* 44: 117-31

Medina FJ, González-Camacho F. 2003. Nucleolar proteins and cell prolifartion in plant cells. *Recent Res. Devel. Plant Biol* 3: 14

Medina FJ, Herranz R. 2010. Microgravity environment uncouples cell growth and cell proliferation in root meristematic cells: the mediator role of auxin. *Plant signaling & behavior* 5: 176-9

Medina FJ, Risueño MC, Morena-Dias de la Espina S. 1983. 3-D Reconstruction and morphometry of fibrillar centres in plant cells in relation to nucleolar activity. *Biology of the cell / under the auspices of the European Cell Biology Organization* 48: 8

Mekhail K, Rivero-Lopez L, Khacho M, Lee S. 2006. Restriction of rRNA synthesis by VHL maintains energy equilibrium under hypoxia. *Cell Cycle* 5: 2401-13

Melese T, Xue Z. 1995. The nucleolus: an organelle formed by the act of building a ribosome. *Current opinion in cell biology* 7: 319-24

Menges M, de Jager SM, Gruissem W, Murray JA. 2005. Global analysis of the core cell cycle regulators of *Arabidopsis* identifies novel genes, reveals multiple and highly specific profiles of expression and provides a coherent model for plant cell cycle control. *The Plant journal : for cell and molecular biology* 41: 546-66

Menges M, Hennig L, Gruissem W, Murray JA. 2002. Cell cycle-regulated gene expression in *Arabidopsis*. *The Journal of biological chemistry* 277: 41987-2002

Menges M, Hennig L, Gruissem W, Murray JA. 2003. Genome-wide gene expression in an *Arabidopsis* cell suspension. *Plant molecular biology* 53: 423-42

Menges M, Murray JA. 2002. Synchronous *Arabidopsis* suspension cultures for analysis of cell-cycle gene activity. *The Plant journal : for cell and molecular biology* 30: 203-12

Menges M, Murray JA. 2006. Synchronization, transformation, and cryopreservation of suspension-cultured cells. *Methods Mol Biol* 323: 45-61

Mergeay M, Verstraete W, Dubertret M, Lefort-Tran M, Chipaux C, Binot RA. 1988. 'MELiSSA'—a microorganisms-based model for 'CELSS' development. *Proceedings at the 3rd European Symposium on Space Thermal Control & Life Support Systems, Noordwijk, The Netherlands*: 4

Millar KD, Kumar P, Correll MJ, Mullen JL, Hangarter RP, et al. 2010. A novel phototropic response to red light is revealed in microgravity. *The New phytologist* 186: 648-56

Miller G, Suzuki N, Ciftci-Yilmaz S, Mittler R. 2010. Reactive oxygen species homeostasis and signalling during drought and salinity stresses. *Plant Cell Environ* 33: 453-67

Mironov VV, De Veylder L, Van Montagu M, Inze D. 1999. Cyclin-dependent kinases and cell division in plants- the nexus. *The Plant cell* 11: 509-22

Miyamoto K, Hoshino T, Hitotsubashi R, Tanimoto E, Ueda J. 2003. Graviresponse and its regulation from the aspect of molecular levels in higher plants: growth and development, and auxin polar transport in etiolated pea seedlings under microgravity. *Uchu Seibutsu Kagaku* 17: 234-5

Miyamoto K, Oka M, Yamamoto R, Masuda Y, Hoson T, et al. 1999a. Auxin polar transport in *Arabidopsis* under simulated microgravity conditions--relevance to growth and development. *Advances in space research : the official journal of the Committee on Space Research* 23: 2033-6

Miyamoto K, Yamamoto R, Fujii S, Soga K, Hoson T, et al. 1999b. Growth and development in *Arabidopsis* thaliana through an entire life cycle under simulated microgravity conditions on a clinostat. *Journal of plant research* 112: 413-8

Mizukami Y. 2001. A matter of size: developmental control of organ size in plants. *Current opinion in plant biology* 4: 533-9

Moller IM. 2001. Plant mitochondria and oxidative stress: Electron Transport, NADPH Turnover, and Metabolism of Reactive Oxygen Species. *Annual review of plant physiology and plant molecular biology* 52: 561-91

Montojo J, Zuberi K, Rodriguez H, Kazi F, Wright G, et al. 2010. GeneMANIA Cytoscape plugin: fast gene function predictions on the desktop. *Bioinformatics* 26: 2927-8

Morena-Dias de la Espina S, Medina FJ, Risueño MC. 1980. Correlation of nucleolar activity and nucleolar vacuolation in plant cells. *European journal of cell biology* 22: 724-9

Morin JP, Preterre D, Keravec V, Thuillez C. 2003. Rotating wall vessel as a new in vitro shear stress generation system: application to rat coronary endothelial cell cultures. *Cell biology and toxicology* 19: 227-42

Morita MT. 2010. Directional gravity sensing in gravitropism. *Annu Rev Plant Biol* 61: 705-20

Morita MT, Tasaka M. 2004. Gravity sensing and signaling. *Current opinion in plant biology* 7: 712-8

Mougey EB, Pape LK, Sollner-Webb B. 1993. A U3 small nuclear ribonucleoprotein-requiring processing event in the 5' external transcribed spacer of Xenopus precursor rRNA. *Molecular and cellular biology* 13: 5990-8

Muday GK, Haworth P. 1994. Tomato root growth, gravitropism, and lateral development: correlation with auxin transport. *Plant physiology and biochemistry : PPB / Societe francaise de physiologie vegetale* 32: 193-203

Muller WG, Walker D, Hager GL, McNally JG. 2001. Large-scale chromatin decondensation and recondensation regulated by transcription from a natural promoter. *The Journal of cell biology* 154: 33-48

Murayama A, Ohmori K, Fujimura A, Minami H, Yasuzawa-Tanaka K, et al. 2008. Epigenetic control of rDNA loci in response to intracellular energy status. *Cell* 133: 627-39

Nagata T, Nemoto Y, Hasezawa S. 1992. Tobacco BY-2 cell line as the ´Hela´cell in the cell biology of higher plants. *Int. Rev. Cytol* 132: 31

Naika M, Shameer K, Mathew OK, Gowda R, Sowdhamini R. 2013. STIFDB2: an updated version of plant stress-responsive transcription factor database with additional stress signals, stress-responsive transcription factor binding sites and stress-responsive genes in *Arabidopsis* and rice. *Plant & cell physiology* 54: e8

Nair GM, Murthi KRS, Prasad MYS. 2008. Strategic, technological and ethical aspects of establishing colonies on Moon and Mars. *Acta astronautica* 63: 6

Nakashima J, Liao F, Sparks JA, Tang Y, Blancaflor EB. 2014. The actin cytoskeleton is a suppressor of the endogenous skewing behaviour of *Arabidopsis* primary roots in microgravity. *Plant Biol (Stuttg)* 16 Suppl 1: 142-50

Naryshkin N, Revyakin A, Kim Y, Mekler V, Ebright RH. 2000. Structural organization of the RNA polymerase-promoter open complex. *Cell* 101: 601-11

NASA. 2014. ISS science for everyone ¨Light Microscopy Module (LMM)¨. *http://www.nasa.gov/mission_pages/station/research/experiments/541.html#publications*

Nitta M, Okamura H, Aizawa S, Yamaizumi M. 1997. Heat shock induces transient p53-dependent cell cycle arrest at G1/S. *Oncogene* 15: 561-8

Ochs RL, Lischwe MA, Spohn WH, Busch H. 1985. Fibrillarin: a new protein of the nucleolus identified by autoimmune sera. *Biology of the cell / under the auspices of the European Cell Biology Organization* 54: 123-33

Oka M, Ueda J, Miyamoto K, Yamamoto R, Hoson T, Kamisaka S. 1995. Effect of simulated microgravity on auxin polar transport in inflorescence axis of *Arabidopsis* thaliana. *Uchu Seibutsu Kagaku* 9: 331-6

Orphanides G, Reinberg D. 2000. RNA polymerase II elongation through chromatin. *Nature* 407: 5

Pardo SJ, Patel MJ, Sykes MC, Platt MO, Boyd NL, et al. 2005. Simulated microgravity using the Random Positioning Machine inhibits differentiation and alters gene expression profiles of 2T3 preosteoblasts. *American journal of physiology. Cell physiology* 288: C1211-21

Paul AL, Zupanska AK, Ostrow DT, Zhang Y, Sun Y, et al. 2012. Spaceflight transcriptomes: unique responses to a novel environment. *Astrobiology* 12: 40-56

Paul AL, Zupanska AK, Schultz ER, Ferl RJ. 2013. Organ-specific remodeling of the *Arabidopsis* transcriptome in response to spaceflight. *BMC plant biology* 13: 112

Pecinka A, Dinh HQ, Baubec T, Rosa M, Lettner N, Mittelsten Scheid O. 2010. Epigenetic regulation of repetitive elements is attenuated by prolonged heat stress in *Arabidopsis*. *The Plant cell* 22: 3118-29

Perbal G. 2001. The role of gravity in plant development. *In: Seibert, G. editor. A world without gravity. Noordwijk, The Netherlands: ESA Publication Division*: 16

Perbal G, Driss-Ecole D, Rutin J, Salle G. 1987. Graviperception of lentil seedling roots grown in space (Spacelab D1 Mission). *Physiologia plantarum* 70: 119-26

Petricka JJ, Nelson TM. 2007. *Arabidopsis* nucleolin affects plant development and patterning. *Plant physiology* 144: 173-86

Phillips T, Shaw K. 2008. Chromatin Remodeling in Eukaryotes. *Nature Education* 1

Planchais S, Glab N, Inze D, Bergounioux C. 2000. Chemical inhibitors: a tool for plant cell cycle studies. *FEBS letters* 476: 78-83

Pontvianne F, Abou-Ellail M, Douet J, Comella P, Matia I, et al. 2010. Nucleolin is required for DNA methylation state and the expression of rRNA gene variants in *Arabidopsis* thaliana. *PLoS genetics* 6: e1001225

Pontvianne F, Matia I, Douet J, Tourmente S, Medina FJ, et al. 2007. Characterization of AtNUC-L1 reveals a central role of nucleolin in nucleolus organization and silencing of AtNUC-L2 gene in *Arabidopsis*. *Molecular biology of the cell* 18: 369-79

Porter AC. 2008. Preventing DNA over-replication: a Cdk perspective. *Cell division* 3: 3

Potuschak T, Doerner P. 2001. Cell cycle controls: genome-wide analysis in *Arabidopsis*. *Current opinion in plant biology* 4: 501-6

Probst AV, Dunleavy E, Almouzni G. 2009. Epigenetic inheritance during the cell cycle. *Nature reviews. Molecular cell biology* 10: 192-206

Raska I, Koberna K, Malinsky J, Fidlerova H, Masata M. 2004. The nucleolus and transcription of ribosomal genes. *Biology of the cell / under the auspices of the European Cell Biology Organization* 96: 579-94

Raska I, Shaw PJ, Cmarko D. 2006. Structure and function of the nucleolus in the spotlight. *Current opinion in cell biology* 18: 325-34

Rasmusson AG, Soole KL, Elthon TE. 2004. Alternative NAD(P)H dehydrogenases of plant mitochondria. *Annu Rev Plant Biol* 55: 23-39

Raynaud C, Mallory AC, Latrasse D, Jegu T, Bruggeman Q, et al. 2014. Chromatin meets the cell cycle. *Journal of experimental botany*

Renaudin JP, Doonan JH, Freeman D, Hashimoto J, Hirt H, et al. 1996. Plant cyclins: a unified nomenclature for plant A-, B- and D-type cyclins based on sequence organization. *Plant molecular biology* 32: 1003-18

Risueño MC, Medina FJ. 1986. The nucleolar structure in plant cells. *Revisiones sobre biologia celular : RBC* 7: 1-154

Risueño MC, Medina FJ, Moreno Diaz de la Espina S. 1982. Nucleolar fibrillar centres in plant meristematic cells: ultrastructure, cytochemistry and autoradiography. *Journal of cell science* 58: 313-29

Roeder RG. 1996. The role of general initiation factors in transcription by RNA polymerase II. *Trends in biochemical sciences* 21: 327-35

Roger B, Moisand A, Amalric F, Bouvet P. 2003. Nucleolin provides a link between RNA polymerase I transcription and pre-ribosome assembly. *Chromosoma* 111: 9

Routh A, Sandin S, Rhodes D. 2008. Nucleosome repeat length and linker histone stoichiometry determine chromatin fiber structure. *Proceedings of the National Academy of Sciences of the United States of America* 105: 8872-7

Rowley A, Johnston GC, Butler B, Werner-Washburne M, Singer RA. 1993. Heat shock-mediated cell cycle blockage and G1 cyclin expression in the yeast Saccharomyces cerevisiae. *Molecular and cellular biology* 13: 1034-41

Rubbi CP, Milner J. 2003. Disruption of the nucleolus mediates stabilization of p53 in response to DNA damage and other stresses. *The EMBO journal* 22: 6068-77

Ruiz-Pesini E, Diez-Sanchez C, Lopez-Perez MJ, Enriquez JA. 2007. The role of the mitochondrion in sperm function: is there a place for oxidative phosphorylation or is this a purely glycolytic process? *Current topics in developmental biology* 77: 3-19

Ruthenburg AJ, Allis CD, Wysocka J. 2007. Methylation of lysine 4 on histone H3: intricacy of writing and reading a single epigenetic mark. *Molecular cell* 25: 15-30

Sabbah S, Raise M, Tal M. 1995. Methylation of DNA in NaCl-adapted cells of potato. *Plant cell reports* 14: 467-70

Sack FD. 1991. Plant gravity sensing. *Int Rev Cytol* 127: 193-252

Sáez-Vásquez J, Caparros-Ruiz D, Barneche F, Echeverria M. 2004. A plant snoRNP complex containing snoRNAs, fibrillarin, and nucleolin-like proteins is competent for both rRNA gene binding and pre-rRNA processing in vitro. *Molecular and cellular biology* 24: 7284-97

Sáez-Vásquez J, Medina FJ. 2008. The Plant Nucleolus. *Adv Bot. Res* 47: 47

Saijo Y, Hata S, Kyozuka J, Shimamoto K, Izui K. 2000. Overexpression of a single Ca^{+2}-dependent protein kinase confers both cold and salt/drought tolerance on rice plants. *Planta J* 23: 9

Samuels AL, Meehl J, Lipe M, Staehelin LA. 1998. Optimizing conditions for tobacco BY-2 cell cycle synchronization - rapid communication. *Protoplasma* 202: 5

Sanchez ML, Caro E, Desvoyes B, Ramirez-Parra E, Gutierrez C. 2008. Chromatin dynamics during the plant cell cycle. *Seminars in cell & developmental biology* 19: 537-46

Santos MP, Dias LP, Ferreira PC, Pasin LA, Rangel DE. 2011. Cold activity and tolerance of the entomopathogenic fungus Tolypocladium spp. to UV-B irradiation and heat. *Journal of invertebrate pathology* 108: 209-13

Schatten H, Lewis ML, Chakrabarti A. 2001. Spaceflight and clinorotation cause cytoskeleton and mitochondria changes and increases in apoptosis in cultured cells. *Acta astronautica* 49: 399-418

Scheer U, Hock R. 1999. Structure and function of the nucleolus. *Current opinion in cell biology* 11: 385-90

Schimmang T, Tollervey D, Kern H, Frank R, Hurt EC. 1989. A yeast nucleolar protein related to mammalian fibrillarin is associated with small nucleolar RNA and is essential for viability. *The EMBO journal* 8: 4015-24

Schwarzlander M, Fricker MD, Sweetlove LJ. 2009. Monitoring the in vivo redox state of plant mitochondria: effect of respiratory inhibitors, abiotic stress and assessment of recovery from oxidative challenge. *Biochimica et biophysica acta* 1787: 468-75

Serrano P, van Loon JJ, Manzano AI, Medina FJ, Herranz R. 2010. Selection of Drosophila Altered Behaviour & Aging strains for microgravity research. *J Gravit Physiol*: http://hdl.handle.net/10261/39192

Serrano P, van Loon JJWA, Medina FJ, Herranz R. 2013. Relation between motility, accelerated aging and gene expression in selected drosophila strains under altered gravity conditions. *Microgravity Sci Technol* 25: 67-72

Shameer K, Ambika S, Varghese SM, Karaba N, Udayakumar M, Sowdhamini R. 2009. STIFDB-*Arabidopsis* Stress Responsive Transcription Factor DataBase. *International journal of plant genomics* 2009: 583429

Shav-Tal Y, Blechman J, Darzacq X, Montagna C, Dye BT, et al. 2005. Dynamic sorting of nuclear components into distinct nucleolar caps during transcriptional inhibition. *Molecular biology of the cell* 16: 2395-413

Shaw P, Brown J. 2012. Nucleoli: composition, function, and dynamics. *Plant physiology* 158: 44-51

Shaw P, Doonan JH. 2005. The Nucleolus. Playing by different rules? *Cell Cycle* 4: 102-05

Shaw PJ, Jordan EG. 1995. The nucleolus. *Annual review of cell and developmental biology* 11: 93-121

Shimazu T, Miyamoto K, Ueda J. 2003. Growth and development, and auxin polar transport of transgenic *Arabidopsis* under simulated microgravity conditions on a three-dimensional clinostat. *Uchu Seibutsu Kagaku* 17: 288-92

Shimotohno A, Umeda-Hara C, Bisova K, Uchimiya H, Umeda M. 2004. The plant-specific kinase CDKF;1 is involved in activating phosphorylation of cyclin-dependent kinase-activating kinases in *Arabidopsis*. *The Plant cell* 16: 2954-66

Sieberer B, Emons A, Vos J. 2007. culturing immobilized plant cells for the TUBUL space experiments on the DELTA and 12S Mission. *Microgravity Sci Technol* 19: 45

Sieberer BJK, H. Franssen-Verheijen, T. Emons, A. M. Vos, J. W. 2009. Cell proliferation, cell shape, and microtubule and cellulose microfibril organization of tobacco BY-2 cells are not altered by exposure to near weightlessness in space. *Planta* 230: 1129-40

Sievers A. 1991. Gravity sensing mechanisms in plant cells. *ASGSB bulletin : publication of the American Society for Gravitational and Space Biology* 4: 43-50

Simon MD, Geim AK. 2000. Diamagnetic levitation: flying frogs and floating magnets. *J. Appl. Phys* 87: 5

Skirycz A, De Bodt S, Obata T, De Clercq I, Claeys H, et al. 2010. Developmental stage specificity and the role of mitochondrial metabolism in the response of *Arabidopsis* leaves to prolonged mild osmotic stress. *Plant physiology* 152: 226-44

Smetana K, Busch H. 1974. The nucleolus and nucleolar DNA. *In: Busch H (ed) The cell nucleolus. Academic, New York* 1: 74

Smyth GK. 2004. Linear models and empirical bayes methods for assessing differential expression in microarray experiments. *Statistical applications in genetics and molecular biology* 3: Article3

Sobol MA, González-Camacho F, Rodríguez-Vilarino V, Kordium EL, Medina FJ. 2005a. Clinorotation influences rDNA and NopA100 localization in nucleoli. *Advances in space research : the official journal of the Committee on Space Research* 36: 9

Sobol MA, Kordium EL, Gonzalez-Camacho F, Rodriguez-Vilarino V, Medina FJ. 2005b. [Altered gravity affects subnucleolus localization of fibrillarin and NopA64, the most important proteins of rRNA processing]. *TSitologiia i genetika* 39: 52-62

Sokol A, Kwiatkowska A, Jerzmanowski A, Prymakowska-Bosak M. 2007. Up-regulation of stress-inducible genes in tobacco and *Arabidopsis* cells in response to abiotic stresses and ABA treatment correlates with dynamic changes in histone H3 and H4 modifications. *Planta* 227: 245-54

Sorrell DA, Marchbank A, McMahon K, Dickinson JR, Rogers HJ, Francis D. 2002. A WEE1 homologue from *Arabidopsis* thaliana. *Planta* 215: 518-22

Sourlingas TG, Sekeri-Pataryas KE. 1996. Aphidicolin large-scale synchronization of rapidly dividing cell monolayers and the analysis of total histone and histone variant biosynthesis during the S and G2 phases of the HEp-2 cell cycle. *Analytical biochemistry* 234: 104-7

Spier RE. 1991. An overview of animal cell biotechnology: the conjoint application of science, art, and engineering. *Biotechnology* 17: 3-18

Springer PS, Holding DR, Groover A, Yordan C, Martienssen RA. 2000. The essential Mcm7 protein PROLIFERA is localized to the nucleus of dividing cells during the G(1) phase and is required maternally for early *Arabidopsis* development. *Development* 127: 1815-22

Springer PS, McCombie WR, Sundaresan V, Martienssen RA. 1995. Gene trap tagging of PROLIFERA, an essential MCM2-3-5-like gene in *Arabidopsis*. *Science* 268: 877-80

Sproul D, Gilbert N, Bickmore WA. 2005. The role of chromatin structure in regulating the expression of clustered genes. *Nature reviews. Genetics* 6: 775-81

Sridha S, Wu K. 2006. Identification of AtHD2C as a novel regulator of abscisic acid responses in *Arabidopsis*. *The Plant journal : for cell and molecular biology* 46: 124-33

Srivastava M, Pollard HB. 1999. Molecular dissection of nucleolin's role in growth and cell proliferation: new insights. *FASEB journal : official publication of the Federation of American Societies for Experimental Biology* 13: 1911-22

Stanek D, Kiss T, Raska I. 2000. Pre-ribosomal RNA is processed in permeabilised cells at the site of transcription. *European journal of cell biology* 79: 202-7

Staves MP. 1997. Cytoplasmic streaming and gravity sensing in Chara internodal cells. *Planta* 203: S79-84

Staves MP, Wayne R, Leopold AC. 1997. The effect of the external medium on the gravitropic curvature of rice (Oryza sativa, Poaceae) roots. *American journal of botany* 84: 1522-9

Steel RGDaJHT. 1980. Principles and Procedures of statistics. . *A. biometerical Approach 2nd Ed. Mac. Gaw Hill book company. New York*

Stepinski D. 2014. Functional ultrastructure of the plant nucleolus. *Protoplasma*

Sterner JM, Dew-Knight S, Musahl C, Kornbluth S, Horowitz JM. 1998. Negative regulation of DNA replication by the retinoblastoma protein is mediated by its association with MCM7. *Molecular and cellular biology* 18: 2748-57

Steward FC, Mapes MO, Kent AE, Holsten RD. 1964. Growth and Development of Cultured Plant Cells. *Science* 143: 20-7

Steward N, Kusano T, Sano H. 2000. Expression of ZmMET1, a gene encoding a DNA methyltransferase from maize, is associated not only with DNA replication in actively proliferating cells, but also with altered DNA methylation status in cold-stressed quiescent cells. *Nucleic acids research* 28: 3250-9

Storey JD, Tibshirani R. 2003. Statistical significance for genomewide studies. *Proceedings of the National Academy of Sciences of the United States of America* 100: 9440-5

Sun X, Linden JC. 1999. Shear stress effects on plant cell suspension cultures in a rotating wall vessel bioreactor. *J Industrial Microbiology and Biotechnology* 22: 4

Sun Y, Dilkes BP, Zhang C, Dante RA, Carneiro NP, et al. 1999. Characterization of maize (Zea mays L.) Wee1 and its activity in developing endosperm. *Proceedings of the National Academy of Sciences of the United States of America* 96: 4180-5

Sundar AS, Varghese SM, Shameer K, Karaba N, Udayakumar M, Sowdhamini R. 2008. STIF: Identification of stress-upregulated transcription factor binding sites in *Arabidopsis* thaliana. *Bioinformation* 2: 431-7

Swaney JS, Patel HH, Yokoyama U, Head BP, Roth DM, Insel PA. 2006. Focal adhesions in (myo)fibroblasts scaffold adenylyl cyclase with phosphorylated caveolin. *The Journal of biological chemistry* 281: 17173-9

Swindell WR, Huebner M, Weber AP. 2007. Transcriptional profiling of *Arabidopsis* heat shock proteins and transcription factors reveals extensive overlap between heat and non-heat stress response pathways. *BMC genomics* 8: 125

Sytnik KM, Popova AF. 1998. Changes in plant mitochondria ultrastructure and respiration intensity in altered gravity. *J Gravit Physiol* 5: P169-70

Tanaka S, Tak YS, Araki H. 2007. The role of CDK in the initiation step of DNA replication in eukaryotes. *Cell division* 2: 16

Tanaka Y, Okamoto K, Teye K, Umata T, Yamagiwa N, et al. 2010. JmjC enzyme KDM2A is a regulator of rRNA transcription in response to starvation. *The EMBO journal* 29: 1510-22

Teale WD, Paponov IA, Palme K. 2006. Auxin in action: signalling, transport and the control of plant growth and development. *Nat. Rev. Mol. Cell Biol.* 7: 847-59

Testillano PS, Gonzalez-Melendi P, Ahmadian P, Risueño MC. 1995. The methylation-acetylation method: an ultrastructural cytochemistry for nucleic acids compatible with immunogold studies. *Journal of structural biology* 114: 123-39

Testillano PS, Sanchez-Pina MA, Olmedilla A, Ollacarizqueta MA, Tandler CJ, Risueño MC. 1991. A specific ultrastructural method to reveal DNA: the NAMA-Ur. *The journal of histochemistry and cytochemistry : official journal of the Histochemistry Society* 39: 1427-38

Thellin O, Zorzi W, Lakaye B, De Borman B, Coumans B, et al. 1999. Housekeeping genes as internal standards: use and limits. *Journal of biotechnology* 75: 291-5

Thiel CS, Paulsen K, Bradacs G, Lust K, Tauber S, et al. 2012. Rapid alterations of cell cycle control proteins in human T lymphocytes in microgravity. *Cell Commun Signal* 10: 1

Timperio AM, Egidi MG, Zolla L. 2008. Proteomics applied on plant abiotic stresses: Role of heat shock proteins (HSP). *Journal of Proteomics* 71: 391-411

Torres Acosta JA, de Almeida Engler J, Raes J, Magyar Z, De Groodt R, et al. 2004. Molecular characterization of *Arabidopsis* PHO80-like proteins, a novel class of CDKA;1-interacting cyclins. *Cellular and molecular life sciences : CMLS* 61: 1485-97

Trono D, Flagella Z, Laus MN, Di Fonzo N, Pastore D. 2004. The uncoupling protein and the potassium channel are activated by hyperosmotic stress in mitochondria from durum wheat seedlings. *Plant Cell Environ* 27: 12

Tsugeki R, Olson ML, Fedoroff NV. 1998. Transposon tagging and the study of root development in *Arabidopsis*. *Gravitational and space biology bulletin : publication of the American Society for Gravitational and Space Biology* 11: 79-87

Tsuji T, Ficarro SB, Jiang W. 2006. Essential role of phosphorylation of MCM2 by Cdc7/Dbf4 in the initiation of DNA replication in mammalian cells. *Molecular biology of the cell* 17: 4459-72

Tsutsumi YM, Patel HH, Huang D, Roth DM. 2006. Role of 12-lipoxygenase in volatile anesthetic-induced delayed preconditioning in mice. *American journal of physiology. Heart and circulatory physiology* 291: H979-83

Tye BK. 1999. MCM proteins in DNA replication. *Annual review of biochemistry* 68: 649-86

Ueda J. 1999. [Plant growth and development, and auxin polar transport in space conditions]. *Uchu Seibutsu Kagaku* 13: 122-3

Ueda J, Miyamoto K, Yuda T, Hoshino T, Fujii S, et al. 1999. Growth and development, and auxin polar transport in higher plants under microgravity conditions in space: BRIC-AUX on STS-95 space experiment. *Journal of plant research* 112: 487-92

Ueno S, Iwasaka M. 1997. Properties of diamagnetic fluid in high gradient magnetic fields. *J Appl Phys* 75: 3

Umeda M, Shimotohno A, Yamaguchi M. 2005. Control of cell division and transcription by cyclin-dependent kinase-activating kinases in plants. *Plant & cell physiology* 46: 1437-42

Umeda M, Umeda-Hara C, Uchimiya H. 2000. A cyclin-dependent kinase-activating kinase regulates differentiation of root initial cells in *Arabidopsis*. *Proceedings of the National Academy of Sciences of the United States of America* 97: 13396-400

Valles JM, Jr., Maris HJ, Seidel GM, Tang J, Yao W. 2005. Magnetic levitation-based Martian and lunar gravity simulators. *Advances in space research : the official journal of the Committee on Space Research* 36: 5

Van de Corput MP, de Boer E, Knoch TA, van Cappellen WA, Quintanilla A, et al. 2012. Super-resolution imaging reveals three-dimensional folding dynamics of the beta-globin locus upon gene activation. *Journal of cell science* 125: 4630-9

Van Leene J, Hollunder J, Eeckhout D, Persiau G, Van De Slijke E, et al. 2010. Targeted interactomics reveals a complex core cell cycle machinery in *Arabidopsis* thaliana. *Molecular systems biology* 6: 397

van Loon JJWA. 2007. Some history and use of the Random Positioning Machine, RPM, in gravity related research. *Advances in space research : the official journal of the Committee on Space Research* 39: 1161-5

van Loon JJWA, Folgering EH, Bouten CV, Smit TH. 2004. Centrifuges and inertial shear forces. *J Gravit Physiol* 11: 29-38

van Loon JJWA, Tranck E, Van Nieuwenhoven FA, Snoeckx LHEH, De Jong HAA, Wubbels RJ. 2005. A brief overview of animal hypergravity studies. *J Gravit Physiol* 12: 6

van Zanten M, Tessadori F, Bossen L, Peeters AJ, Fransz P. 2010. Large-scale chromatin de-compaction induced by low light is not accompanied by nucleosomal displacement. *Plant signaling & behavior* 5: 1677-8

van´t Hof J. 1986. Control points within the cell cycle. *In The Cell Division Cycle in Plants, ed. JA Bryant, D Francis, Cambridge: Cambridge Univ. Press.*: 14

Vandepoele K, Raes J, De Veylder L, Rouze P, Rombauts S, Inze D. 2002. Genome-wide analysis of core cell cycle genes in *Arabidopsis*. *The Plant cell* 14: 903-16

Vassilev LT. 2006. Cell cycle synchronization at the G2/M phase border by reversible inhibition of CDK1. *Cell Cycle* 5: 2555-6

Verkest A, Manes CL, Vercruysse S, Maes S, Van Der Schueren E, et al. 2005a. The cyclin-dependent kinase inhibitor KRP2 controls the onset of the endoreduplication cycle during *Arabidopsis* leaf development through inhibition of mitotic CDKA;1 kinase complexes. *The Plant cell* 17: 1723-36

Verkest A, Weinl C, Inze D, De Veylder L, Schnittger A. 2005b. Switching the cell cycle. Kip-related proteins in plant cell cycle control. *Plant physiology* 139: 1099-106

Vogt SS, Butler RP, Haghighipour N. 2012. GJ 581 update: additional evidence for a Super-Earth in the habitable zone. *Astronomische Nachrichten (Astronomical Notes)* 333: 17

Volkmann D, Baluska F, Lichtscheidl I, Driss-Ecole D, Perbal G. 1999. Statoliths motions in gravity-perceiving plant cells: does actomyosin counteract gravity? *FASEB journal : official publication of the Federation of American Societies for Experimental Biology* 13 Suppl: S143-7

Volkov RA, Medina FJ, Zentgraf U, Hemleben V. 2004. Organization and molecular evolution of rDNA, nucleolar dominance, and nucleolus structure. *Prog. Botany* 65: 41

Wada Y, Miyamoto K, Kusano T, Sano H. 2004. Association between up-regulation of stress-responsive genes and hypomethylation of genomic DNA in tobacco plants. *Molecular genetics and genomics : MGG* 271: 658-66

Wang G, Kong H, Sun Y, Zhang X, Zhang W, et al. 2004. Genome-wide analysis of the cyclin family in *Arabidopsis* and comparative phylogenetic analysis of plant cyclin-like proteins. *Plant physiology* 135: 1084-99

Wang H, Fowke LC, Crosby WL. 1997. A plant cyclin-dependent kinase inhibitor gene. *Nature* 386: 451-2

Wang Y, Maharana S, Wang MD, Shivashankar GV. 2014. Super-resolution microscopy reveals decondensed chromatin structure at transcription sites. *Scientific reports* 4: 4477

Weber M, Schubeler D. 2007. Genomic patterns of DNA methylation: targets and function of an epigenetic mark. *Current opinion in cell biology* 19: 273-80

Wei Q, Li J, Liu T, Tong X, Ye X. 2013. Phosphorylation of minichromosome maintenance protein 7 (MCM7) by cyclin/cyclin-dependent kinase affects its function in cell cycle regulation. *The Journal of biological chemistry* 288: 19715-25

Went FW. 1928. Wuchsstoff und Wachstum. *Receuils des Travaux Botanica Neerlandica* 25: 117

West G, Inze D, Beemster GT. 2004. Cell cycle modulation in the response of the primary root of *Arabidopsis* to salt stress. *Plant physiology* 135: 1050-8

Wolf DA, Schwarz RP. 1991. Analysis of gravity-induced particle motion and fluid perfusion flow in the NASA-designed rotating zero-head-space tissue culture vessel. *NASA Technical Paper*

Wolf DA, Schwarz RP. 1992. Experimental measurement of the orbital paths of particles sedienting within a rotating viscous fluid as influenced by gravity. *NASA Technical Paper*

Xu D, Bai J, Duan Q, Costa M, Dai W. 2009. Covalent modifications of histones during mitosis and meiosis. *Cell Cycle* 8: 3688-94

Yang YH, Dudoit S, Luu P, Lin DM, Peng V, et al. 2002. Normalization for cDNA microarray data: a robust composite method addressing single and multiple slide systematic variation. *Nucleic acids research* 30: e15

Yata K, Esashi F. 2009. Dual role of CDKs in DNA repair: to be, or not to be. *DNA repair* 8: 6-18

Yoder TL, Zheng HQ, Todd P, Staehelin LA. 2001. Amyloplast sedimentation dynamics in maize columella cells support a new model for the gravity-sensing apparatus of roots. *Plant physiology* 125: 1045-60

Yu J, Li B, Dai P, Ge S, Cheng X. 2009. Study on the interaction among molecules and the determination of DNA by light scattering with a new type rhodanine derivative. *Spectrochimica acta. Part A, Molecular and biomolecular spectroscopy* 74: 875-80

Yuge L, Hide I, Kumagai T, Kumei Y, Takeda S, et al. 2003. Cell differentiation and p38(MAPK) cascade are inhibited in human osteoblasts cultured in a three-dimensional clinostat. *In vitro cellular & developmental biology. Animal* 39: 89-97

Zhang J, Campbell RE, Ting AY, Tsien RY. 2002. Creating new fluorescent probes for cell biology. *Nature reviews. Molecular cell biology* 3: 906-18

Zhang W, Zou X. 2012. Synchronization ability of coupled cell-cycle oscillators in changing environments. *BMC systems biology* 6 Suppl 1: S13

Zhou Y, Wang H, Gilmer S, Whitwill S, Fowke LC. 2003. Effects of co-expressing the plant CDK inhibitor ICK1 and D-type cyclin genes on plant growth, cell size and ploidy in *Arabidopsis* thaliana. *Planta* 216: 604-13

Zhu J, Jeong JC, Zhu Y, Sokolchik I, Miyazaki S, et al. 2008. Involvement of *Arabidopsis* HOS15 in histone deacetylation and cold tolerance. *Proceedings of the National Academy of Sciences of the United States of America* 105: 4945-50

Zilberman D. 2008. The evolving functions of DNA methylation. *Current opinion in plant biology* 11: 554-9

Zinchuk V, Zinchuk O, Okada T. 2007. Quantitative colocalization analysis of multicolor confocal immunofluorescence microscopy images: pushing pixels to explore biological phenomena. *Acta histochemica et cytochemica* 40: 101-11

Zupanska AK, Denison FC, Ferl RJ, Paul AL. 2013. Spaceflight engages heat shock protein and other molecular chaperone genes in tissue culture cells of *Arabidopsis* thaliana. *American journal of botany* 100: 235-48